NTNU
Norwegian University of Science and Technology
Marine Technology, Systems Department

M.Sc. THESIS

Tilte: **Variable Inlet and Exhaust Valve Operation in Medium Speed Marine Diesel Engines**	**Delivered:** **11.06.2010** **Availability:** **Open**
Student: **Hans Steffen Ravnanger Sæle**	**Number of pages:** **161**

Abstract:

This thesis was successfully completed through five main parts. First a lingering issue of great importance was dealt with in order to start the use of the provided simulation model. This task was imperative to accurate simulation results as it aimed to ensure matching definitions between simulation software and the engine manufacturer. A satisfactory result was quickly obtained.

Secondly some sections are spent mapping the potential performance benefits of a camless valve train. This part has its reference in automotive industry and gives strong indications that great potential lies in valve train modifications. This chapter serves as the main basis for evaluating the results from variable valve control simulations.

Third there was a great deal of model modifications required to obtain the propulsion engine model needed to fit the scope of this thesis. This gave life to an additional task as the provided generator engine model had to be recalibrated for å different operational purpose. Recalibration was completed and model operation showed good matching to the measured performance data provided by the manufacturer.

Fourth there was a need for valve train modifications in order to successfully simulate variable valve control. This was solved through systematic use of a set of parameters that had the ability of manipulating the lift curve. These scaling factors were able to provide a satisfactory result regarding lift manipulation. Some minor limitations regarding curve shaping were evident as no manipulation to the raw data was performed.

The fifth and most central part of the thesis concerns the simulated valve strategy experiments. A set of strategies previously performed in the automotive industry was reproduced using the Rolls Royce KRM-6 model. When matching the results of these two studies on finds that the results are quite similar. Miller timing strategies prove to be the most beneficial of all showing a potential bsfc reduction of up to almost 9 percent. There are however indications that a Miller timing hybrid might give lesser harmful emissions. Optimal operation of the engine is determined on the basis of each of the strategies that proved beneficial. By this it will be evident that optimal operation using the best strategy yields the most beneficial operation.

Key Words:

Variable Valve Control
Medium speed Diesel Engine
GT-Power

Advisors:

Harald Valland, Nabil Al Ryati

Address:
NTNU
Department of Marine Technology
N-7491 Trondheim

Location:
Marinteknisk Senter
O. Nielsens vei 10

Tel: +47 73 595501
Fax: +47 73 595697

ASSIGNMENT TEXT

The overall objective of the task is to get quantitative evaluation of engine performance improvements that can be obtained by means of variable valve operation. The study should be based on the use of theoretical performance simulation using GT-POWER.

The assignment should be prepared based on following points:

- A single-cylinder model of the Rolls-Royce K-type engine should be established. The model should be capable of simulating all relevant engine operating conditions (speed and power)
- Variable valve operation should be demonstrated by the simulation model. Following modifications of the valve lift function should be considered:
    - Unchanged valve lift function – changing crank angle at valve opening
    - Unchanged shape of valve lift function – variable max valve lift
    - Unchanged shape of valve lift function – variable length (duration) of valve opening
- At one characteristic engine operating point the simulation model should be applied for analysing the effect of variable valve operation on typical performance variables like mean indicated pressure, thermal efficiency, volumetric efficiency, and exhaust temperature.
- The concept of optimum valve operation at a given engine operating point should be defined. The simulation model should be used to determine optimum valve operation.
- Two typical application of variable valve operation should be analysed:
    - Control of air supply to the cylinders in a Lean Burn Gas Engine
    - Implementation of the Miller cycle in a diesel engine

The assignment text must be included as a part of the MSc report.

The report should be written like a research report, with an abstract, conclusions, contents list, reference list, etc. During preparation of the report it is important that the candidate emphasizes easily understood and well written text. For ease of reading the report should contain adequate references at appropriate places to related text, tables and figures. On evaluation, a lot of weight is put on thorough preparation of results, their clear presentation in the form of tables and/or graphs, and on comprehensive discussion.

All used sources must be completely documented. For textbooks and periodicals, author, title, year, page number and eventually figure number must be specified.

It is assumed that the student should take initiative for establishing satisfactory contact with his teacher and eventual advisors.

In accordance with current regulations NTNU reserves the right to use any results from the project work in connection with teaching, research, publication, or other activities.
Two -2- copies of the report are required. A complete copy of all material on digital form on CD-ROM in Word-format or other relevant format should be handed in together with the written material.

The project report must be delivered no later than June 14th 2010.

Department of Marine Technology, 2010-02-26

Harald Valland
Professor

PREFACE

This report is written as the master thesis of Hans Ravnanger Sæle at NTNU Marine Technology – Systems Department during the spring of 2010. The thesis is treating the principles of variable valve control on medium speed diesel engines. A literature study founds the basis for this thesis which is also written by Hans Ravnanger Sæle during the fall of 2009. Experiments are done to support this literature study is the central part of this thesis and the results are presented with reference to automotive industry research on a smaller scale engine. Experiments are based on strategies that have a certain known theoretical potential. A Rolls Royce KRM-6 engine model is prepared to show this potential in principle. Simulations of the KRM's compression ignition process are realized using software called GT Power to get as accurate simulation results as possible. Results are discussed on the basis of a set of predetermined performance parameters. The thesis gets an unexpected additional task when having to recalibrate the entire engine model that initially is for generator purposes only. The calibration work proves to be quite time consuming and constitutes a substantial part of the thesis. From last year's literature study an uncompleted task remains and this is dealt with initially in this thesis.

Trondheim, 11.06.2010

Hans Steffen Ravnanger Sæle

CONTENTS

FIGURES

TABLES

APPENDIXES

1 INTRODUCTION

"For economical and environmental reasons there is a drive to improve engine performance, especially to reduce fuel consumption and exhaust emissions. The operation of inlet and exhaust valves has impact on engine performance. Engine power, specific fuel consumption and exhaust emissions may be improved by means of variable valve timing and valve operation, especially at off-design operating conditions. As typical examples variable valve operation may be used for reduction of NO_x emissions in diesel engines by means of the Miller cycle. In Lean Burn gas engines the air-fuel ratio at low engine power may also be controlled by means of variable valve operation."

"Powerful engine performance simulation programs have been developed that can be adopted for most engine types. One such simulation program, GT-POWER, is available at Department of marine technology at NTNU and will be used in this assignment."

(Extraction from the assignment text, Valland 2010)

Initially there was an unfinished task in need of additional treatment. The issue of matching valve actuation definitions between simulation software and engine manufacturer was insufficiently treated in (1) . Finishing this task will therefore constitute the first part of this thesis.

The student will demonstrate variable valve operation by use of a Rolls Royce KRM-6 simulation model. At two characteristic engine operating points the simulation model is applied for analysing the effect of variable valve operation on the basis of typical performance variables like mean indicated pressure, thermal efficiency, volumetric efficiency, and exhaust temperature. Several strategies are used for each of the two off-design operation points. Wherever possible the concept of optimum valve operation at a given engine operating point is defined for each of the proposed strategies. The simulation model is used to determine optimum valve operation.

Making the simulation model run properly has offered several challenges. The initial model was suitable only for generator operation and could not simulate severe load or speed changes. Recalibration became a great part of this thesis as such work is demanding and time consuming. In addition to this GT Power does not offer complete variable valve control solutions and the software had to be manipulated in order to implement as systematic approach for continuous variable valve control via the already existent cam based valve train.

2 VALVE LIFT DEFINITIONS

During the project assignment written in the fall semester of 2009, the issue of whether or not lift definitions in GT-Power are matching those of Rolls Royce itself was addressed. Unfortunately it was not solved in a satisfactory way. Before starting experiments on valve timing I needed to complete this task by resolving the issues concerning valve definitions. It is imperative to getting accurate simulation results that lift definitions in GT-Power and Rolls Royce are corresponding. Therefore we need to prove that this is the case, if not a solution must be presented.

Practically measurements of valve lift are usually not done on the cam itself. In Rolls Royce's case measurements are done on the top of the pushrod which transfers energy from the cam to the rocker arm. As stated in the project assignment, Rolls Royce define valve opening as the crank angle when the pushrod is lifted 1.8 mm. The reason for this is the shape of the cam. As can be seen from the figure below the start of the cam profile's ramp is not well pronounced making the actual start of the lift hard to register by practical measurement.

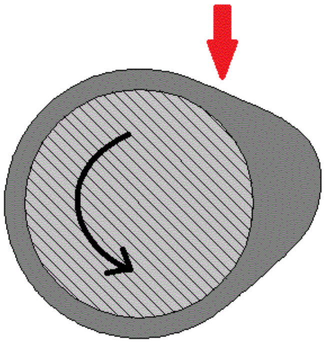

FIGURE 1 - CAM PROFILE ILLUSTRATION

To find which angle, expressed in cam angle degrees, GT-Power defines as valve opening we open GT-Post to view results for a simple simulation done randomly using the KRG model. From GT-Post we open the cylinder template and view results for valves and ports. All post simulation information regarding engine operation results can be found in GT Post.

Part Information

Print ...

Part: Cyl-1

Template: EngCylinder

Attribute Value	Unit	Case / Case# 1
Intake Port Pressure, Average	bar	2.53679
Intake Port Temperature, Average	K	324.596
Exhaust Port Pressure, Average	bar	2.09009
Exhaust Port Temperature, Average	K	631.912
Intake Valve Close, Crank Angle at	deg	-129.764
Intake Valve Open, Crank Angle at	deg	291.764
Exhaust Valve Close, Crank Angle at	deg	432.439
Exhaust Valve Open, Crank Angle at	deg	109.561

FIGURE 2 - VALVE/PORTS RESULTS FROM GT POST

From Fig. 2 we see that GT-Power simulations register opening of the valve happening at 291.764°. Below we observe that this crank angle represents the initial lift of the valve and not the lift at 1.8mm as defined by Rolls Royce. The ramp of the lift does not seem to be excluded by GT Power by looking at Fig. 3.

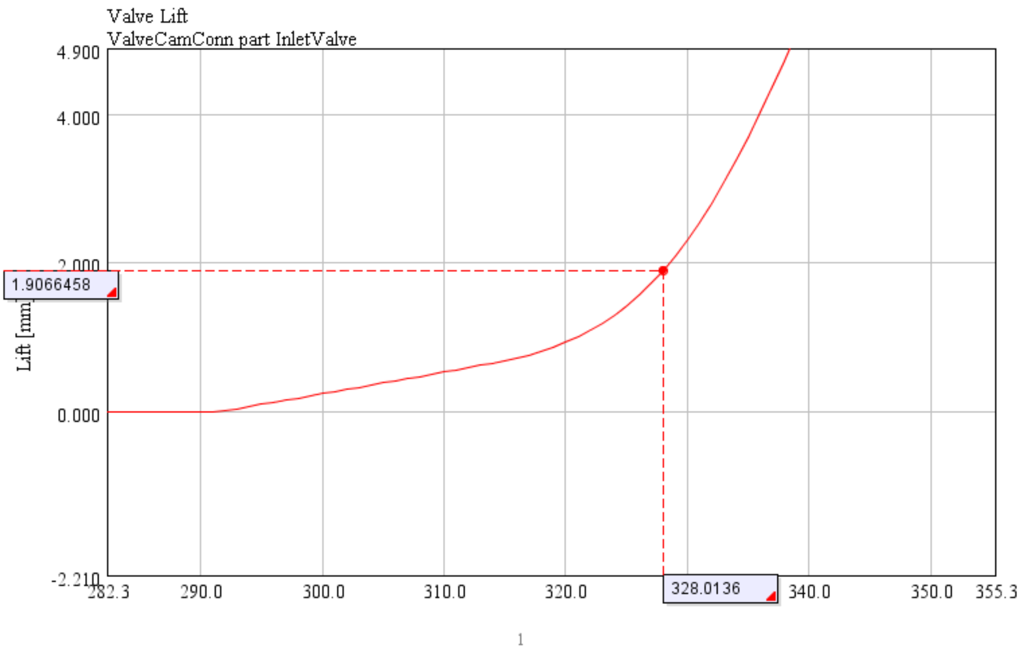

FIGURE 3 – INLET VALVE LIFT (RESOLUTION DOES NOT ALLOW FOR 1.8 MM VIEW)

The fact that the ramp of the lift is excluded by companies such as Rolls Royce is in fact taken into consideration by the GT-Power designers. A parameter named "*Valve Event Reporting Height*" is implemented into the program to deliberately exclude the ramp of the lift. An explanation of this variable is found in the help navigator of GT-Power:

"Height at which the angle of valve-open and valve-close RLT variables will be reported or a dependence reference object. Some companies reference their valve opening and closing timing angles to a lift greater than 0.0 so that the ramps at the start and end of the lift curve are excluded. Please note that this attribute only applies to the RLT variables reported in this connection and not those reported in adjacent 'EngCylinder' parts. ("def" = 0.0)"

Further exploration of the engine model show that Valve Event Reporting Height for the intake valve has been implemented at a value of 1.8mm, which is in accordance with Rolls Royce definitions.

Template:	ValveCamConn
Object:	InletValve
Object Comment:	Derived from Valve Reference Object InLE516-97
Comment:	

Attribute	Unit	Object Value	Part Override
Part Giving Angle (def=Attached Cylinder)		def	...
Driver Object Giving Angle		ign	...
Variable Profile Dependency Object		ign	
Flow Coefficient Lift Unit		LiftOverDiam	
Valve Type for RLT Variable Calculations		intake	
Valve Event Reporting Height	mm	1.8	
Valve Event Lift Flag		valve	
Preprocess Plot Request		☑	
Heat Conduction "Flange"		ign	...

This will in effect mean that the lift values below 1.8mm are not used as dependence reference objects and thus presenting a result of a simulation corresponding to an actual Rolls Royce engine testing.

Not being able to display the crank angle at lift equal to 1.8mm is based on the resolution of the array implemented to GT-Power. Using linear interpolation an estimate for the crank angle can be presented:

$$\theta = \frac{y_{2}-y_{1}}{y_{2}-y_{1}} \cdot (\theta_{2}-\theta_{1}) + \theta_{1}$$

Applying this formula to the array of crank angle versus lift height we can find an approximate value for the angle when 1,8mm occurs.

47	325.0128	1.4329939
48	326.01306	1.5736523
49	327.01334	1.7311358
50	328.0136	1.9066458
51	329.0139	2.1014
52	330.01416	2.3177488

FIGURE 4 - EXTRACT FROM INLET LIFT ARRAY

$$\theta = \frac{1{,}8000000 - 1{,}7311358}{1{,}9066458 - 1{,}7311358} \cdot (328{,}0136 - 327{,}013334) + 327{,}013334 = 327{,}0494616°$$

We clearly see that a substantial part of the cycle (in terms of crank angle) is used at the ramp of the cam profile, almost 40°. This supports the motivation companies have for excluding the ramps of valve opening and closing when applying simulation software such as GT-Power.

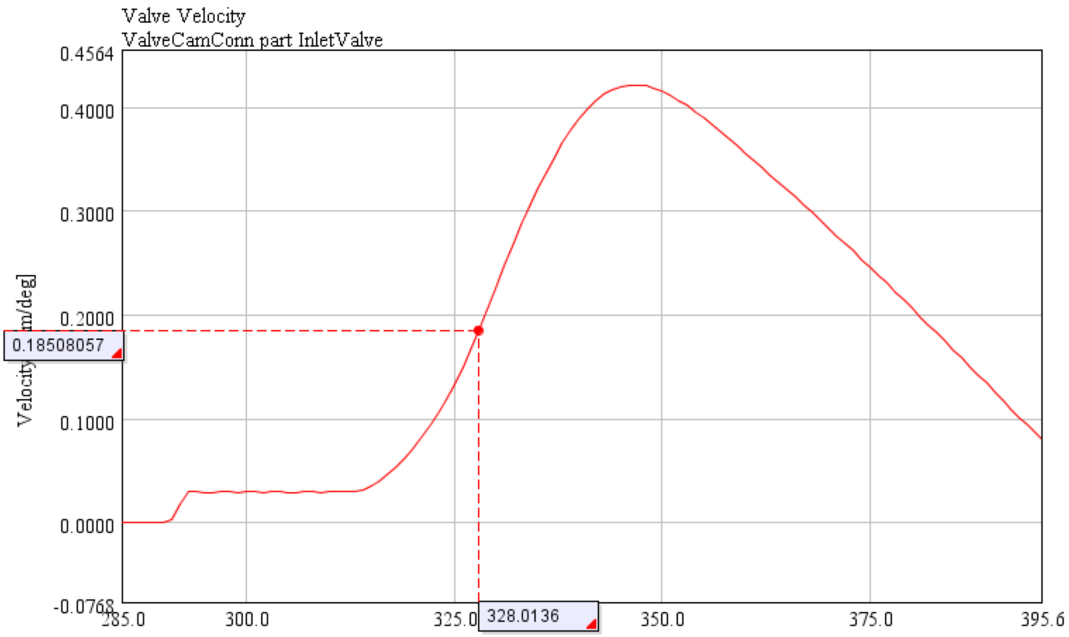

FIGURE 5 – INLET VALVE VELOCITY

As can be seen from the velocity graph above, Rolls Royce defines valve opening close to the peak value of acceleration located at the turning point of the velocity curve. At this point Rolls Royce can register the most valve movement per turning angle, making measurements more apparent. This might be the reason itself for defining valve opening as crank angle when lifting 1.8mm.

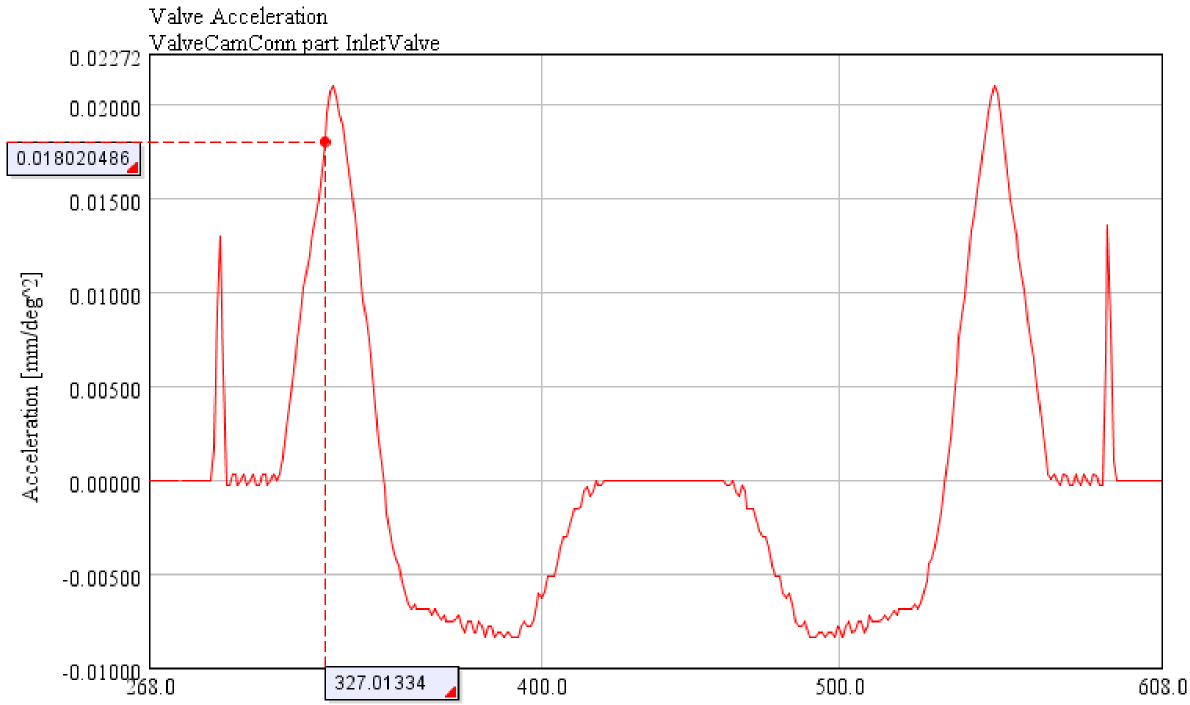

FIGURE 6 - INLET VALVE ACCELERATION

We can thus conclude that this subject requires no further investigation, due to the fact that no valve height is reported outside the range of Rolls Royce lift definitions. I was also able to identify the motivation for using 1.8 mm by analyzing valve velocity and acceleration.

3 CAMLESS ENGINE PERFORMANCE BENEFITS

Before presenting any results of the simulations completed in this thesis, a brief review is made of what can be expected from a camless engine in terms of performance benefits. This review is meant as a supplement to the explanations made in (1). According to (2) a camless high speed engine was built at Ford Research Laboratory. I will use this engine as a reference to present the potential of engine performance improvement when using a camless valve train. This engine uses an electro hydraulic solution to make a continuously variable valve control system. No mechanical springs are used, although we know from (1) that springs are possibly needed to support the hydraulics on the larger medium speed engines.

Being able to build an engine without a camshaft, total weight reduces and possibly also the volume requirement of the unit. This makes a camless engine desirable compared to its competitors. The main challenge to manufacturers making VVA solutions is recuperation of the kinetic energy needed to create valve lift. Unable to return this energy to the system, the camshaft solution is hard to beat on economical terms. Earlier the camshafts fixed lift lead to conflicting requirements for various operating conditions, but was considered an acceptable compromise due to the simplicity and reliability of this valve train. In more recent times there is a growing focus on fuel economy and harmful exhaust emissions pushing the designers to create innovative solutions. The camless engine is one of these solutions representing an engine with less compromised performance.

So what can be expected from an engine with the full ability to vary all parameters concerning valve lift and timing continuously? We need to map the various ways VVA is used to gain benefit from the desirable improvement in engine operation. Some of these are already mentioned in (1).

3.1 INTAKE TIMING

Given the ability to control the intake event is an essential part of the valve control benefit potential. Here lies the ability to manipulate the charge air trapped at the start of each cycle. A new starting point can be set for any given operation.

3.1.1 FASTER BURN RATE

To achieve satisfactory combustion efficiency during a cycle fast burn rate is required to complete most of the combustion within the early stages of expansion. A fast burn rate is highly dependent on both sufficient turbulence and mixing of the fuel and air inside the cylinder. Using fixed valve lift at low engine speeds, the lesser air flow into the cylinder is entering through a relatively larger area by Bernoulli. This means that intake air velocity is lower, causing insufficient turbulence to achieve the required burn rate. There are two solutions to this problem. The intake valve could be timed to open at a later point where the piston down stroke speed is enough to create sufficient air intake speed. The other possibility is to reduce intake valve lift in order to increase flow speed of the inlet air.

3.1.2 THROTTLING LOSS REDUCTION

As mentioned in (1) throttling loss is reduced in SI engines as the throttle may be kept fully open during load reduction. The full potential of the air flow is maintained, but the intake valve is timed to reduce the effective volume of fresh air into the cylinder. Late or early intake valve closing may be used to achieve this effect. In (2) early inlet closing is referred to as the preferred method. On diesel or CI engines this is referred to as Miller timing. The goal of such timing in CI engines is to reduce the temperature during combustion so that NOx formation is prevented to some extent. NOx is mainly formed in local hot spots. This effect is reduced due to the lower overall combustion temperature. Given less time to trap air, such inlet valve timing is often supported by tuning. This means opening the inlet valve at an exact point where pressure dynamics in the inlet manifold create a ram charging effect.

3.1.3 TORQUE INCREASE

Common for engines using camshaft valve trains, torque curves show a distinct peak in the mid speed range. At both low and high speeds torque is deteriorated as a result of the performance compromise of the fixed valves. (2) present numbers of torque increase that represent a flatter curve and with a 10% gain in torque in the overall range as well as a 50% gain to the lower range. Mainly this effect in VVA engines is achieved due to improvement of the volumetric efficiency. This is obtained by fully utilizing the ram charging effect. At low speeds the intake is timed to close in order to obtain the maximum effective compression ratio. This is because the ram charging potential is at its lowest here. Variable valve actuation is used to make the best possible compromise between ram charging and compression ratio across the engine speed range. As a consequence, varying the effective compression ratio can happen without variation to the expansion ratio. Reducing the compression ratio in a turbo charged diesel engine improves cycle efficiency. A smaller volume of air is trapped at a higher pressure meaning that less work has to be done by the piston itself.

3.2 EXHAUST TIMING

Exhaust timing is important in order to control the effects on end-of-cycle properties. Exhaust closing is determining events like valve overlap, time for blow down and internal exhaust gas recirculation.

3.2.1 OPTIMIZING EXPANSION RATIO

Higher torque and better fuel efficiency at low speeds can be achieved by retarding the exhaust valve opening. At high speeds the exhaust is opened early to give time for blow-down. At lower speeds however, an equally early opening would be wasteful, making the expansion stroke short of its potential. Exhaust valve opening can be retarded almost as far as to the bottom dead center. For optimal torque and fuel efficiency this timing should be optimized through the whole speed range.

3.2.2 EXHAUST GAS RECIRCULATION

Timing of the exhaust valve also provides the ability to control the amount of residual gas in the cylinder at the point of recharging. First of all this means no external EGR unit. Second, the residual gas in the cylinder helps lower the peak combustion temperature due to partial displacement of some excess oxygen in the premix (1). This results in less production of nitrogen oxides. Two methods exist for valve controlled EGR. Early closure of the exhaust valve will keep the last part of exhaust contained in the cylinder prior to recharging. Extensively late closing of the exhaust valve may cause some of the exhaust gases to be pumped back into the cylinder. According to (1), the last method causes a loss of torque at low speeds. Problems concerning EGR are wear-inducing contaminants found in the residual gas and its effect on increasing the acidity of engine oil. This can in turn result in an inefficient engine.

3.3 VARIABLE LIFT HEIGHT

Another advantage of continuous variable valve actuation is being able to set a lift height dependent on engine speed. This promotes the ability to manipulate the characteristics of the combustion itself.

3.3.1 ENERGY REDUCTION

Less consumption of energy may be achieved compared to the fixed cam driven valve trains. At lower speeds smaller valve lift may be desirable, thus the energy spent on lifting a valve decreases, proving the existence of potential energy savings in a certain lower part of speed range.

3.3.2 INLET AIR VELOCITY

As engine speed decreases in a conventional cam driven engine the intake air velocity is reduced. The reason for this is the coherent reduction of the mean piston speed. This rate of movement of the piston is what creates the pressure difference necessary to drive the intake airflow. Therefore, when the mean piston speed decreases and less air is pulled through the area of the valve during the intake stroke, air intake velocity is reduced accordingly. However this air velocity reduction can be avoided by applying a VVA valve train. A shorter lift at lower engine speeds reduces the area through which the intake air flows, thus maintaining the desired air flow velocity. A certain velocity is desirable to maintain sufficient turbulence and mixing of the air fuel composition. In turn this affects the burn rate as mentioned above. Certain flow patterns can be achieved by giving different lift to the two inlet valves, thus creating two different streams of inlet air. Some researchers claim that this effect the charge motion in to a greater extent than the cylinder head design (2). Improving charge air motion is known to improve combustion stability at idle and emissions in general.

3.4 IMPROVED IDLE

Since close to idle running is one of the operating conditions within the scope of this thesis, I wish to make a brief note on what to expect in this particular operation. One of the most influential factors to idle instability is residual gas in the cylinders. Minimizing the amount of residual gas is imperative to ensure stabile combustion during idling. This can be done by controlling the valve overlap, timing the valves for optimal scavenging. When able to tune valve timing and valve lift, lower idle speeds are possible resulting in significant reductions in fuel consumption. This is supported by research using cam lobes designed for low speed operation (2).

3.5 VALVE VELOCITY

Controlling the velocity of valve motion provides benefits in terms of consumed energy and improved volumetric efficiency.

3.5.1 VOLUMETRIC EFFICIENCY

Engines using camshaft valve trains hold a fixed relation between engine speed and velocity of valve motion. The only way to move the valve faster is to increase engine speed. Camless engines may govern fast valve motion at low speeds, using hydraulic force which is independent on the crankshaft speed. Consequently we can get closer to the desired rectangular shape of the lift curve as the movement portions of the lift occupy a smaller area. Improving the volumetric efficiency is a contributing factor to increased engine torque. Increased torque can be achieved both at low and high speeds using variable valve control.

3.5.2 ENERGY CONSUMPTION

On the other hand low speed operation needs a lower relative valve motion velocity. This means that hydraulic pressure may be reduced to minimize the energy consumed by this actuation. Also the possible use of a pendulum spring system described in (1), will further contribute to recuperate the energy needed for valve lift. As previously mentioned the traditional cam shaft valve train is efficiently recuperating the energy spent on valve actuation. Good matching is vital for any valve control solution that aims to compete in a wide engine spectrum.

4 BERGEN K-ENGINE

The engine used to make computer models for this assignment is a Rolls Royce KRG 6 engine. This abbreviation tells us that the engine is a K-type in line generator engine with six cylinders. Before commencing the main part of this master project, a list of important engine data will be presented to give further understanding of the dimensions of this motor. Additionally some general information about the K-type engine will be provided.

Main engine data				
Number of cylinders	-	6	8	9
Cylinder Bore	mm	250	250	250
Piston Stroke	mm	300	300	300
Rated Power (MCR)	kW	1165	1555	1750
Mean Effective Pressure	bar	22,00	22,00	22,00
Rated Speed	o/min	720	720	720
Speed Ideling	o/min	450	450	450
Mean Piston Speed	m/s	7,20	7,20	7,20
Displacement	l	88	118	133

TABLE 1 - MAIN EINGINE DATA

The type K is a four stroke engine built in Vee- and in-line versions. These turbocharged engines all have 250mm bore and 300mm stroke and turbo charging is based on pulse drive. The KRG is delivered in 3,5,6,8 and 9 cylinders. Type K variants (KRM, KVM, KRG and KVG) have identical components as far as possible. For customers using K engines for generator sets as well as propulsion purposes, this means lower expenses on spare parts.

Piston cooling is provided by oil from the main lubricating oil system. Cooling oil is led through the connecting rod up to the nodular cast iron pistons. Both crank case and cylinder block is made from the same material as the pistons. Large hatches on each side of the crank case and cylinder block allow easy access for maintenance work. The figure below shows a KRM engine which is similar to the KRG.

The cylinder heads are made from a compacted graphite cast iron which has gained popularity in engine manufacturing due to its low weight and it's fatigue properties at high temperatures. Valve- seats and guides on both inlet and exhaust ducts are centrifugally cast from a special alloy cast iron. Assembly of these components is done by shrink fitting.

All valves on K-engines are equipped with a "ROTOCAP" valve rotor that turns the valves slightly with each lift. This feature ensures that deposits stuck between the seat and valve face are wiped away. Valve rocker arms are lubricated by the valve lubrication system. Due to safety concerns over fuel oil leakage, the system is separate from the main lubrication system. The oil tank and filters is engine mounted and the entire system is engine driven.

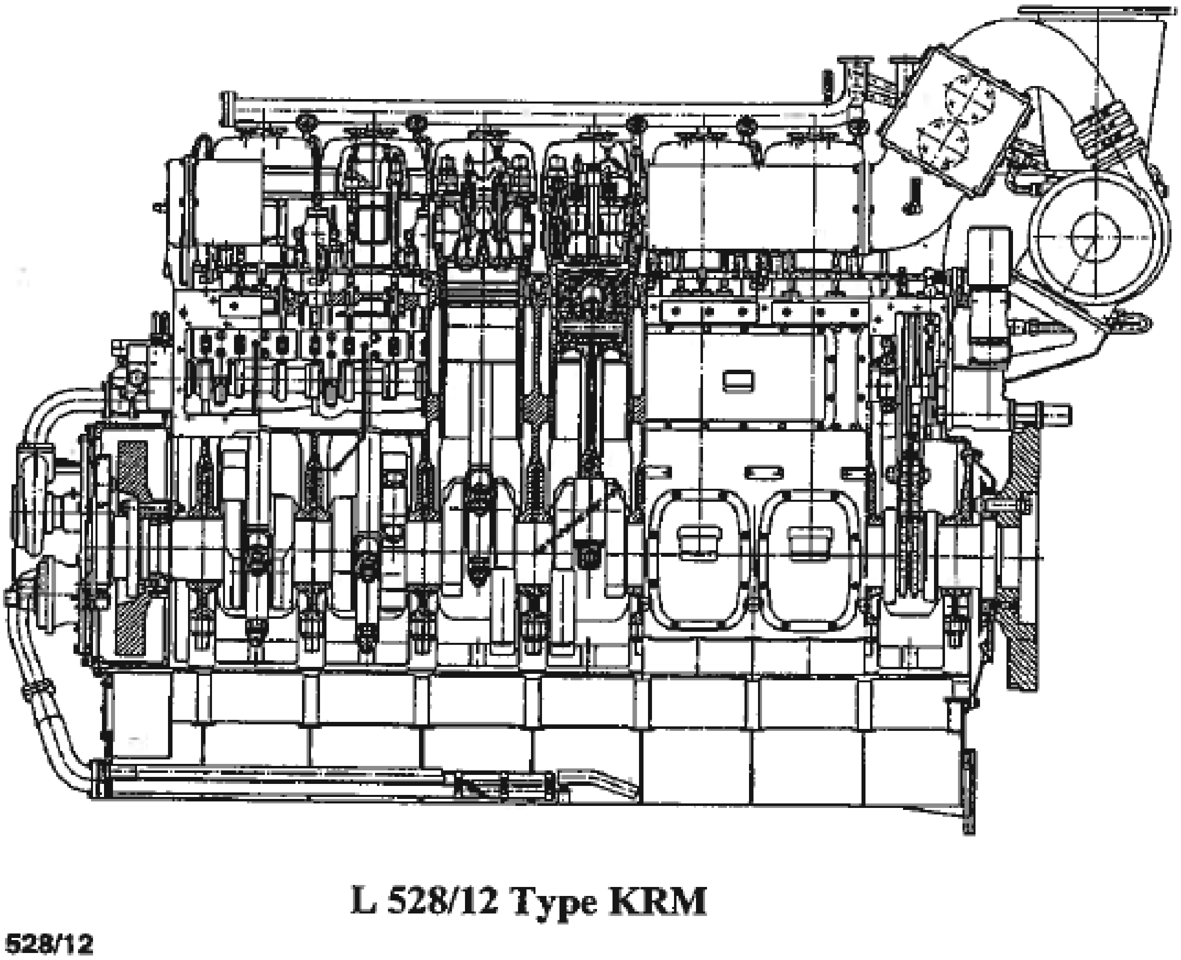

FIGURE 7 - KRM 6 ILLUSTRATION

On the top right of the figure the turbo charger, air intake receiver and exhaust is shown. The left portion of the figure is a cutaway showing the inside of the crankshaft, sleeves and cylinder heads. The valves are also visible on the figure. Some differences exist between this KRM propulsion motor and the KRG on which the GT-Power model is based. Considering the scope of this thesis, there are no crucial differences except potentially different turbochargers. This issue will be readdressed.

5 MODEL PREPARATIONS

When the one cylinder model was calibrated in (1), constant values were inserted to the templates representing the charge air cooler outlet and the turbine inlet respectively. These values will no longer be realistic if the engine speed and load of this model is reduced. Therefore we need to establish corresponding input values for these templates using the full scale model. However, as this model is representing a KRG generator motor, reducing the speed of the full scale is somewhat complicated. I first need to modify the model to represent a propulsion motor. Modifications require complete understanding of the model structure and its sub systems. I will start with the fuel system.

5.1 KRG-6 FUEL SYSTEM

The speed of this engine is intended to be constant thus the model might only be calibrated for a narrow range of speeds. To gain further understanding of the limitations of the full scale KGR model we start by investigating the fuel injection control system as speed/load dependent limitations are suspected.

5.1.1 FUEL MASS CONTROLLER

Added to the full scale model is a fuel mass control template that calculates the total fuel mass to be injected and divides this mass equally between the six cylinders. The controller targets a certain engine performance parameter at a part load condition by adjusting the quantity of fuel. Target parameters can be either of the following:

- bmep – brake mean effective pressure
- brake torque
- brake power kW/HP
- imep – indicated mean effective pressure

For this particular model brake power in kilowatts is the target quantity as the motor is serving an electrical power generation purpose. Sensors connected to the crank template pick up power and speed, which in turn are forwarded to the fuel mass controller. A similar sensor on the air intake receiver forwards the air mass flow to the controller. There are effectively three input parameters to this control template. In addition the power from the crankshaft is fed forward to a monitor that compares real time power to the target power.

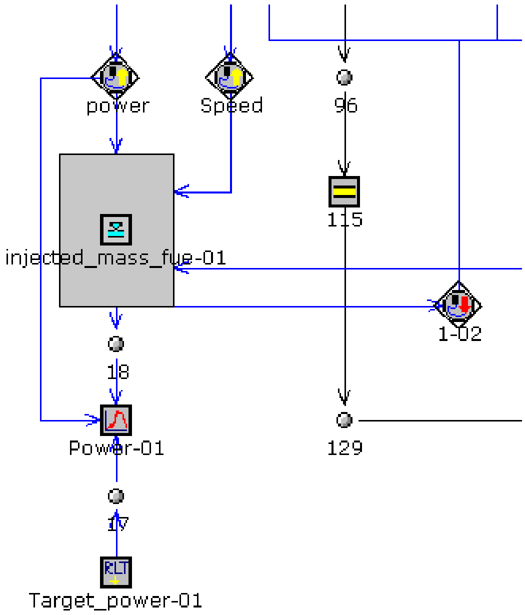

FIGURE 8 -FUEL MASS CONTROLLER

The schematic view above shows how the three input parameters are forwarded to the control template. The air mass flow sensor is outside the range of the image, only the arrow coming in from the right side is visible. We also see the power monitor and its relation to the target power template. The arrow going out from the control template represents the fuel line distributing an equal amount of fuel between the engine cylinders.

The target power of the full scale model is currently 780 kW corresponding to a total of 130 kW per cylinder. This number lies close to the obtained value from simulations using the one cylinder engine. The value that was obtained was 131.064 kW. These values are obtained running the engine at 720 rpm for both models.

5.1.2 FUEL INJECTOR

When the fuel mass for a given target power is evenly distributed among cylinders this value serves as input to the direct injection injector template. This template may be used to inject fluid into any cylinder, pipe or flow split, but primarily it is used on direct injection diesel engines. The start of injection is determined in this template, the mass of fuel is determined from the controller and the injection profile is set as function of crank angle. This template presents a challenge in terms of engine speed reduction. When speed is reduced and fuel mass flow changes correspondingly, the nozzle discharge coefficient in this template is affected. From fluid dynamics we know this coefficient as:

"…the ratio of the mass flow rate at the discharge end of the nozzle to that of an ideal nozzle which expands an identical working fluid from the same initial conditions to the same exit pressure." (3) .

From the help navigator in GT-Power this statement regarding the nozzle coefficient is found. It explains that the realistic range of "cnozz" is dependent on the type of profile provided to the fuel injector template. In our models the injector relies on a pressure profile which determines the injection pressure at certain crank angles. When given a pressure profile, provided by Rolls Royce Marine, the coefficient represents a realistic value when within the range 0.60 – 0.75. Correspondingly the mass flow rate needs to lie within the range of 60 – 75% of its theoretical maximum. We start by investigating this parameter as it is suspected that the injection pressure profile needs extension.

5.2 LOAD- AND SPEED RANGE OF KRG-6

Mapping the range of the current model is important as “cnozz” might shift out of bounds when simultaneously running on lower speeds and loads. The experiment concerning load- and speed range will therefore be conducted by creating a series of cases for each simulation, reducing the speed for each of the load settings; 25, 50, 75, and 100% MCR. This means that the results from each simulation will provide us data for these loads and speeds in the range 450 - 720rpm. 450 rpm is assumed to be close to idle based on available engine data. After assessing the simulations and confirming that correct target power is reached for each case, a table can be presented showing the effect on “cnozz”.

Speed [rpm]/Load	**100 % MCR**	**75 % MCR**	**50 % MCR**	**25 % MCR**
720	0.744	0.740	0.679	0.382
650	0.742	0.667	0.627	0.374
600	0.743	0.618	0.593	0.371
550	0.745	0.571	0.559	0.368
500	0.751	0.560	0.524	0.367
450	0.761	0.568	0.482	0.367

From the table we observe that the KRG model fails at lower loads and speeds. This is due to the calibration work previously done to the model. (4) used this model and calibrated it for his PhD thesis, and for the purpose of his study the engine was set to run under constant speed and load conditions. There was no need for the model to function outside the scope his thesis. Using the KRG-6 model in this study on variable valve control will require the model to represent a propulsion engine. At this time it does not and recalibration is required.

5.3 CALIBRATION METHOD

Calibration is done in a particular manner described by the GT-Power manual (5). This method requires that certain steps are followed precisely. As the full description is quite comprehensive I will provide a brief summary of the procedure in this report. The steps described below represent a routine to be repeated for all the existing test bed cases. There are ten cases of measurement data for the KRM engine, see appendix W.

5.3.1 REMOVING THE TURBOCHARGER

In the first step, measured turbocharger performance data is imposed on the model by removing the TC templates and replacing them with templates for predefined environment conditions. These templates now represent charge air cooler outlet downstream of the cylinder and the turbine inlet at the end of exhaust receiver. Measured boost pressure and temperature is imposed to the charge air cooler substitute and the back pressure is defined in the turbine replacement template. For this step the air flow rate is checked to be within limits after simulation. If there are deviations of more than 3% here, retuning is required. Likely causes of discrepancies are listed in (5).

5.3.2 MODEL WITH NO TURBINE

In the second step the compressor is connected to the upstream intake system, and an environment with a proper back pressure is left where the turbine used to be. The compressor is then manually set to turn at a measured speed and the mass flow is corrected by using a multiplier to match the measured data. This mass flow should be the same as the mass flow of the previous step.

5.3.3 MODEL WITH NO COMPRESSOR

Turbine and exhaust is added to the model from the first step. An environment template is now replacing the compressor and intercooler. In this step the turbine is forced to rotate at measured rotational speed. At this configuration mass flow rate is again checked. If needed the turbine's mass flow multiplier may be adjusted within a defined range to correct air flow rate. Calibration in this step is more complicated for waste gate- and variable geometry turbines. However, this is not the case in my study.

5.3.4 CALIBRATE THE POWER

In this step, the steady state power is found for the compressor and turbine respectively from step 2 and 3. If the numbers are equal then all is well. Adjustment of either turbine- or compressor efficiency multiplier is allowed within a range of 0.95 – 1.05. In this case the compressor efficiency should be adjusted first to calibrate the compressor outlet temperature. Second turbine efficiency can be adjusted to match turbine- and compressor power.

5.4 TOOLS FOR CALIBRATION

Certain tools exist in GT-Power to help simplify the process of calibration. This is an iterative process and great time benefit can come from using these tools.

5.4.1 DIRECT OPTIMIZER

The "Direct Optimizer" allows for definition of one or more independent variables. These variables will be adjusted automatically within a given range to match a predefined operating point. This is done by targeting a known value for this point. Other values might be used as goal for optimization as well. This tool is also able to find an optimal point; either a maximum or minimum value. Definition of a certain design limit may also be a desirable approach.

The "Direct Optimizer" works by requesting a range of the independent variable as well as the resolution of this range. If the initial value is 1 and the parameter range is 1 as well we have the case shown below.

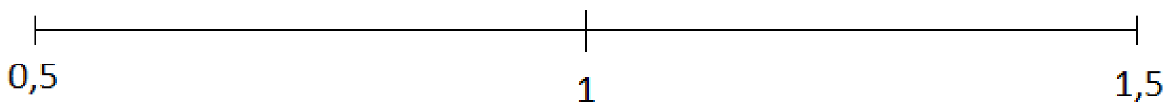

FIGURE 9 - DIRECT OPTIMIZER ALGORITHM ILLUSTRATION

The resolution determines the division of this range. Lower percentage corresponds to more divisions within the range. The optimizer algorithm works by checking the extreme values. If the higher extreme value results in a value closer to the target reference than the median, only the top half of the range is subject for further investigation. The new median (1.25) of the top half is then checked. The process is repeated for the halved range and the algorithm continues to cut each range in half by checking up and down from the updated median.

5.4.1.1 INDEPENDENT VARIABLES

In order to recalibrate the model to perform equal to KRM test bed data, we must find the parameters most influential to combustion. Such parameters can be utilized to obtain performance close to a predetermined reference (here measured performance data). The value of these parameters must be adjusted seperately for several performance cases in order to maintain realistic combustion for each case as well as matching the reference data of KRM within reasonable limits. Adjustment will be done automatically by the software through tools such as the Direct Optimizer.

5.4.2 DESIGN OF EXPERIMENTS

When interested in the effect of a change to one or more variables, GT-Power allows setting up a DOE that may provide valuable information. Based on given changes made to several parameters, DOE results will provide a clear indication of which parameters produce a given variable change. Results are presented in an interactive menu where the user is allowed to continuously change the parameter in question and see the direct consequences in a graphical representation. Such a tool is extremely useful when investigating what changes might follow from adjusting certain parameters. The DOE results are found in GT-Post which means that a full simulation is needed. However several following test simulations might not be required as DOE results show the user what is needed to obtain a certain effect.

5.5 RECALIBRATION OF KRG-6

As the KRG model currently is the only model available to me, I need to make alterations to it in order to study valve control at low speed/load conditions. Similar to the KRG-6 engine we know there exists a KRM-6 that basically has the same physical dimensions, and this engine is applied to propulsion purposes similar to what is needed for this study. Even though I have no access to such a model, I should be able to recalibrate the KRG model against KRM reference data. In this way I should be able to obtain results representing a KRM-6 engine by modifying the model of the KRG-6 engine.

A complete set of test bed data for the KRM-6 is found in appendix V. These show performance parameters at 10 different operating conditions. Speed and load is varying from idling speed of 450 rpm (221kW) to speeds of over 850 rpm (1470 kW). Each case represents a reference for calibration. To get a complete range of operating conditions we must calibrate the KRG model against each of these ten cases separately.

5.5.1 INITIAL CONCERNS

Starting the calibration process I identify certain elements of the model that is suspected to need some alterations.

5.5.1.1 TURBOCHARGER MATCHING

One vital concern when attempting to recalibrate the KRG model against KRM test bed data is to see wether turbocharger maps are matching. This means if the types of turbocharger on the two engines are different, there might occur problems when moving out of the optimal working area of the KRG. From (6) I compare the technical data and find indications that the turbocharger types match up. This means the calibration work can commence. If, at completion of calibration, the turbocharger still shows signs of mismatching, the issue will be readdressed.

5.5.1.2 COMBUSTION MODEL SIMPLIFICATION

Due to the scope of this thesis I wish to simplify the combustion model in order to lower its sensitivity in terms of speed/load dependency. The current combustion model is a semi-predictive model dependent on three Wiebe-functions that determine the rate of heat release. Given that this thesis seeks to investigate the effect of valve control, we might obtain sufficient accuracy using a ROHR model dependent on only one Wiebe function. However investigation shows that this option is no longer available in the new version of GT-Power (v7.0.0). This means that the three-Wiebe model that we are currently using is in fact the most simple one. I will therefore continue using this model throughout the recalibration of the KRG model. In GT-Power, the combustion model is title? "EngCylCombDIWiebe" and is described in the GT-Power Help Navigator. An excel sheet acts as support to this model in order to determine the Wiebe constants (Appendix X).

5.5.2 INJECTION PRESSURE CALIBRATION

In the KRG-model there exists an array of injection pressures for certain crank angles. This is a predetermined array of injection pressures corresponding to the operating point of the KRG model. In the case of my thesis I need to manipulate this injection curve to allow change according to speed and load. Considering the physical properties of the injection system on this engine, the pressure profile will mainly be dependent on the engine speed. As speed decreases the injection pressure will decrease. GT-Power provides the possibility of scaling curves like the injection pressure profile through a multiplier. This multiplier may be parameterized and made dependent on other reference objects such as speed or load. This parameter will be one of our independent variables used to recalibrate the KRG model.

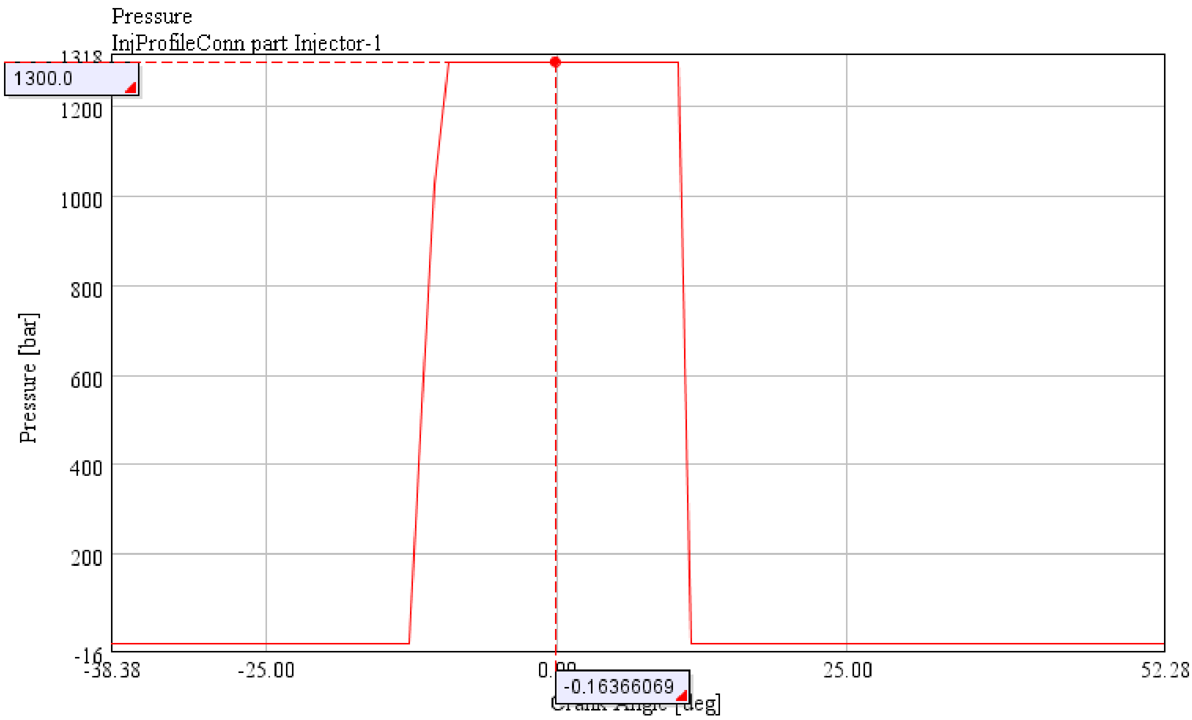

FIGUR 1 - INJECTION PRESSURE PROFILE

The figure above shows an example in which the injection pressure profile has been scaled to 100% of its original magnitude (pressure profile multiplier equal to 1.0). Multiplier values through the range of reference cases are obtained using GT-Power's "Direct Optimizer". Brake power was defined as a target reference and by automatically adjusting the pressure multiplier, the optimizer attempted to match the performance parameters of the given operating point. A dependency was found in order to improve the nozzle discharge coefficient within the range of operating conditions. The pressure profile multiplier ranges from 0.4-1.3 throughout cases 1-10 with increments of 0.1 between cases.

However, the pressure profile multiplier alone was not able to solve the calibration issue for the injector completely. The problem was finally solved by extending the range of dependence between the crank-angle and bmep such that injection duration is load dependent over the whole operating range as well.

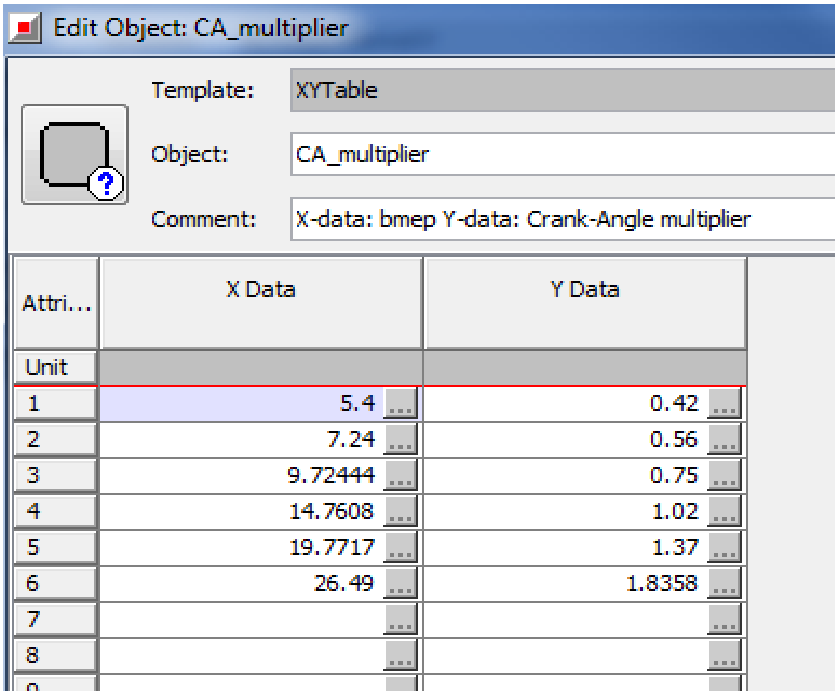

FIGURE 10 - SCALING OF INJECTION DURATION IS DEPENDENT ON LOAD

The figure above shows how the duration determinant (here Crank-Angle multiplier) changes with respect to mean effective pressure. In the initial KRG-6 model this array was narrower. This had to be extended to fit KRM-6, which was done such by creating a linear dependency between load and injection duration across the operating range. Tuning the injection pressure and duration solved the issue of the nozzle discharge coefficient. I now have an injection model that adapts to both speed and load.

5.5.3 CALIBRATING FOR RATE OF HEAT RELEASE (ROHR)

The combustion model may also require alterations as speed and load is variable. Similar to the injection pressure curve, there are multipliers for each of the three RHOR curve exponents determined by “EngCylCombDIWiebe”. The multipliers determine the magnitude of the premixed-, main and tail exponent of the ROHR-curve. The main exponent is parameterized and now represents an independent variable. I now have to find values for this parameter which yields realistic performance data compared to the KRM reference.

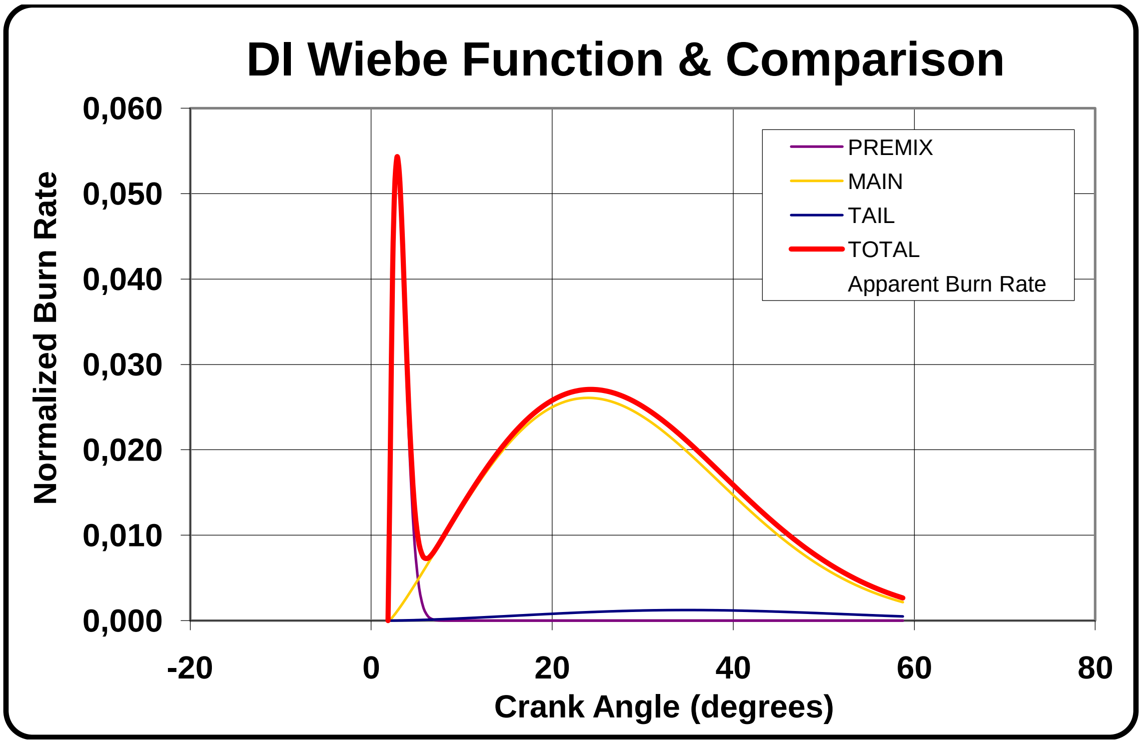

FIGURE 11 - ROHR FROM DI WIEBE COMBUSTION FROM GTI EXCEL SHEET

The figure above shows a general example of a ROHR curve. We can clearly see how the three exponents give different contributions to the total rate of heat release. In this thesis it was found sufficient to parameterize the main exponent in order to calibrate for maximum cylinder pressure. The actual dependency of this parameter on speed and load will be presented in the figure below. Similar to the injection duration, the dependency range of this parameter had to be extended to reach all KRM-6 operating points. The resulting array of mean effective pressures and multiplier values is shown below.

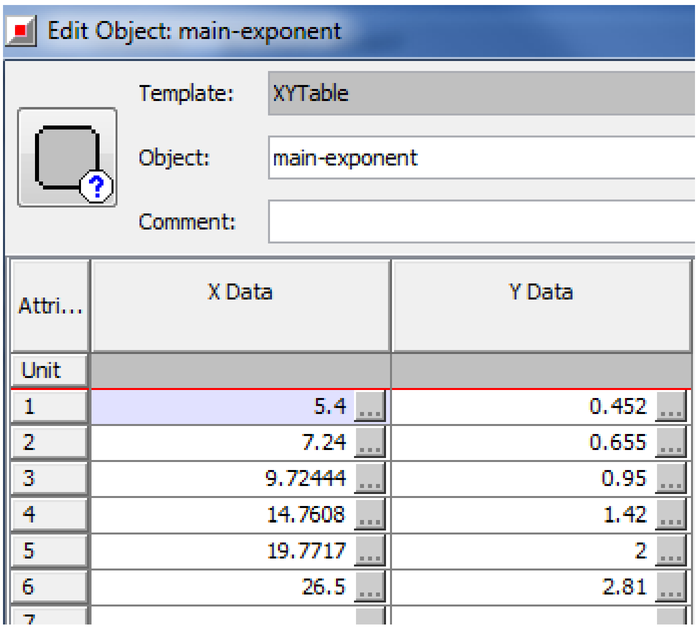
Edit Object: main-exponent

Template: XYTable

Object: main-exponent

Comment:

Attri...	X Data	Y Data
Unit		
1	5.4	0.452
2	7.24	0.655
3	9.72444	0.95
4	14.7608	1.42
5	19.7717	2
6	26.5	2.81
7		

FIGURE 12 - ROHR MAIN EXPONENT MULTIPLIER FOR 3 WIEBE-FUNCTION

This array ensures that a ROHR dependency exists for the complete load range. Without this extension, ROHR would become too high at low loads as the program always uses the nearest multiplier when out of bounds. Theoretically a bmep lower than 7.24 Bar, would correspond to a 0.655 multiplication if the range was not extended. A bmep of 5.4 Bar is considered sufficiently low for the KRM-6 model.

5.5.4 FRICTION MEAN EFFECTIVE PRESSURE

A parameter is established in order to define engine friction as a function of the speed and load. The value of this parameter is mainly used to calibrate for brake mean effective pressure. Fmep is tuned in order to meet the reference values for bmep. Results are presented in the calibration results summary.

5.5.5 BACK PRESSURE

In order to obtain a correct mass flow through the engine compared to the reference data sheet, back pressure was estimated for each of the ten cases. A range of 1.0-3.0 Bar was found. This might not be the best way to go about this issue, but at the moment it serves as my only option. By iteration a value for back pressure was set to give a correct charge air mass flow through the inlet manifold.

5.5.6 INITIAL RESULTS OF CALIBRATION

I went about the calibration process by obtaining a set of input parameters from the reference data sheet in appendix V. There were four known parameters concerning the state of operation suitable for this purpose:

- Engine Speed
- Mass of injected fuel
- Inlet Receiver Temperature
- Inlet Receiver Pressure

For each measured case of the data sheet I mainly used the three independent parameters described earlier to obtain simulation data matching the measured data. Back pressure was used to calibrate for mass flow, main ROHR exponent multiplier was used to calibrate for maximum cylinder pressure and finally friction mean effective pressure was independently varied through iteration to obtain the correct mean effective pressure. To match simulation results to the measured cases the following list of parameters had to be checked for severe deviations:

Performance Checkpoints:

- Air Mass Flow
- Maximum Cylinder Pressure
- Brake mean Effective Pressure
- Brake Specific Fuel Consumption

Downstream Checkpoints:

- Exhaust Temperature
- Turbine Inlet Temperature
- Exhaust Mass Flow

5.5.6.1 PERFORMANCE RESULTS

All results for this initial calibration round was transferred to an excel work book so deviations could be represented in graphs. Below these graphs are presented in order to investigate the results:

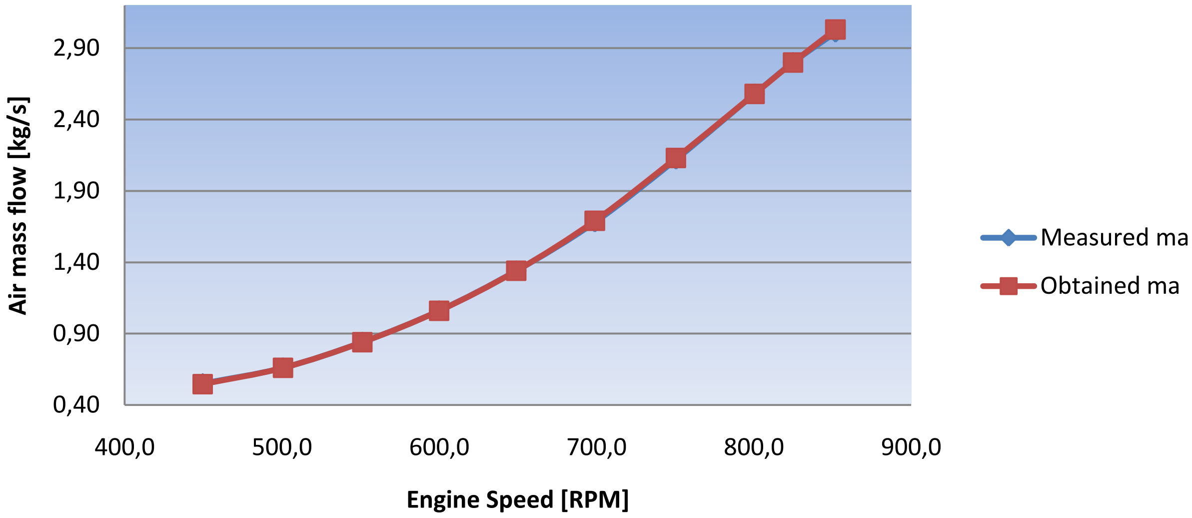

FIGURE 13 - MASS FLOW OF AIR IN THE INLET RECEIVER

The flow of air into the system was easily matched to the measured data. We see no real deviations from the measured data curve. This parameter is left free of further investigations.

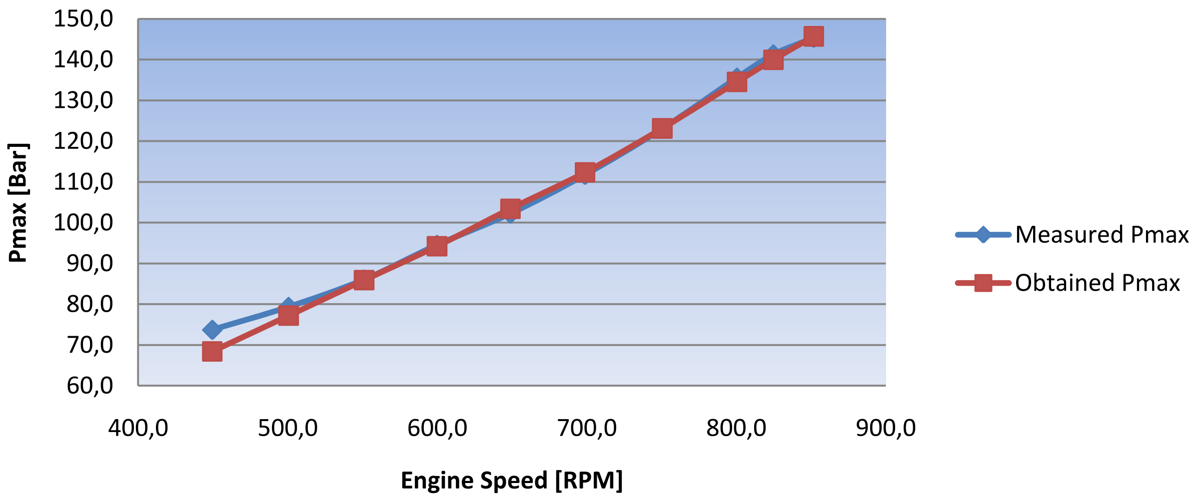

FIGURE 14 - MEAN VALUE OF MAXIMUM CYLINDER PRESSURE

For the maximum cylinder pressure we see deviations in the first two cases of -7.2 % and -2.7 % respectively. The deviations are severe, especially for case one. We will need to find alternative means to calibrate for this parameter.

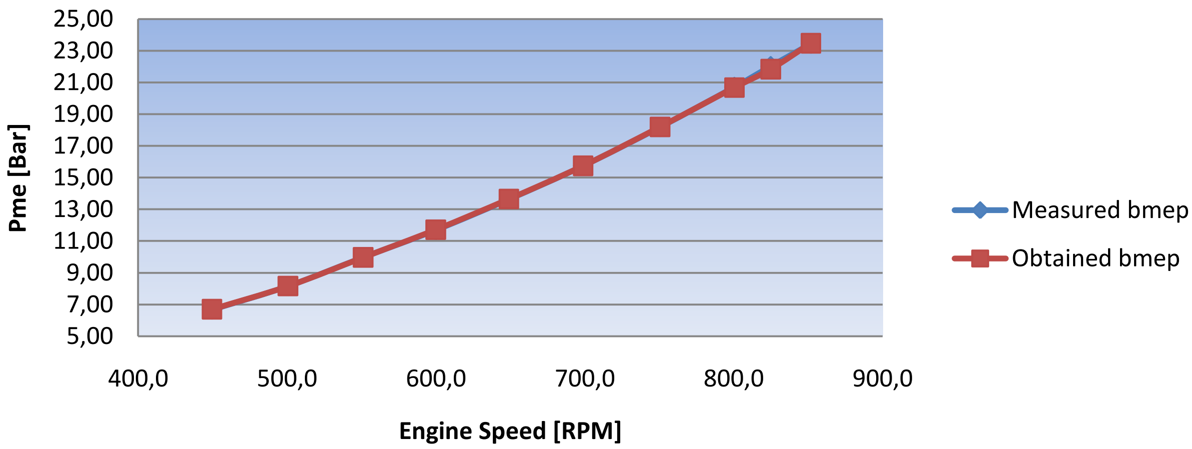

FIGURE 15 – BMEP

Friction mean effective pressure provides good matching concerning brake mean effective pressure. No need for further investigation at this point.

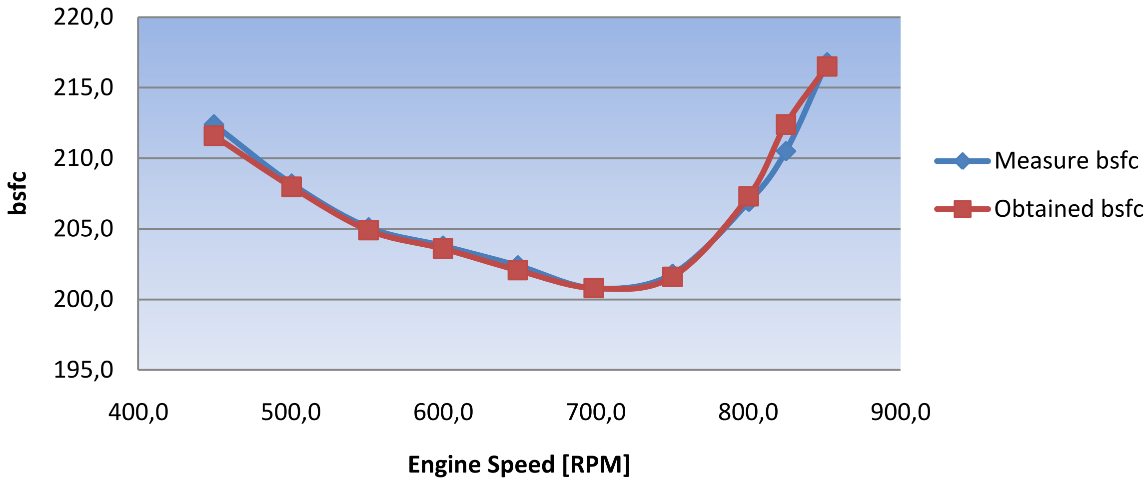

FIGURE 16 - BRAKE SPECIFIC FUEL CONSUMPTION

Deviations showing on the graph above concerns case nine. The value obtained by simulations is in this case 0.9% higher than the measured value. Such a deviation is within acceptable limits. However the issue will be readdressed as soon as a second calibration round is completed.

5.5.6.2 DOWNSTREAM RESULTS

I looked for matching of the downstream conditions of the engine to see if the current in-cylinder process is serving as a good representation of the KRM 6 engine.

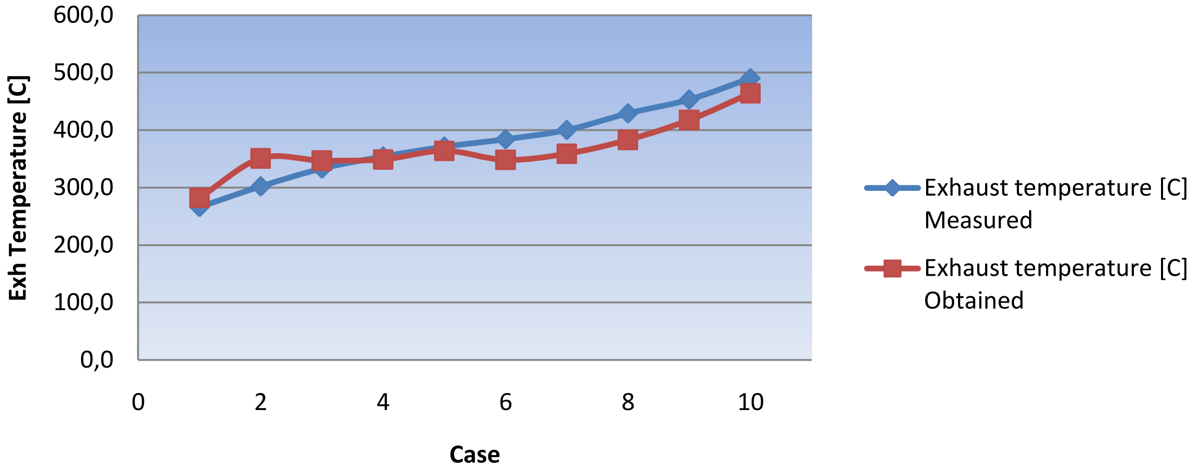

FIGURE 17 - MEAN OF TEMPERATURES RECORDED AFTER THE EXHAUST PORTS

Although most of the previous parameters have shown good matching to the measurements the exhaust temperatures are not matching well. This might indicate that some measures of cooling in the exhaust system are different between KRG and KRM engines. Also there might be an issue to consider regarding the cylinder heat transfer functions.

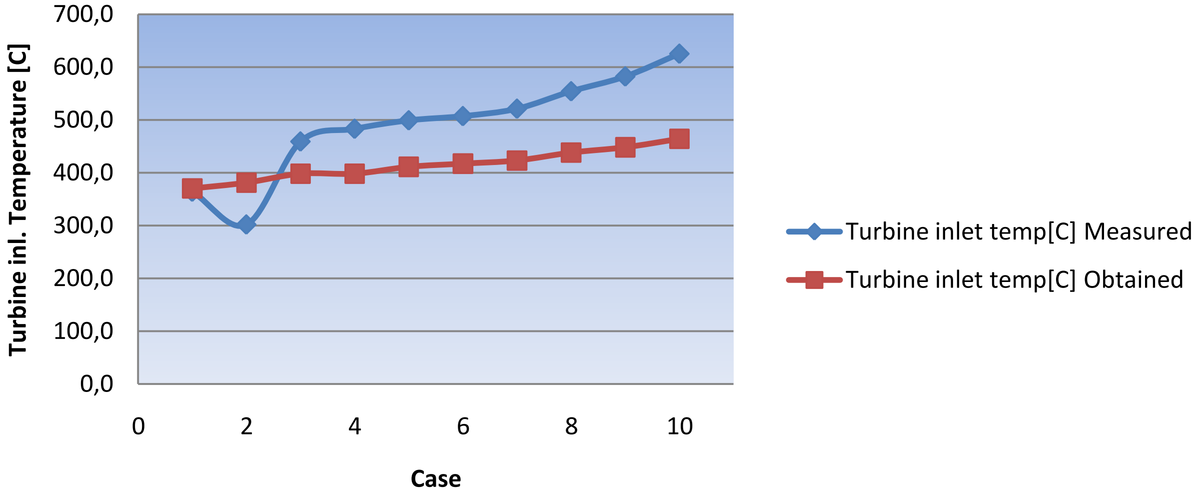

FIGURE 18 - MEAN OF TEMPERATURES RECORDED AT THE TWO TURBINE INLETS

Inlet temperature at the turbine is determined by the wall temperatures downstream as well as the initial exhaust temperatures. Using the solver for wall temperatures we obtain values shown above. Solving this problem will be dealt with by removing the solver and imposing a range of assumed temperatures that produce more reasonable results. Such assumptions must be reevaluated at a later stage.

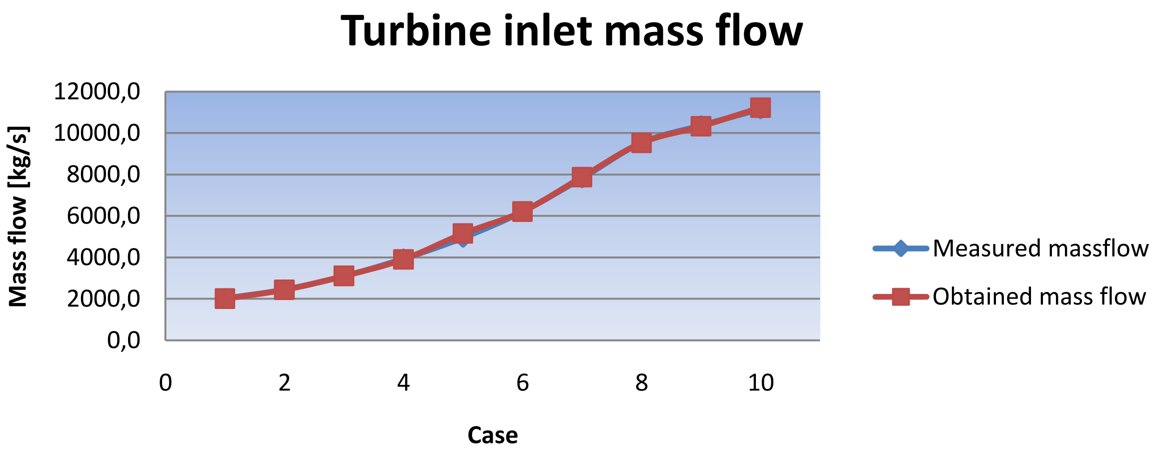

FIGURE 19 - SUM OF MASS FLOWS INTO THE TWO TURBINE DUCTS

The turbine inlet mass flow seems to be within acceptable limits.

5.5.7 NEW CONCERNS

In light of the calibration results obtained at this point some changes have to be made in order to make the KRM model function properly. First of all reconsiderations to the combustion model are made. All the changes below are results of an iterative search for errors and improvements made in cooperation with (4).

5.5.7.1 NEW COMBUSTION MODEL

In the current combustion model we use the possibility for scaling the magnitude of ROHR's main exponent. Although this provides matching for most cases we are not able to make it fit perfectly. A new Wiebe function is therefore imposed on the model called Wiebe6. Through this model the shape of the ROHR curve is kept equal to default values and burning duration is made load and speed dependent. This is a more logical approach considering how diesel engines work in principle. Increased load should require a longer burning period.

5.5.7.2 PREDICTION OF ENGINE FRICTION

Imposing an assumed engine friction to obtain a certain mean effective pressure cannot be considered good practice as no values are known for this parameter. Such an approach can only be defended in search of other problems in areas like the exhaust. The general idea is for this approach to help locate sources of error by overruling certain elements manually. We therefore continue the use of GT-Powers ability to predict friction now that a solution is provided for the cylinder heat transfer issues. This solver relies on factors related to mean piston speed, peak cylinder pressure in addition to a constant. For each load case a certain friction mean effective pressure is calculated and automatically included into the process.

5.5.7.3 NEW CYLINDER HEAT TRANSFER

As the exhaust receiver temperatures show large deviations from measurement data, suspicions arise to whether the cylinder heat transfer between the two models should remain unchanged. As the KRG model is calibrated for a certain speed and limited load variations this is not likely the case. When solving this issue, I will attempt to make the heat convection multiplier load dependent. A solution was found where this multiplier has the initial value 1 for large cycle periods, but for an interval of crank degrees -128 to 130 the convection is parameterized and made load dependent to simulate an increased convection event during this particular period (combustion).

In addition to the alterations regarding transport of heat from the combustion chamber, changes were also made to the wall temperatures. The previous KRG model used a wall temperature solver that automatically defined temperatures on the cylinder wall surface. Recalibration of this solver requires data that cannot be obtained at the time. The engine manufacturer was asked to find some additional engine data, but replied that K-engines are somewhat outdated making such data unobtainable. To solve this issue a simplified wall temperature reference object was created called “simple-Twall-model”. This model defines temperatures at the piston crown, cylinder head and at the cylinder wall. With reference to the help navigator a dependency was created between load and temperatures at the cylinder head and piston. Arrays were made for these two, defining temperatures at the surface. Temperature at cylinder walls is a more complicated issue and was set to a constant value of 400K, as recommended by the help navigator.

5.5.8 NEW RESULTS

As previously stated, the new model changes were made through an iterative process. I will now present the ultimate result of this process, reevaluating the calibration data regarding performance and downstream temperatures.

5.5.8.1 NEW PERFORMANCE RESULTS

New excel sheets were added to the calibration workbook. The following graphs represent the matching of the final calibration and initial measurements.

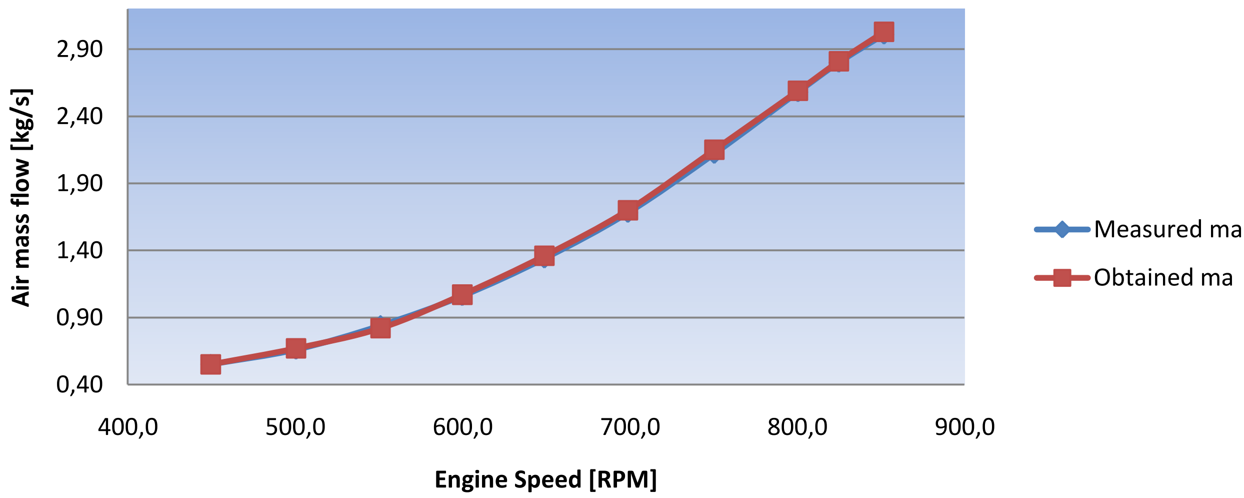

FIGURE 20 - RECALIBRATED AIR MASS FLOW

As seen from the diagram no real changes were needed in order to keep sufficient matching between air mass flows. This parameter is still calibrated using assumed values for back pressure. This approach is considered sufficient for the model use at this point.

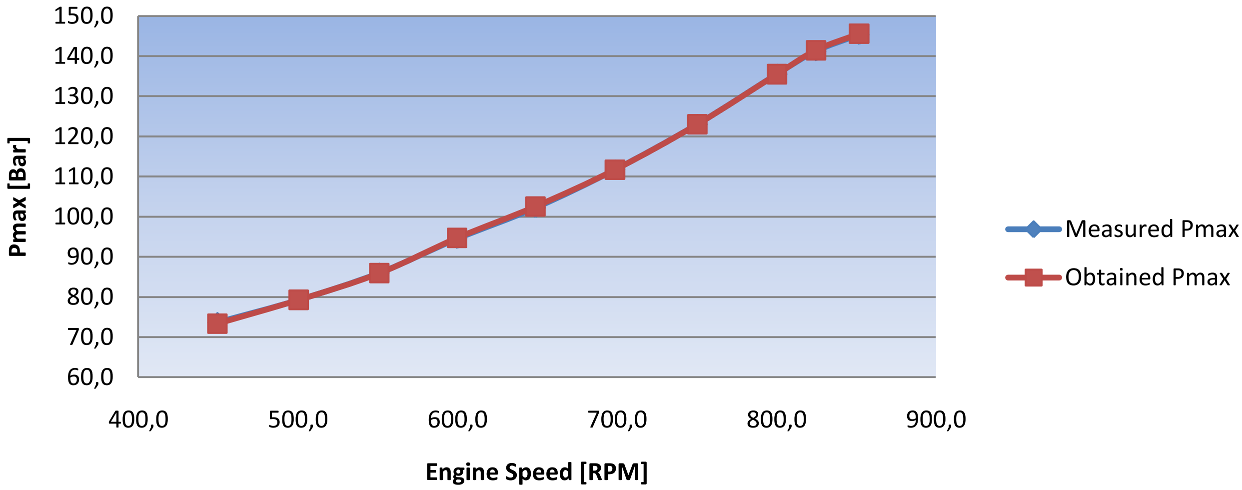

FIGURE 21 - RECALIBRATED MAXIMUM CYLINDER PRESSURE

Comparing this graph to the initial calibration results we see an improvement in the low- and high speed regions. The simulation data are now matching well within the measurement reference. The new changes to the model made the second calibration process faster than the first. The conclusion is that adjusting the burning period is a far better approach than scaling the magnitude of the main heat release exponent.

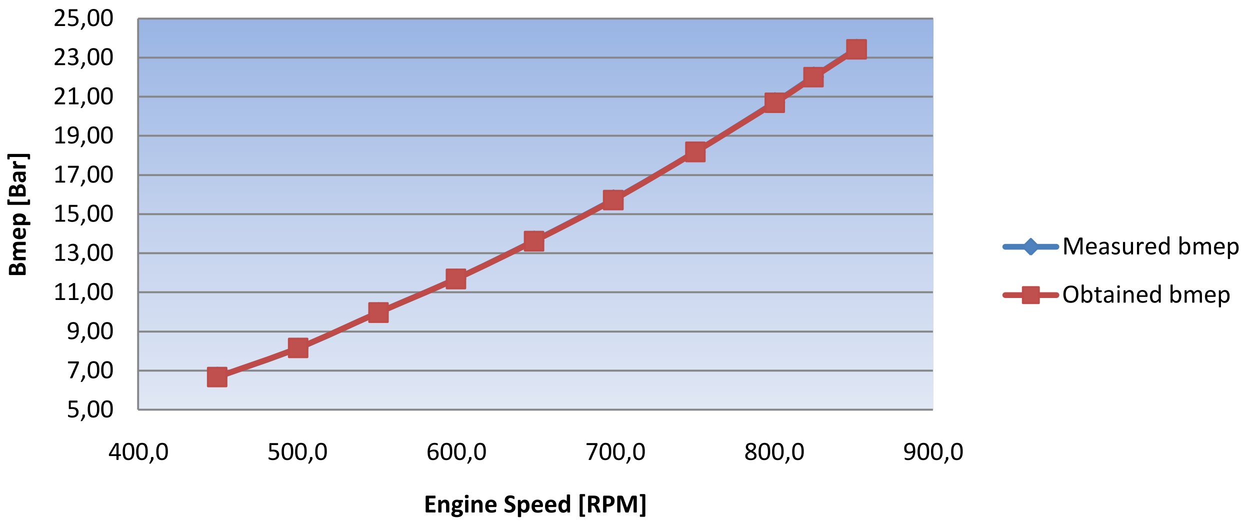

FIGURE 22 - RECALIBRATED BMEP

Considering that bmep already was sufficiently calibrated for in the first attempt, we only verify that the newly obtained values still represents a good match.

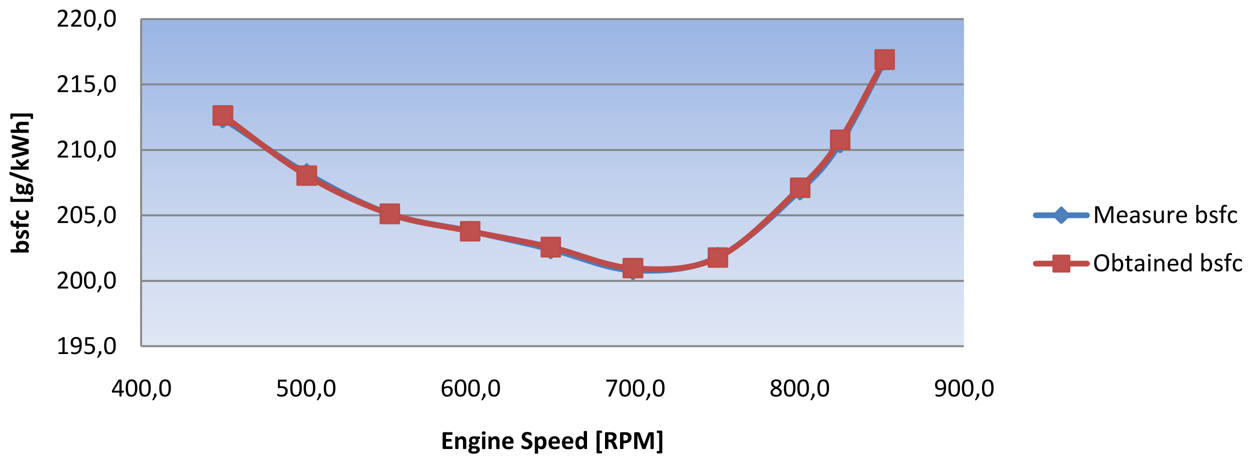

FIGURE 23 - RACALIBRATED BREAK SPECIFIC FUEL CONSUMPTION

Only two of the cases from the previous calibration showed inconsistency. Now we see that these problem areas have been provided with a solution. An overall solution to the previously mentioned issues has proved to be beneficial for this performance parameter as well.

The presented data now show that recalibrated KRG model successfully puts out performance data that are consistent with the KRM reference. However the real issue was the temperatures in the exhaust receiver thus we still have to investigate the effects of the new changes downstream.

5.5.8.2 NEW DOWNSTREAM RESULTS

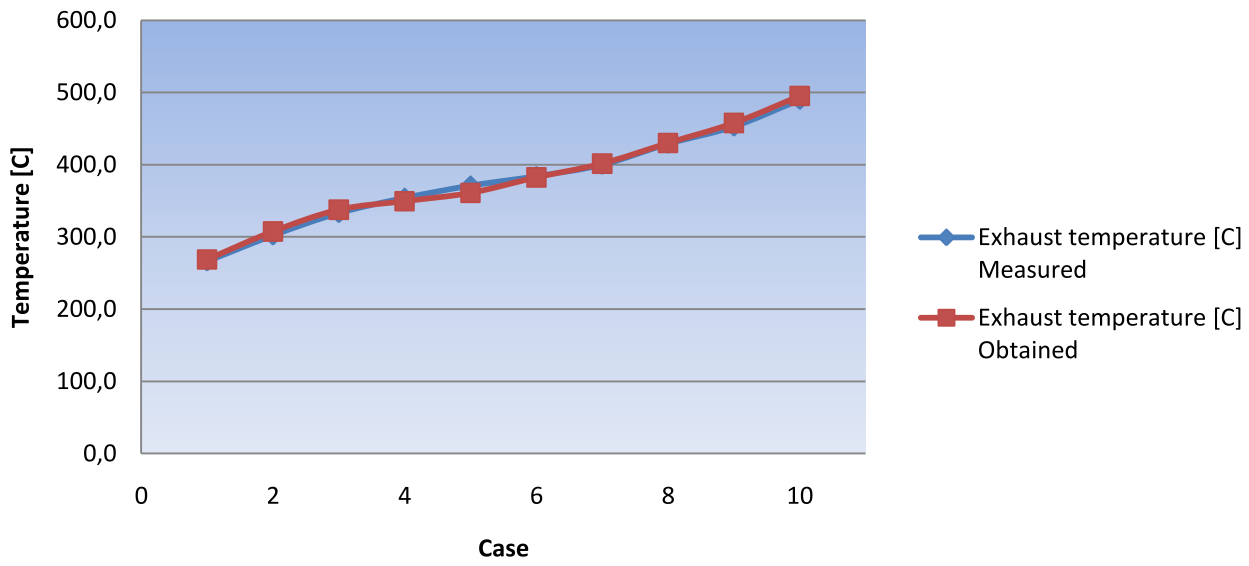

FIGURE 24 - RECALIBRATED EXHAUST RECEIVER TEMPERATURES

The newly obtained exhaust receiver temperatures (average) show much closer correspondence to the measurements from the reference data sheet. This is a result of the changes made to the cylinder heat transport model as well as removal of the wall temperature solver downstream. These results are sufficiently close to the measurement data, allowing me to continue evaluation of downstream conditions.

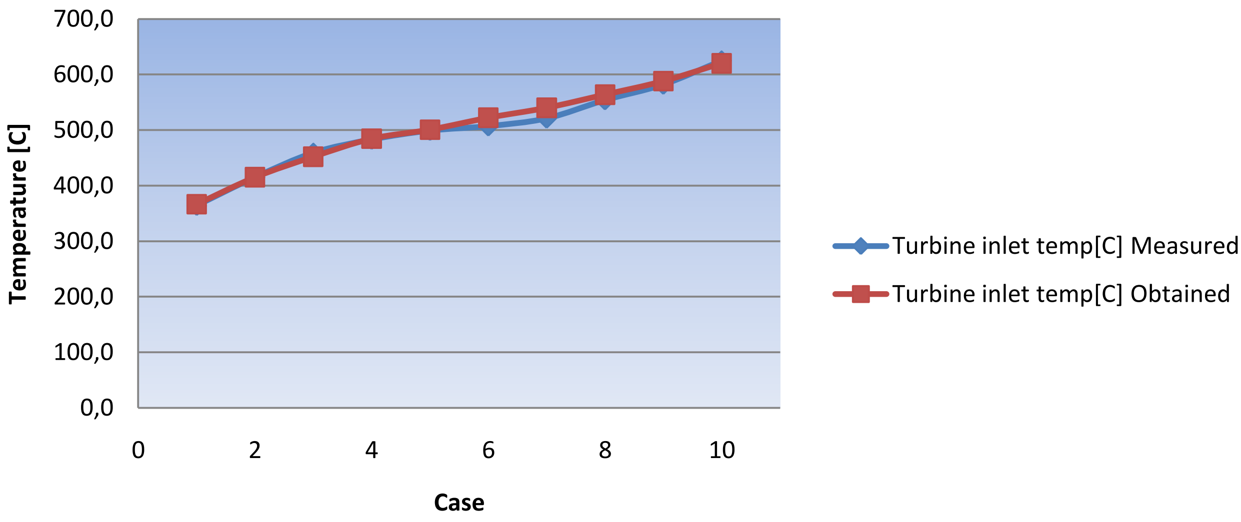

FIGURE 25 - RECALIBRATED TURBINE IINLET TEMPERATURES

Previous data for turbine inlet temperatures might have been the least consistent of all previous results. Serving as the final boundary condition it is crucial for these data to match well. As can be seen from the graph above this is now the case. Results of recalibration show almost identical mass flow registered at the inlet of the KRM-6 turbine. It was however verified by Rolls Royce that turbines are different on KRG and KRM engines. Maps for KRM are no longer obtainable, but considering the scope of this assignment it is sufficient to obtain correct boundary conditions.

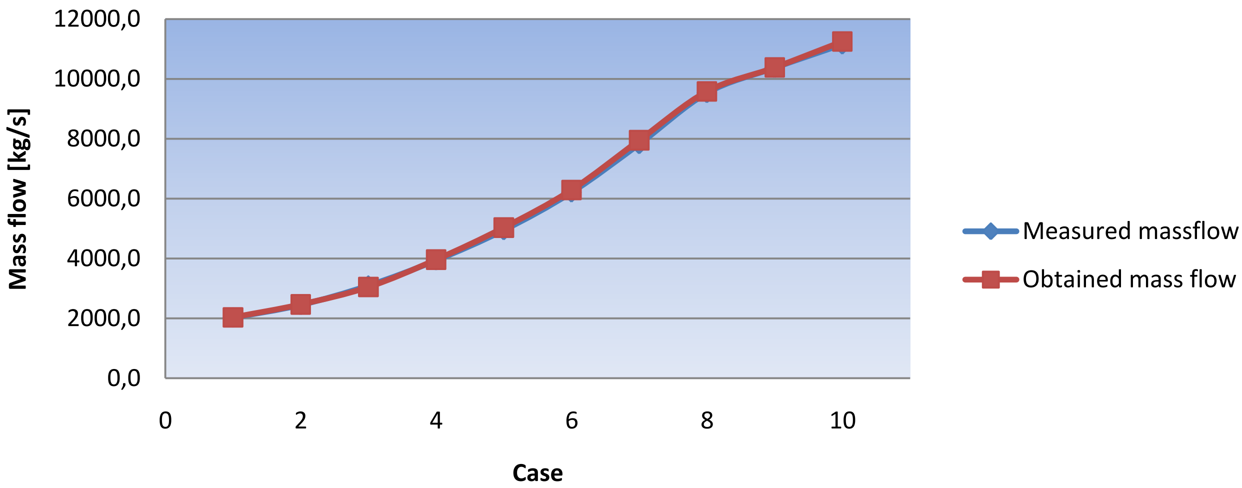

FIGURE 26 - RECALIBRATED TURBINE INLET MASS FLOW

Turbine mass flow results still show consistency compared to the measured values. No changes were expected to these values.

5.6 MODEL PREPARATIONS COMPLETED

I now consider the KRG-6 model to perform identically to what can be expected from a KRM-6 engine model. I now have a model able to serve propulsive purposes as initially desired. Therefore I consider the recalibration process finalized and successful. All calibration parameters are now hidden from the user interface in order to present a tidy simulation model for further use. This is done by inserting the load dependent parameters as objects in arrays that show the necessary dependency to mean effective pressure. The electronic appendix "Arrays Load Dependency" show a complete list of these hidden parameters.

As operating six cylinders seems to yield sufficiently short simulation time for valve control experiments no time will be spent on reducing the model to one cylinder as planned. Six cylinders are used with a predetermined fuel flow for ten operating points along a propeller curve. This means that running of the model is bound to these ten points as no new fuel flow will be calculated automatically for transients. Given the time and the scope of this thesis, a discrete set of operating points along the propeller load curve is considered sufficient. The aim is to show the principle of how beneficial engine operation is obtainable through continuous valve operation. I believe this model to be suitable for such a purpose.

6 VALVE TRAIN MODIFICATIONS

Now that calibration of the model makes it able to perform equal to the Rolls Royce KRM-6 propulsion engine there remains only the need for a valve train able to control all valve events independently. Lift, timing and duration must be individually determinable in order to do this. Chapter 6 will identify the possibilities provided by GT-Power for this kind of manipulation. GT-Power is originally not set up for variable valve control. This might cause for unwanted consequences, but this chapter aims to produce a valve control system in the best possible manner.

6.1 VALVE LIFT HEIGHT REGULATION

One of the main concerns regarding variable valve control is managing to continuously adjust the height the valve is lifted. In GT-Power this can be done by scaling the lift curve that is preset by the manufacturer and directly implemented into GT-Power using a multiplier. An example illustrated in figure 27 show how the inlet lift multiplier is able to decrease lift height. The parameter is reduced in steps from the original value of 1.2 down to 0.3 of its original height. 1.2 is a value obtained by calibration of the model and serves as the 100% lift with valve lash and push rod compressibility factors included.

Somehow adjusting the lift multiplier in GT Power is not enough. The properties of the curve are not preserved properly as this software originally has no intention of simulating total valve control. This manipulation of cam shaft actuation must be extended.

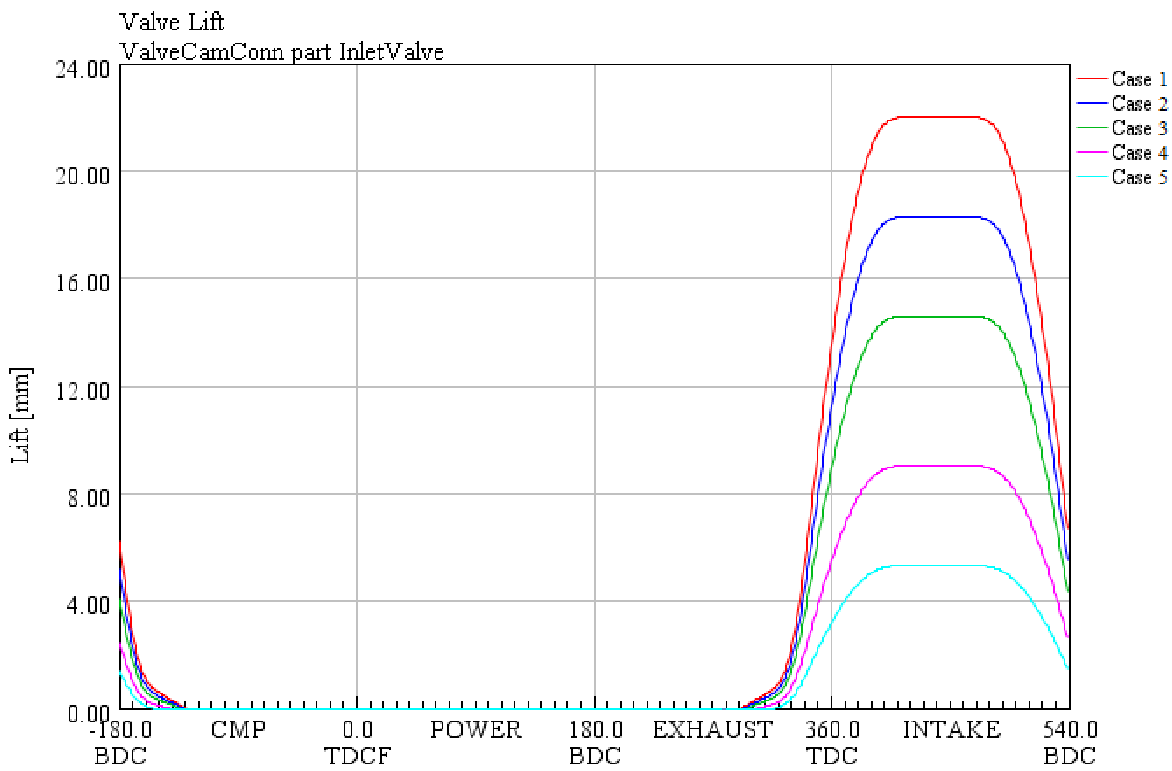

FIGURE 27 - INLET VALVE LIFT WITHOUT ADJUSTMENTS

As can be seen from the figure above there are issues regarding the opening and closing event of this curve. As the height is scaled down below 50% there is a tendency of late opening and early closing. Wanting to open and close at the same time in all cases there is a need to adjust time of opening and the duration of the lift itself. Below is a new figure showing the lift curves after making the necessary adjustments. A parameter named “cam timing angle” is determining when opening occurs and hence I advanced this slightly so that IVO occurs at the correct cam angle in all cases.

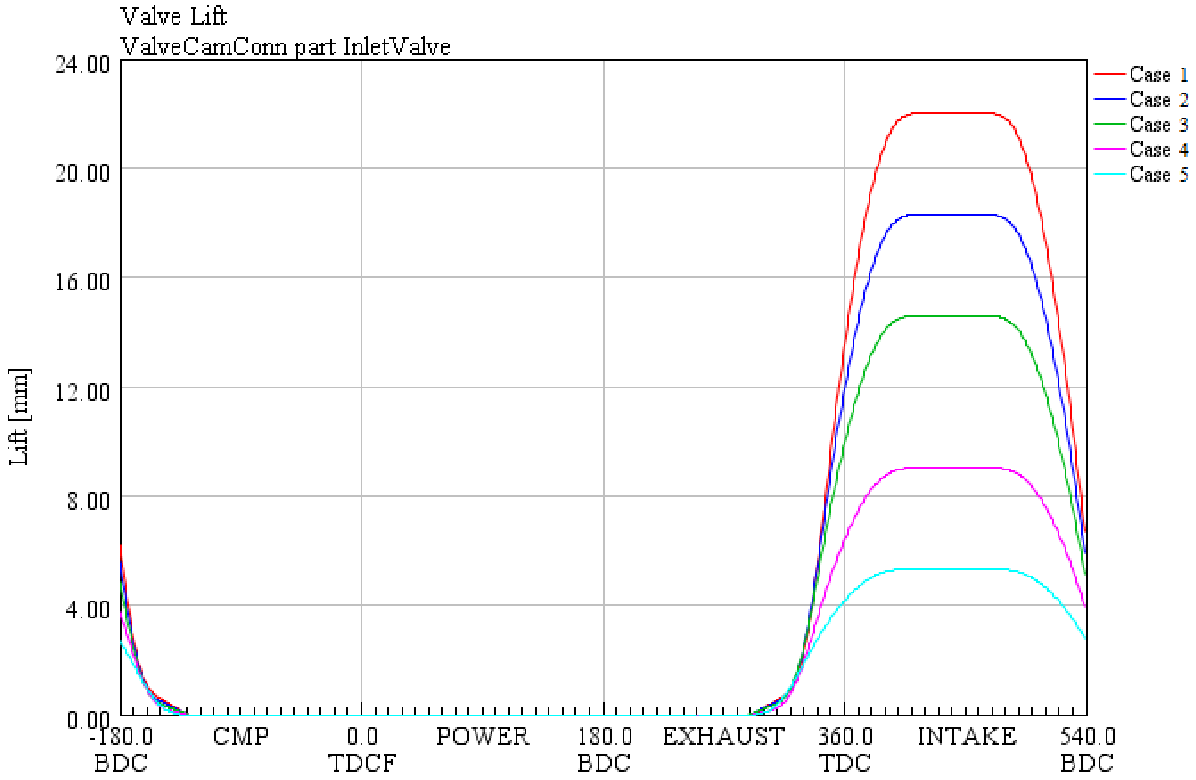

FIGURE 28 - INLET VALVE EVENT WITH ADJUSTMENTS

Regarding closing of the valve, a possibility exists enabling me to extend the duration of the lift. This inlet angle multiplier is parameterized and increased sufficiently to ensure proper closing.

What concerns acceleration of the valve, total valve control requires a reduced lift which does not compromise the acceleration, making the lift rounded during opening and closing. However this requires me to manipulate the raw valve lift data which would be too extensive for this thesis.

6.2 VALVE LIFT DURATION

Producing variable valve closing events means changing the lift duration from the point of opening to either a later or earlier point. This is done using the lift angle multiplier. Adjusting it for several cases means making it a parameter in the case setup of GT Power. Below is an example of varying lift duration.

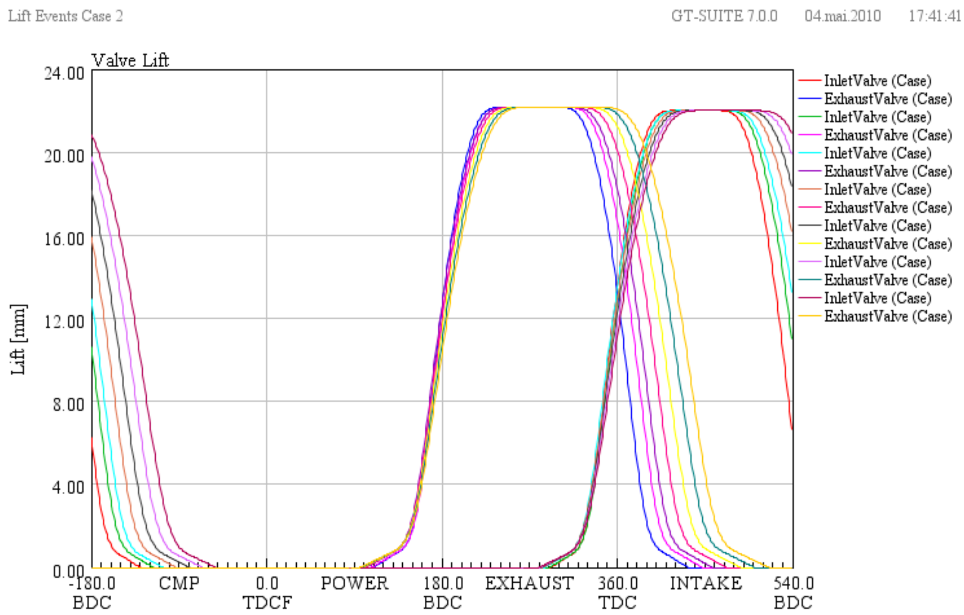

FIGURE 29 - LIFT DURATION ILLUSTRATION

A slight rounding of the opening end movement is inevitable as the lift curve is somewhat stretched. Fixing this would again mean manipulating the raw data for every case. Varying the duration as presented in the figure above is considered satisfactory for this thesis.

6.3 LIFT PHASE SHIFTING

As the least complex modification, the phase shifting of the lift curve is done by simply redesigning a new set of values to the cam angle multiplier. This effectively moves the lift curve in the direction of my choosing. The shape of the curve remains completely intact, as illustrated in figure 30.

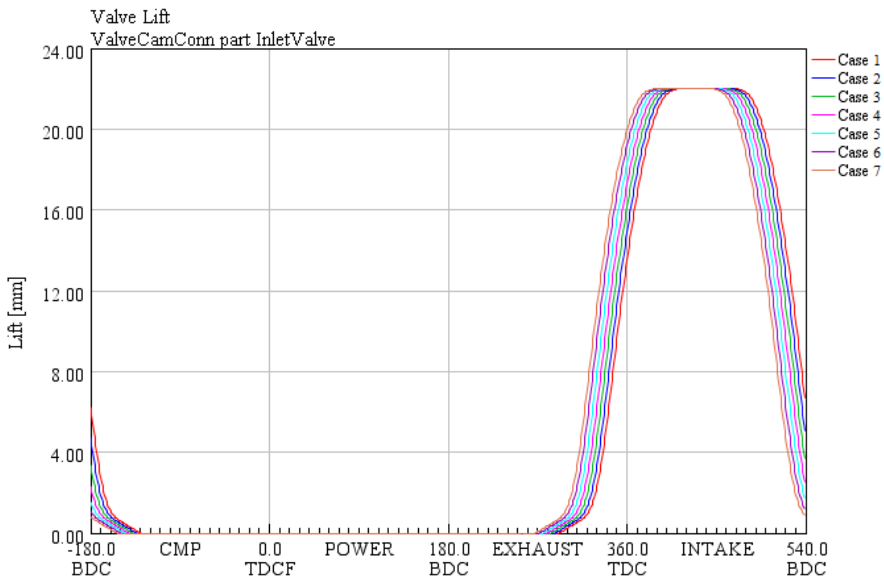

FIGURE 30 - INLET VALVE PHASE SHIFTING

When changing the IVC event one must be careful to adjust the start of cycle definition in GT Power accordingly to get reliable results from simulations.

7 FRAMEWORK

Before starting simulation of the experiments yet to be established, we need to create a framework around the engine in question. This means defining a certain realistic scenario when applying a newly developed system for variable valve actuation to this medium speed diesel engine.

7.1 SETTING

In the sense that the variable valve control system is considered to be new for this type of engine we imagine the engine itself being recently produced and situated at a test bed facility. It has also been established that the engine is to be used for propulsion purposes. This situation implies that testing of the valve control system should follow a scheme similar to a standard engine test run for marine applications. For propulsion machinery the speed is not constant during such a test. In practice the engine is propelling a water brake creating the resistance equal that of a propeller. After priming, flushing and clearance validation of the crankshaft the engine is put through a test run. Running the engine takes several hours and is sometimes done in the presence of the customer. First the engine will be fired up and kept at idle until warm. Then the engine load is increased in steps and kept running at these loads for some time to monitor performance. Usually, the final steps reach loads above 100% MCR to make sure the engine can withstand overload to a certain degree.

Below a propeller load curve is shown in a diagram of engine load limits. Note that the diagram is made to serve illustrational purposes only. The horizontal red lines indicate a proposed setup for which engine speeds may be subject of research in this thesis. As indicated in the diagram loads of 25, 50, 75 and 100% are usually subject for test run.

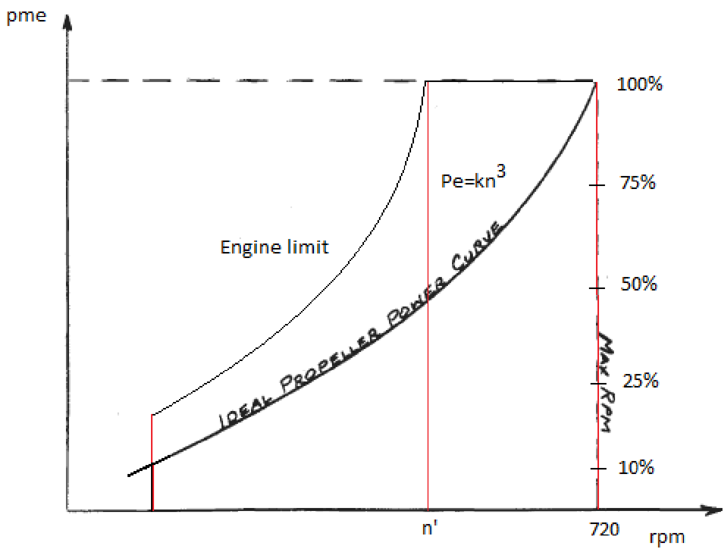

FIGURE 31 - ENGINE LOAD LIMITS ILLUSTRATION

When using continuous variable valve control one might manage to improve combustion quality at instances that are initially less than optimal for this engine. After completing simulations for a standard test run performance parameters will be collected in graphs. These data serve as reference to performance data collected after simulating a set of valve control strategies. Valve control will be applied to the areas where performance has the greatest potential for improvement.

8 VARIABLE VALVE CONTROL

Using the framework outlined above, the goal is to improve part load conditions by manipulating the motions of both inlet- and exhaust valves on the KRM engine. Performance parameters will be registered for a standard run at ten points along the propeller curve while preserving the camshaft controlled valve settings. A systematic approach to timing and scaling the valve lift will be outlined based on a short literature study on different valve control strategies. A number of these strategies will be subject to experimental research.

8.1 TIMING STRATEGIES

Before moving on to the experiment simulations I quickly reevaluate the different valve control strategies to gain a more systematic view of their purpose.

8.1.1 INLET VALVE PHASING ONLY

Phasing of the inlet valve opening in GT-Power is done by redefining the “Cam Timing Angle”. This is done by converting the value to an independent parameter. Late phasing of the inlet to an angle after top dead center is one strategy to maintain high inlet air velocities at lower loads. This way the air entering the cylinder is pulled in by the vacuum created as the piston moves downward. Using variable valve control one may choose to recharge using one or two valves. In the latter case one achieves higher velocities, but the same flow pattern as before. Using only one valve the flow pattern is altered, increasing tumble and swirl to enhance mixing properties. The turbulence will be stronger, but less homogenous. Directed valves may enhance the swirl pattern additionally. The increased turbulence will support combustion stability and thus enables leaner combustion without severe cycle to cycle variations. This is highly recommended in the lean burn gas engine cycle in terms of avoiding throttling and the use of the dual fuel strategy. Using this valve timing strategy one might avoid having to switch fuel types at low speed. At low speed, torque is potentially increased by advancing IVC due to increased volumetric efficiency. High speed operation requires retarding of IVC to improve η_v.

8.1.2 EXHAUST VALVE PHASING ONLY

The ability to vary the exhaust valve event means not having to make a compromise between expansion work at low speed and exhaust stroke pumping work at high speed. Phasing the exhaust valve opening to a later point increases the work output of the expansion. Another benefit from this is the extra time for hydro carbons to oxidize in the cylinder and the reduction of HC emissions because of this. A third consequence of retarded exhaust event is increase of valve overlap. This increases the dilution of residual gases in the cylinder that are unwanted in low speed/part load operation.

At high speeds an earlier EVO produces benefits in terms of reduced pumping work as more time is given for blow down prior to BDC. This will serve its purpose if the pumping work reduction is greater than the loss in expansion work. Later EVC serves assisting to scavenging, but increases pumping work.

8.1.3 DUAL EQUAL PHASING

Phasing of the lift array in GT-Power is easily done. In the part editor of the valves one merely modify the “Cam Timing Angle” of both inlet and exhaust valves equally using predefined parameters. Retarding cam timing in this case actually delays the overlap without changing its duration. This will cause exhaust gas to be drawn back into the cylinder at exhaust pressure. Benefits from this are reduction of NOx emissions caused by internal EGR, recycling of hydro carbons and reduction of intake pumping work.

8.1.4 DUAL INDEPENDENT PHASING

Independent phasing of the valve events produce great benefits. This enables optimization in idle, part load and high speed operation providing great flexibility. Slight refinement of dual equal phasing at part load may give a more optimal solution. The ability to vary overlap is useful for combustion stability at idle by increasing residual gas dilution.

8.2 LIFT STRATEGIES

Given an operating condition one may desire to alter the height of valve lift from the seat. The reasons may differ depending on the situations already described. Goals such as energy consumption improvement, charge air velocity enhancement are among the most common for lift strategies. This subject will not be extensively dealt with here as it turns out the simplified combustion model does not handle the issue of resulting swirl and mixing from altered inlet flow characteristics. This fact was discovered at a late point of the project work, and implementing a more advanced cylinder flow model requires data lacking at this point. However lift event strategy principles were extensively treated in (1) and there is reason to believe that benefit is obtainable on medium speed diesel engines equal to the benefits showed in automotive research technology.

9 SIMULATION EXPERIMENTS

In the results of the following experiments I wish to analyze alterations in engine performance caused by manipulation of valve event timing. Parameters like mean indicated pressure, thermal efficiency, volumetric efficiency and exhaust temperatures as well as brake specific fuel consumption are used to represent the performance in each experiments. Every experiment is divided into several cases. Separate cases are made for subdivisions within an experiment. For example early and late phasing is analyzed separately as well as running the experiment on two different operating points.

Initial performance was analyzed using the standard valve train. This represents the cam shaft valve train without any modifications. From these data I identified two cases that show potential for performance improvement, one load case below the original optimum and one above this. The basis for choosing these two operating points was brake specific fuel consumption.

9.1 STANDARD PERFORMANCE

Running the model for the first time after recalibration produced a full set of results. These data were collected to found a basis for creating valve control strategies in further experiments. All results from GT Power were exported into an excel work sheet where graphs were made to serve as representation for the original engine performance. These results are represented in the following sections.

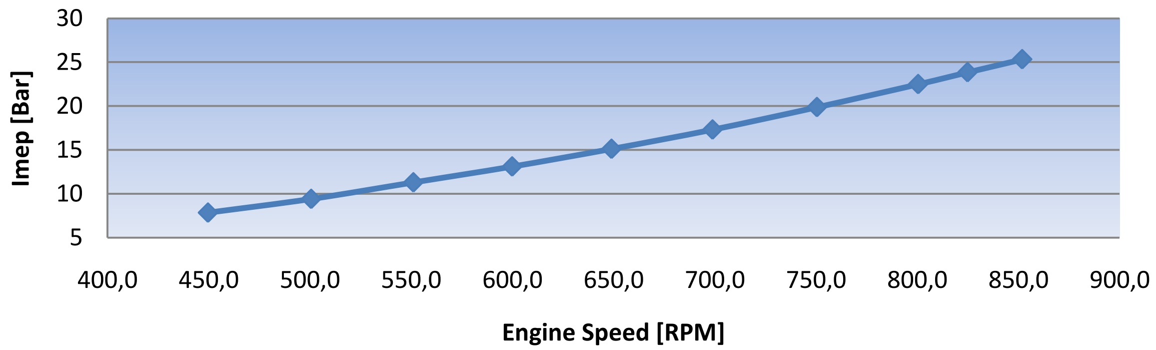

FIGURE 32 - STANDARD MEAN INDICATED PRESSURE

The above figure is a representation of the load curve based on the ten cases used for recalibrating the model. The model is now able to simulate along this curve.

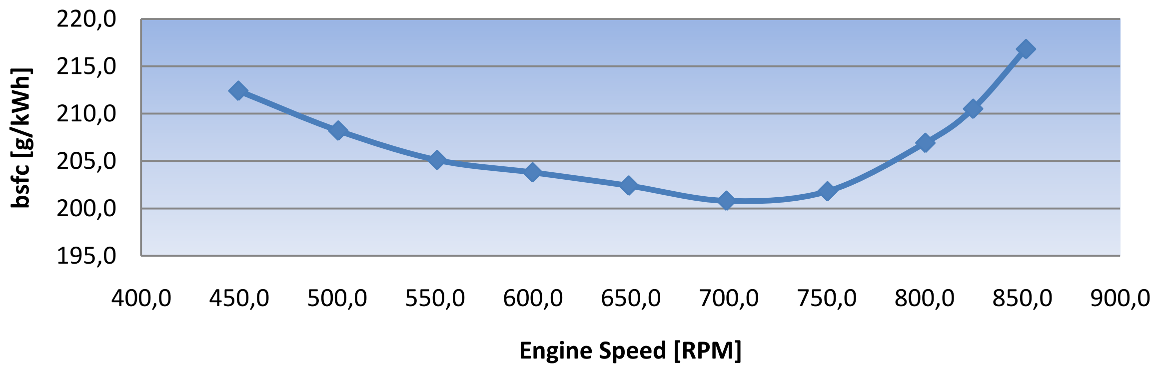

FIGURE 33 - BSFC OF STANDARD RUN ALONG LOAD CURVE

As load and speed is increased we see bsfc decreasing to an optimum at 720 rpm which is approximately 85% MCR a common optimum for marine engines. On the basis of this graph two operating points were chosen in order to provide a valve control solution capable of improving bsfc. I chose case two (500 rpm) and case 9 (825 rpm) for further investigation as these are cases with great potential for improvement outside of 100% MCR and idle.

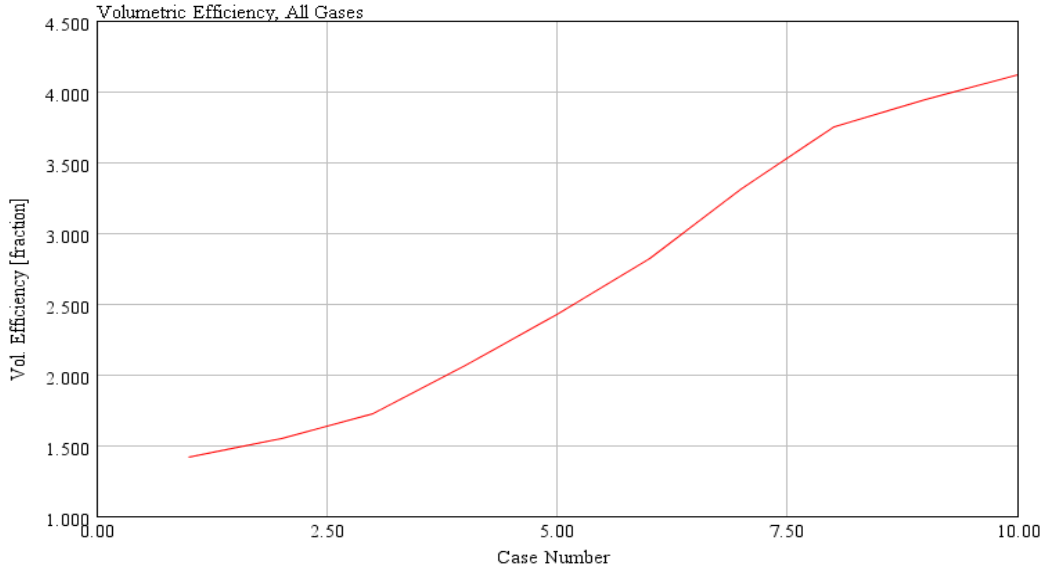

FIGURE 34 - VOLUMETRIC EFFICIENCY AT EACH LOAD CONDITION

As a reference for further experiments volumetric efficiency is stored as a function of all ten load conditions. This is done for thermal efficiency as well, shown in the figure below.

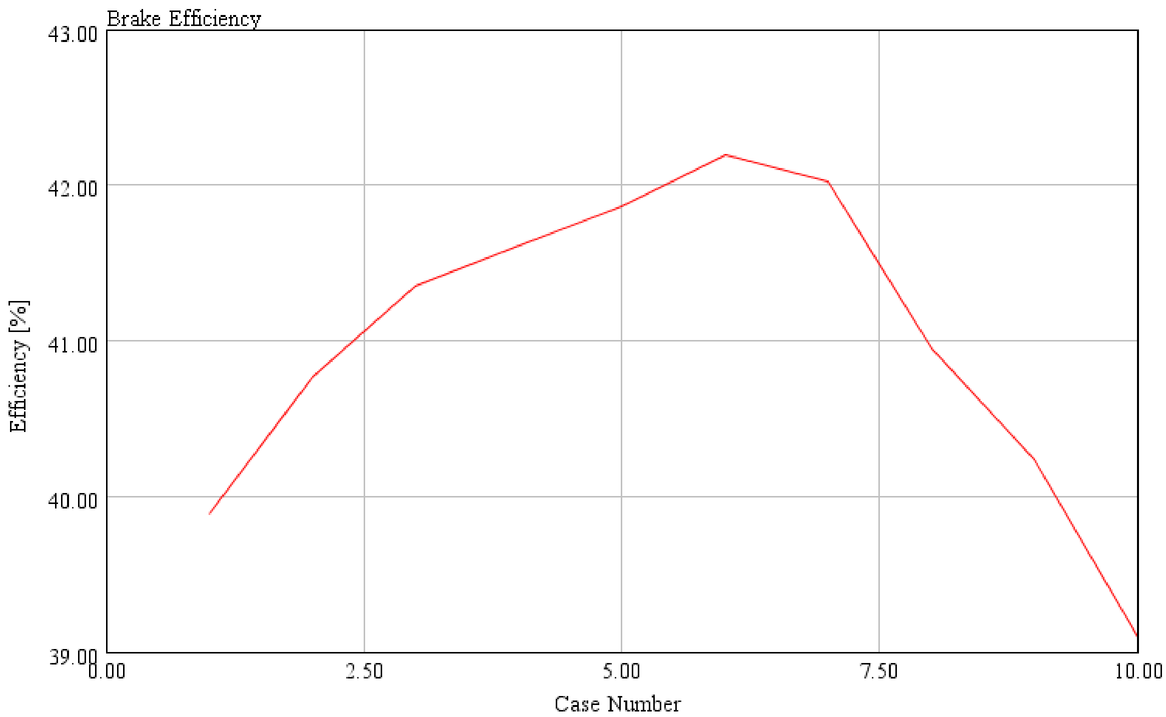

FIGURE 35 - OVERALL/THERMAL EFFICIENCY

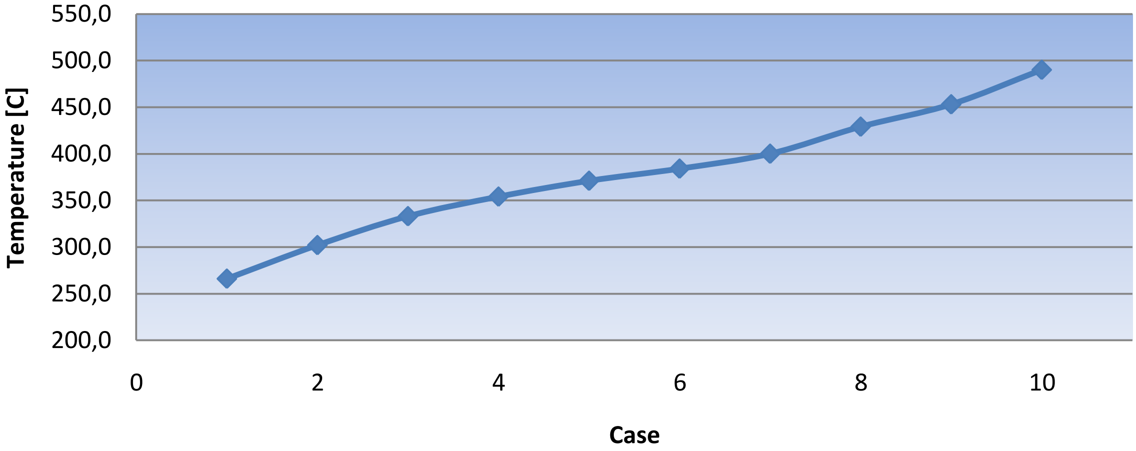

FIGURE 36 - EXHAUST TEMPERATURE AS FUNCTION OF LOAD

A plot (Fig. 36) of the exhaust temperature is made to serve as a future reference for valve control experiments. We see a clear inclination as load increases.

No extensive commenting is made on these figures as they serve merely as a reference. I already confirmed that performance correspond to the real measurements made on the KRM-6 engine. Modification of the valve train and experiments concerning valve control should in theory be able to improve conditions that suffer from compromise at this point.

9.2 TIMING EXPERIMENTS

To create a basis for comparison the valve timing experiments follow the same strategy as an automotive industry study (7). In this paper a heavy duty high speed diesel engine served as subject for bsfc investigation using valve control. Experiments made by (7) are reproduced for the Rolls Royce KRM-6 in order to evaluate own results against the results in (7). Note that the results concerning bsfc will be underestimated on the bigger KRM-6 which will be subject to running over a longer time span whilst developing greater overall power. This means that every unit of bsfc reduction on the KRM-6 will have greater significance when compared to the high speed diesel engine used by (7).

9.2.1 SHIFTING EVO WITH FIXED EVC

In this experiment EVO was both advanced and retarded from its default value of 51 degrees cam angle. Using the latter strategy I expected to be able to increase low load torque as more time is used for expansion. However, no significant results were found in any of the two chosen load cases for this strategy. Advanced and retarded EVO was successfully reproduced on the KRM-6, and results actually correspond well with (7) which could not find any bsfc benefit either. Early EVO is expected to have a wasteful effect on the expansion stroke at low load. This was confirmed as a decrease in volumetric efficiency followed from advancement of EVO. Only a slight torque increase was shown at low load when retarding EVO. Although this is supportive of the initial theory a bsfc decrease of 0.7% may not be regarded as useful in this experiment. The full results for EVO variation on case 2 and 9 is shown in appendix A.

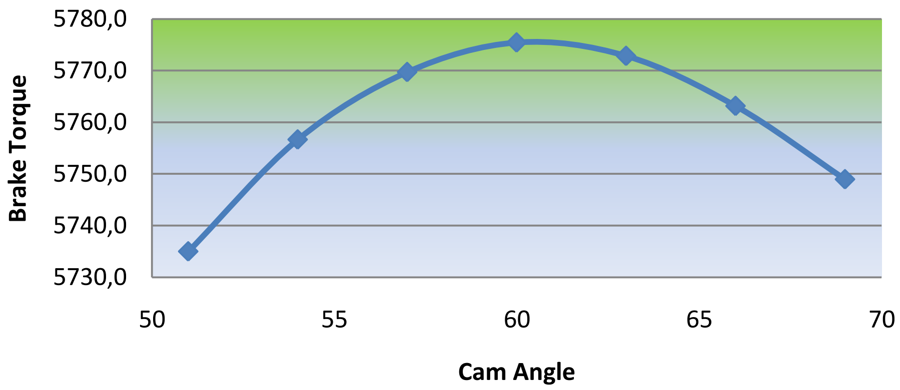

FIGURE 37 - TORQUE AS FUNCTION OF LATE EVO AT 500 RPM

We see a tendency that EVO retardation is beneficial up to a certain point where the exhaust opening event occur too late. 51 degrees cam angle is the standard EVO case.

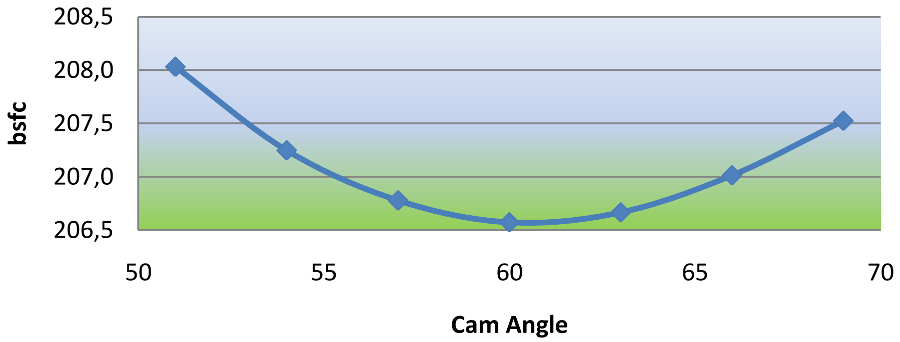

FIGURE 38 - BSFC AS FUNCTION OF LATE EVO AT 500 RPM

There is an optimum regarding bsfc in this strategy. This result is however not strong enough to confirm that our goal for this strategy is reached. To verify a result as valid for a given potential I search for substantial life cycle improvements in terms of either fuel consumption or emissions.

9.2.2 EARLY IVC WITH FIXED IVO

This is the strategy similar to Miller and Atkinson cycles. In (7) it proved to be the most beneficial of the proved strategies in terms of fuel consumption. Bsfc was reduced by 6- and 2.3 percent by using early (Miller) - and late (Atkinson) IVC respectively. In my study, the numbers were actually greater than the results produced in (7).

9.2.2.1 EARLY IVC AT 500 RPM AND 5735 NM

Below is a waterfall diagram showing how valves are closed progressively earlier through the ten cases.

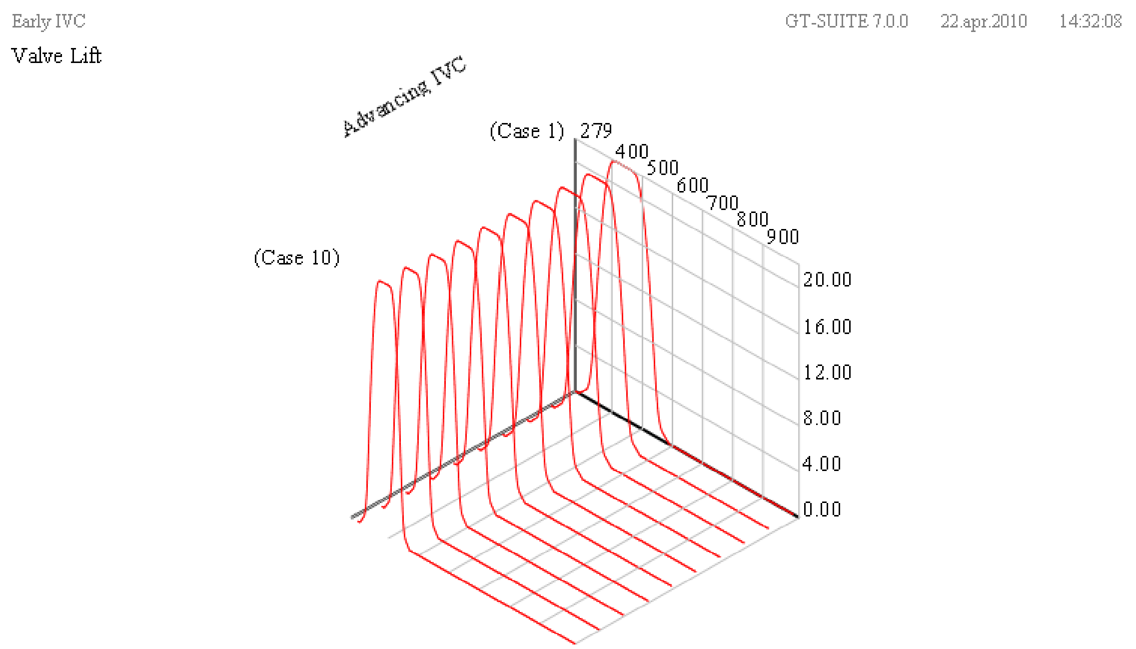

FIGURE 39 - ADVANCING THE INLET VALVE CLOSING AT 500 RPM

The figure above serves as verification of lift height and shape. We also see how closing is advanced more for each of the ten cases.

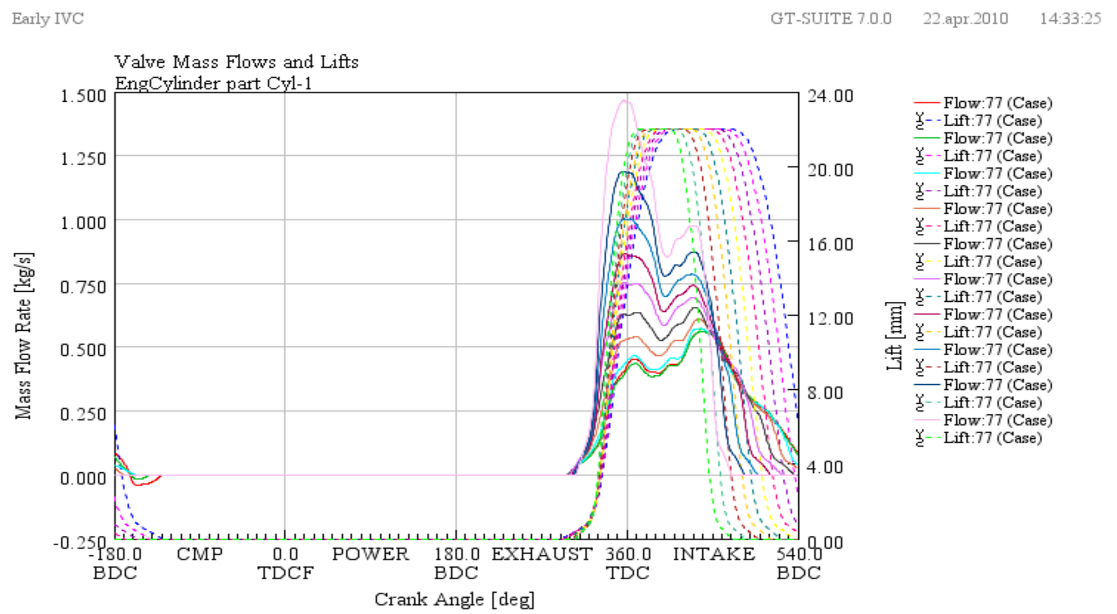

FIGURE 40 - EARLY IVC LIFT VS. MASS FLOW AT 500 RPM

The figure above shows how the mass flow rate increases through the inlet valve as the experiments are set up to demand equal amounts of trapped mass in the cylinder at IVC. Back flow is eliminated in most of the cases. We also see that the mass flow pattern changes as the peak occurs earlier in the most advanced IVC events. This is due to the high piston speed in the mid part of the intake stroke. Theoretically this could cause problems concerning too high inlet flow velocities. Some swirl and turbulence is desirable, but too much could have a negative effect on combustion if fuel droplets were to reach the cylinder wall and lower the combustion efficiency. As my model have no accurate flow connection between inlet pipe flow and cylinder swirl and turbulence, locating this point is not possible at this time. Data for cylinder flow patterns are lacking at this time.

Below diagrams are presented to show how performance is improved when closing the intake valve early. The aim of this strategy is to expand the charge air trapped inside the cylinder prior to compression. This will in turn lower the initial charge temperature. Note that standard IVC happens at a crank degree equivalent to approximately 277 cam angle degrees. Expressing valve events in Cam angle degrees is the default in GT Power.

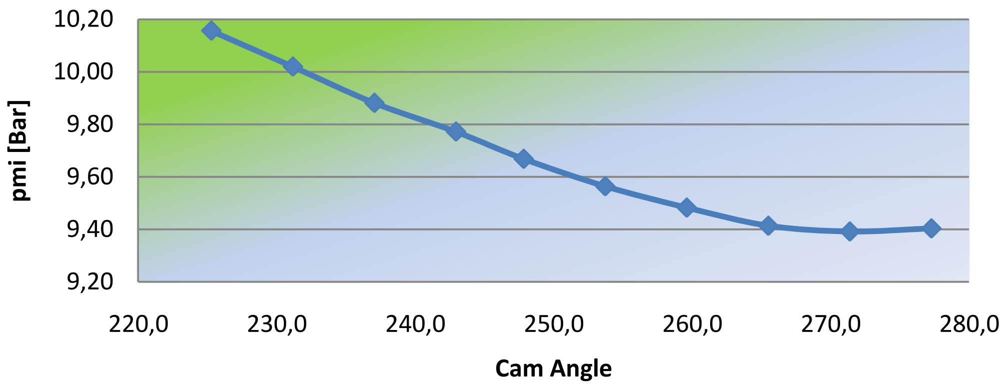

FIGURE 41 - NET MEAN INDICATED PRESSURE AS A FUNCTION OF EARLY IVC AT 500 RPM

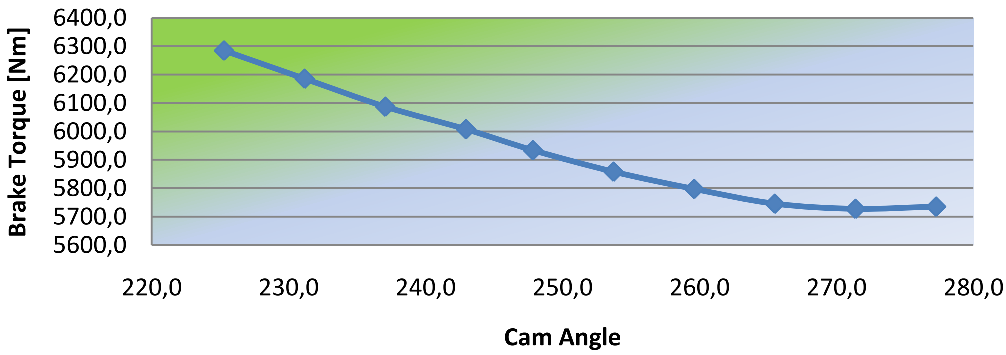

FIGURE 42 - TORQUE AS A FUNCTION OF EARLY IVC AT 500 RPM

Brake torque follows the mean indicated pressure proportionally and is only used here to verify the relation for practical purposes. In further studies only net mean indicated pressure is needed to identify torque variation correspondence to the various valve control experiments.

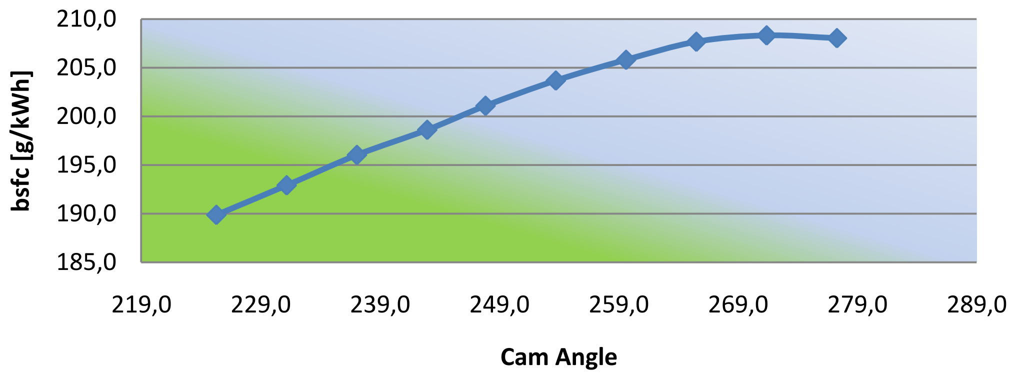

FIGURE 43 - BSFC AS FUNCTION OF EARLY IVC AT 500 RPM

The ability to develop more torque on the same amount of injected fuel per cycle indicates that a lower amount of fuel is used per unit of energy produced by the engine. Brake specific fuel consumption is a useful measurement for this issue and is shown in the graph above. We clearly see how advancing the IVC causes fuel savings. The highest recorded saving is just shy of 9% using this strategy. This requires the cylinder to be able to benefit from the increased mass flow rate in case 10 (IVC at 225 degrees Cam Angle). The average flow velocity through the inlet valve is not increased significantly. However peak velocity is increased by 42% compared to the standard IVC in case 1.

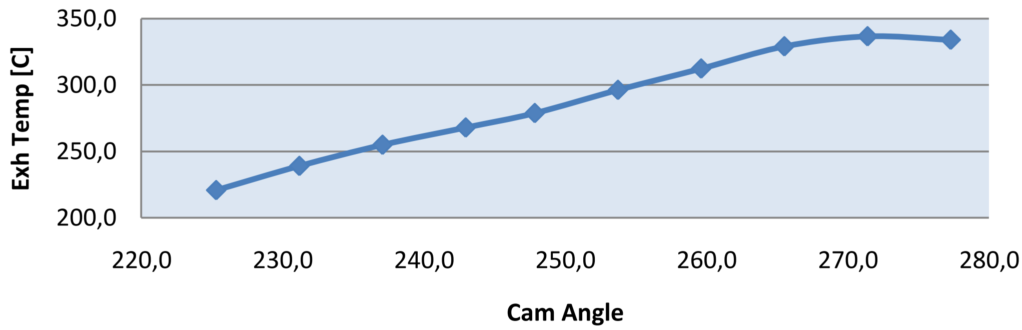

FIGURE 44 - EXHAUST TEMPERATURE AS A FUNCTION OF EARLY IVC AT 500 RPM

We see from the graphs above that we benefit greatly from closing the intake at an early stage in the process. However in this case we assume that the variable geometry turbine is capable of delivering an increased boost pressure in order to keep the trapped mass constant. The temperature graph show we have less temperature difference across the turbine, making the variable geometry essential to validate these results.

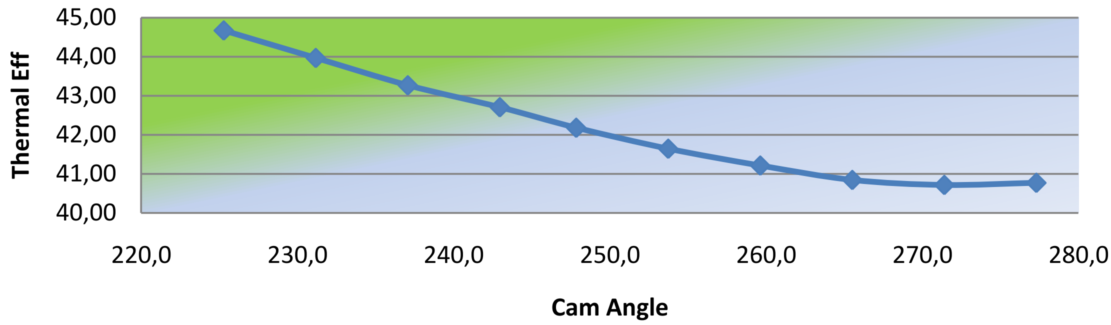

FIGURE 45 - THERMAL EFFICIENCY AS A FUNCTION OF EARLY IVC AT 500 RPM

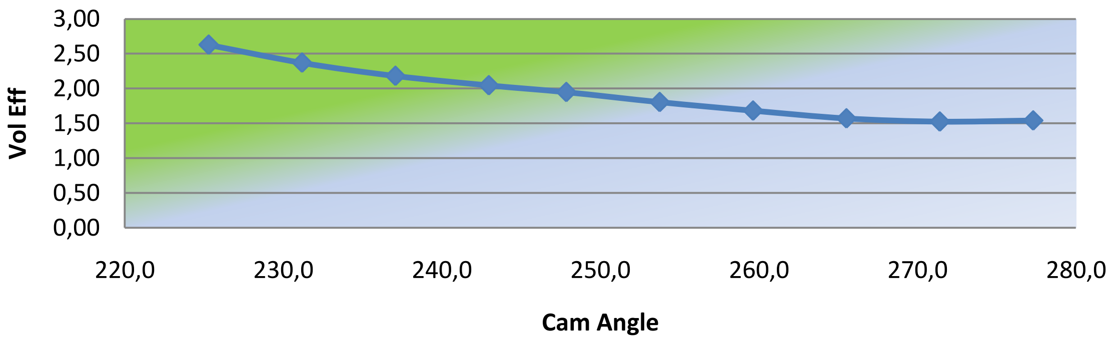

FIGURE 46 - VOLUMETRIC EFFICIENCY AS A FUNCTION OF EARLY IVC AT 500 RPM

We see a significant increase in volumetric efficiency due to the high mass flow. A larger portion of the inlet air is blown through the engine during valve overlap when the mass flow rate is at its peak during the advanced IVC events.

$$\eta_V = \frac{2\dot{m}_a}{\rho_{a,0} V_d N}$$

Results are verified by the formula above as all parameters in the denominator are constant through the experiment. The increase in blow-by air is not necessarily positive however. Too much fresh air in the exhaust manifold will compromise the exhaust temperatures if excessive blow by occurs, giving the turbine a hard time creating the required boost for a given trapped mass requirement. Due to the simplicity of my model I am not able to identify the exact optimal valve strategy for this case. Possibly it is located somewhere within the presented range. Since great improvements in both thermal and volumetric efficiency are evident, these results indicate great potential for energy savings in the diesel industry as of today.

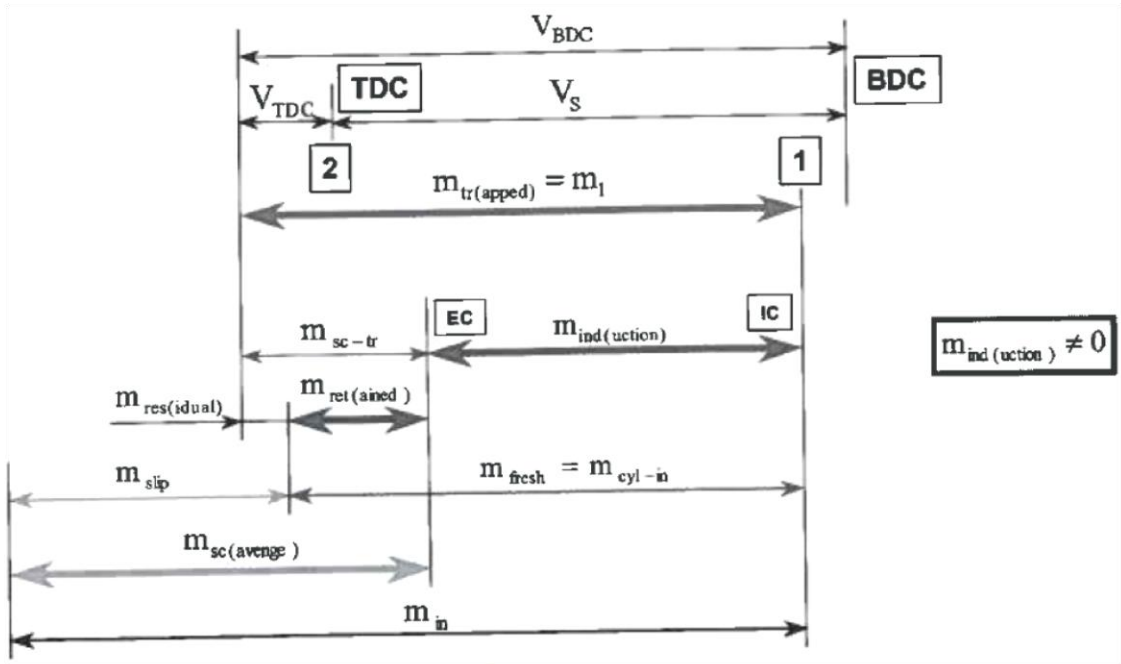

FIGURE 47 - INLET AIR DISTRIBUTION (8)

From the figure we see the relation of trapping potential and mass actually going into the cylinder. It is logical to presume that we at some point get a blow by too great to benefit the diesel process. Full set of results for this experiment in appendix B.

9.2.2.2 EARLY IVC AT 825 RPM AND 15464 NM

Considering the high speed case using early inlet valve closing, fuel savings are obtained compared to the amount of energy produced by the engine. The same tendencies are seen in mass flow versus lift as in the low speed case, see appendix C. I will briefly present the most important results from this experiment.

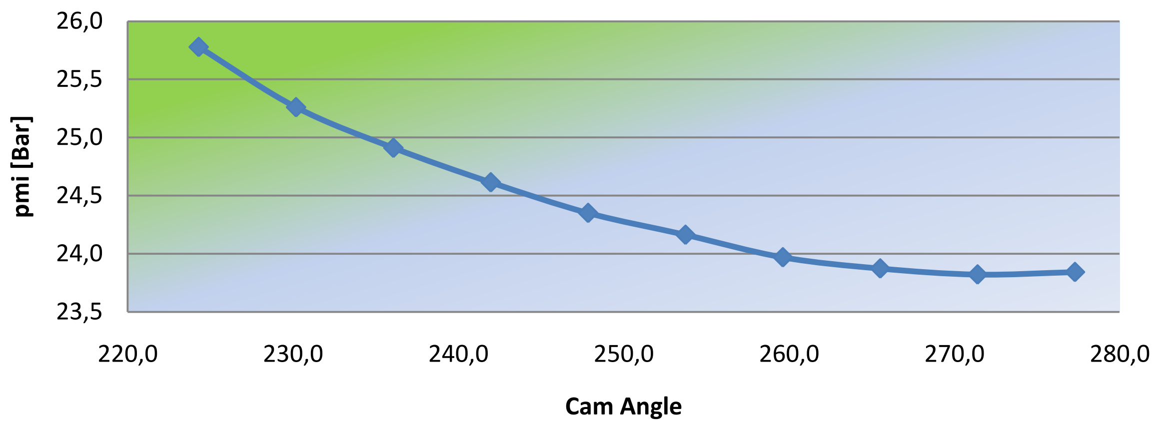

FIGURE 48 - NET MEAN INDICATED PRESSURE AS A FUNCTION OF EARLY IVC AT 825 RPM

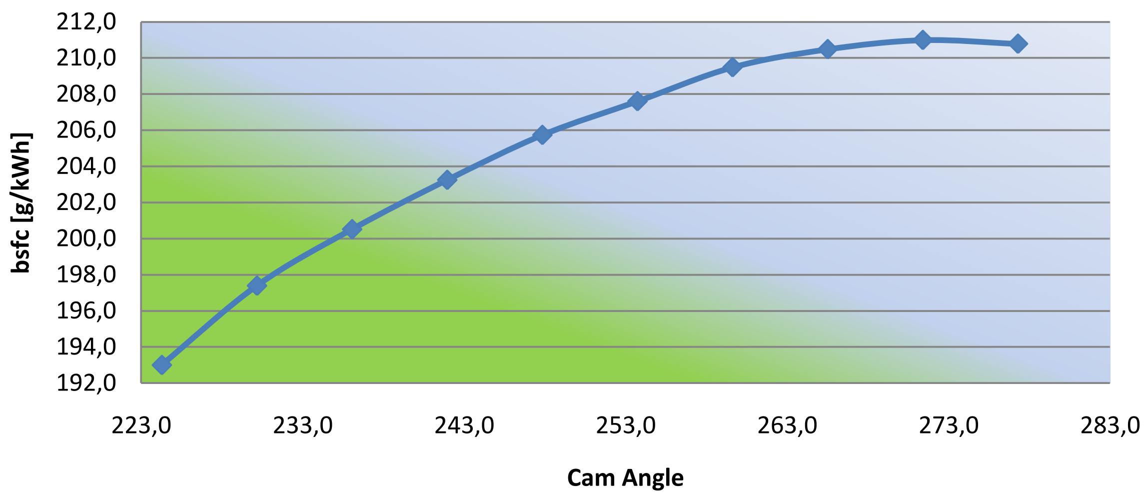

FIGURE 49 - BRAKE SPESIFIC FUEL CONSUMPTION AS A FUNCTION OF EARLY IVC AT 825 RPM

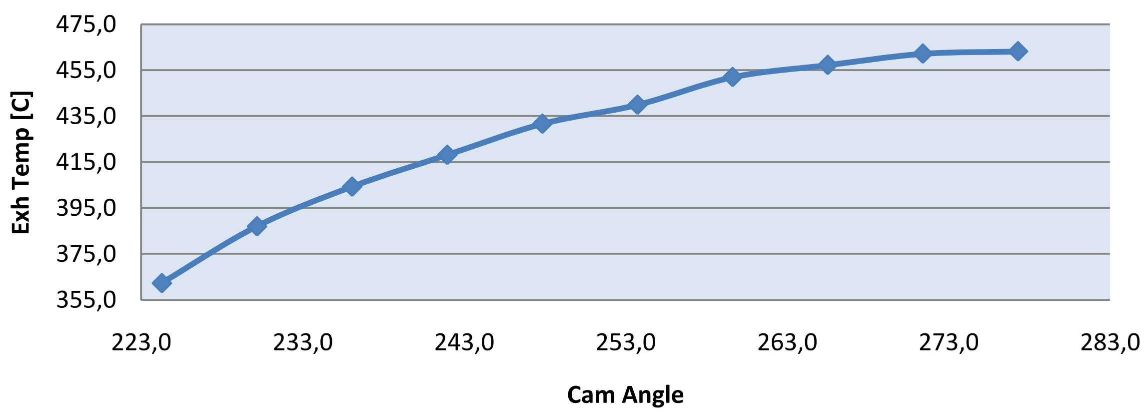

FIGURE 50 - EXHAUST TEMPERATURE AS A FUNCTION OF EARLY IVC AT 825 RPM

At some point along the exhaust temperature curve a lower limit for operating a turbine with variable geometry exists. This will probably contribute to limit the fuel saving potential of these strategies.

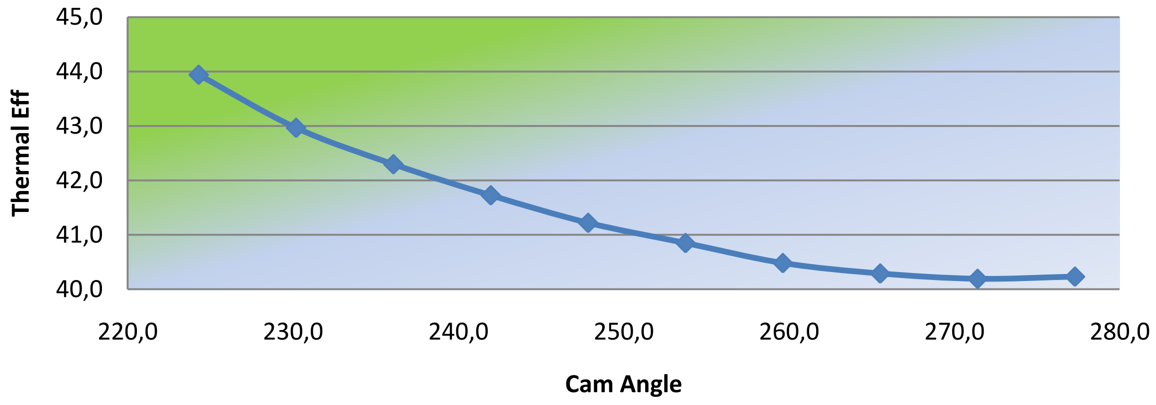

FIGURE 51 - THERMAL EFFICIENCY AS A FUNCTION OF EARLY IVC AT 825 RPM

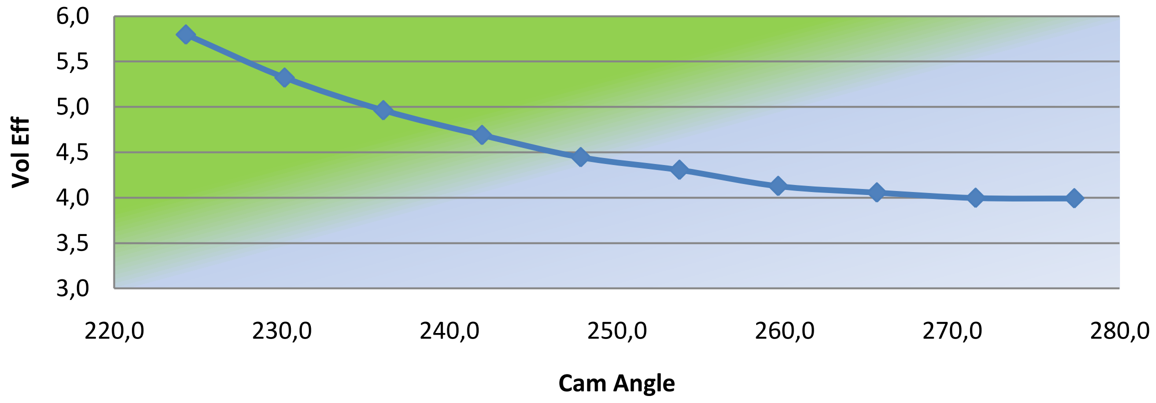

FIGURE 52 - VOLUMETRIC EFFICIENCY AS A FUNCTION OF EARLY IVC AT 825 RPM

It is evident that this strategy produces similar results when performed in high speed operation, thus the same arguments can be made for both the low- and high speed case. To quantify this event a fuel saving of 8.4% is recorded as the maximum of this experiment. Arguments regarding volumetric efficiency and its effect on performance will not be repeated in this section. There is no tendency for the thermal efficiency to drop along the range of this experiment. Further extension might show a volumetric efficiency high enough to ruin thermal efficiency.

9.2.3 LATE IVC WITH FIXED IVO

A benefit in bsfc of 2.3% was recorded in (7). From our results we see great potential of matching and even exceeding this result, based on the KRM-6 of engine.

9.2.3.1 LATE IVC AT 500 RPM AND 5735 NM

In the low speed case we successfully manage to reproduce the experiment and get a fuel saving of 2.6%. Analyzing the performance will tell us if this number is plausible in terms of engine limitations. Full results in appendix D.

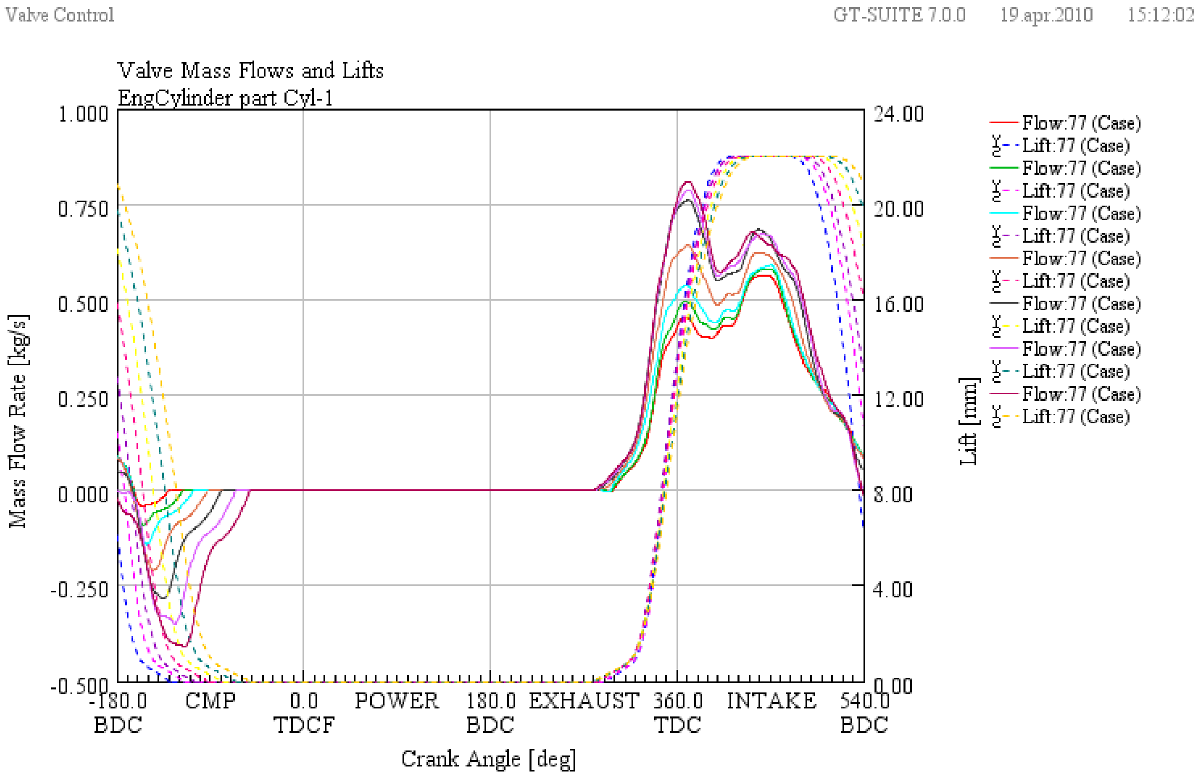

FIGURE 53 - LATE IVC LIFT VS. MASS FLOW AT 500 RPM

The desired back flow is evident from the figure above causing reduction to the effective compression ratio. Effect of this on the cylinder conditions and emissions will be dealt with at a later point.

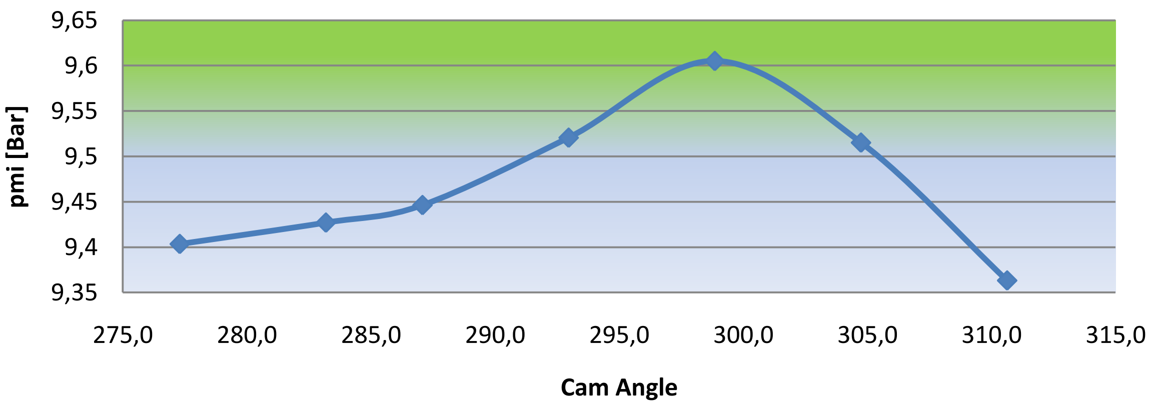

FIGURE 54 - NET MEAN INDICATED PRESSURE AS A FUNCTION OF LATE IVC AT 500 RPM

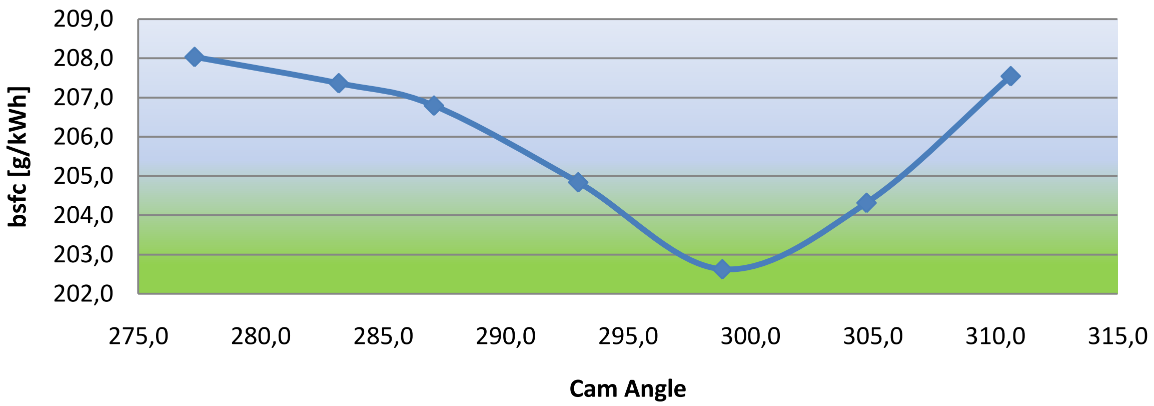

FIGURE 55 - BRAKE SPECIFIC FUEL CONSUMPTION AS A FUNCTION OF LATE IVC AT 500 RPM

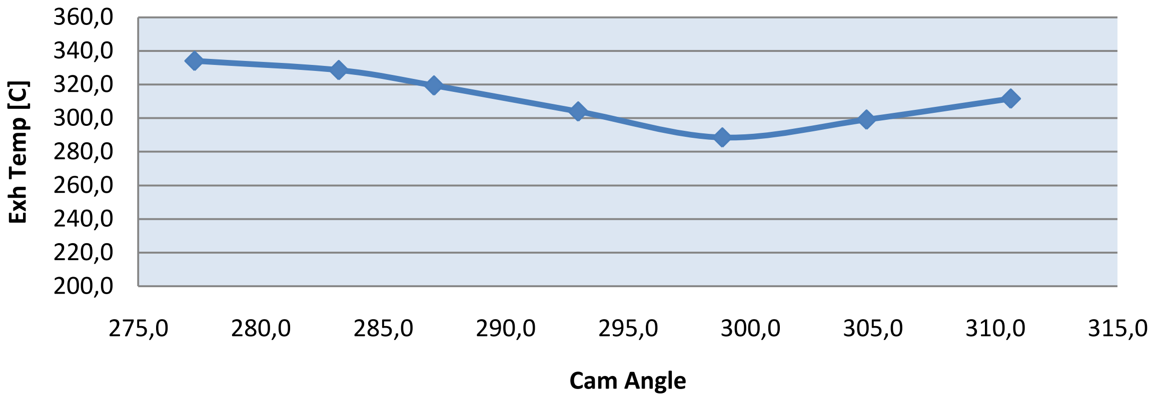

FIGURE 56 - EXHAUST TEMPERATURE AS A FUNCTION OF LATE IVC AT 500 RPM

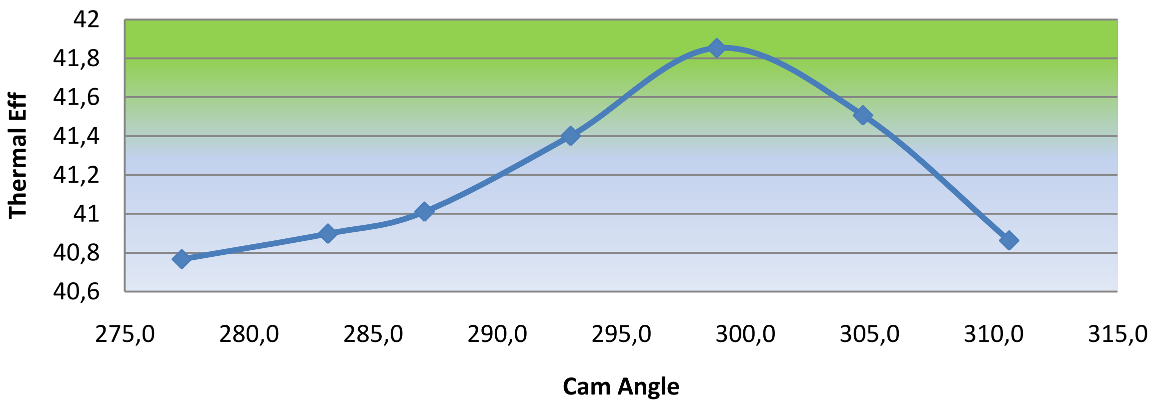

FIGURE 57 - THERMAL EFFICIENCY AS A FUNCTION OF LATE IVC AT 500 RPM

There is clearly an effect at the latest cases of IVC where the desired effect is lost. Too much of the effective compression ratio is lost creating a massive back flow into the inlet manifold. Flows in the opposite direction of the inlet air could possibly disrupt the flow characteristics of inlet air that often is used in engine tuning.

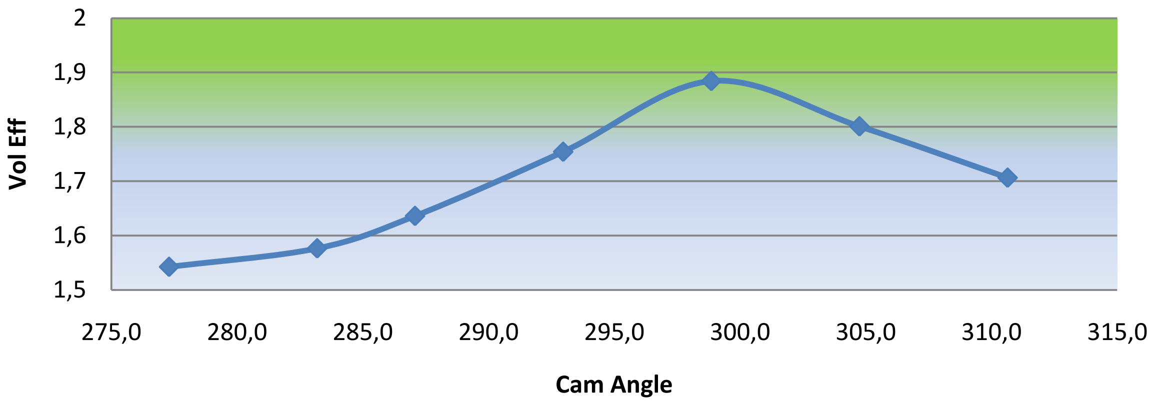

FIGURE 58 - VOLUMETRIC EFFICIENCY AS A FUNCTION OF LATE IVC AT 500 RPM

Closing the inlet valve at a later point than standard setup IVC creates results showing an optimum regarding bsfc. Delaying IVC to about 300 degrees cam angle produces a benefit of 2.6%. Even later IVC will steal too much from the compression ratio to produce any benefit. This figure serves as the maximum obtainable in my experiments and it is very close to the results of (7) confirming that this technology is transferrable to medium speed diesel engines. The percentage is even more significant on the larger KRM due to a higher power output and longer running of the engine making the total amount of fuel saved larger relative to the engine presented in (7).

9.2.3.2 LATE IVC AT 825 RPM AND 15464 NM

Running the Atkinson cycle in the high speed case does not produce as much benefit to bsfc as the low speed case. However the savings I obtain in my experiment are quite substantial. 4.8% lower bsfc is recorded at the most by reproducing the Atkinson cycle for the KRM-6 engine. The results presented below represent a given interval set by the user. Some extension was made showing that bsfc benefits quickly flattened out. The reason for not presenting these numbers is an unrealistically high boost pressure outside- and possibly within this range. This is correlated to the massive backflow that is caused by compression. Results for this strategy in appendix E.

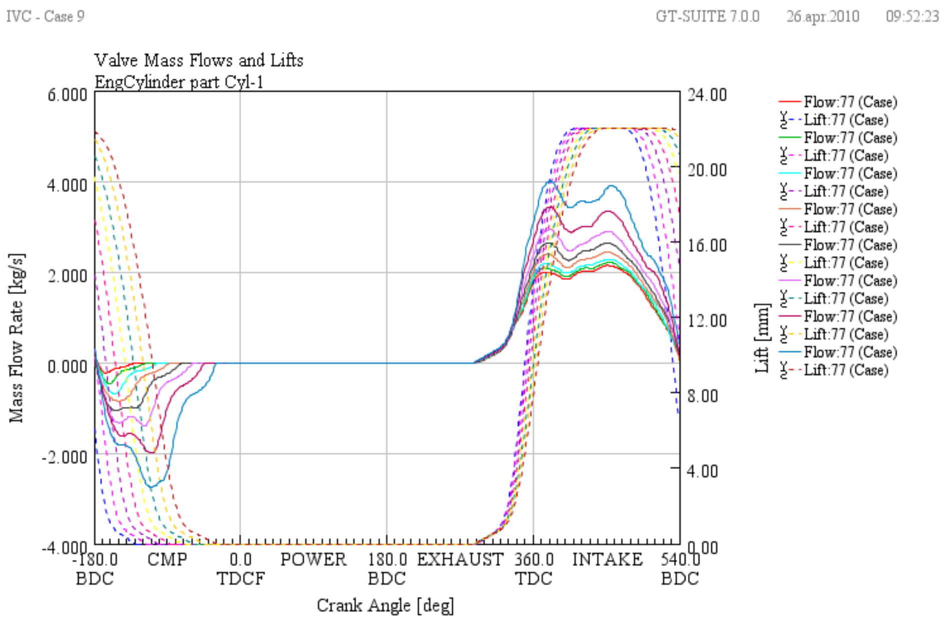

FIGURE 59 - FLOW VS. MASS FLOW AT IVC AT 825 RPM

Quite substantial backflow is evident in the late cases. The figure above shows that inlet closing event is retarded to a possible unrealistically late point. Almost no time is left for compression in the last cases. Compression is thus supported by a high boost pressure to maintain a constant trapped mass. From my experiments I see that boost pressure compensation is rapidly increasing already from case 5 making this a more realistic point of optimal timing. This can be seen in the jump shown in the initial mass flow rate development. Case 5 is closing the inlet valve around -115 degrees leaving about two thirds of the compression left unspoiled. Bsfc benefit from this case is 2.4% matching the maximum obtained results of (7). The experiment setup is set to have as few variables as possible. When keeping trapped mass constant we need to be attentive to parameters that might be out of bounds like the boost pressure in this case. The pressure at cycle end in cases 6-8 show unrealistic values and will be discarded from the following graphs.

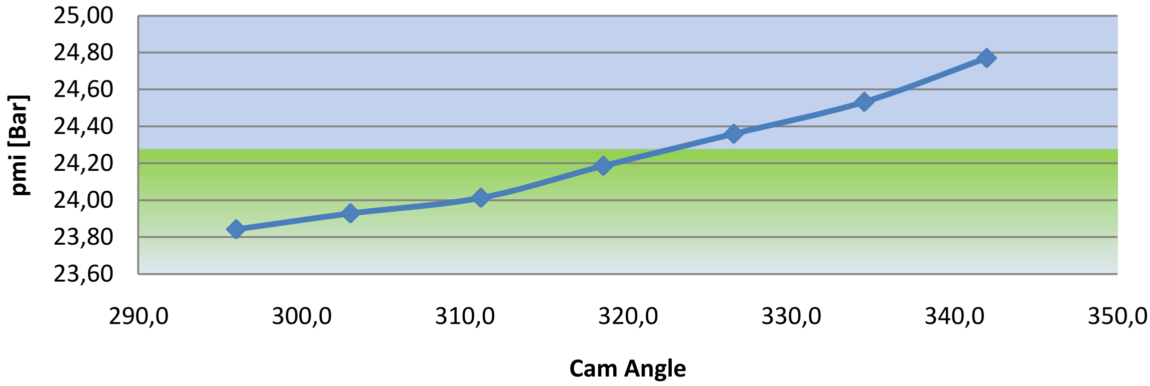

FIGURE 60 - NET MEAN INDICATED PRESSURE AS A FUNCTION OF LATE IVC AT 825 RPM

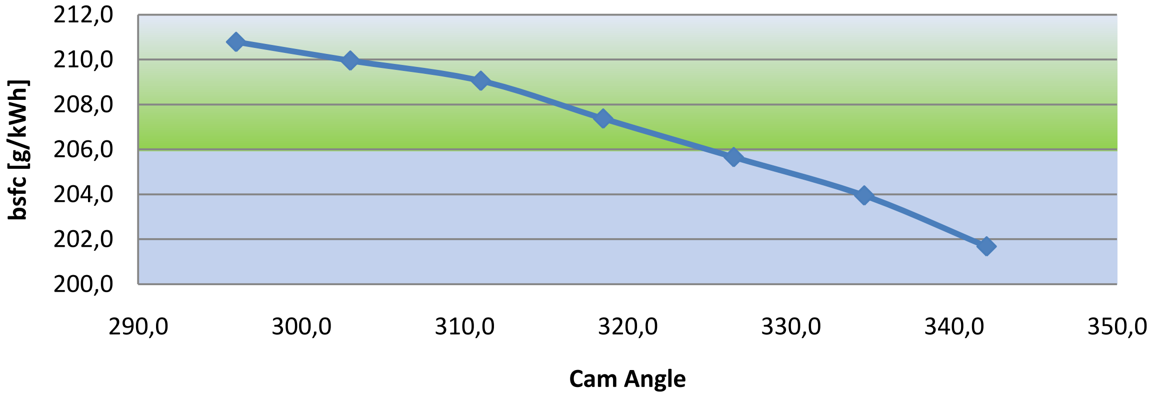

FIGURE 61 - BRAKE SPECIFIC FUEL CONSUMPTION AS A FUNCTION OF LATE IVC AT 825 RPM

Gradient colors are implemented to indicate beneficial results. Gradient stop is set at case five as the post cases are discarded from the results on the basis explained above.

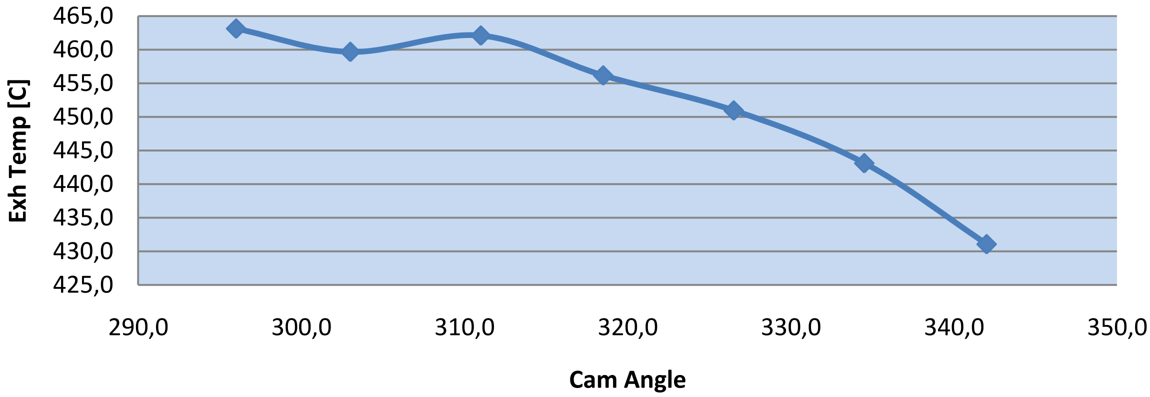

FIGURE 62 - EXHAUST TEMPERATURE AS A FUNCTION OF LATE IVC AT 825 RPM

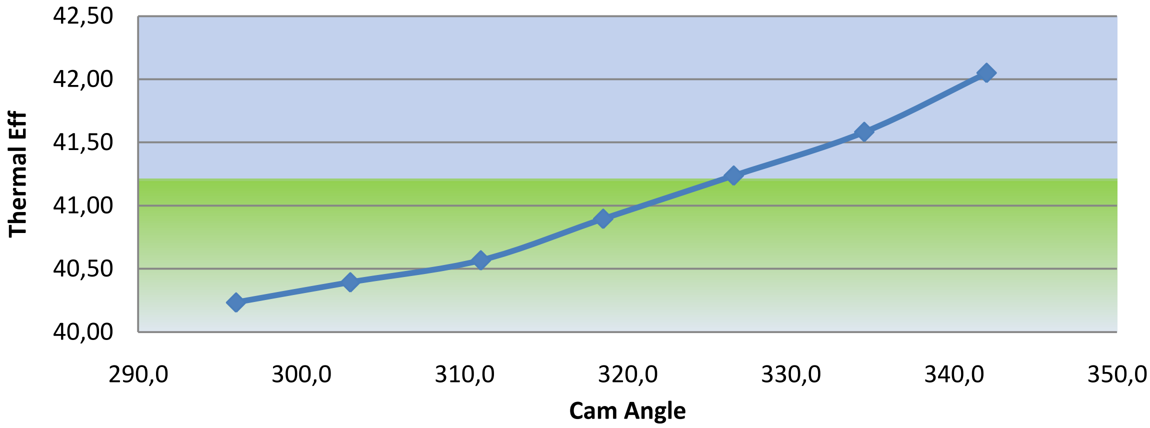

FIGURE 63 - THERMAL EFFICIENCY AS A FUNCTION OF LATE IVC AT 825 RPM

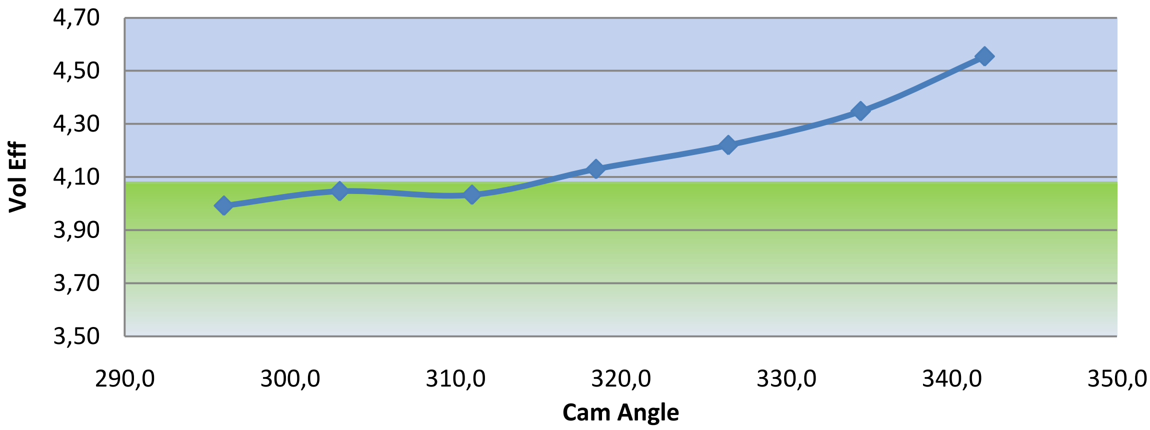

FIGURE 64 - VOLUMETRIC EFFICIENCY AS A FUNCTION OF LATE IVC AT 825 RPM

All graphical results seem to escalate slightly past case five due to possibly unrealistic boost pressure imposed on the cycle. Given the circumstances and the scope of this task I recognize that the principle of Atkinsons and Millers cycle as successful when used on a medium speed diesel engine.

9.2.4 EXHAUST PHASING

From (7) no benefit in bsfc is expected when phase shifting the whole exhaust event to an earlier EVO. A small reduction is expected in the opposite case however, where the event is shifted to occur at a later point than the standard one. On the KRM-6 the exhaust event originally occurs at 51 degrees cam angle. This corresponds to 102 crank degrees. The following chapters will show the results from reproducing these strategies in GT Power.

9.2.4.1 EARLY EXHAUST PHASING AT 500 RPM AND 5735 NM

Graphical results for this strategy are presented in appendix F. The following diagram shows the experiments that were carried out by shifting the whole exhaust event to an earlier point. In the same figure we see the effect on the mass flow through the valve.

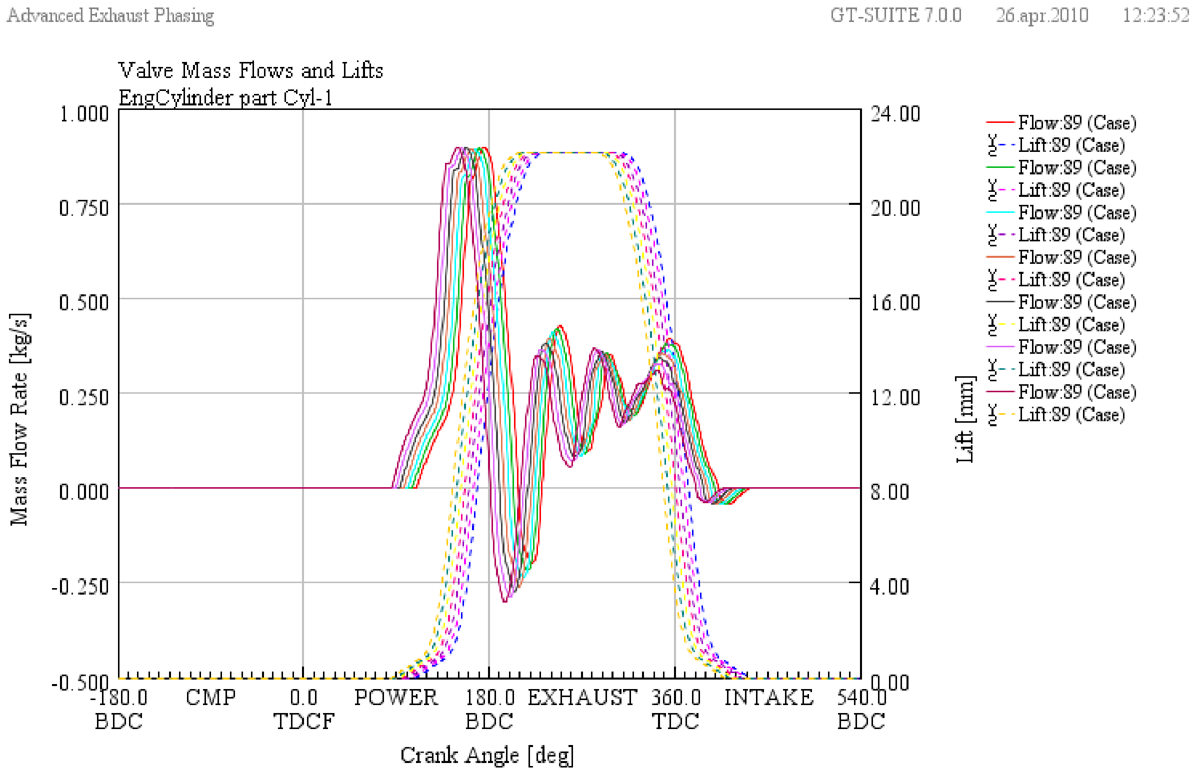

FIGURE 65 - ADVANCING THE EXHAUST EVENT AT 500 RPM

Mass flow pattern suffers little from alteration in this strategy. Losing time for valve overlap is critical at speeds close to idle. A low amount of residual gases is desirable to ensure combustion stability at this point. Little overlap results in poor scavenging causing a high amount of residuals in the cylinder charge. Opening the exhaust at an earlier point is also reducing the expansion stroke which in turn impacts torque output. Less expansion produces less torque.

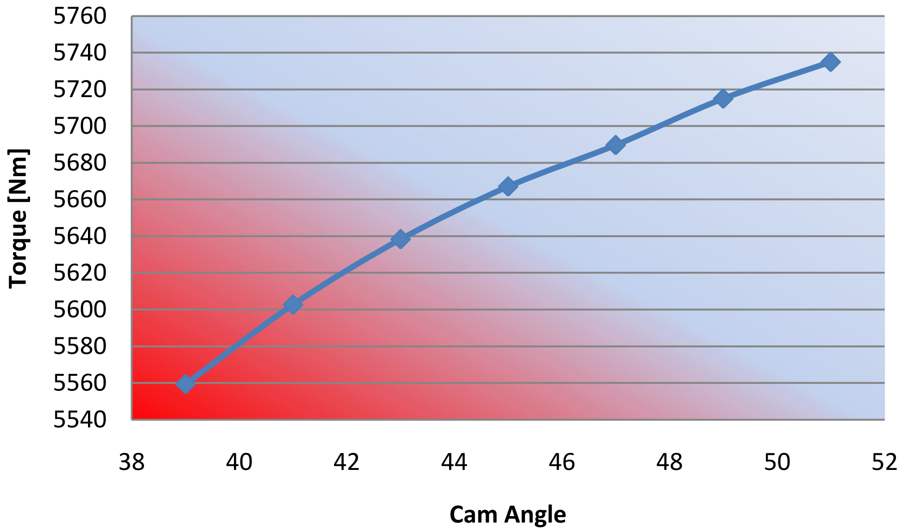

FIGURE 66 - TORQUE REDUCTION CAUSED BY EARLY EVO AT 500 RPM

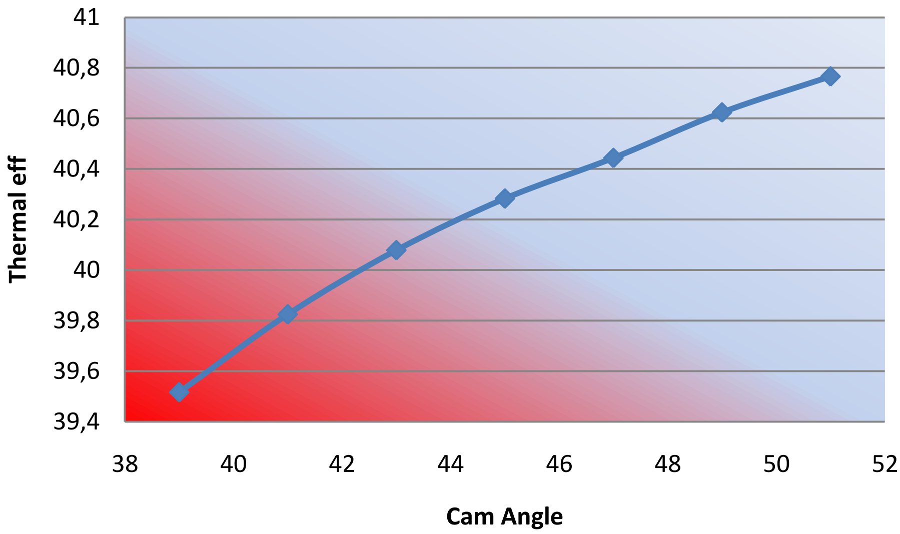

FIGURE 67 - ADVANCED EXHAUST PHASING EFFECT ON THERMAL EFFICIENCY AT 500 RPM

Losing torque will in turn cause a reduction in the thermal efficiency as fuel flow is kept constant through the experiments. Engine friction is controlled to stay constant in all cases.

9.2.4.2 EARLY EXHAUST PHASING AT 825 RPM AND 15464 NM

Expectedly we have no benefit to bsfc using this strategy. The same arguments can be used as for the previous section. I will only present the diagram showing lift and flow relations to verify that the experiment has a similar outcome. Further results can be viewed in appendix G.

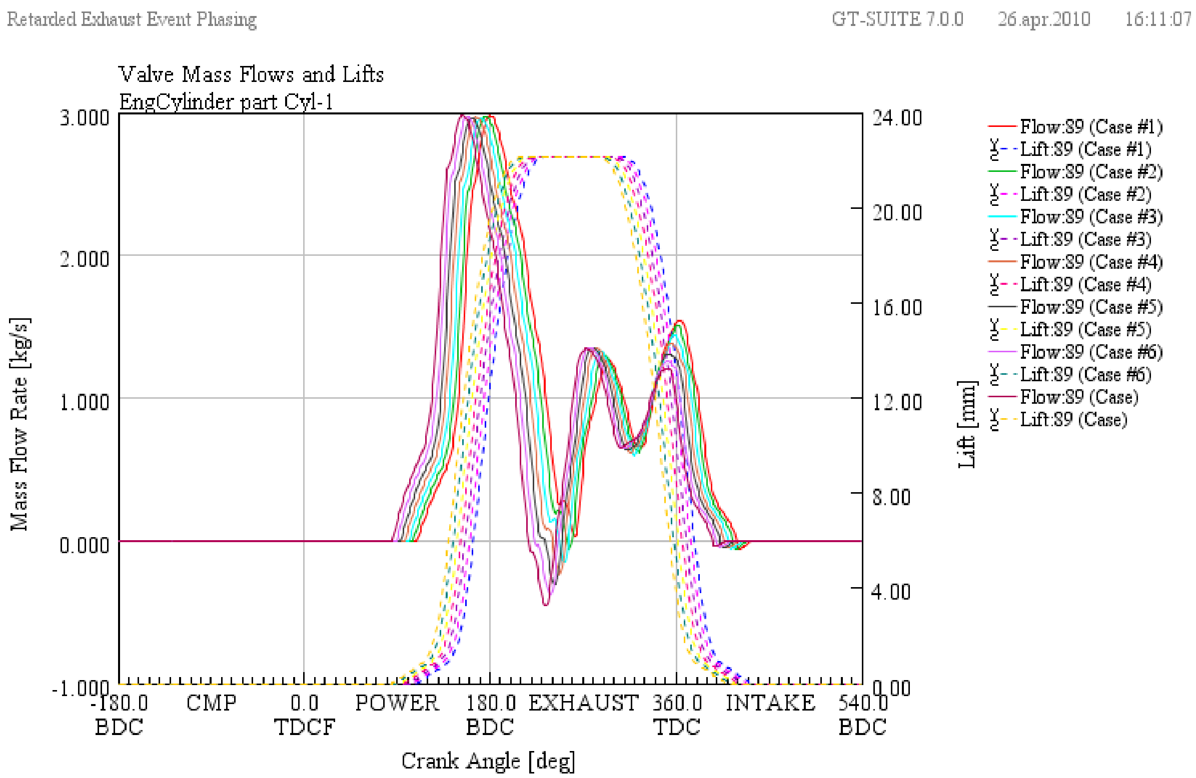

FIGURE 68 - ADVANCING THE EXHAUST EVENT AT 825 RPM

Clearly the strategy reproduces the same effect at high speed. To comment on effects at this operation attention must be made to the peak mass flow at the late part around TDC. We see that flow is restricted when decreasing the overlap. However early opening of the exhaust valve will give more time for blow down, which in high speed mode is desirable.

9.2.4.3 LATE EXHAUST PHASING AT 500 RPM AND 5735 NM

Driving the exhaust event to occur at a later point has been found to produce some bsfc benefit. First a control diagram for mass flow is verifying that the current strategy has no disrupting effect on the flow through the valves. The resulting benefit for this experiment is 0.53% reduction of bsfc. (7) presented a similarly sized value of 1% bsfc reduction using the same range of phase shifting. Extending the range might be interesting in search of greater benefit to fuel consumption, however the experiment was dimensioned similarly to the one made by (7). Full results in appendix H.

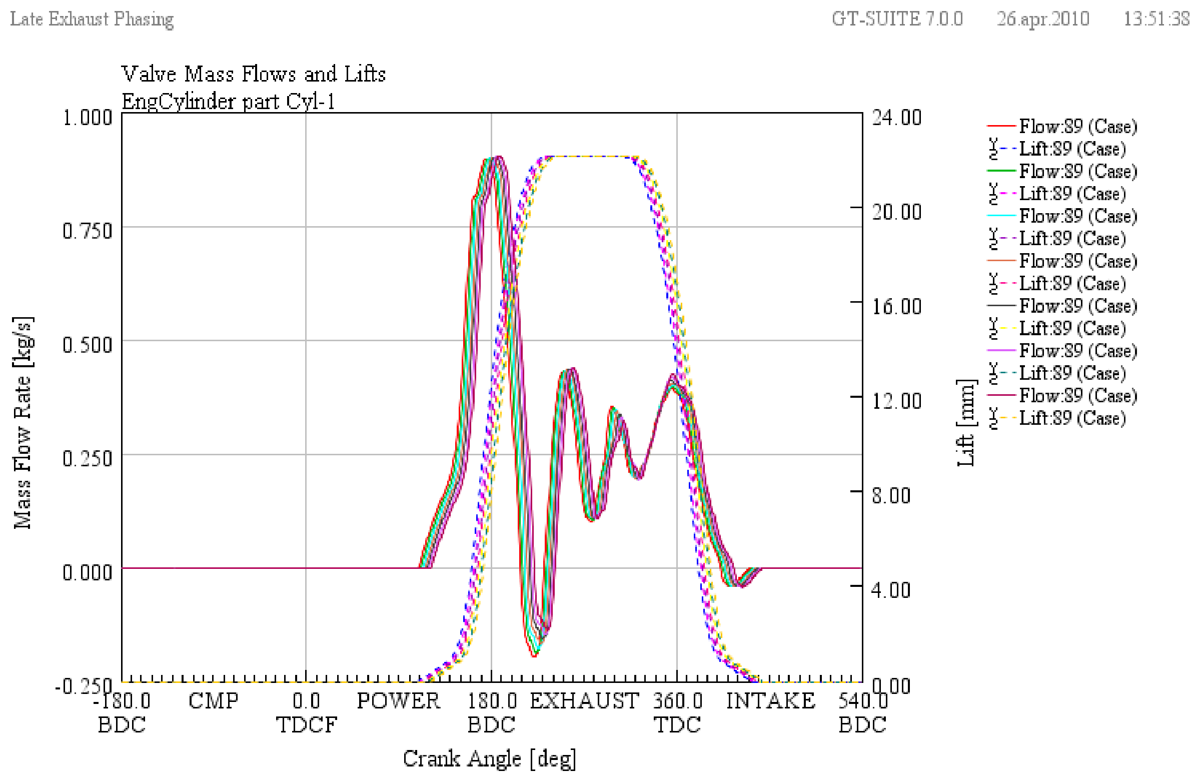

FIGURE 69 - RETARDING THE EXHAUST EVENT AT 500 RPM

The figure above show how the valves open and closes at a later time for each of the cases generated in this experiment. A late exhaust valve closing will effectively increase valve overlap giving more time for scavenging of the cylinder. Less residual gas will be present in the start of cycle air charge.

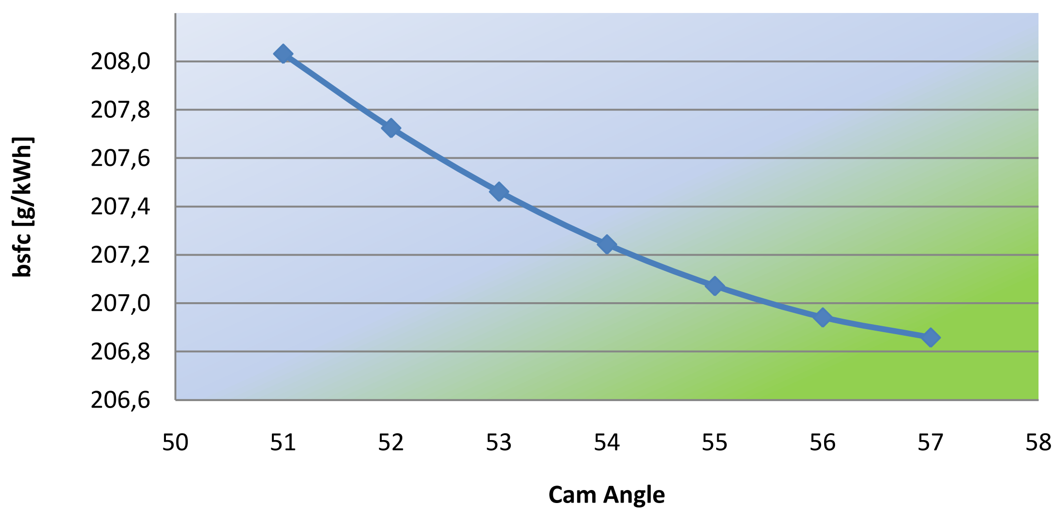

FIGURE 70 - BRAKE SPECIFIC FUEL CONSUMPTION AS A FUNCTION OF LATE EXHAUST PHASING

Interpreting the curve above one would conclude that the maximum fuel saving potential might be located slightly outside of this range. The curve seems to be approaching an optimum. Considering the scope of this thesis no time has been spent on extending this range for the Rolls Royce KRM-6.

9.2.4.4 LATE EXHAUST PHASING AT 825 RPM AND 15464 NM

Shifting the entire exhaust valve event to a later point does not produce any fuel benefit at high speed. However, some increase in volumetric efficiency is evident from the simulation results.

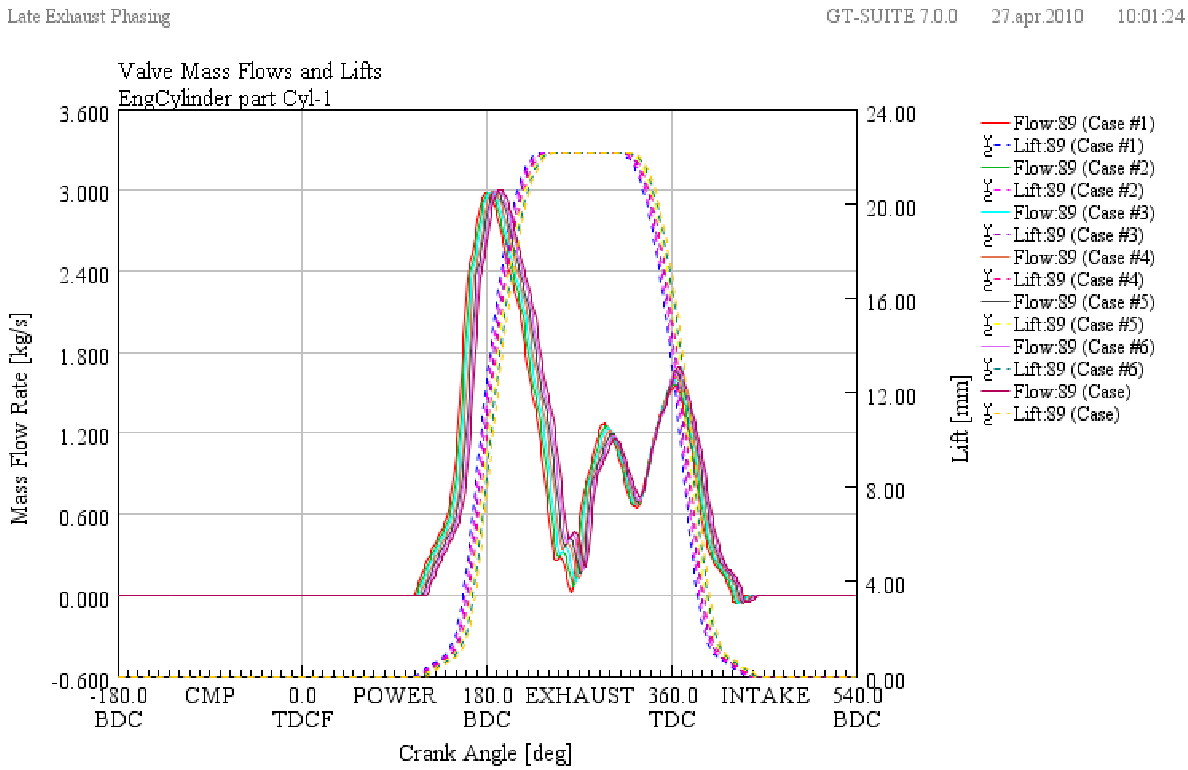

FIGURE 71 - RETARDING THE EXHAUST EVENT AT 825 RPM

Very little back flow of exhaust to the cylinder is recorded during simulations of this experiment. This means that internal EGR at this load point is dysfunctional.

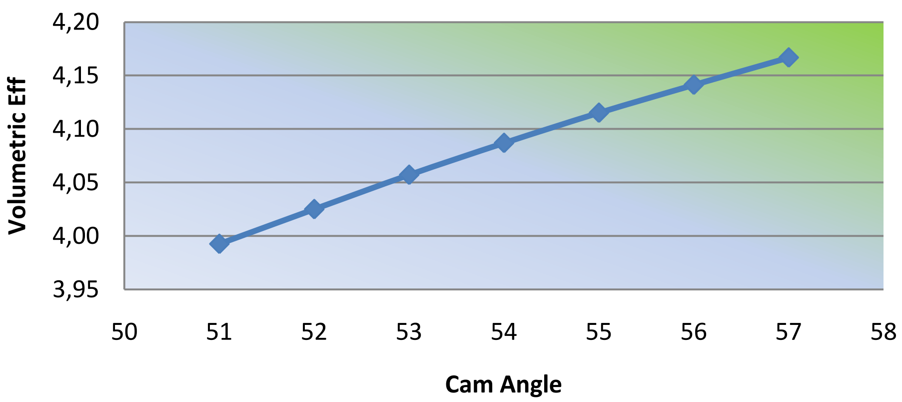

FIGURE 72 - INCREASE IN VOLUMETRIC EFFICIENCY

Although no fuel can be saved using this strategy there is an increase in the amount of air going in as a result of the increased overlap. Exhaust temperature has a slight declination caused by the excess blow by air. All results in appendix I.

9.2.5 INLET PHASING

Shifting the lift curve to an earlier opening point is another way of increasing the valve overlap. This strategy is suspected to produce significant results in the low speed area.

9.2.5.1 EARLY INLET PHASING AT 500 RPM AND 5735 NM

According to (7) there is potential in this strategy to reduce bsfc by approximately 4 percent. Such results were however not obtained except for a slight optimum located at about IVO of 135 degrees cam angle.

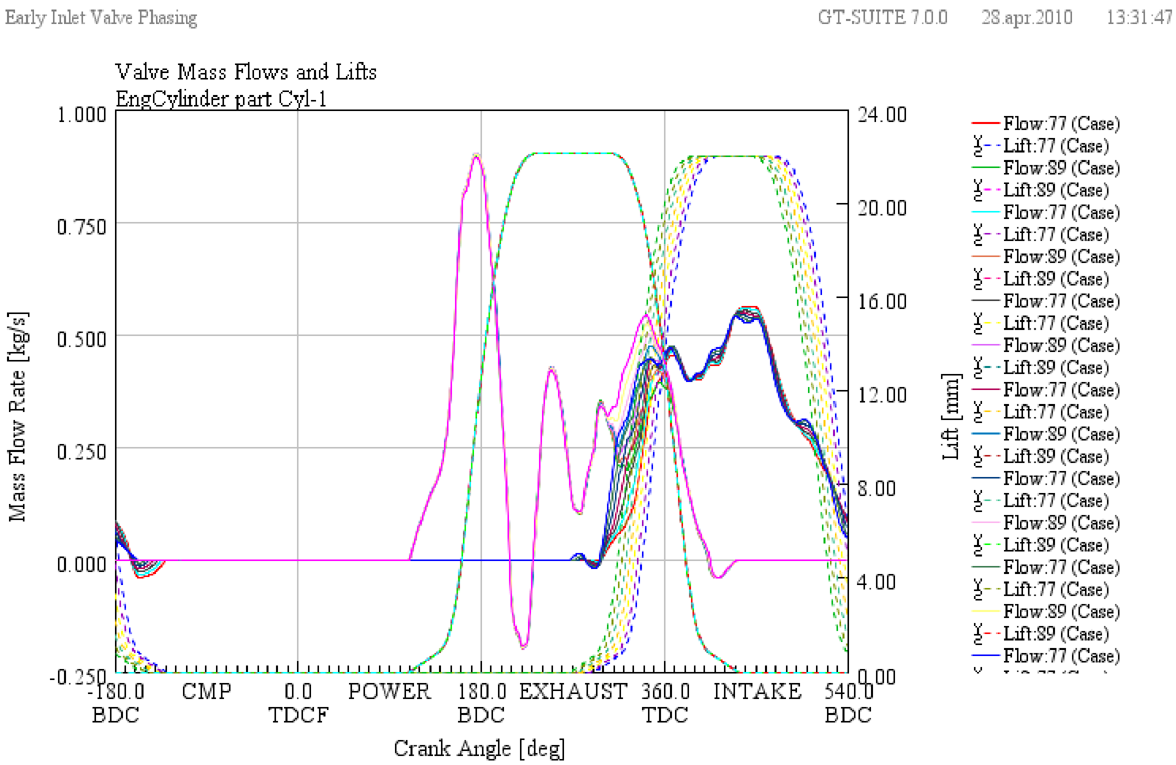

FIGURE 73 - ADVANCED INLET VALVE EVENT AT 500 RPM

The effect of increased overlap is evident. Inlet mass flow increases more rapidly as the valve opens earlier. This seems to be correlated to the dynamics of the exhaust mass flow. The exhaust flow is strengthened by the changing inlet event as inlet air is pulled in displacing the exhaust gas.

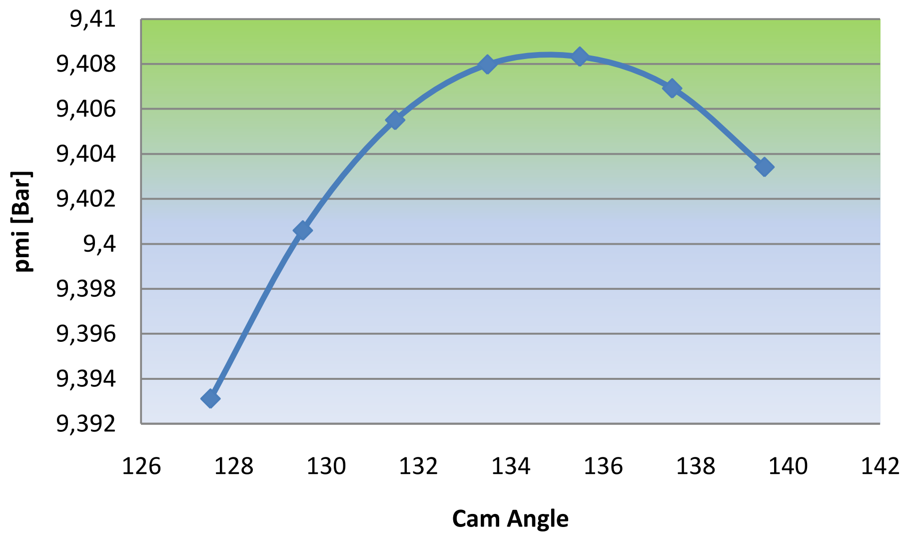

FIGURE 74 - NET MEAN INDICATED PRESSURE AS A FUNCTION OF EARLY INLET VALVE PHASING AT 500 RPM

Note that the pressure axis of the figure above presents a narrow range. The change in pmi is small and the benefit is lost after 135 cam angle degrees. This result causes no significant bsfc benefit as expected from (7). See appendix J for further results.

9.2.5.2 EARLY INLET PHASING AT 825 RPM AND 15464 NM

The dynamics of the valve flows seem to be affected in the same way as it was in the previous section. However no benefit is achievable at all. We see from the graph below how flow dynamics are similar to low speed.

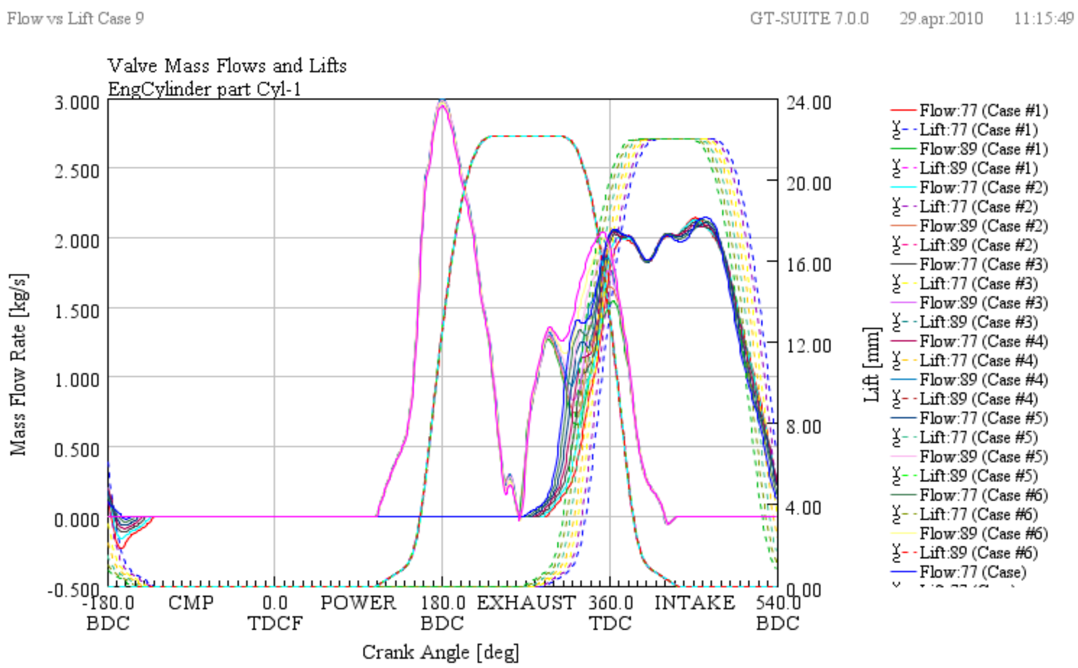

FIGURE 75 - ADVANCED INLET VALVE EVENT AT 825 RPM

Boost pressure in this case has been kept constant as inlet valve phasing did not alter the amount of trapped mass in the cylinder. Additional boost might enhance the charge motion characteristics, but will not be treated in this thesis. Results for this experiment are shown in appendix K.

No benefit was found retarding the inlet valve event and presenting the results in appendixes L and M will be considered sufficient at this point.

9.2.6 RETARDING AND ADVANCING EVO AND IVO BY THE SAME ANGLE

Although this strategy did not produce any beneficial results in (7) it is reproduced in this thesis in search for greater fuel saving potential. The experiment is carried out by four sections where both valve events are retarded and advanced 24 crank angle degrees for low- and high speed operation respectively.

9.2.6.1 LATE VALVE OPENING AT 500 RPM AND 5735 NM

Adjusting the inlet valve opening event is one of the ways to control air supply to the cylinders. This strategy could therefore also be relevant for valve control on a lean burn gas engine. The results achieved in this experiment show some potential as an optimum is located somewhere around 60 degrees EVO and 149 degrees IVO.

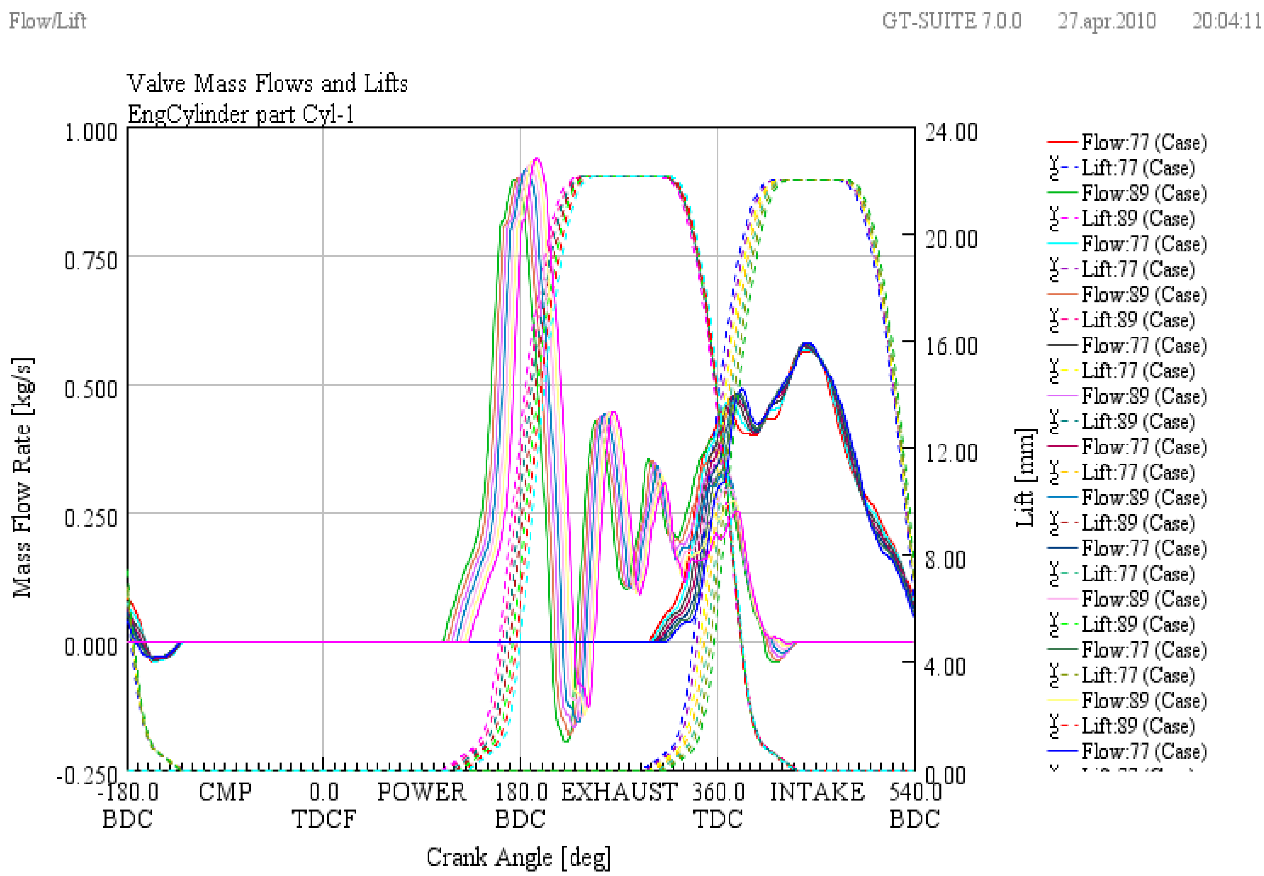

FIGURE 76 - OPENING BOTH VALVES LATE AT 500 RPM

Torque is gained from the increase of expansion stroke until being caught up with valve overlap reduction. More work is required for pumping gases out through the exhaust port and the small torque gain is eventually lost.

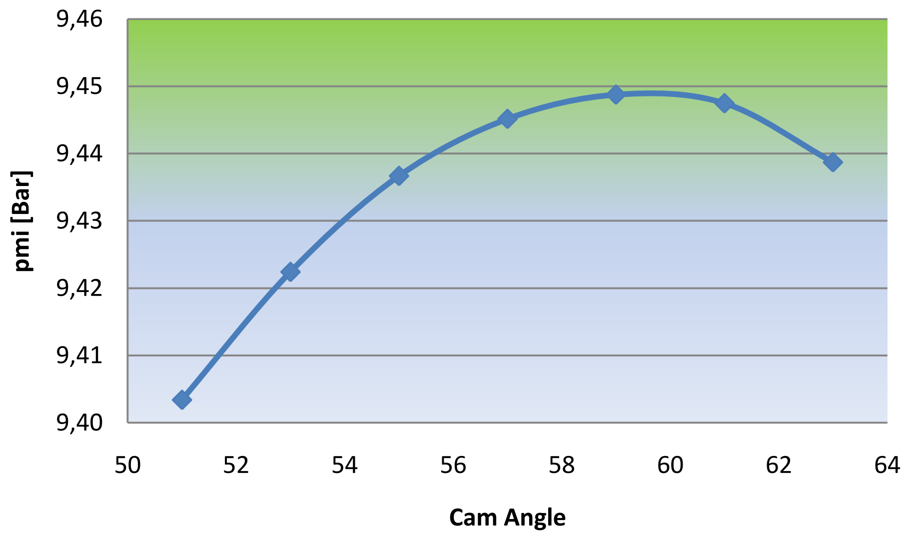

Given a constant fuel flow to the cylinders this increase in power output dictates a proportional decrease in bsfc and an improved thermal efficiency. Total bsfc reduction for this strategy is 0.6%. These results are presented in appendix N.

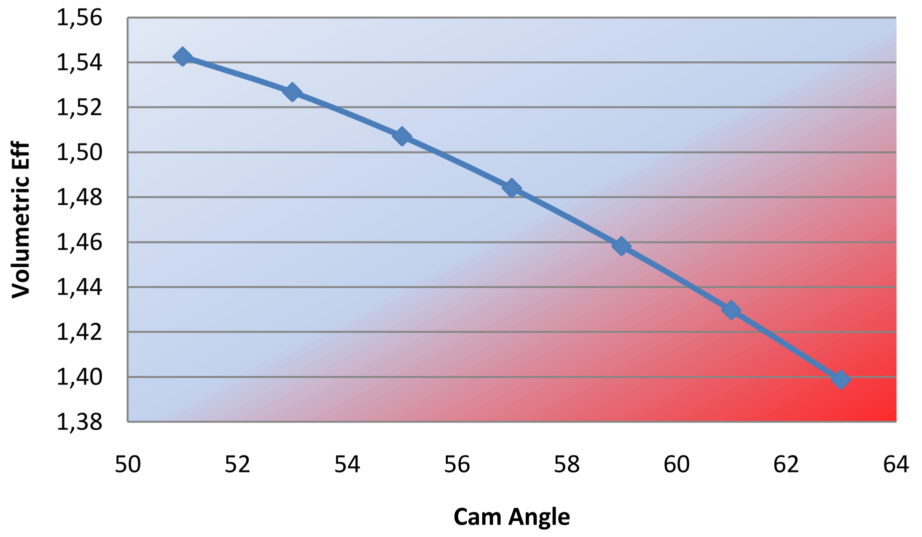

As the valve overlap is reduced by retarding the IVO, volumetric efficiency is lost. Lesser blow by air is used for scavenging of the cylinder. We see how this could be used to control air supply in a lean burn gas engine. These engines require air/fuel ratio to stay constant in order to serve its purpose and through valve control this ratio can be adjusted for any operation.

The following experiments produced no beneficial results to fuel consumption:

- Late dual valve opening at 825 rpm and 15464 Nm
- Early dual valve opening at 500 rpm and 5735 Nm
- Early dual valve opening at 825 rpm and 15464 Nm

The results for these strategies are presented in appendixes O, P and Q respectively.

9.2.7 DUAL RETARD OF IVC AND EVC

Another strategy that produced promizing results in (7) was retarding both valve closing events to a later point than the original valve events. Reductions in bsfc of 3 and 4 percent were found in the low and high speed cases respectively. Keeping the trapped mass constant by adjusting the boost pressure together with this type of valve control had significant impact on mass flow through both the valves. Significant fuel savings were found in this thesis as well. This was done by retarding the IVC and EVC by 77 and 83 crank angle degrees respectively. This is range is quite a substantial part of the given stroke, but I would rather choose too great a range than one that is too small in order to cover the area where benefit is produced. This range was used in both high speed and low speed operation.

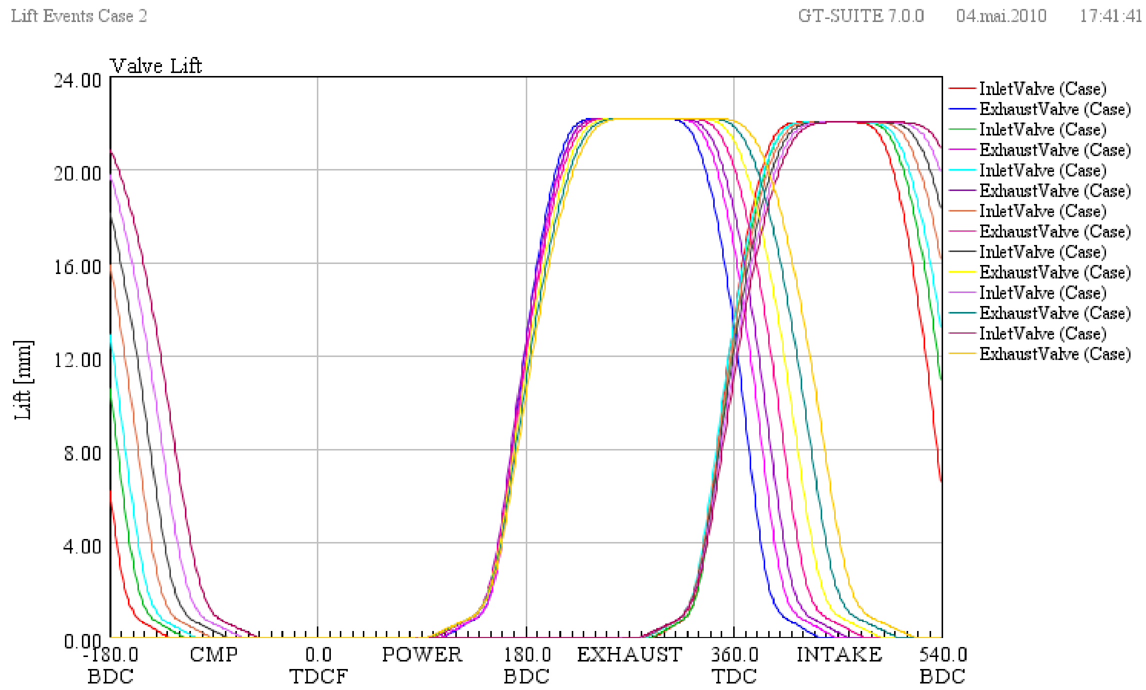

FIGURE 77 - DELAYED EVC AND IVC AT 500 RPM AND 825 RPM

We see how the event variation is covering a large area of its given stroke. IVC in the 8th case is probably too late compared to the effective stroke left to compress the charge. I will control the outer points of this experiment by analyzing the boost pressure required to maintain constant trapped mass.

9.2.7.1 RETARDING CLOSING EVENTS AT 500 RPM AND 5735 NM

As seen from the flow characteristics through the valves below there are a substantial effect from boosting the charge air supply. Identifying the realistic boost pressure is outside the scope of this thesis, however I would assume that case 4 or 5 is on the verge of exceeding realistic values of what is possible in terms of boosting the charge pressure. This judgment is based on the imposed pressure escalation from case 5 through 8.

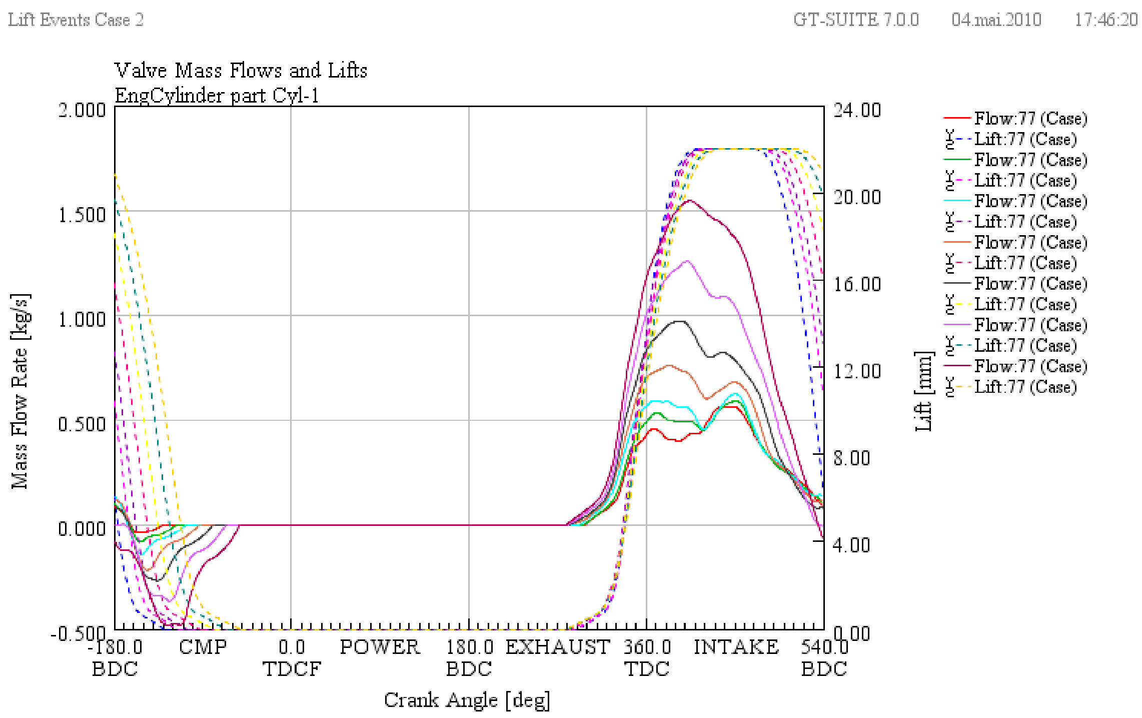

FIGURE 78 - INLET AIR MASS FLOW AT 500 RPM

For case five mass flow is indicated by the black line in the diagram above. There is a clear escalating effect in mass flow caused by adjusting the boost pressure too high. Boost pressure is adjusted by an inlet receiver pressure multiplier. Analyzing this multiplier shows the same jump at this point. Given that case five represents our boundary, there exists a potential of reducing bsfc by 2.5 percent using this strategy at low load for the KRM engine.

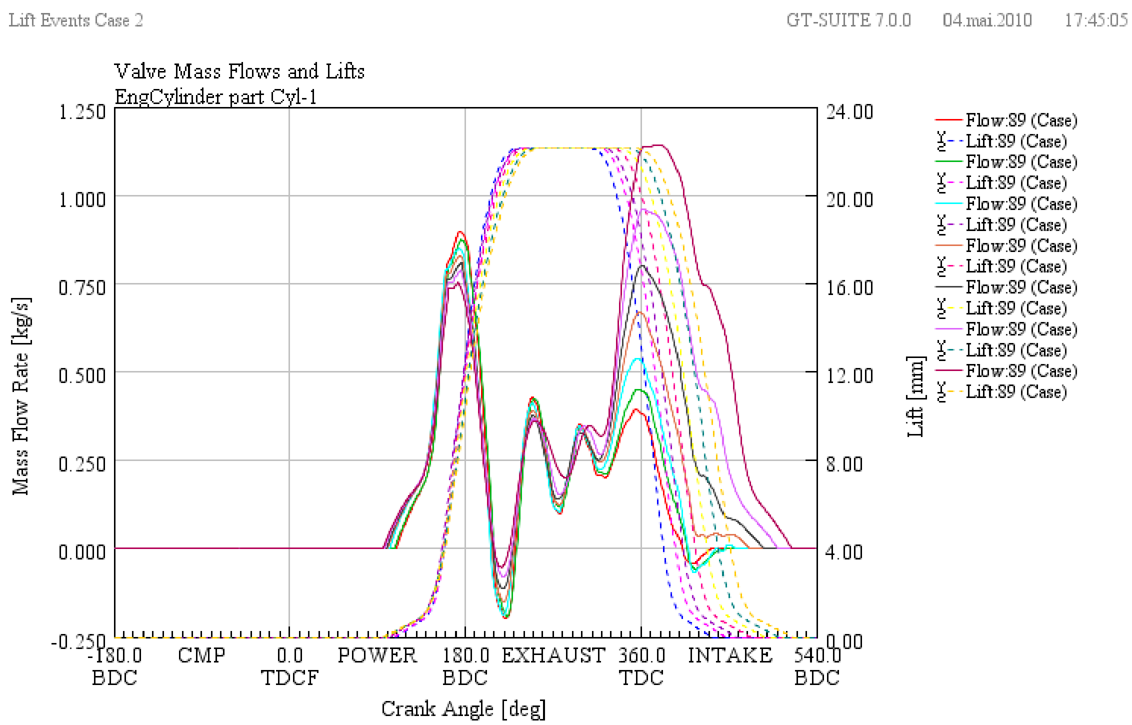

FIGURE 79 - EXHAUST MASS FLOW AT 500 RPM

The same escalating effect is present in the exhaust mass flow, indicating a great deal of blow-by occurring as the exhaust valve is left open far into the intake stroke. Note that case four represents a valve operation which eliminates back flow of exhaust to the cylinder charge. This is valuable in low load operation to ensure smooth running and stabile combustion.

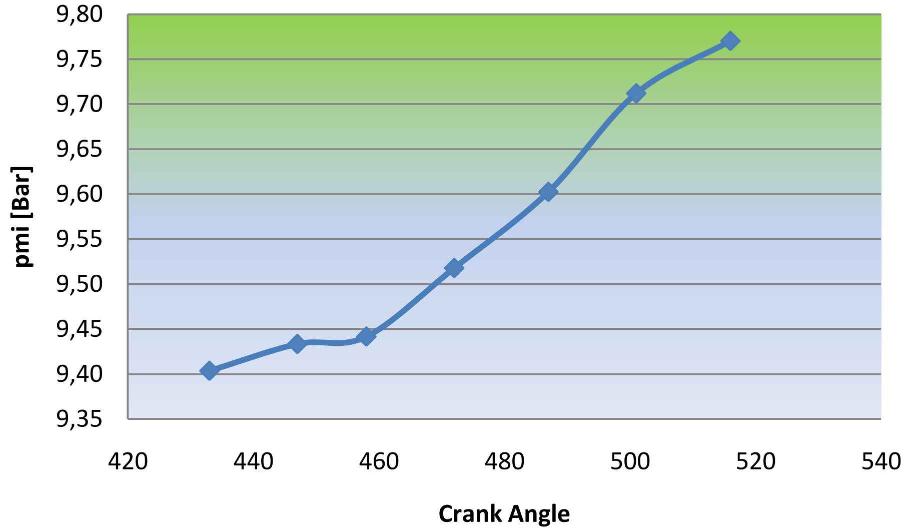

FIGURE 80 - NET MEAN INDICATED PRESSURE AT 500 RPM

A closer look at the net mean indicated pressure shows how the boost affects combustion properties. Escalation occurs during cases four and five in which an excessive boost pressure is needed to ensure the required trapped mass amount. The same can be seen from the volumetric efficiency presented below.

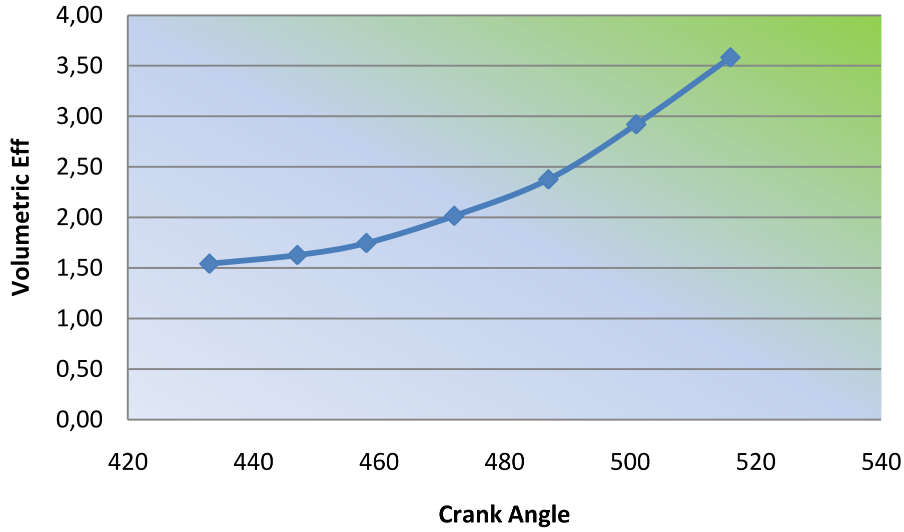

FIGURE 81 - VOLUMETRIC EFFICIENCY AT 500 RPM

Complete set of graphical results in appendix R.

9.2.7.2 RETARDING CLOSING EVENTS AT 835 RPM AND 15464 NM

Reproducing the experiment for the high speed case produces results of similar character to the previous section. These results are however lacking the significant magnitude of reduction regarding the fuel consumption. A maximum bsfc reduction of one percent is recorded in this strategy. True to the principle I recognize that keeping the exhaust closed for the majority of the exhaust stroke increases torque output. This is producing a benefit in thermal efficiency due to the constant fuel mass inserted per cycle.

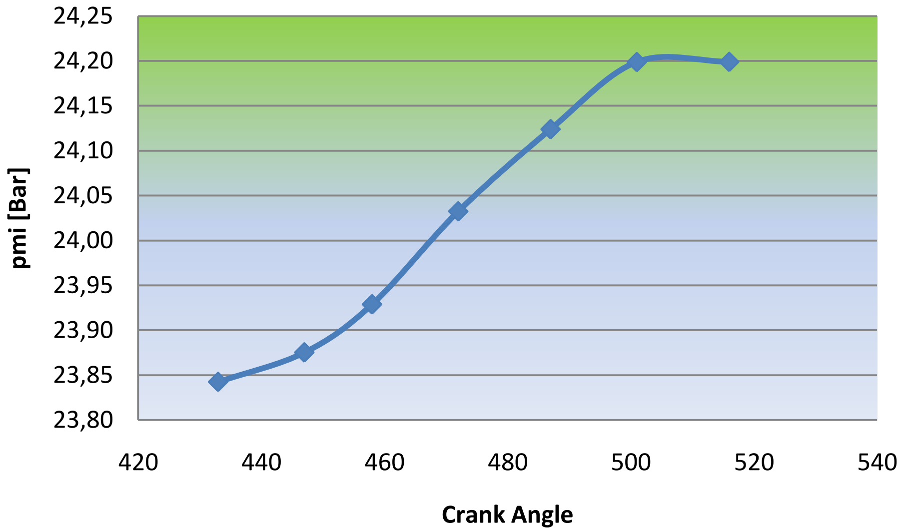

FIGURE 82 - NET MEAN INDICATED PRESSURE AS A FUNCTION OF CRANK ANGLE AT 825 RPM

Case four is recorded as the maximum fuel saving potential in this thesis due to the suspicions of unrealistic boost pressure values. As the aim is to illuminate the principles of valve control on a medium speed diesel engine, it is considered sufficient at this time.

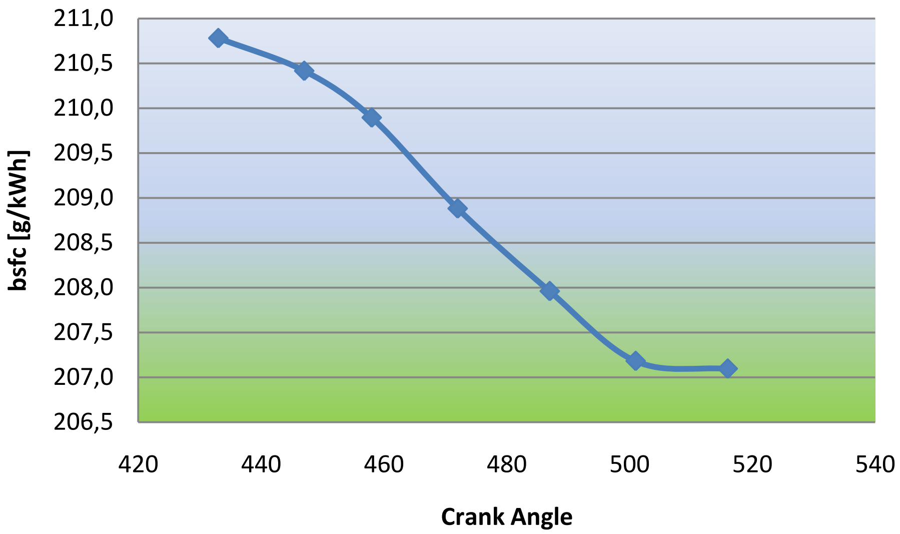

FIGURE 83 - BRAKE SPECIFIC FUEL CONSUMPTION AS A FUNCTION OF CRANK ANGLE

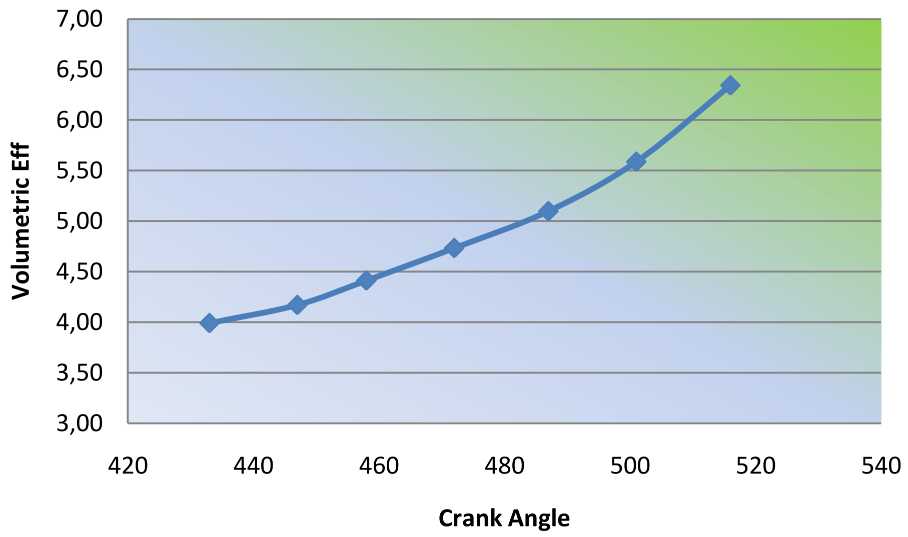

FIGURE 84 - VOLUMETRIC EFFICIENCY AS A FUNCTION OF CRANK ANGLE

Complete results for this strategy in appendix S.

9.3 EMISSIONS

In order to give further evaluation of the results produced in the experiments, attention is paid to the emissions produced in the strategies with the best results. Today there is a lot more focus on "green" technologies. Emissions requirements have become a driving force for combustion engine development as a cause of this. Economy has less impact on final engineering solutions as engineers are pushed to utilize more advanced technology despite the higher cost. As the combustion process itself is believed to hold a limited potential with regard to exhaust emissions engineers give focus to exhaust after-treatment. Although this is an important development, exhaust after treatment tends to be less cost efficient. Valve control may serve a substantial part in reducing emissions from combustion. The main focus here is to optimize the process in all its operating conditions, meaning less fuel is spent without reducing functionality and or payload of the vessel. In addition to this, the automotive industry has shown examples where valve control has provided beneficial impact on specific amounts of unwanted substances such as NOx, carbon based emissions and particles.

Although my model contains some limitations concerning in-cylinder flow simulation I will search for results in the strategies that are the most promising.

9.3.1 MILLER/ATKINSON VALVE TIMING

Expected from the Miller and Atkinson cycle is the ability to reduce the specific heat of the charge making combustion possible at a lower temperature and with less NOx forming hot spots. The model used to simulate combustion in GT-Power seems to contain some limitations in the effect that valve timing is supposed to have on the initial cylinder charge. As the inlet valve closes GT-Power considers a trapped charge with predetermined properties, meaning that some of the physical impact from valve events might be lost. Given the time and scope of this thesis I will analyze the effect obtained by the strategies presented above.

9.3.1.1 EARLY IVC WITH FIXED IVO

Closing the inlet air supply before completing the downward motion of the piston makes for an expansion of the trapped charge. This affects the charge by lowering the temperature even further at the start of compression. Total mean combustion temperature is lowered and fewer hot spots is expected. Although no significant reduction is found in the maximal combustion temperature of this experiment, there was a massive effect on the temperature in the unburned zone. Surrounding conditions showed a 9.2 percent lower temperature compared to the standard configuration. This is supportive of the theory regarding lesser hot spots during combustion. Due to the simplicity of my combustion model no recordings are made of combustion NOx concentration. However there were recordings of most other emissions. The effect of early IVC on some of these is presented below.

VVT Config	IVC [Cam Degrees]	CO (ppm)	CO2 (ppm)	Hydrocarbon (ppm)
Standard	277.3	0.87	57004.20	0.43
Early 1	271.4	0.87	57069.00	0.43
Early 2	265.5	0.86	56323.50	0.43
Early 3	259.6	0.85	55452.40	0.43
Early 4	253.7	0.81	53211.60	0.40
Early 5	247.8	0.79	51554.10	0.39
Early 6	242.0	0.75	48863.40	0.38
Early 7	236.1	0.71	46022.80	0.35
Early 8	230.2	0.66	42821.00	0.33
Early 9	224.3	0.61	39200.10	0.30

TABLE 2 - EMISSIONS REDUCTION IN HIGH SPEED OPERATION USING EARLY INLET VALVE CLOSING

Substantial emission reductions are evident from the table above. Carbon monoxide, carbon dioxide and unburned hydro carbons are reduced by 30, 31 and 30 percent respectively when comparing the most successful case to standard valve configuration.

VVT Config	IVC [Cam Degrees]	CO (ppm)	CO2 (ppm)	Hydrocarbon (ppm)
Standard	277.3	1.35	53319.70	0.41
Early 1	271.4	1.37	53906.90	0.42
Early 2	265.5	1.36	53106.30	0.41
Early 3	259.6	1.30	50440.20	0.38
Early 4	253.7	1.24	47640.20	0.37
Early 5	247.8	1.16	44494.80	0.34
Early 6	243.0	1.10	42269.10	0.32
Early 7	237.1	1.02	39424.50	0.30
Early 8	231.2	0.93	35998.90	0.27
Early 9	225.3	0.84	32357.90	0.25

TABLE 3 - EMISSIONS REDUCTION IN LOW SPEED OPERATION USING EARLY INLET VALVE CLOSING

High speed operation is able to produce better relative emission results in all areas compared to low speed. Carbon monoxide, carbon dioxide and unburned hydro carbons are reduced by 38.0, 39.3 and 39.0 percent respectively.

9.3.2 LATE IVC WITH FIXED IVO

The other way to reduce the effective compression ratio is to keep the inlet valve open for some time after BDC, causing a backflow of air to the inlet manifold. This reduction gives the same effective temperature reduction in the unburned zone (8 percent mean temperature reduction in low speed operation). On the other hand an optimum seems to exist regarding the carbon based emissions in this strategy.

VVT Config	IVC [Cam Degrees]	CO (ppm)	CO2 (ppm)	Hydrocarbon (ppm)
Standard	277.3	1.35155	53319.7	0.40572
Late 1	283.2	1.3329	52354.7	0.398355
Late 2	287.1	1.30174	50817.8	0.382475
Late 3	293.0	1.22546	47668.5	0.360142
Late 4	298.9	1.15999	44735.9	0.341003
Late 5	304.7	1.29907	46948.4	0.356125
Late 6	310.6	1.51502	49734.9	0.381714

TABLE 4 - EMISSIONS REDUCTION IN LOW SPEED OPERATION USING LATE INLET VALVE CLOSING

Case four stands out as the optimal case for clean emissions during low speed. Carbon monoxide, carbon dioxide and unburned hydro carbons are reduced by 14, 16 and 16 percent respectively.

VVT Config	IVC [Cam Degrees]	CO (ppm)	CO2 (ppm)	Hydrocarbon (ppm)
Standard	296.0	0.87	57004.20	0.43
Late 1	303.0	0.86	56086.50	0.43
Late 2	311.0	0.86	56131.20	0.43
Late 3	318.5	0.84	54835.00	0.42
Late 4	326.5	0.83	53914.20	0.41
Late 5	334.5	0.81	52681.50	0.40
Late 6	342.0	0.79	50750.30	0.39
Late 7	350.0	0.79	49860.50	0.38

TABLE 5 - EMISSIONS REDUCTION IN HIGH SPEED OPERATION USING LATE INLET VALVE CLOSING

Promising results are recorded also for the high speed operation for this strategy. Carbon monoxide, carbon dioxide and unburned hydro carbons are reduced by 6.9, 7.6 and 7.0 percent respectively. Cases six and seven are discarded on the basis explained previously.

9.3.2.1 CONCLUSION – MILLER/ATKINSON VALVE TIMING

Given the simulation results presented above there is a clear indication that early closing of the inlet valves give greater benefits for emissions than closing late. It can be confirmed that this strategy is the most beneficial of all strategies presented in this thesis. This result is supported from (7) where the same strategy was preferred. In all Miller- and Atkinson experiments performed in this thesis a lowered mean cylinder temperature was proven. Even though no NOx concentration numbers could be recorded this fact indicates that benefits regarding NOx emissions is obtainable in real life.

9.3.3 LATE VALVE EVENT CLOSING

Configuring both valve closing events to occur at a late point was among the strategies providing most beneficial to bsfc. Naturally this strategy contains elements from the Atkinson cycle by closing the inlet valve at a late point. At low speed this strategy proves more efficient than its Atkinson equivalent (Atkinson imposed on the same operating point) and is potentially a more desirable solution if emission levels are similar or even lowered.

Case	EVC [Crank Angle]	IVC [Crank Angle]	CO (ppm)	CO2 (ppm)	Hydrocarbon(ppm)
1 (Standard)	433	591	1.35	53319.70	0.41
2	447	604	1.29	51347.30	0.40
3	458	614	1.18	48792.20	0.37
4	472	627	1.04	43574.50	0.33
5	487	641	0.88	37268.60	0.28
6	501	654	0.71	30419.70	0.23
7	516	668	0.58	24916.30	0.19

TABLE 6 -EMISSIONS REDUCTION IN LOW SPEED OPERATION USING LATE VALVE EVENTS CLOSING

We see promising emission results using this strategy as well. However the result does not completely match the early IVC at low speed operation, however in comparison with late IVC with fixed IVO this strategy is superior. Carbon monoxide, carbon dioxide and unburned hydro carbons in this experiment are reduced by 35.0, 30.1 and 30.0 percent respectively. Case six and seven is discarded on the previously explained basis.

Case	EVC [Crank Angle]	IVC [Crank Angle]	CO (ppm)	CO2 (ppm)	Hydrocarbon (ppm)
1 (Standard)	433	591	0.87	57004.20	0.43
2	447	604	0.83	54925.10	0.42
3	458	614	0.77	52665.10	0.40
4	472	627	0.72	49965.30	0.38
5	487	641	0.67	47071.70	0.35
6	501	654	0.61	43121.90	0.32
7	516	668	0.53	37881.50	0.28

TABLE 7 - EMISSIONS REDUCTION IN HIGH SPEED OPERATION USING LATE VALVE EVENTS CLOSING

Carbon monoxide, carbon dioxide and unburned hydro carbons in this experiment are reduced by 17.2, 12.3 and 11.6 percent respectively. Cases five, six and seven are discarded on previously explained basis. Compared to late closing at a late stage this strategy produces better results regarding exhaust emissions. This means that in any case retarding the inlet closing events for both valves will serve as a cleaner solution over late inlet valve closing alone. We now see the importance of being able to control valves continuously in order to change strategies when load and speed is changed.

9.3.4 CONCLUSION EMISSIONS

As shown by results above the best solution to both high speed and low speed operation seems to be Miller valve timing. Closing the inlet valve early is preferred in all cases where a bsfc benefit is proved. Emissions for experiments without benefit to bsfc have not been included in this thesis. However attention could be paid to cases where bsfc is nearly constant. There is no such case recorded in the simulations of this thesis. All emission results in appendix T.

10 CONCLUSION

A simplified model of the Rolls Royce KRM-6 engine, capable of simulating all relevant engine operating points regarding power and speed was established. This was done by recalibrating a KRG-6 model previously used for simulation of a generator load operation. Calibration work proved to constitute a great deal of the initial work load and was carried out after reevaluating possible benefits from camless operation. The latter section was meant as a supplement to the literature study carried out in (1). It also served as a reference to the final simulation results as the desired outcome was stated in advance.

In order to recieve any simulation results from combustion cycle enhancement using valve control, the model needed even more preparations. GT-Power is based on traditional cam shaft valve train propulsion. However parameters used for adjusting the valve lift curve enabled the user to manipulate the curves in a satisfactory manner. Some further adjustments were desired to get the curve shapes exactly right, but parameters for lift manipulation was nevertheless limited.

Valve control experiments concerning valve timing were based on a study from the automotive industry. Valve control is most proven in this part of engine manufacturing industry. Strategies from (7) were reproduced in order to hold a proper basis for comparison. In both (7) and this thesis, Miller timing strategies were found most beneficial to bsfc as well as emissions. There were however a Miller timing hybrid strategy showing even more potential in emissions reduction. This strategy did not only close the inlet valve at a late point. Exhaust valves were closed at an approximately equally late point. Results are presented in appendixes for performance and emissions. For given strategies a proposed optimal valve operation was determined on the basis of simulation results. In some cases where no clear optimum could be found the best valve operation configuration was based on engine performance limitations assumed to lie within the range of the experiments. Close matching was found when comparing most of the strategies to (7), there were however one strategy that did not live up to its potential. Early Inlet Valve Event Phasing was believed to produce great benefit at low speed operation. No such results were obtained when reproducing the strategy for the KRM-6.

To conclude for this thesis as a whole I would say that the main principle of continuous valve control on a medium speed diesel engine has been shown. Potential fuel savings has in some cases shown to be of great magnitude. The values obtained show a matching to the reference from automotive industry. Marine energy production units compared to automotive applications are operated for longer periods in time. In addition the marine engines are bigger in terms of power. This would indicate that these engines will be underestimated compared to an automotive engine when compared on the basis of bsfc savings. 5 percent reduction in bsfc on a large medium speed engine would yield a much higher total mass of fuel saved in a life cycle perspective.

11 FURTHER WORK

Through calibration and the use of the KRM-6 model some areas of improvement are identified. As a natural part of completing a task one realizes that some areas will remain undone. As a substitute for taking on the extra challenges I wish to make a chapter in this thesis of what further work is needed to enhance the quality of this paper.

11.1 CYLINDER FLOW

GT-Power offers possibilities of implementing dependence objects to simulate in-cylinder flow on basis of certain reference objects. Initial state of the charge, cylinder geometry and imposed conditions are among the categories that serve as a reference. Swirl patterns and development of in cylinder tumble can be determined using these references. Lack of data regarding swirl and tumble in the KRM-6 flow dynamics prevents me from simulating a realistic in-cylinder flow. Combustion is based on initial charge properties and a load dependent rate of heat release.

There is also no clear reference present to create a proper link between the inlet valve flows and cylinder charge motions. We have shown that inlet air velocity is affected greatly by controlling the valve actuation. Further work should be done by providing data for the cylinder air flow references above. Using the standard cam based valve train this flow could be properly simulated for standard valve operation. Then additional analysis could be done by linking the flow parameters to the valve actuation variables so that flow alterations would become clear when proposing a certain VVC strategy. As no link is present in GT-Power one would have to create parameter based links between inlet air velocity and cylinder flow dynamics and initial charge properties on a theoretical basis.

11.2 LIFT EXPERIMENTS

To validate the effect of work done in the previous chapter, lift height variation experiments should be carried out and completed. The valve flow velocity change has already been proven to be dependent on the lift height as area and trapped mass is kept constant. (7) does not provide any results regarding variable valve lift. Another reference would thus be needed. Such reference should be easily obtainable through theory or papers published in the automotive industry.

11.3 SYSTEM IMPLEMENTATION

In (1) a reliable valve control system independent on the crank mechanism is analyzed through study of recent subject literature. The two spring pendulum valve actuation design with electronic latching presented by (9) is shown in appendix U .This technology was regarded as very promising. This system is highly compatible with common rail fuel supply, a technology increasingly available on modern day diesel applications. The system is also fairly simple compared to the vast variety of tasks it is capable of performing. The fact that this system suffers from none of the major problems that prevent complete valve control on medium speed diesel engines, is its best advantage against its competitors. The system schematics are shown in appendix U. Supplying complete energy consumption calculations for this system using valves in KRM dimensions would provide better indication to system benefits compared to cam shaft operation of the original valve train.

11.4 TUNING

Continuous variable valve control requires a different kind of turbocharger in order to vary boost pressure according to given strategies. Variable geometry turbines are needed to create the conditions valid for this thesis. No such turbocharger model has been used in this thesis. Boost pressure has been adjusted manually to ensure a constant trapped mass for each of the proposed strategies. Using a turbocharger in any engine yields pressure pulses in the inlet manifolds. In this thesis only constant inlet dynamics have been simulated. The ability to simulate pressure pulses would enable the tuning aspect of valve control possibly increasing or decreasing the potential of currently proposed strategies. GT-Power should in theory be capable simulating a dynamic inlet manifold pressure of a given load. Such conditions should be implemented to make the model more realistic.

11.5 MORE VALVE CONTROL STRATEGIES

As this thesis based its valve control experiments on a given study carried out by (7) there might be more timing strategies possible of creating a bsfc benefit to a medium speed diesel engine. Further research should be able to discover more studies that could serve as reference for new valve actuation strategies. If not, strategies should be made and investigated to further map the potential performance benefits in medium speed diesel engines.

11.6 LIFE CYCLE ANALYSIS

When a certain bsfc benefit is ascertained one may study the running of the engine in a life cycle perspective. This may be done either from a manufacturer's view with a main focus on carbon foot print and other emissions requirements, or alternatively from the users angle with a main focus on life cycle cost. 5 percent savings in bsfc may add to a great economic savings depending on the size of engine and hours of use and mean time between failures. As my engine is particularly outdated and only a limited record of operation is obtained at this point, no life cycle calculations have been presented. However were data obtainable, it would be interesting to see the potential cost and emission savings through the life of such an engine.

11.7 ENGINE PERFORMANCE

In some of the valve control experiments the obtainable benefits sometimes appeared to be unlimited. This might be correlated to the fact that charge boost pressure is set manually and gives life to unrealistic turbocharger performance. To me, little is known about variable geometry turbines at the time of writing. It is however assumed that an increased charge boost pressure is obtainable. The magnitude of this boost pressure on a KRM-6 engine is unknown. Optimal valve operation is therefore determined on the assumption that the boost pressure through variable geometry has limitations within the range of these experiments. There lies great potential for improvement in this part of the thesis. However realistic turbocharger operation in connection with variable valve requires a great deal of data on a turbocharger that does not exist at this time.

To further improve model performance the fuel controller template should be reestablished in the model. This could enable me to target a certain load for each of the strategies and the given fuel consumption benefit would be evident in a lower injected mass per cycle. The bsfc benefit in this thesis is recorded as more torque is gained for a given fuel flow. The first case is considered the most realistic in terms of ship operation at sea as a certain load is needed to perform certain tasks.

12 ACKNOWLEDGEMENTS

I would very much like to convey my heartfelt to staff members at NTNU Marine Technology Systems Department; Professor Harald Valland and PhD candidate Nabil Al Ryati.

Al Ryati has spent a great deal of time in the final stages of his PhD thesis no less, to mentor me in my hours of need. His knowledge regarding GT-Power is unequaled at the institute and was of inestimable aid when getting to grips with the software.

Professor Valland by virtue of his superior understanding of diesel engine operation, kindly provided invaluable guidance throughout the project. He instigated the vital connection between Al Ryati and myself, ensured unhindered access to required software and - in short - ensured I knew how to operate it.

Additionally I would like to direct thanks to Rolls Royce Marine, Engines Bergen. Especially engineer Even Høgset Olsen who has generously served as an important source of information about the KRM-6 engine and its applications.

13 WORKS CITED

1. **Sæle, Hans.** *Variabel ventilstyring av medium speed dieselmotorer.* Trondheim : NTNU, 2009.

2. **Levin, M. M. Schechter and M. B.** *Camless Engine.* s.l. : Society of Automotive Engineers, 1996.

3. **Answers Corporation.** www.answers.com. *www.answers.com.* [Online] 2010.

4. **Ryati, Nabil Al.** 2010.

5. **Gamma Technologies Inc.** Correlating an engine model to measured data. s.l. : Gamma Technologies, 2006, p. Chapter 10.

6. *Project Guide Marine Propulsion Plant.* s.l. : Rolls Royce Marine AS Engines Bergen, 2001.

7. **Stobart, Jiamei Deng and Richard.** *BSFC Investigation Using Variable Valve Timing.* Laougbourough : SAE, 2009.

8. **Stapersma.** *Diesel Engines Volume Two - Turbocharging.* Delft : TU Delft, 2009.

9. **Zeng (David) Lou - LGD Technology, LLC.** *Camless Variable Valve Actuation Designs with Two-Spring Pendulum and Electrohydraulic Latching.* s.l. : SAE , 2007.

14 ABBREVIATIONS

BDC:	Bottom dead center
Bmep:	Brake mean effective pressure
Bsfc:	Brake specific fuel consumption
CMP:	Compression
CO:	Carbon monoxide
CO_2:	Carbon Dioxide
DI:	Direct injection
EGR:	Exhaust gas recirculation
EVO:	Exhaust valve opening
EVC:	Exhaust valve closing
Imep:	Indicated mean effective pressure
IVO:	Inlet valve opening
IVC:	Inlet valve closing
KRG-6:	Engine type specification indicating a 6 cylinder in-line K-type engine for generator
KRM-6:	Engine type specification indicating a 6 cylinder in-line K-type engine for propulsion
MCR:	Max Continuous Rating
MSc.:	Mater of Science
NO_x:	Oxides of nitrogen
Pmi:	Mean indicated pressure
ROHR:	Rate of heat release
RPM:	Revolutions per minute
Stud.techn.:	Student of Technology
TDC:	Top dead center
VVA:	Variable valve actuation
VVC:	Variable valve control

APPENDIX A: EVO VARIATION WITH FIXED EVC

Early EVO with fixed EVC at 500 rpm and 5735

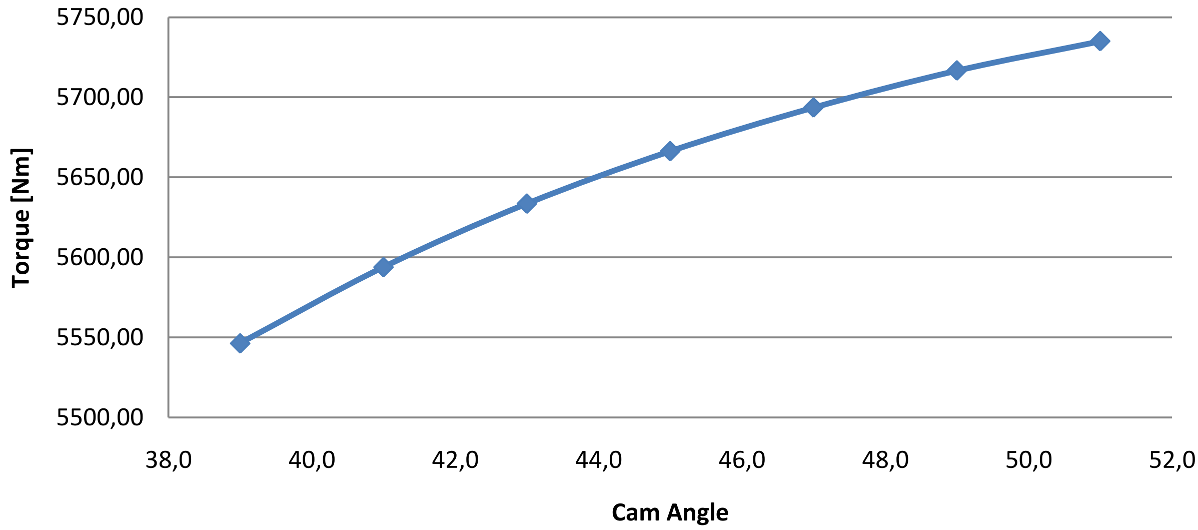

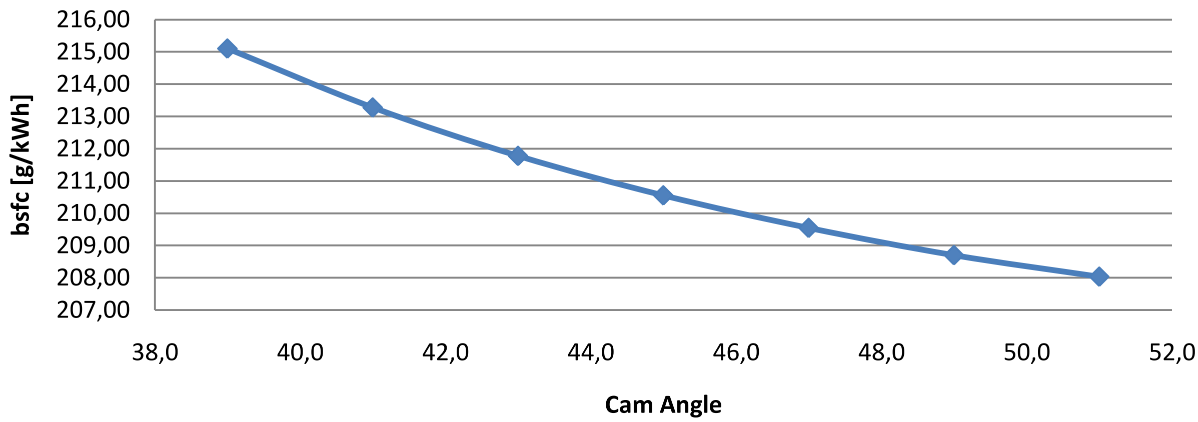

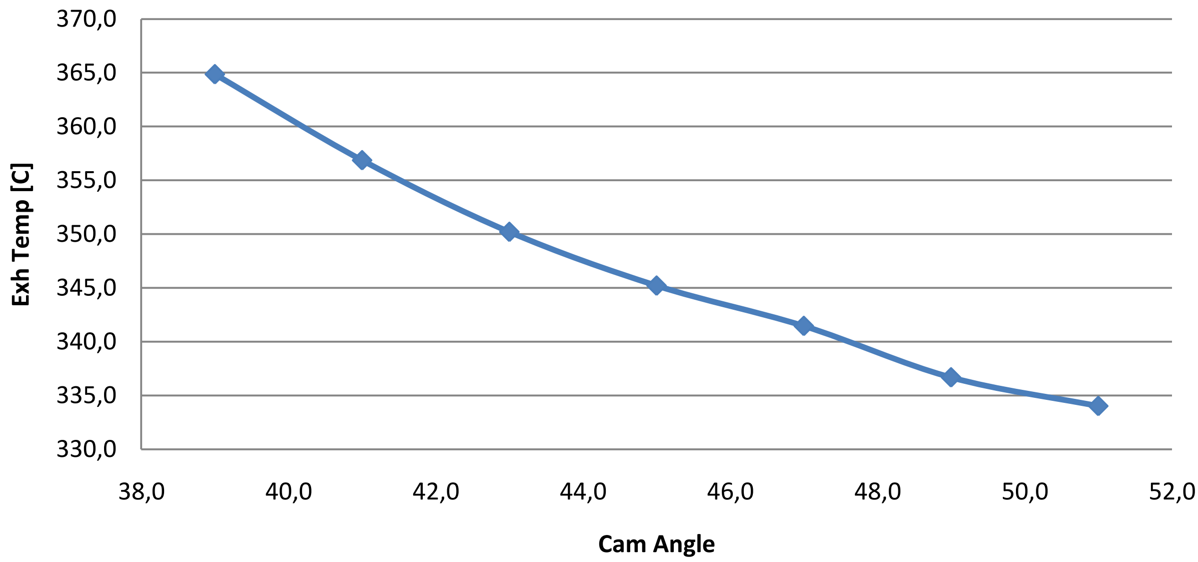
370,0
365,0
360,0
355,0
350,0
345,0
340,0
335,0
330,0
Exh Temp [C]
38,0
40,0
42,0
44,0
46,0
48,0
50,0
52,0
Cam Angle

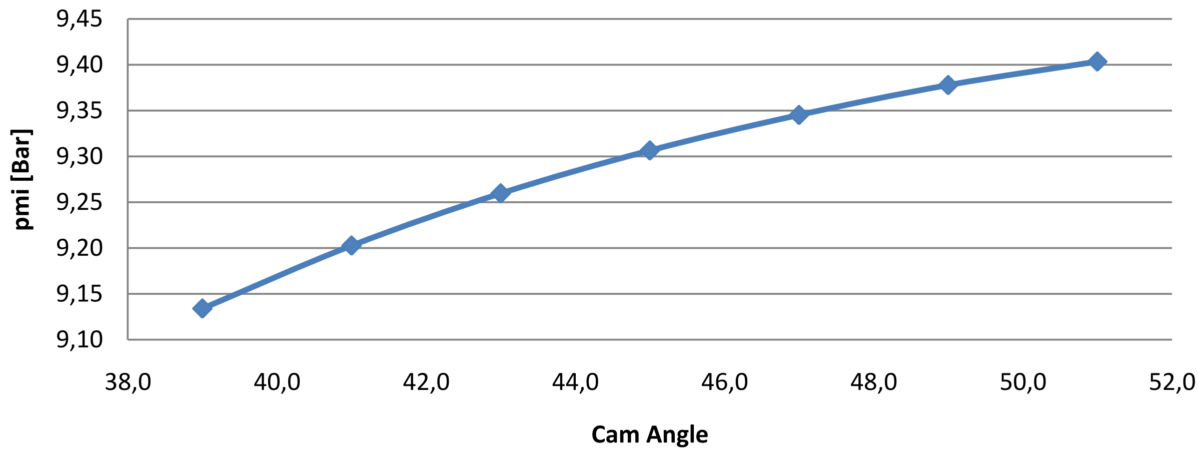
9,45
9,40
9,35
9,30
9,25
9,20
9,15
9,10
pmi [Bar]
38,0
40,0
42,0
44,0
46,0
48,0
50,0
52,0
Cam Angle

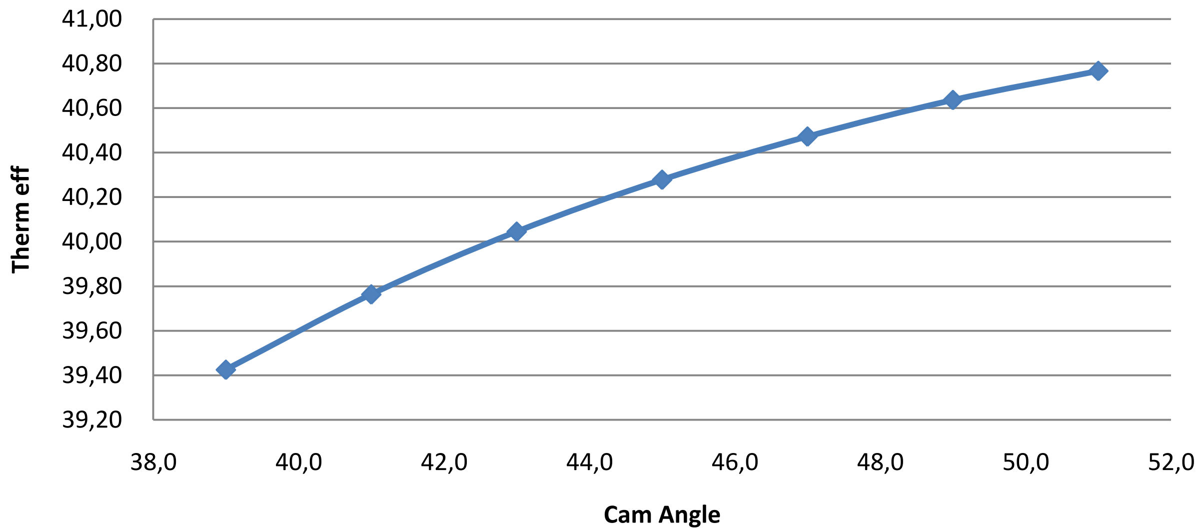
Therm eff
41,00
40,80
40,60
40,40
40,20
40,00
39,80
39,60
39,40
39,20
38,0
40,0
42,0
44,0
46,0
48,0
50,0
52,0
Cam Angle

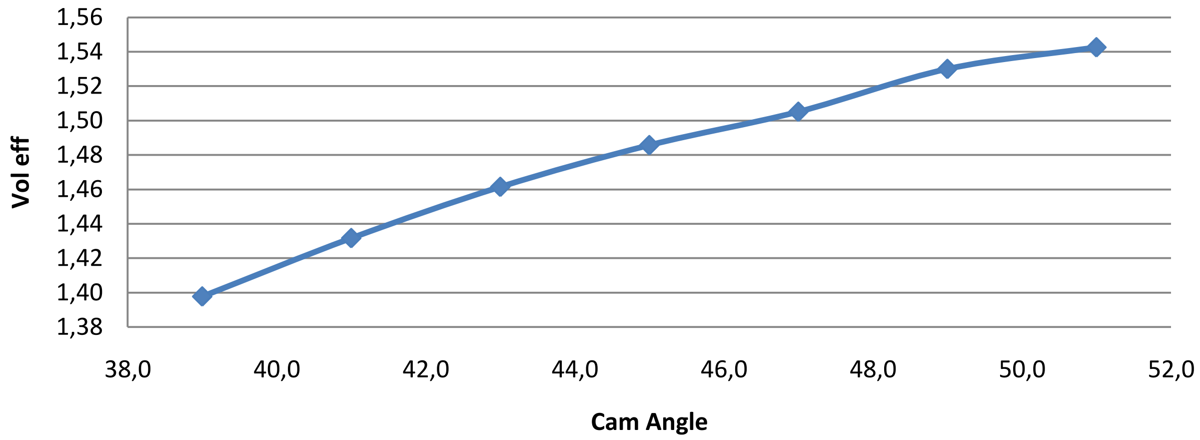
Vol eff
1,56
1,54
1,52
1,50
1,48
1,46
1,44
1,42
1,40
1,38
38,0
40,0
42,0
44,0
46,0
48,0
50,0
52,0
Cam Angle

Late EVO with fixed EVC at 500 rpm and 5735

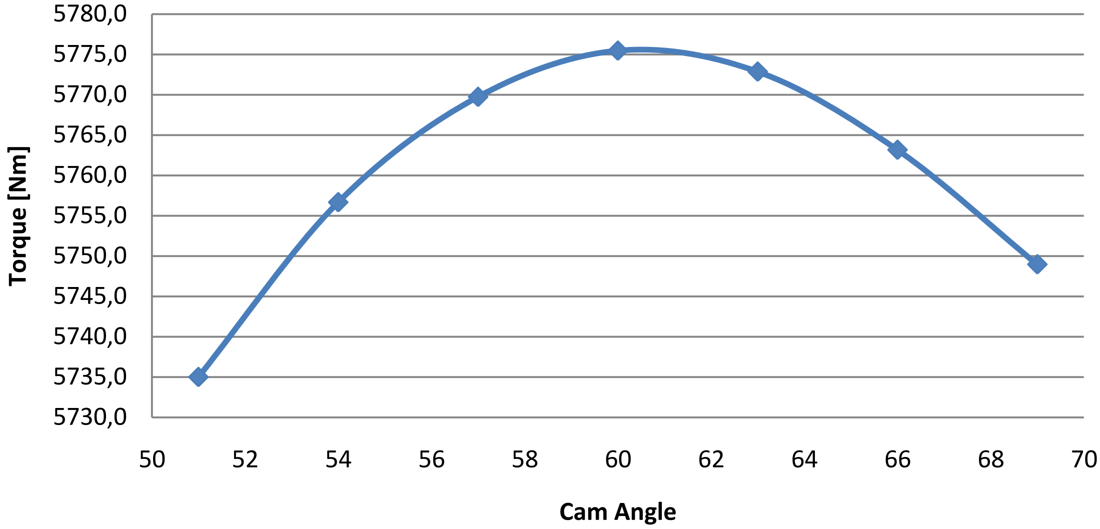

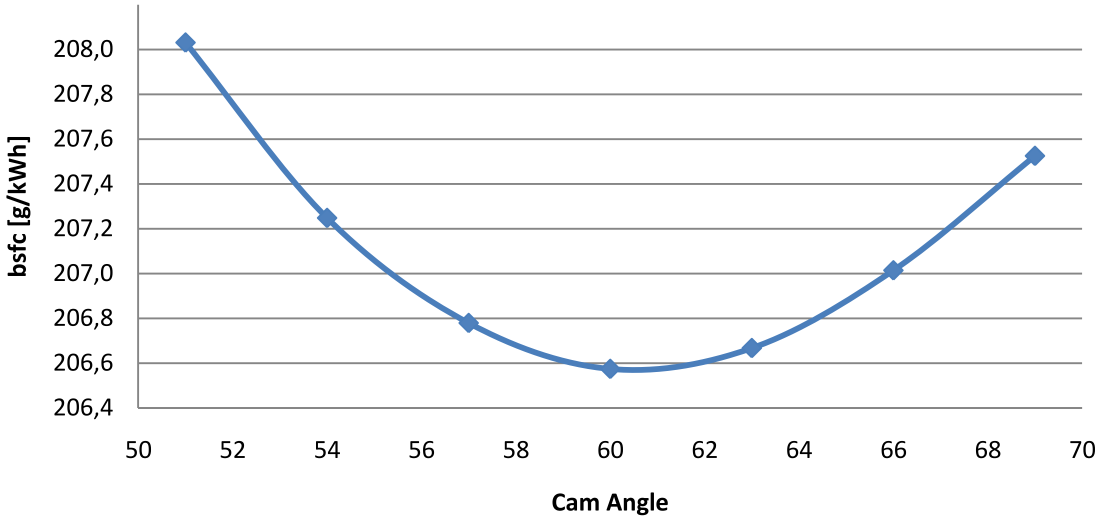

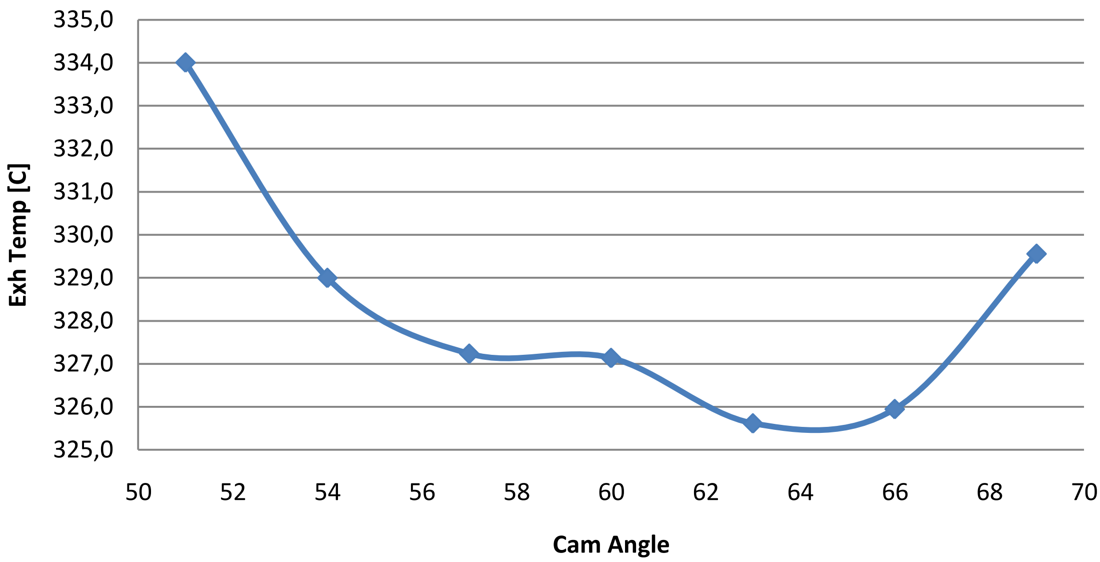

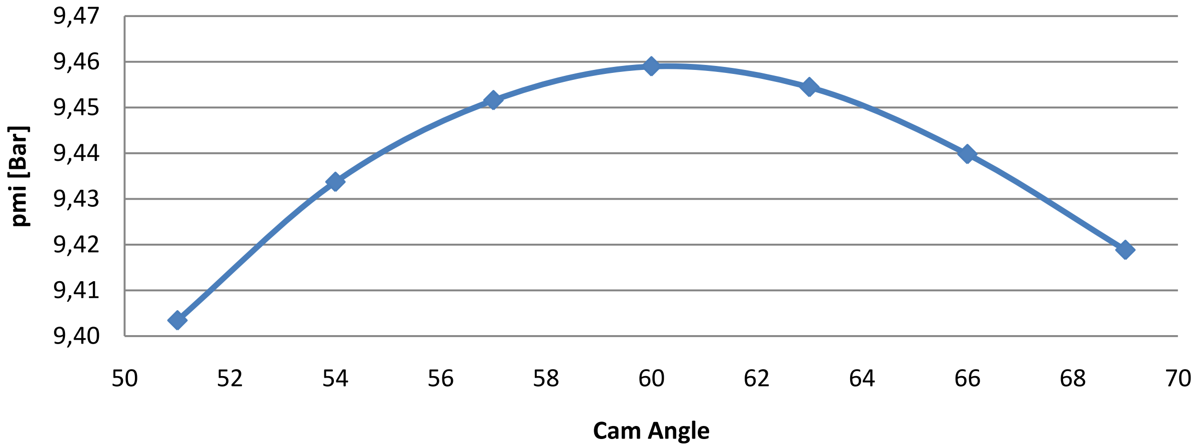
pmi [Bar]
9,47
9,46
9,45
9,44
9,43
9,42
9,41
9,40
50
52
54
56
58
60
62
64
66
68
70
Cam Angle

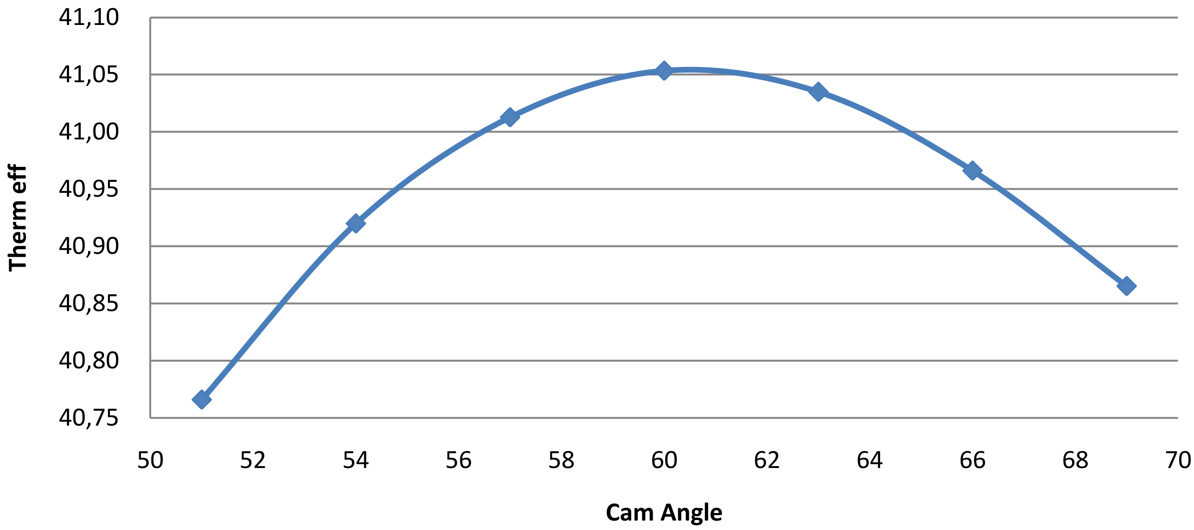
Therm eff
41,10
41,05
41,00
40,95
40,90
40,85
40,80
40,75
50
52
54
56
58
60
62
64
66
68
70
Cam Angle

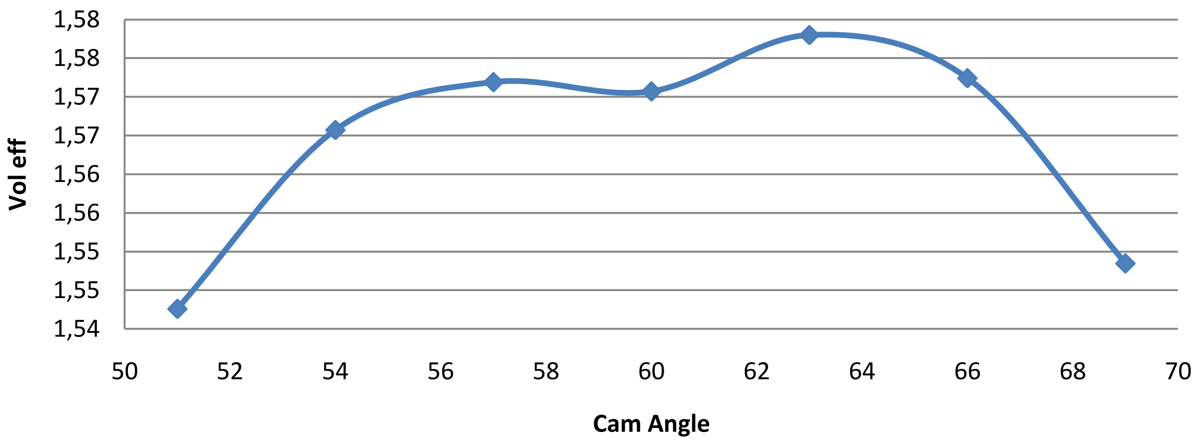
Vol eff
1,58
1,58
1,57
1,57
1,56
1,56
1,55
1,55
1,54
50
52
54
56
58
60
62
64
66
68
70
Cam Angle

Early EVO with fixed EVC at 825 rpm and 15464 Nm

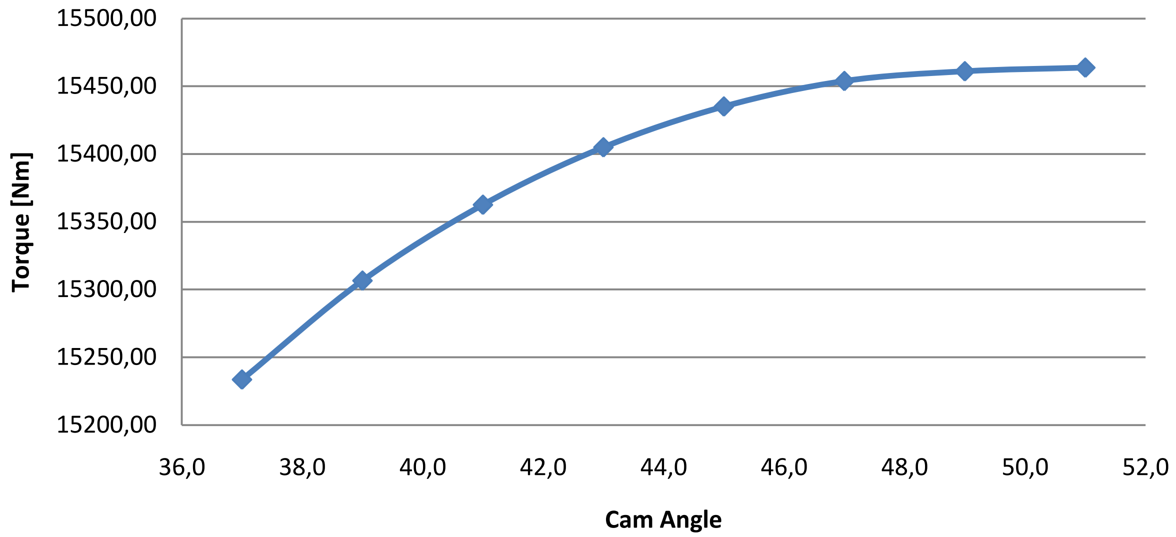

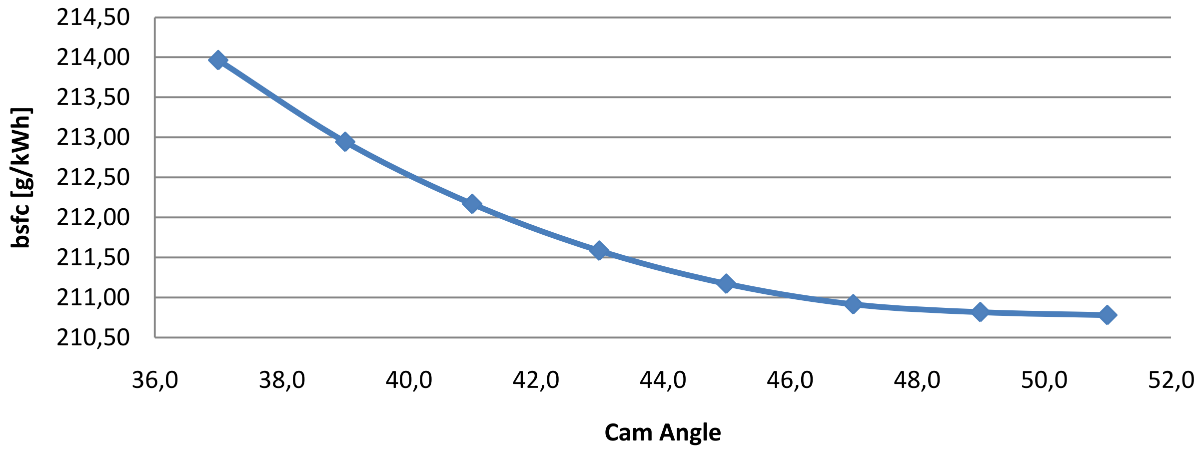

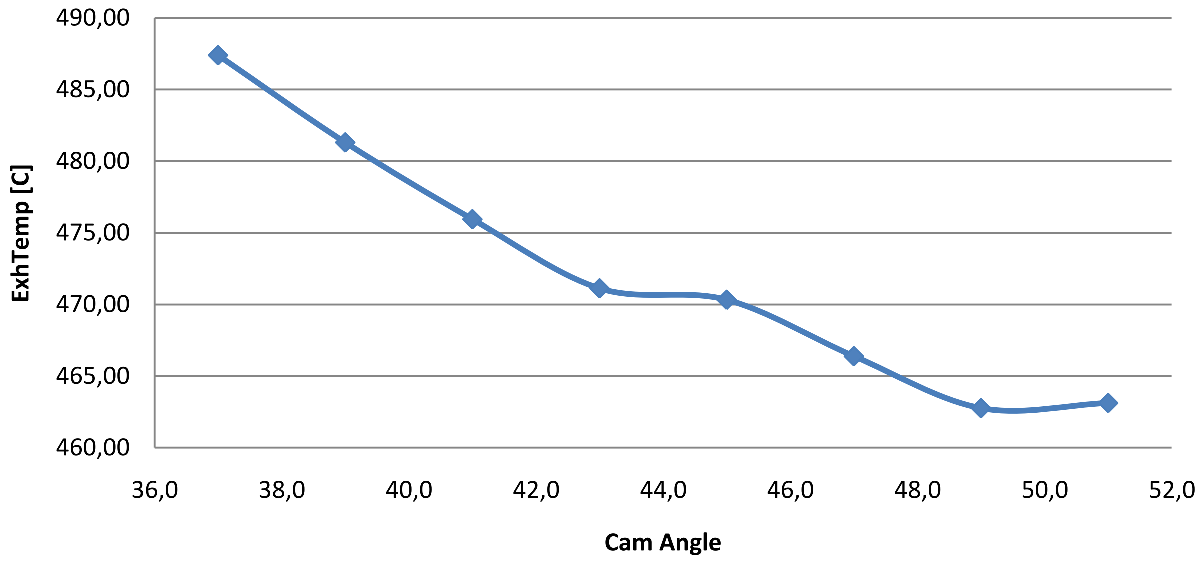

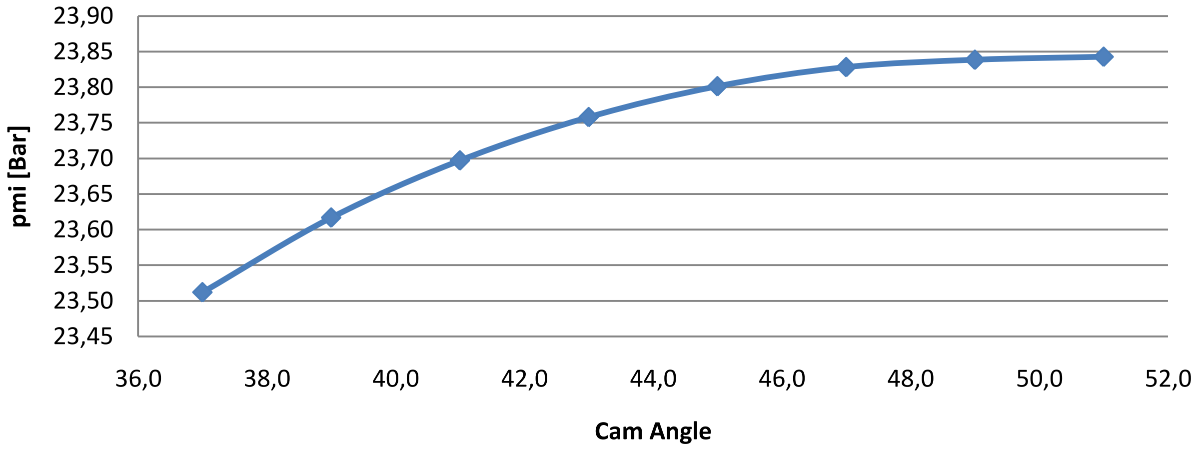
23,90
23,85
23,80
23,75
23,70
23,65
23,60
23,55
23,50
23,45
pmi [Bar]
36,0
38,0
40,0
42,0
44,0
46,0
48,0
50,0
52,0
Cam Angle

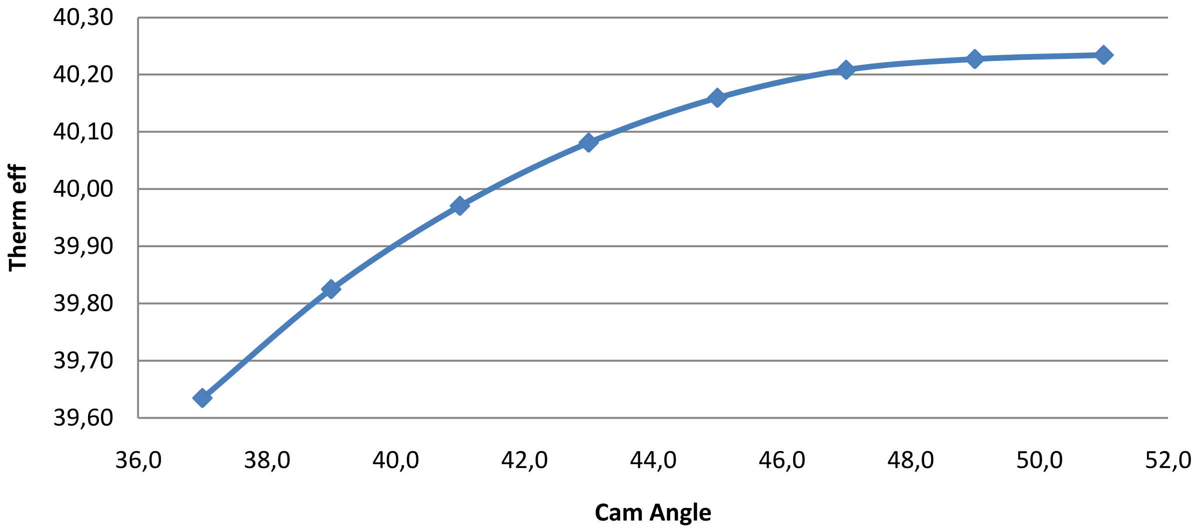
40,30
40,20
40,10
40,00
39,90
39,80
39,70
39,60
Therm eff
36,0
38,0
40,0
42,0
44,0
46,0
48,0
50,0
52,0
Cam Angle

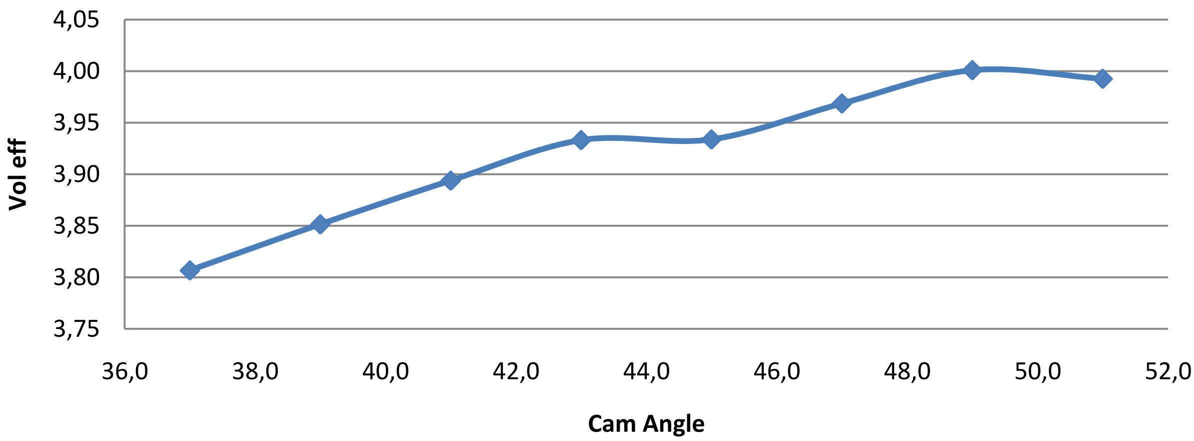
4,05
4,00
3,95
3,90
3,85
3,80
3,75
Vol eff
36,0
38,0
40,0
42,0
44,0
46,0
48,0
50,0
52,0
Cam Angle

Late EVO with fixed EVC at 825 rpm and 15464 Nm

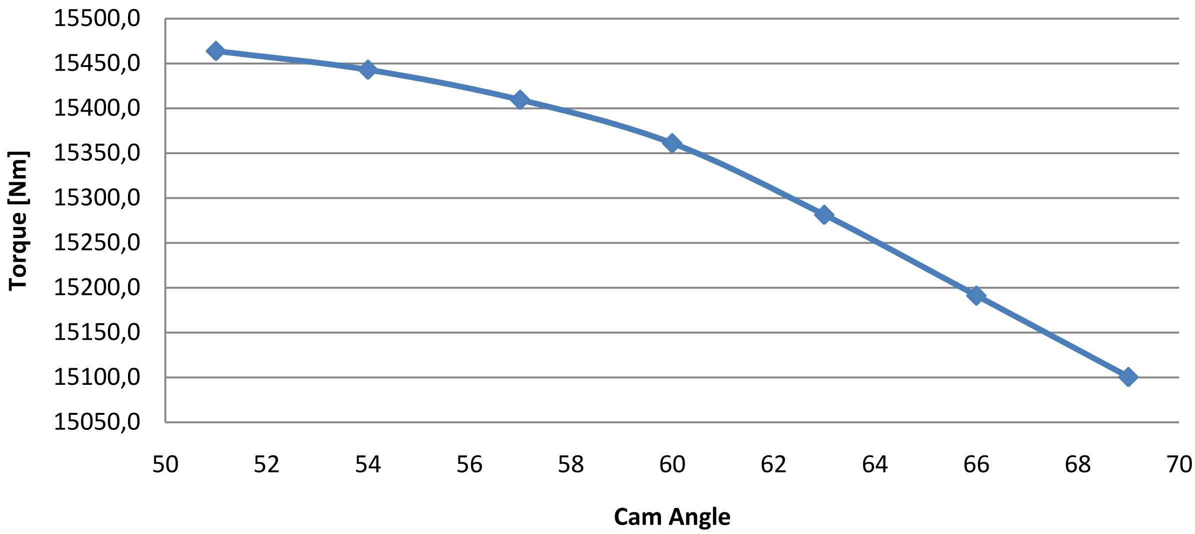

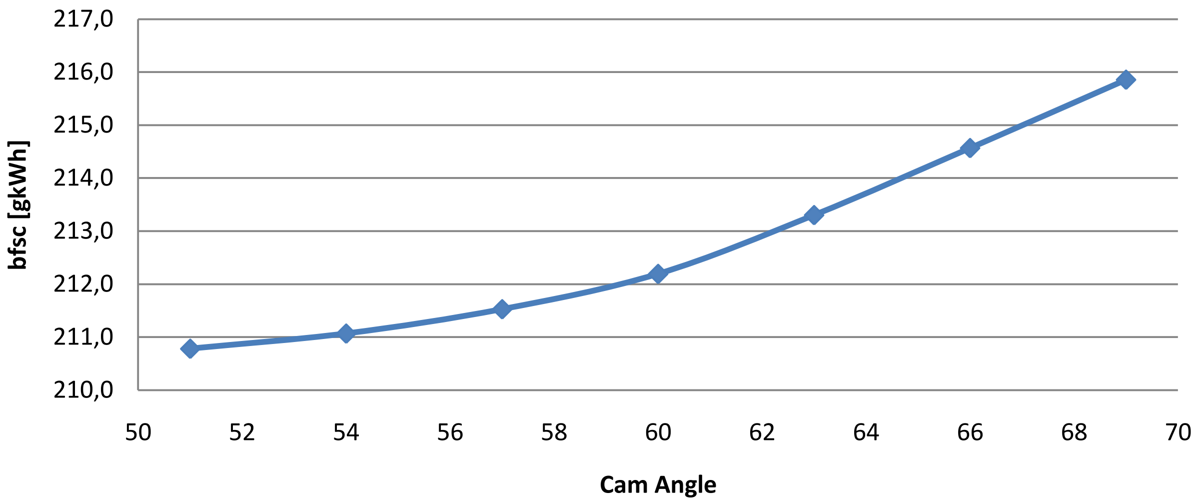

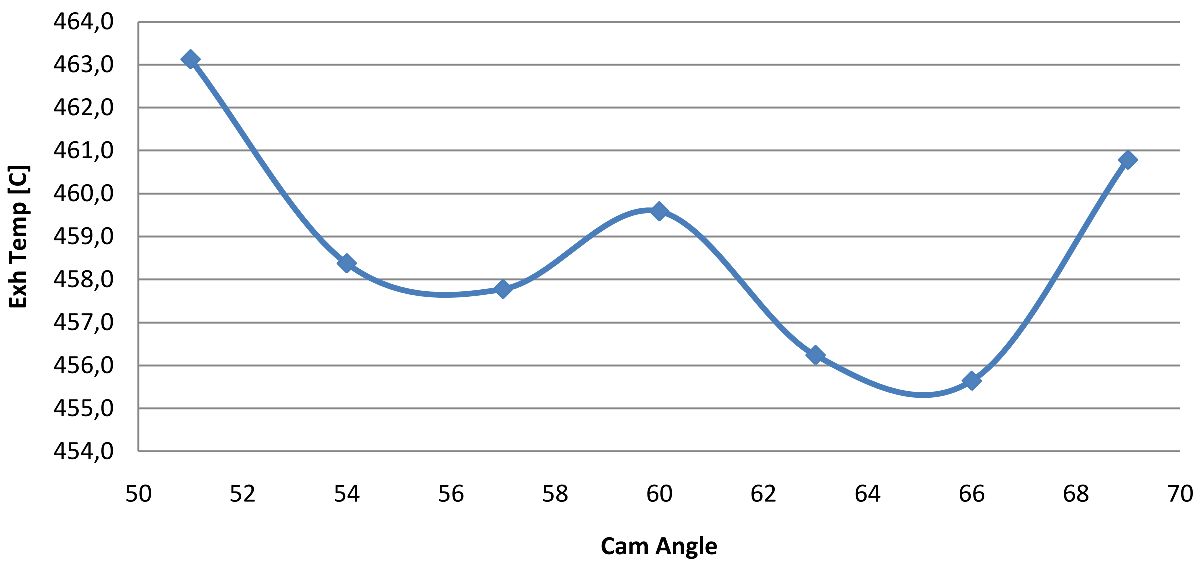

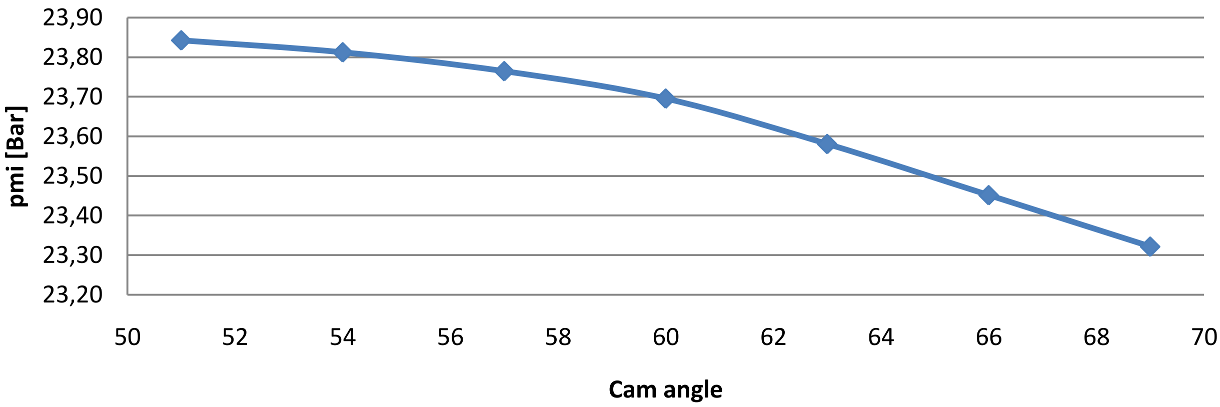
pmi [Bar]
23,90
23,80
23,70
23,60
23,50
23,40
23,30
23,20
50
52
54
56
58
60
62
64
66
68
70
Cam angle

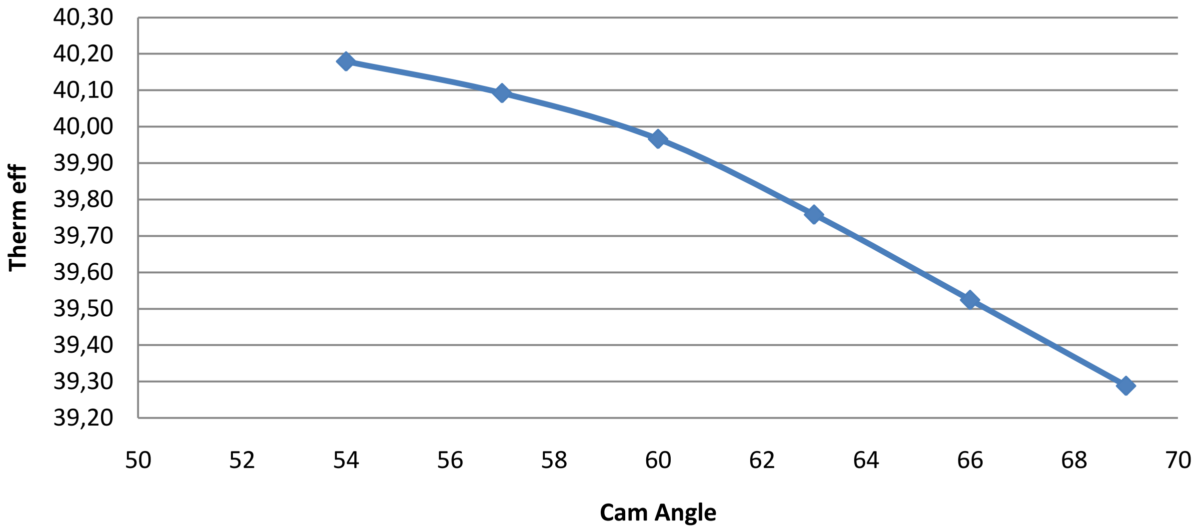
Therm eff
40,30
40,20
40,10
40,00
39,90
39,80
39,70
39,60
39,50
39,40
39,30
39,20
50
52
54
56
58
60
62
64
66
68
70
Cam Angle

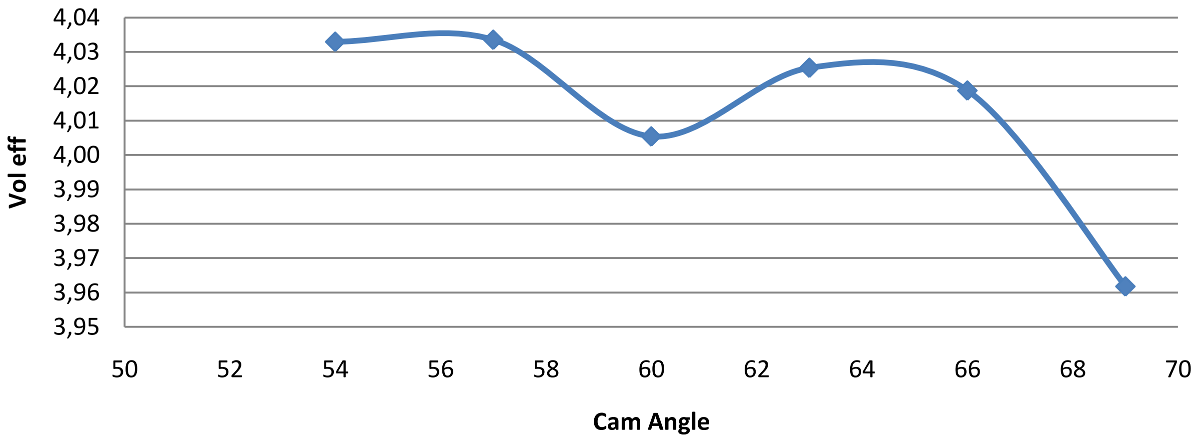
Vol eff
4,04
4,03
4,02
4,01
4,00
3,99
3,98
3,97
3,96
3,95
50
52
54
56
58
60
62
64
66
68
70
Cam Angle

APPENDIX B: EARLY IVC AT 500 RPM AND 5735 NM

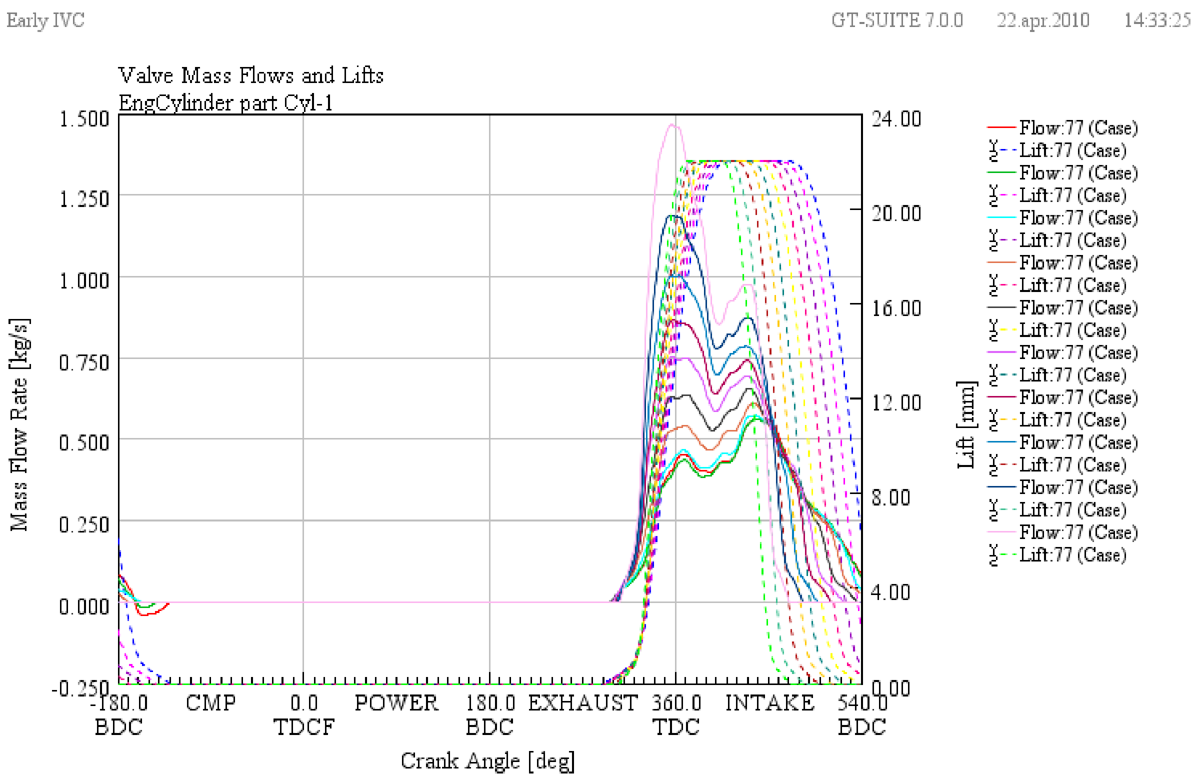

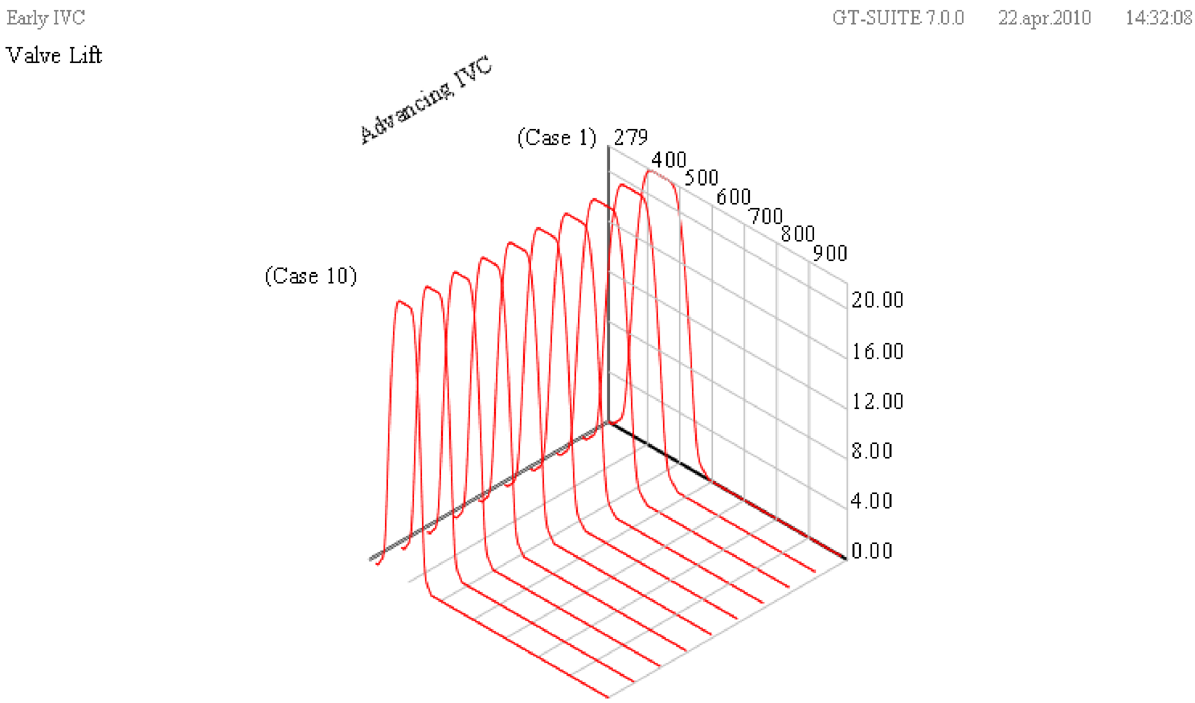

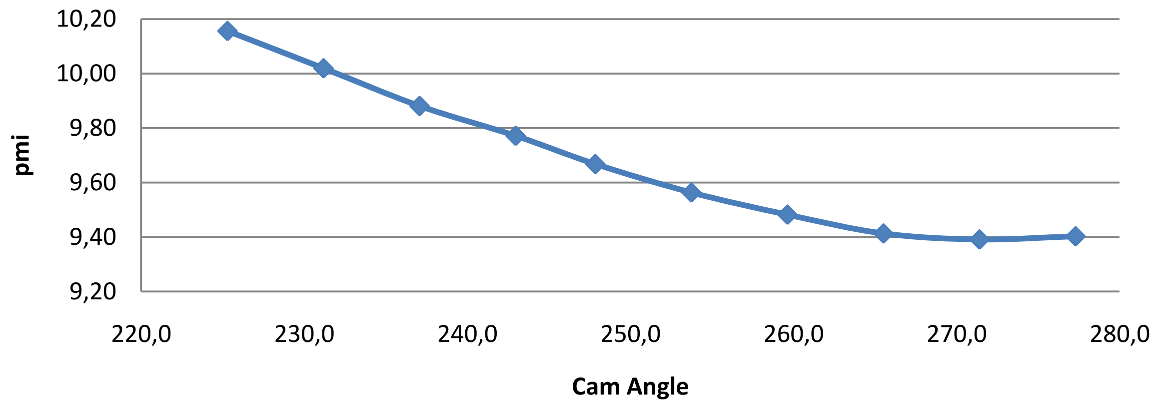
pmi
10,20
10,00
9,80
9,60
9,40
9,20
220,0
230,0
240,0
250,0
260,0
270,0
280,0
Cam Angle

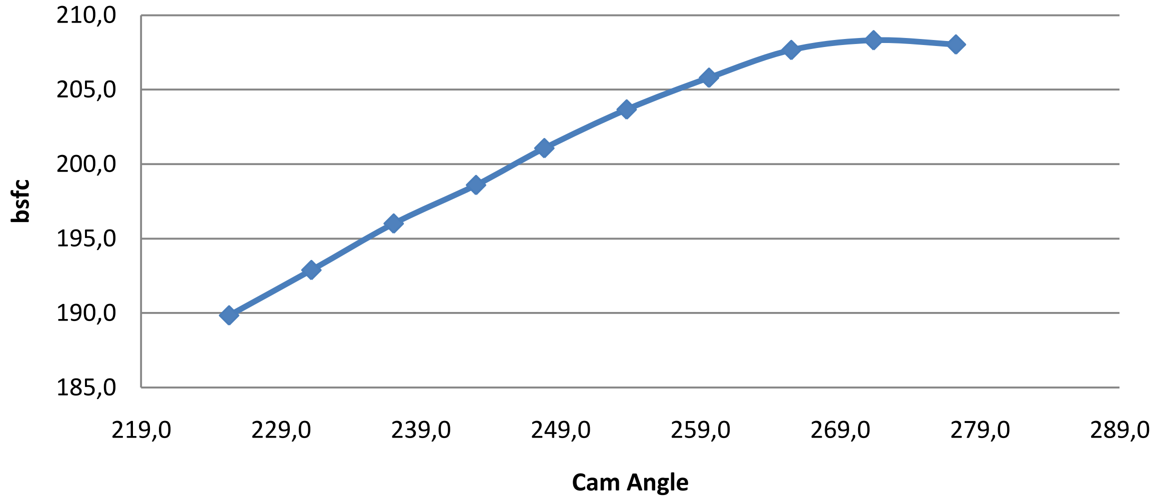
bsfc
210,0
205,0
200,0
195,0
190,0
185,0
219,0
229,0
239,0
249,0
259,0
269,0
279,0
289,0
Cam Angle

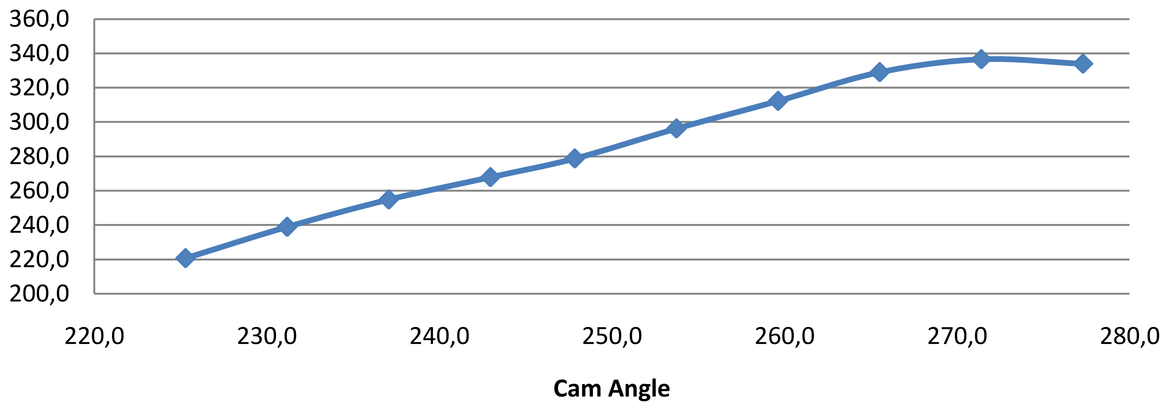
360,0
340,0
320,0
300,0
280,0
260,0
240,0
220,0
200,0
220,0
230,0
240,0
250,0
260,0
270,0
280,0
Cam Angle

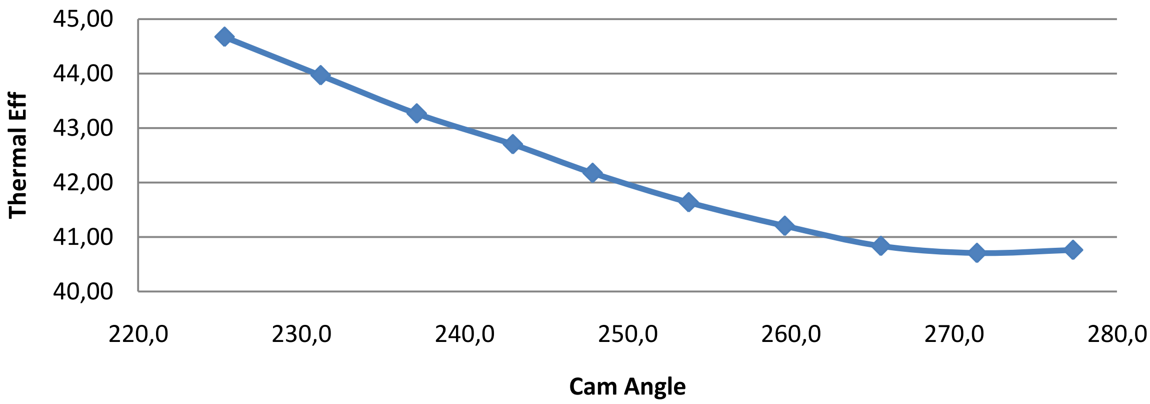
Thermal Eff
45,00
44,00
43,00
42,00
41,00
40,00
220,0
230,0
240,0
250,0
260,0
270,0
280,0
Cam Angle

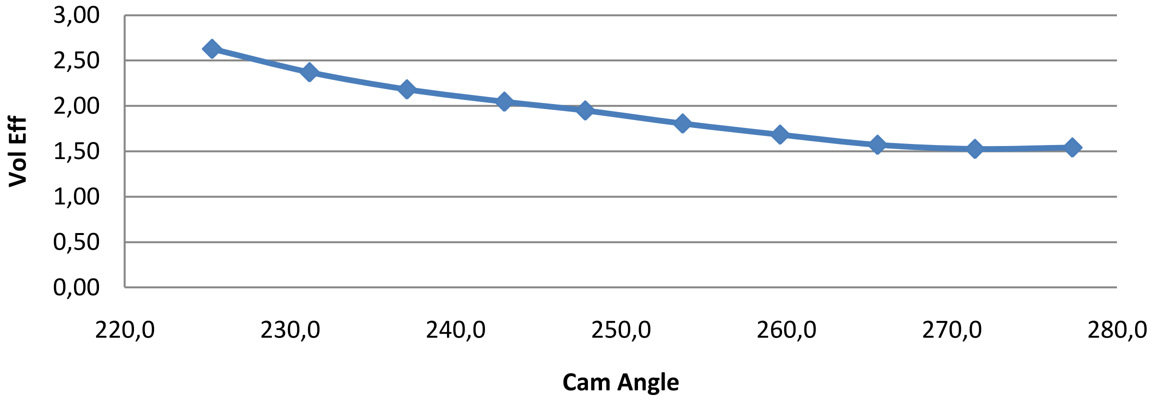
Vol Eff
3,00
2,50
2,00
1,50
1,00
0,50
0,00
220,0
230,0
240,0
250,0
260,0
270,0
280,0
Cam Angle

APPENDIX C: EARLY IVC AT 825 RPM AND 15464 NM

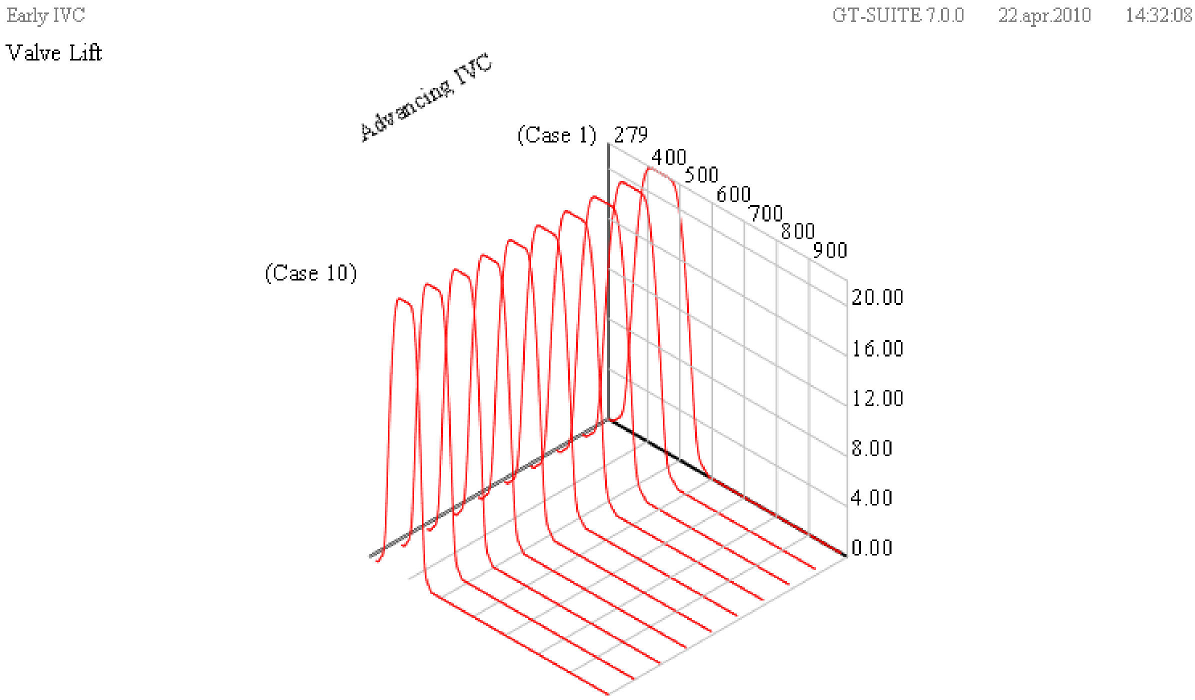

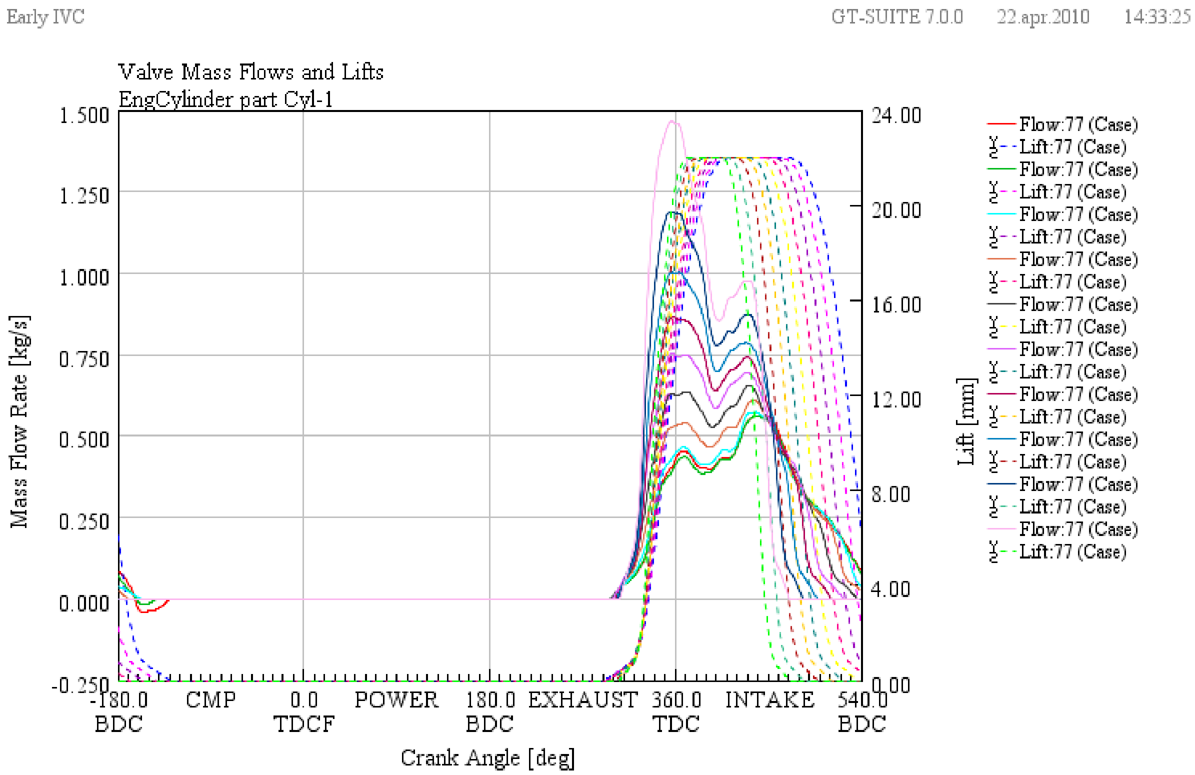

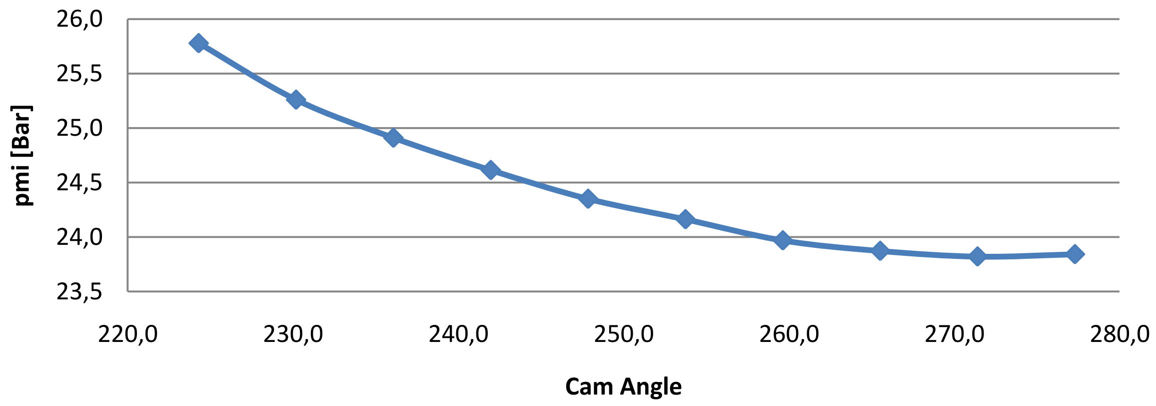
pmi [Bar]
26,0
25,5
25,0
24,5
24,0
23,5
220,0
230,0
240,0
250,0
260,0
270,0
280,0
Cam Angle

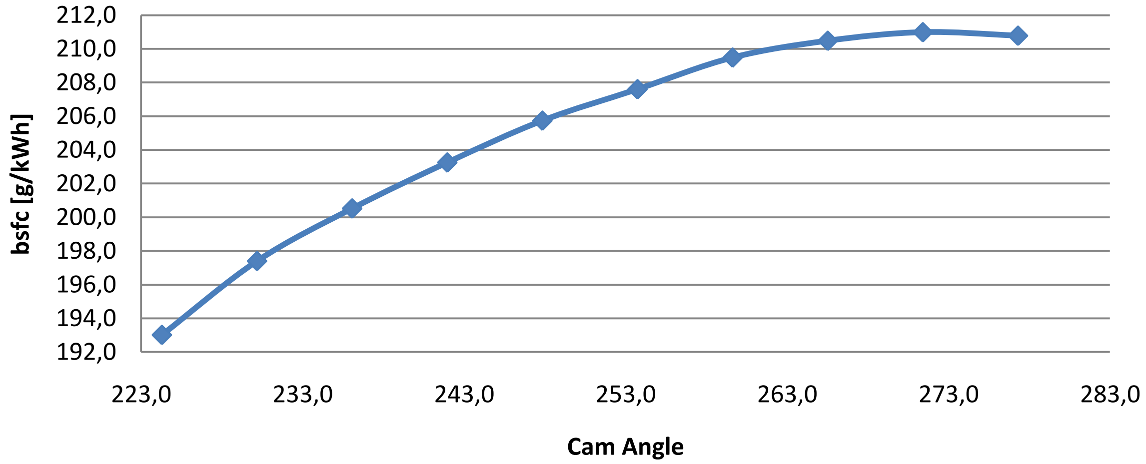
bsfc [g/kWh]
212,0
210,0
208,0
206,0
204,0
202,0
200,0
198,0
196,0
194,0
192,0
223,0
233,0
243,0
253,0
263,0
273,0
283,0
Cam Angle

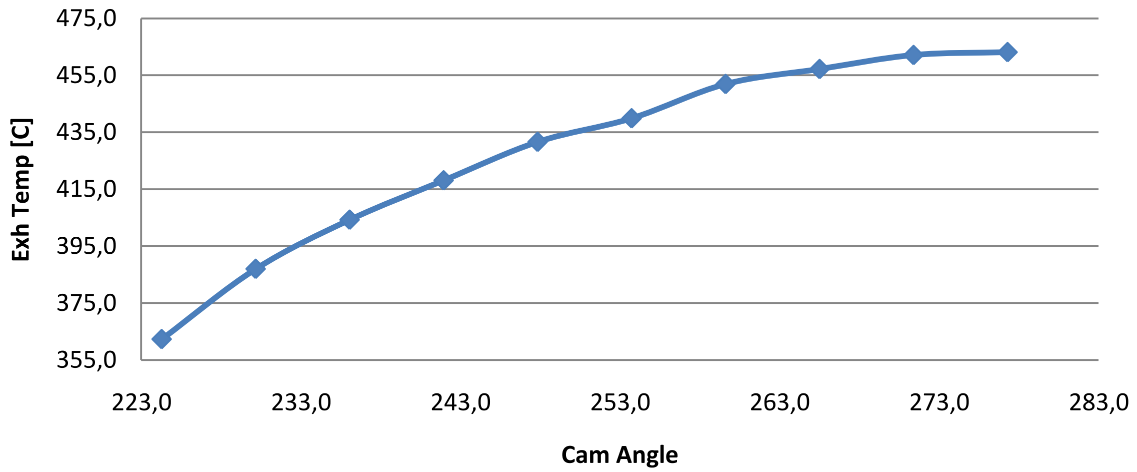
Exh Temp [C]
475,0
455,0
435,0
415,0
395,0
375,0
355,0
223,0
233,0
243,0
253,0
263,0
273,0
283,0
Cam Angle

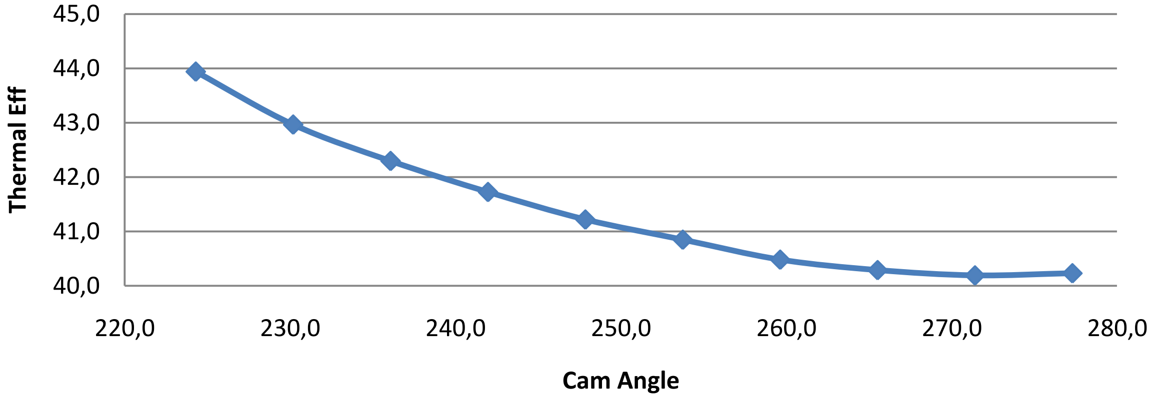
Thermal Eff
45,0
44,0
43,0
42,0
41,0
40,0
220,0
230,0
240,0
250,0
260,0
270,0
280,0
Cam Angle

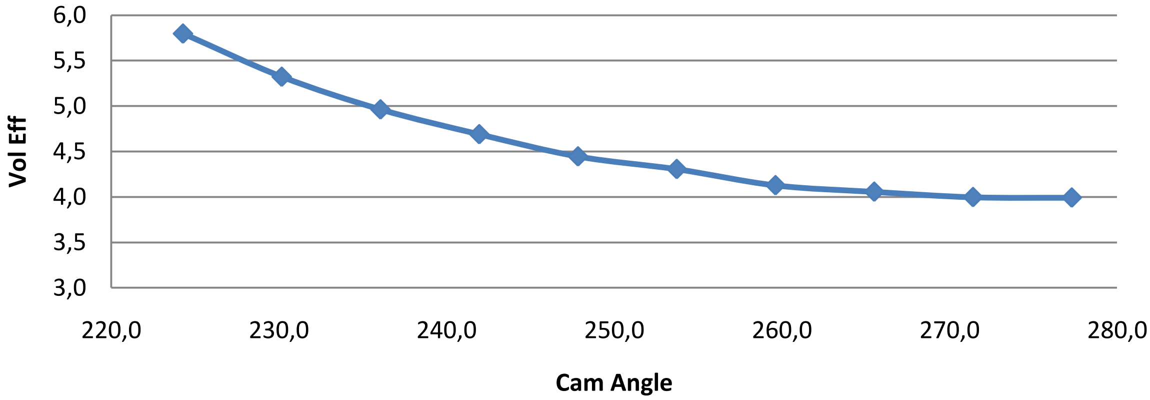
Vol Eff
6,0
5,5
5,0
4,5
4,0
3,5
3,0
220,0
230,0
240,0
250,0
260,0
270,0
280,0
Cam Angle

APPENDIX D: LATE IVC AT 500 RPM AND 5735 NM

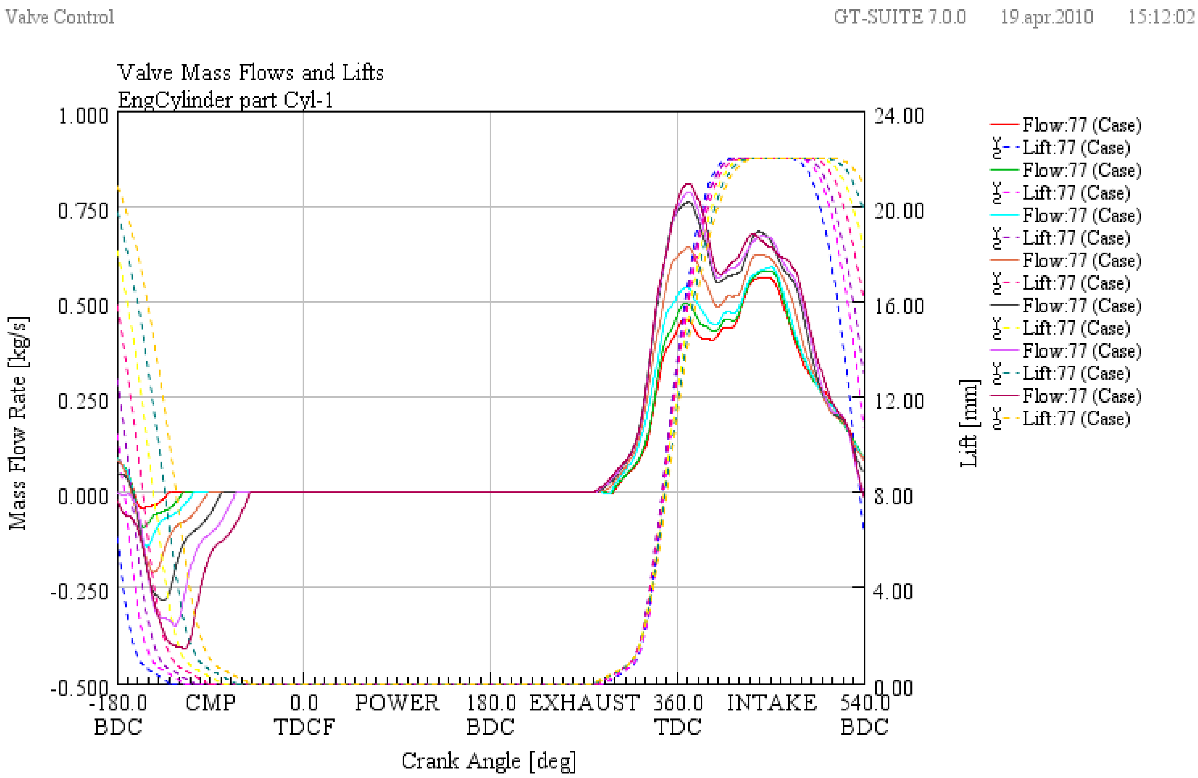

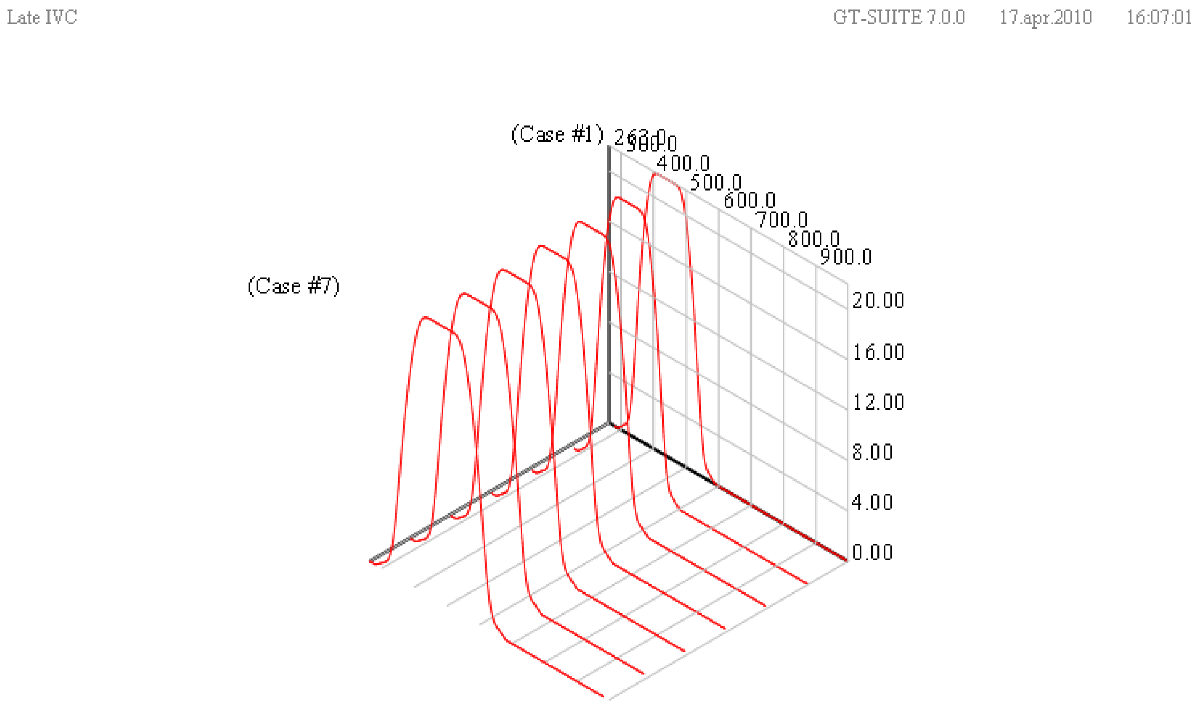

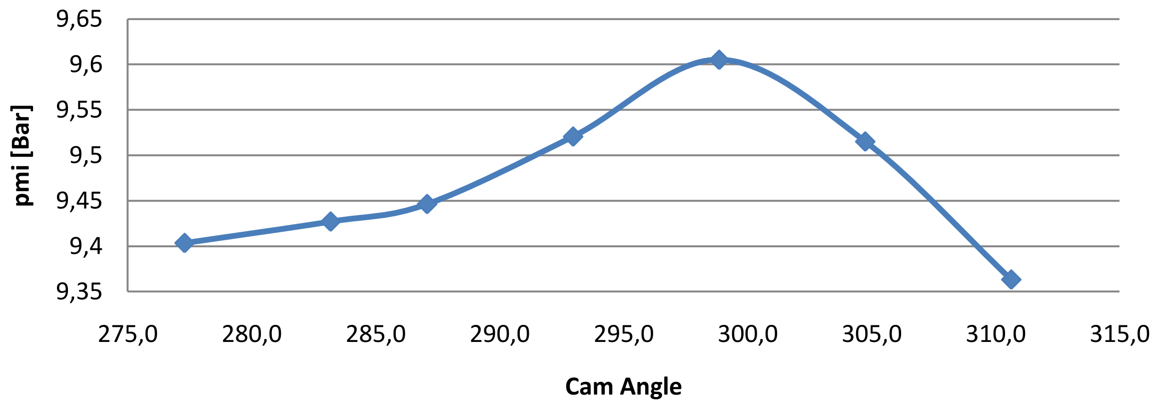
pmi [Bar]
9,65
9,6
9,55
9,5
9,45
9,4
9,35
275,0
280,0
285,0
290,0
295,0
300,0
305,0
310,0
315,0
Cam Angle

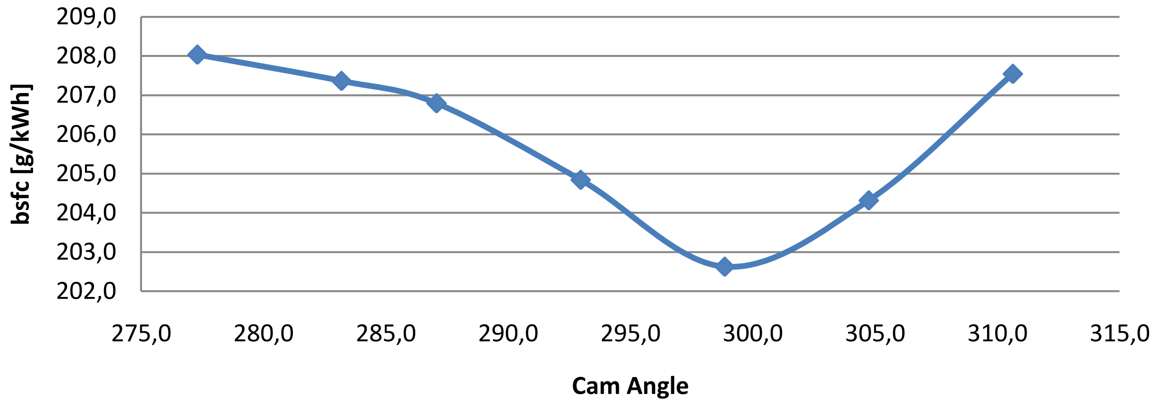
bsfc [g/kWh]
209,0
208,0
207,0
206,0
205,0
204,0
203,0
202,0
275,0
280,0
285,0
290,0
295,0
300,0
305,0
310,0
315,0
Cam Angle

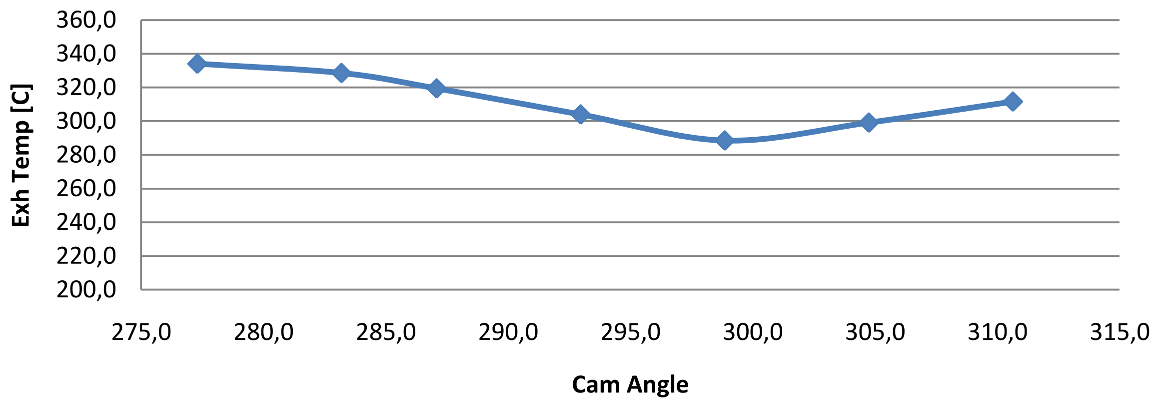
Exh Temp [C]
360,0
340,0
320,0
300,0
280,0
260,0
240,0
220,0
200,0
275,0
280,0
285,0
290,0
295,0
300,0
305,0
310,0
315,0
Cam Angle

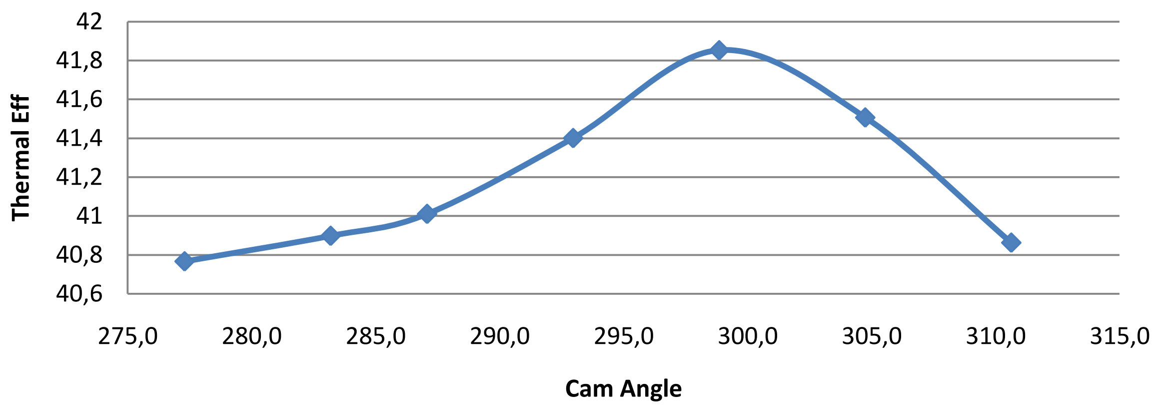
Thermal Eff
42
41,8
41,6
41,4
41,2
41
40,8
40,6
275,0
280,0
285,0
290,0
295,0
300,0
305,0
310,0
315,0
Cam Angle

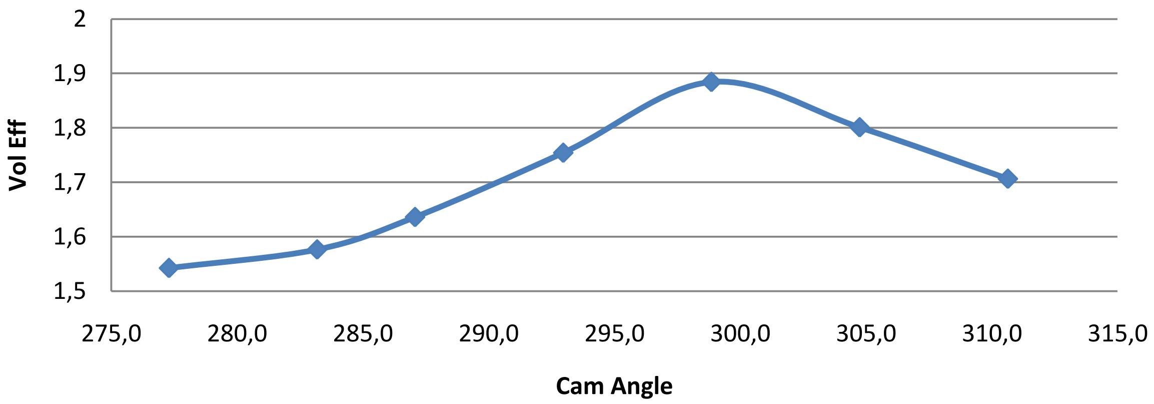
2
1,9
1,8
1,7
1,6
1,5
Vol Eff
275,0
280,0
285,0
290,0
295,0
300,0
305,0
310,0
315,0
Cam Angle

APPENDIX E: LATE IVC AT 825 RPM AND 15464 NM

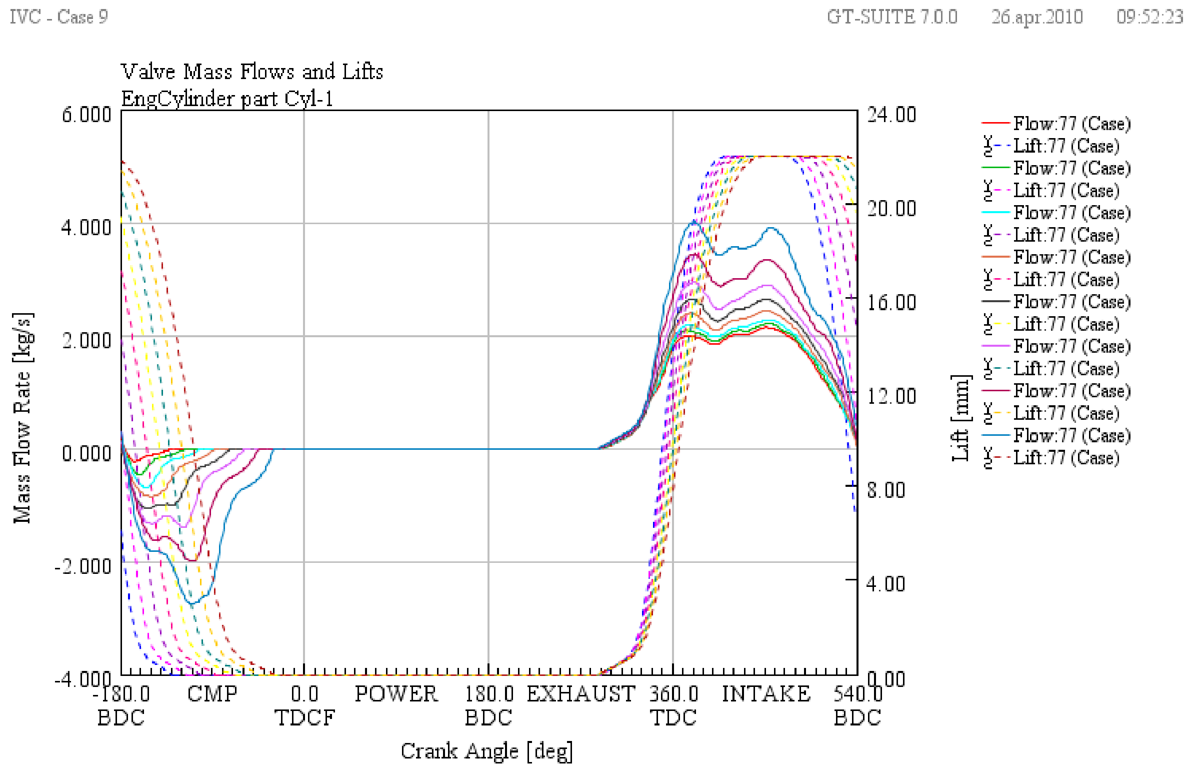

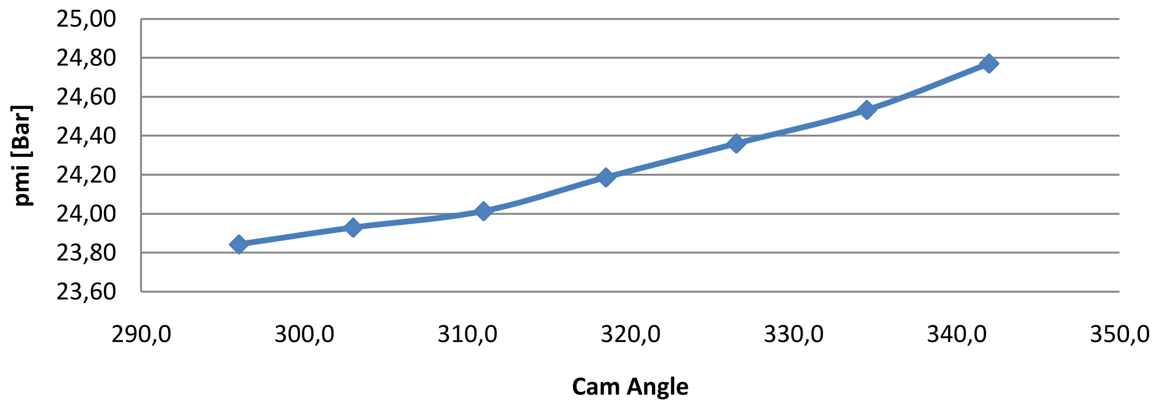

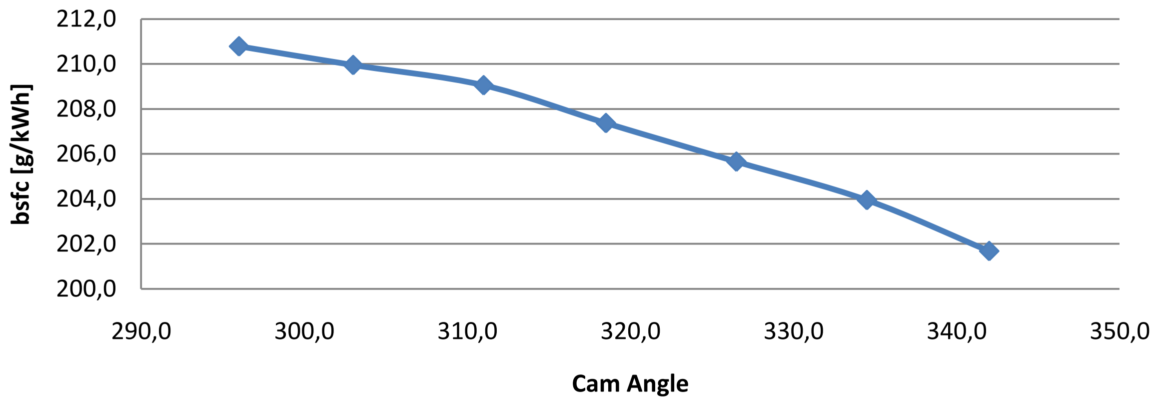
212,0
210,0
208,0
206,0
204,0
202,0
200,0
bsfc [g/kWh]
290,0
300,0
310,0
320,0
330,0
340,0
350,0
Cam Angle

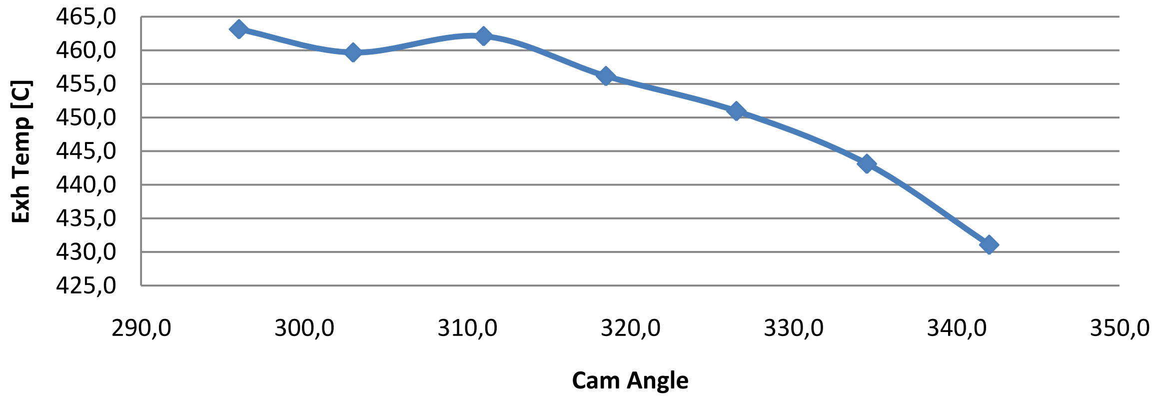
465,0
460,0
455,0
450,0
445,0
440,0
435,0
430,0
425,0
Exh Temp [C]
290,0
300,0
310,0
320,0
330,0
340,0
350,0
Cam Angle

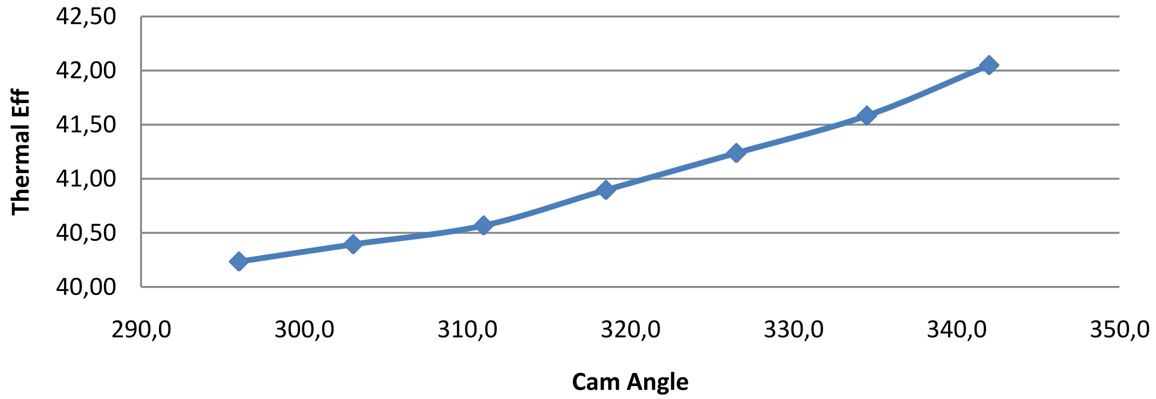
42,50
42,00
41,50
41,00
40,50
40,00
Thermal Eff
290,0
300,0
310,0
320,0
330,0
340,0
350,0
Cam Angle

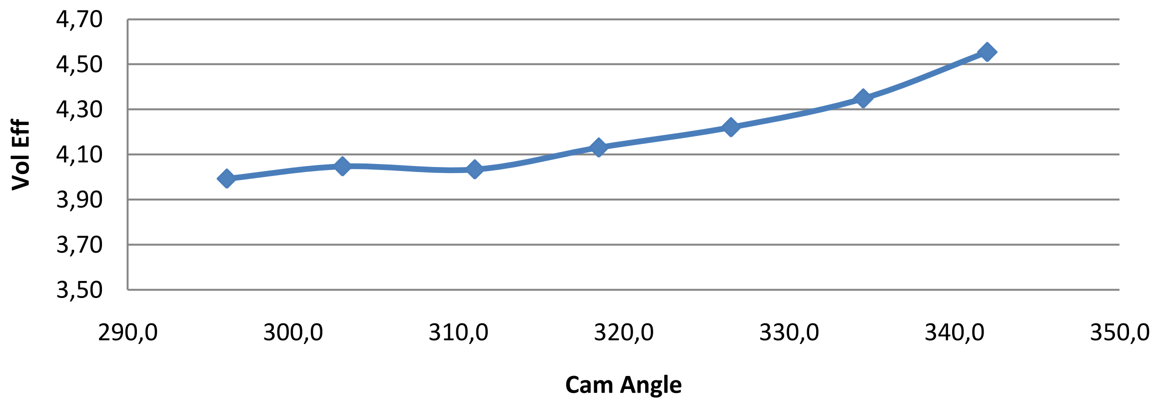
4,70
4,50
4,30
4,10
3,90
3,70
3,50
Vol Eff
290,0
300,0
310,0
320,0
330,0
340,0
350,0
Cam Angle

APPENDIX F: EARLY EXHAUST PHASING AT 500 RPM AND 5735 NM

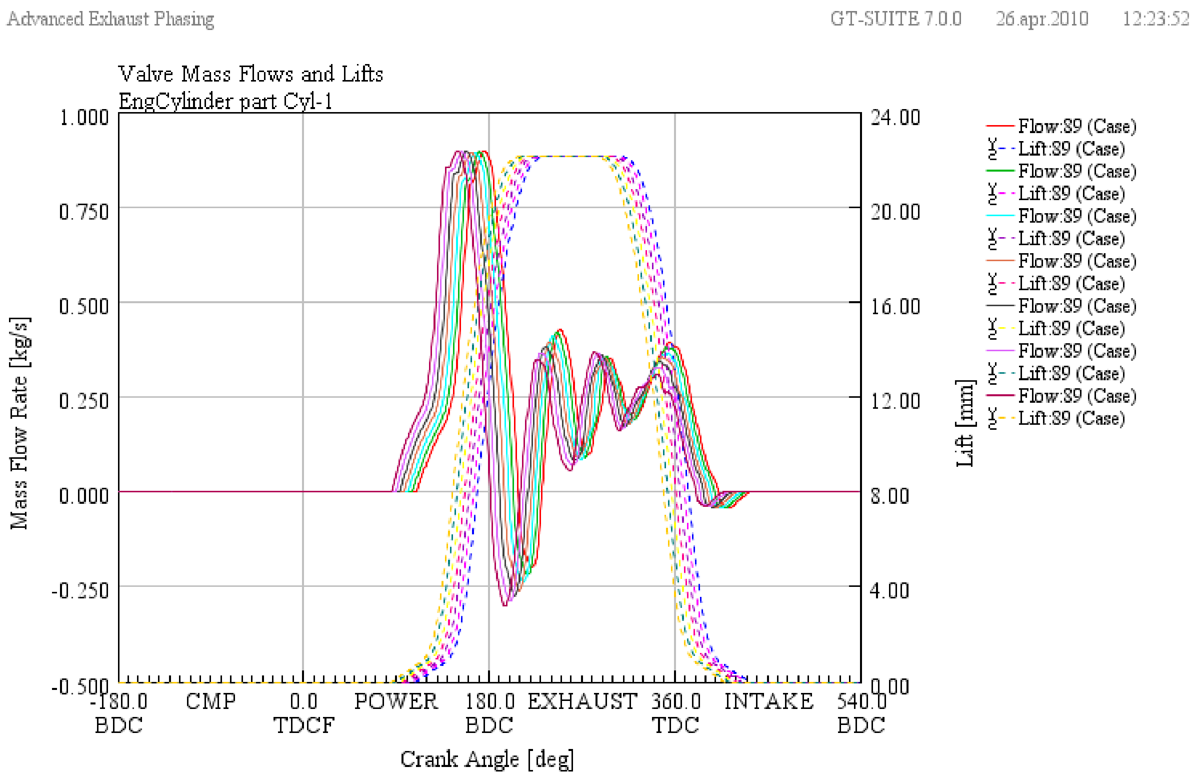

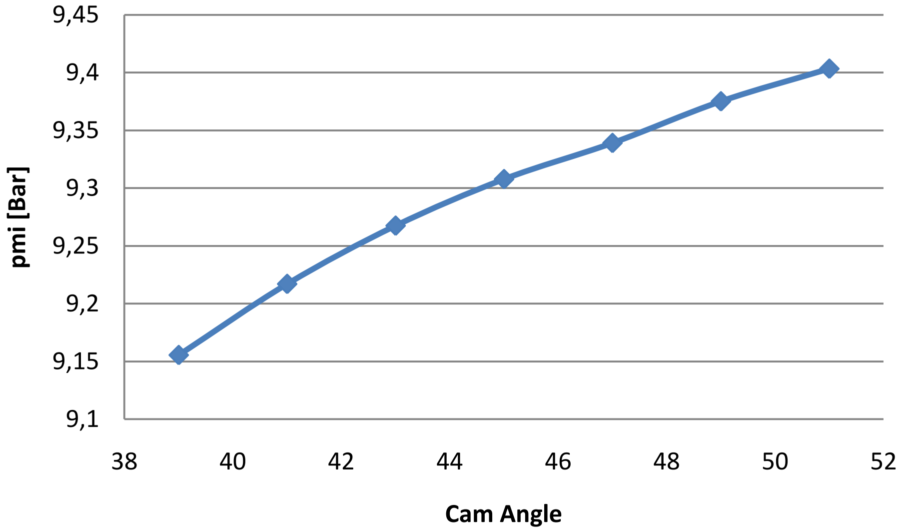

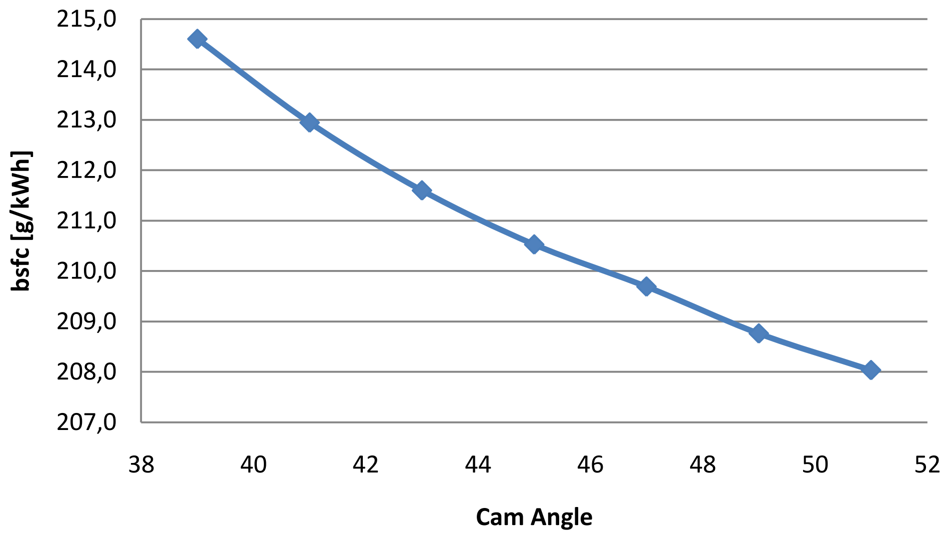
215,0
214,0
213,0
212,0
211,0
210,0
209,0
208,0
207,0
bsfc [g/kWh]
38
40
42
44
46
48
50
52
Cam Angle

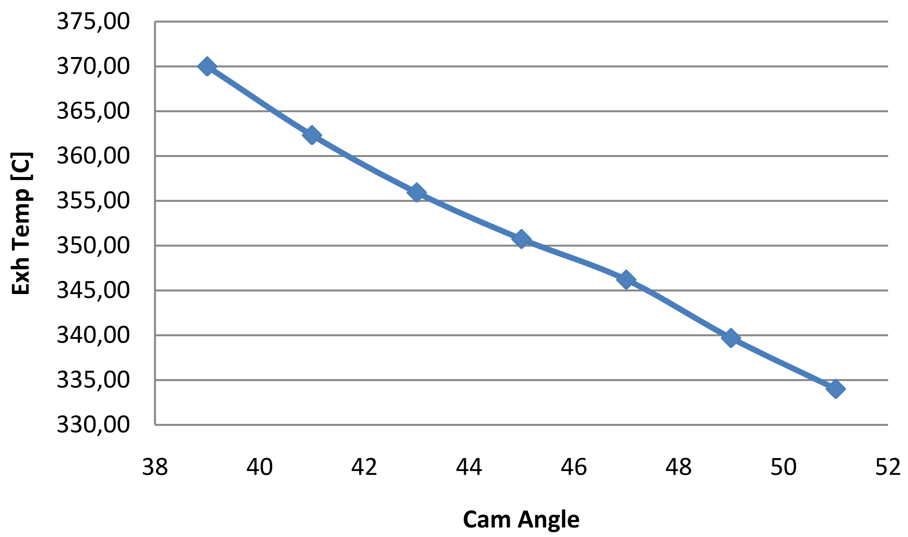
375,00
370,00
365,00
360,00
355,00
350,00
345,00
340,00
335,00
330,00
Exh Temp [C]
38
40
42
44
46
48
50
52
Cam Angle

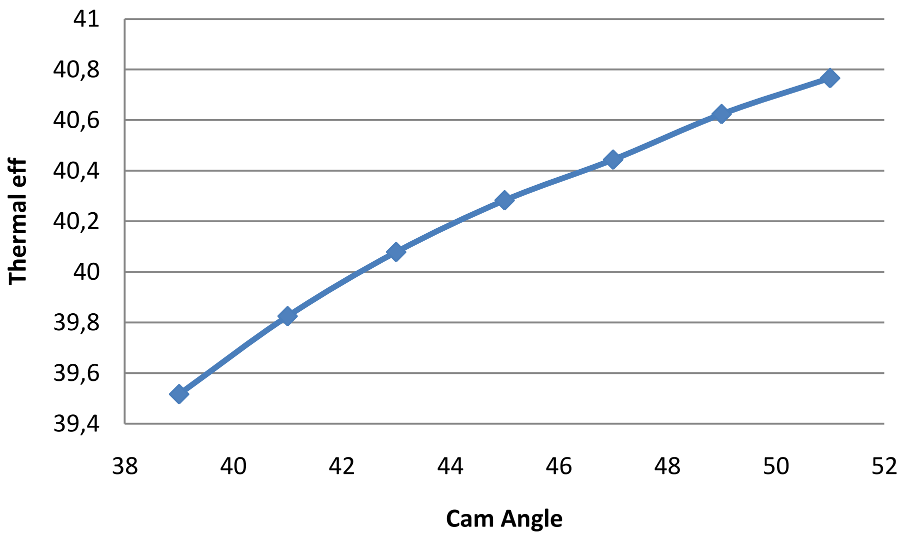
Thermal eff
41
40,8
40,6
40,4
40,2
40
39,8
39,6
39,4
38
40
42
44
46
48
50
52
Cam Angle

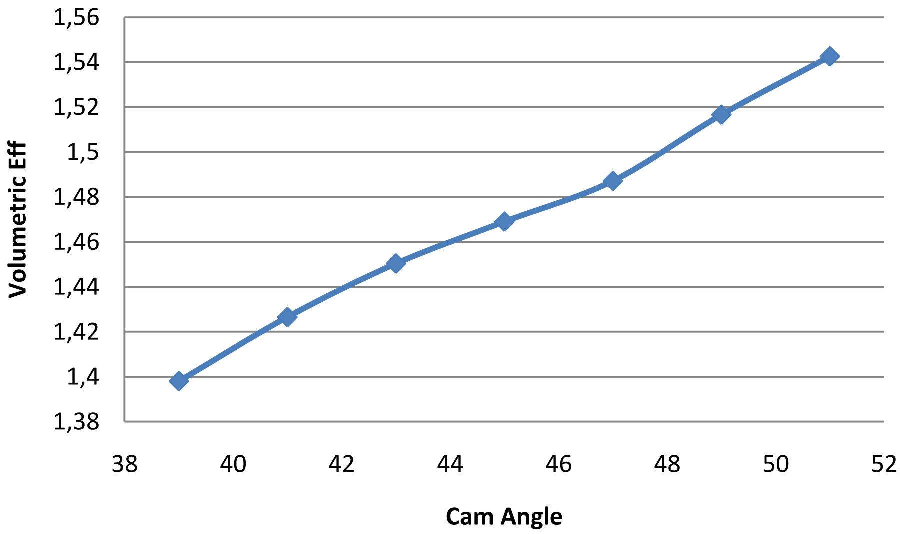
Volumetric Eff
1,56
1,54
1,52
1,5
1,48
1,46
1,44
1,42
1,4
1,38
38
40
42
44
46
48
50
52
Cam Angle

APPENDIX G: EARLY EXHAUST PHASING AT 825 RPM AND 15464 NM

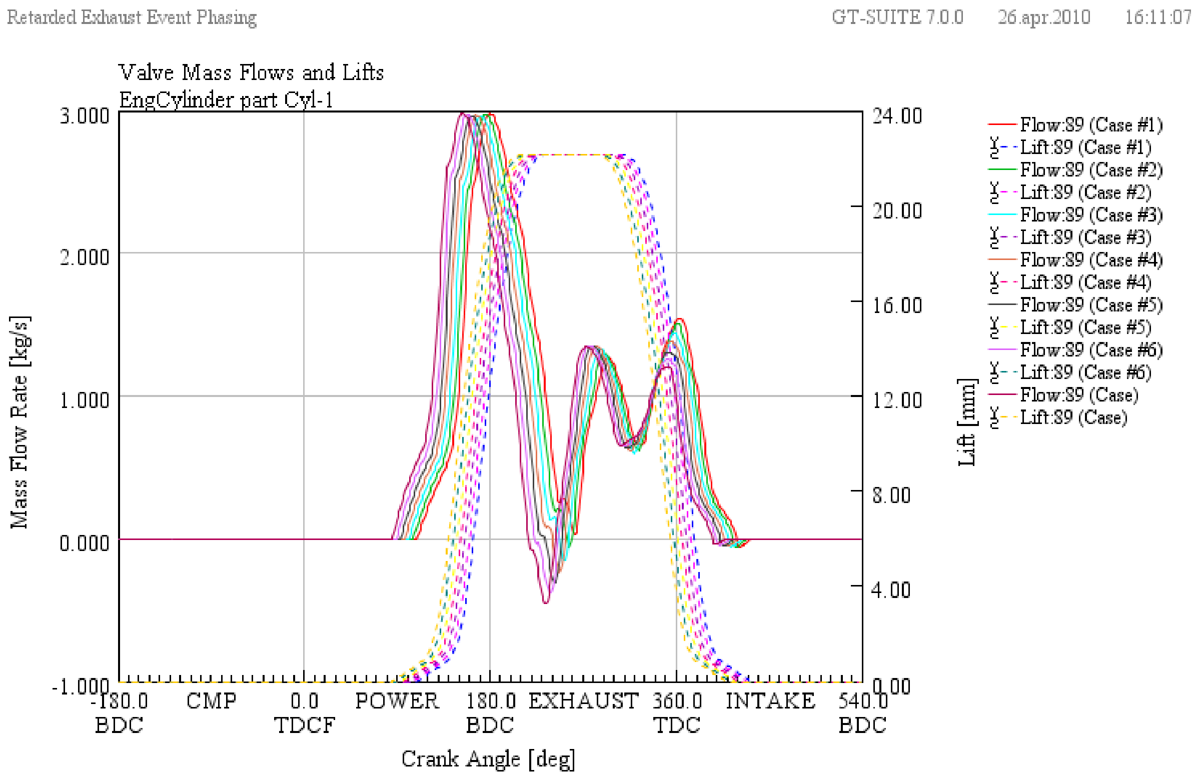

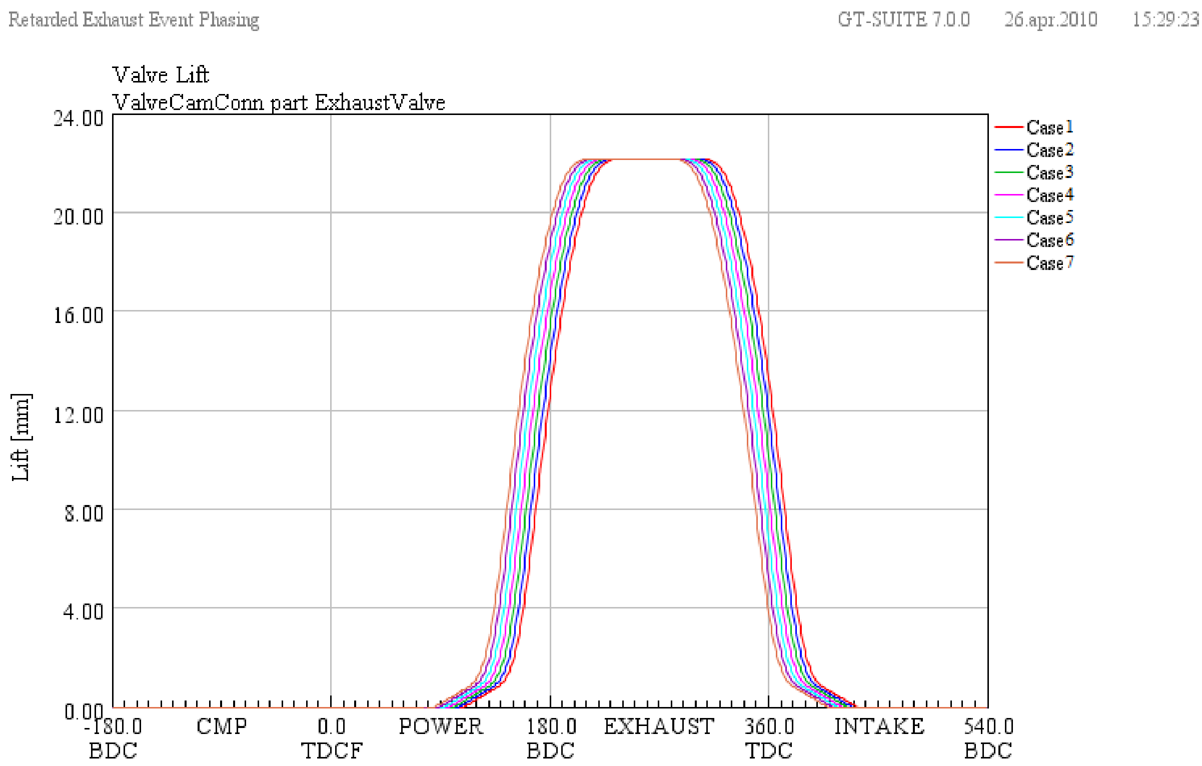

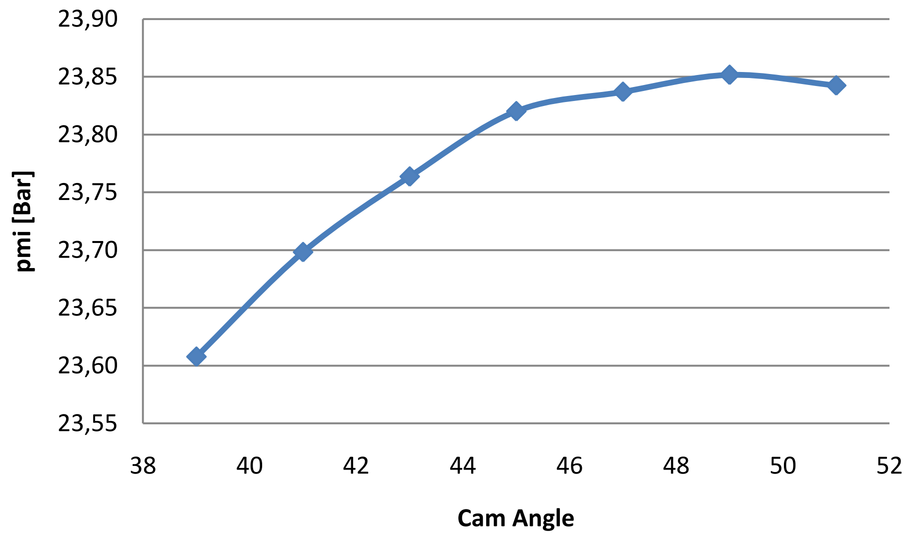
pmi [Bar]
23,90
23,85
23,80
23,75
23,70
23,65
23,60
23,55
38
40
42
44
46
48
50
52
Cam Angle

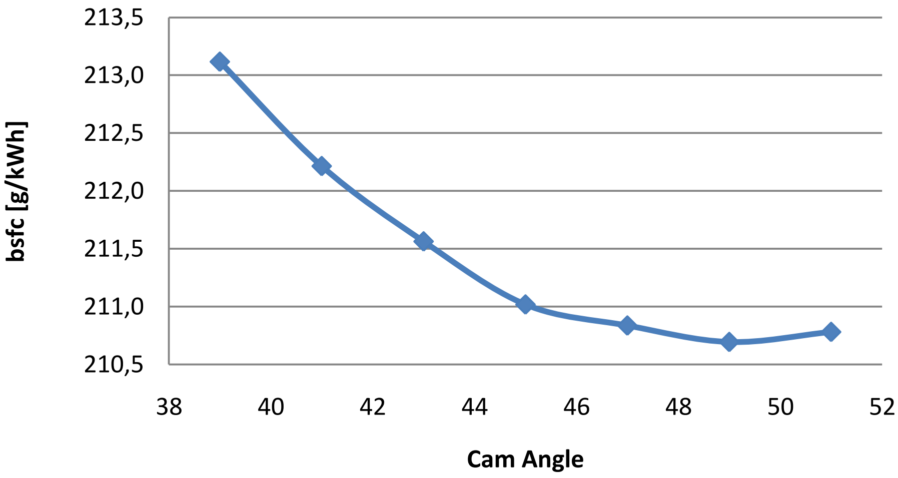
bsfc [g/kWh]
213,5
213,0
212,5
212,0
211,5
211,0
210,5
38
40
42
44
46
48
50
52
Cam Angle

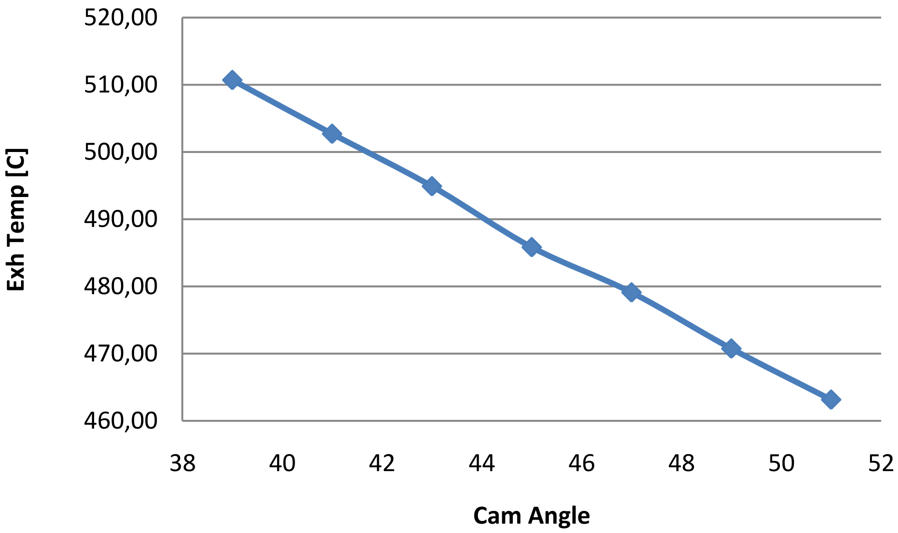
Exh Temp [C]
520,00
510,00
500,00
490,00
480,00
470,00
460,00
38
40
42
44
46
48
50
52
Cam Angle

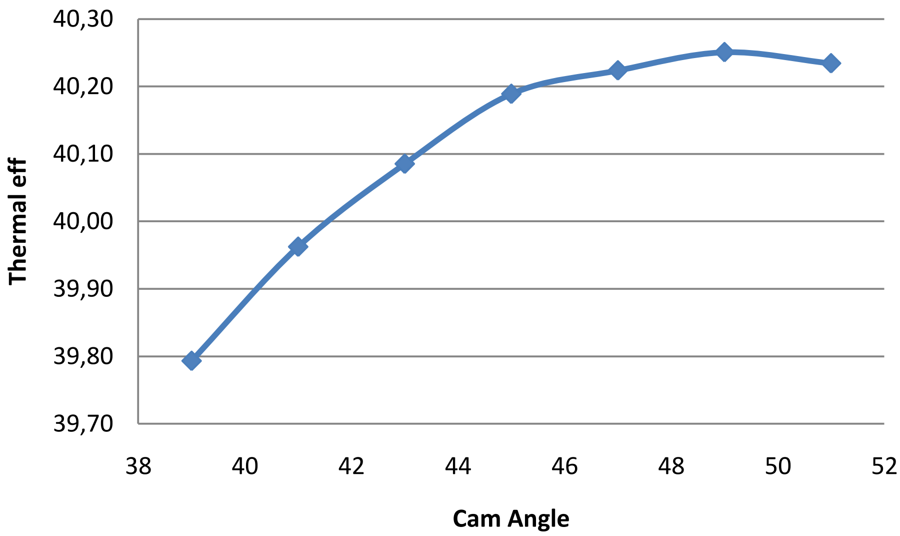
Thermal eff
40,30
40,20
40,10
40,00
39,90
39,80
39,70
38
40
42
44
46
48
50
52
Cam Angle

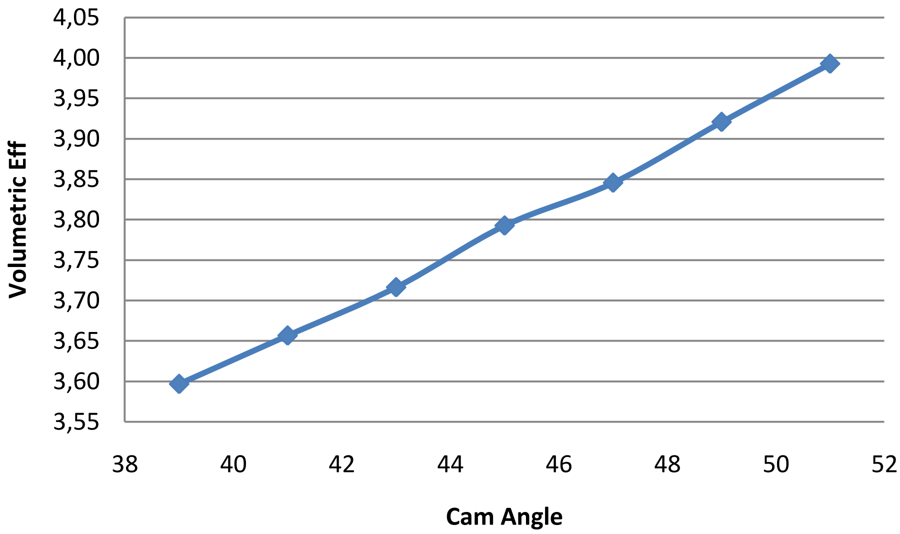
Volumetric Eff
4,05
4,00
3,95
3,90
3,85
3,80
3,75
3,70
3,65
3,60
3,55
38
40
42
44
46
48
50
52
Cam Angle

APPENDIX H: LATE EXHAUST PHASING AT 500 RPM AND 5735 NM

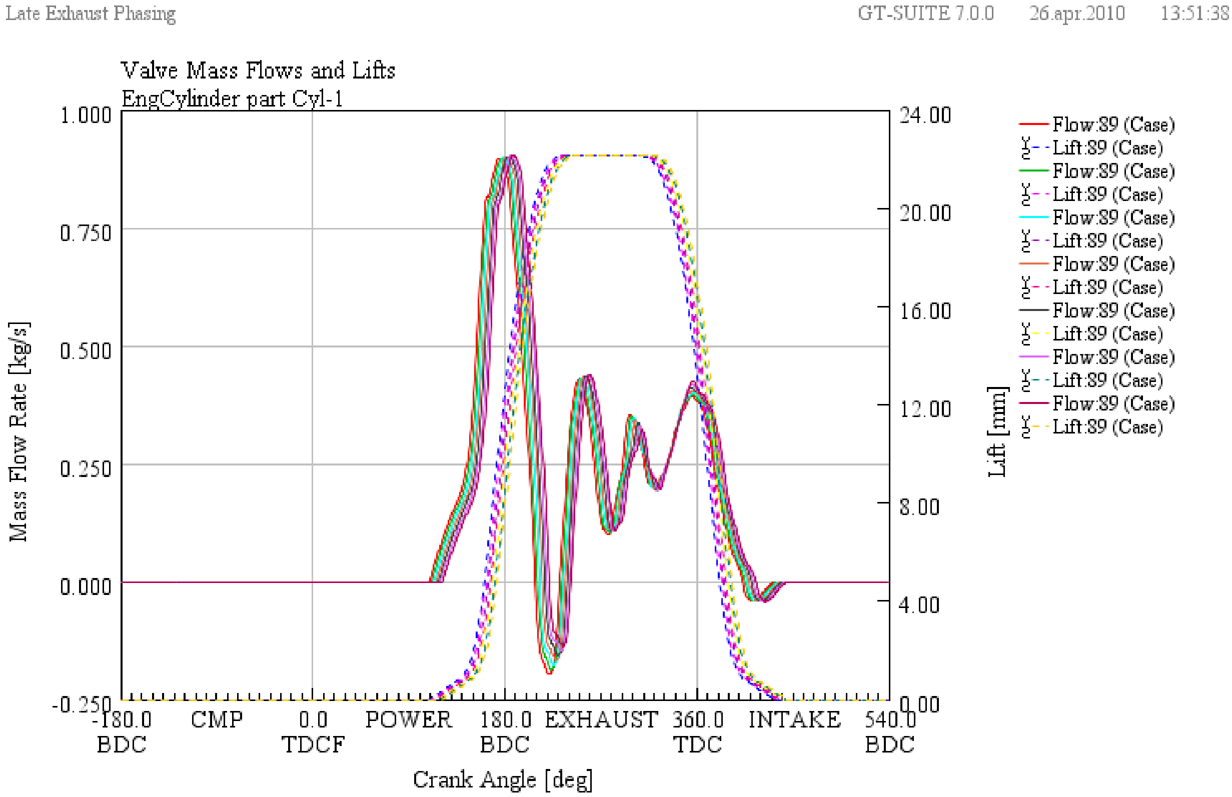

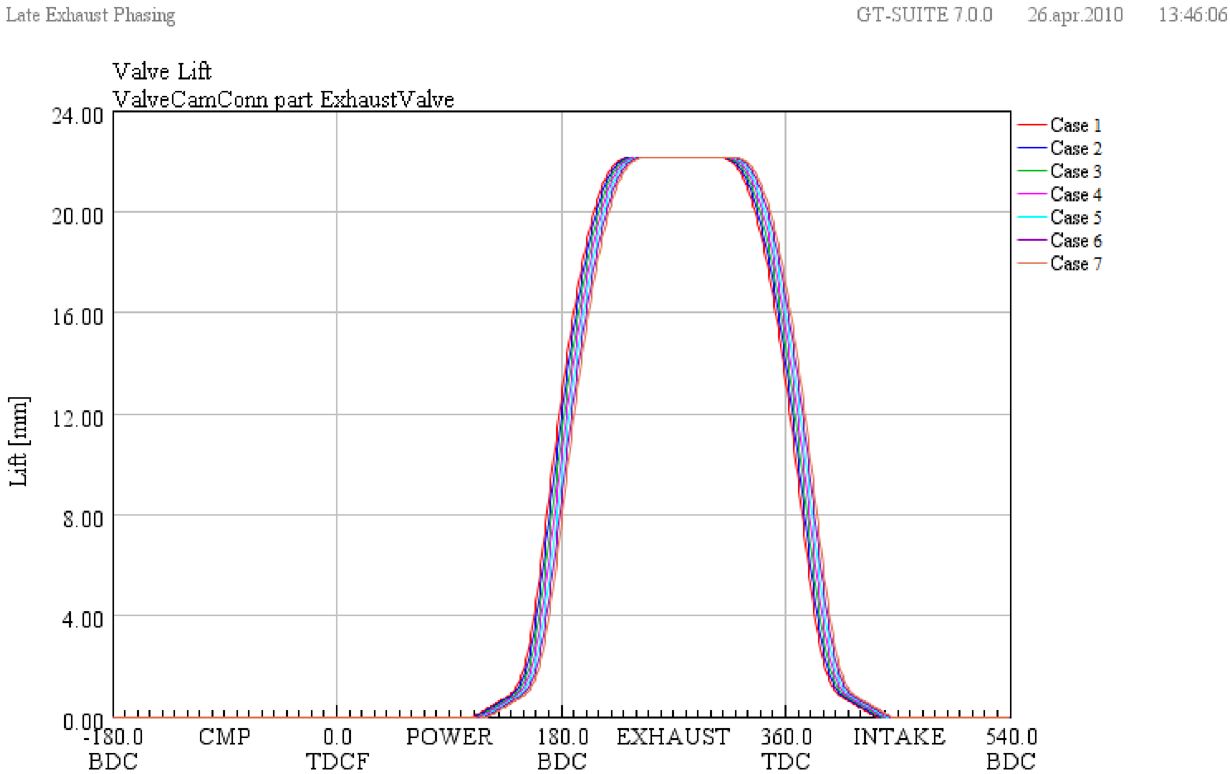

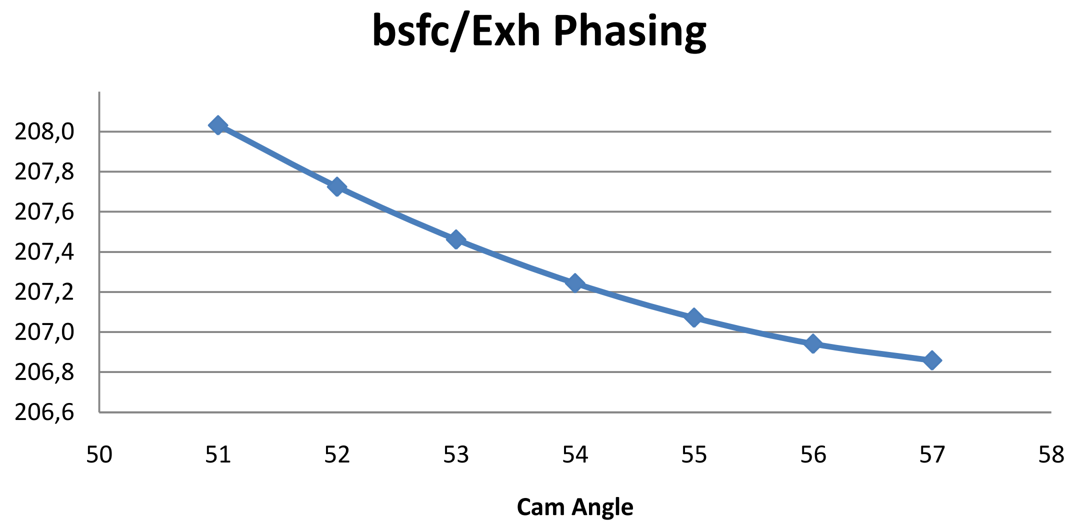
bsfc/Exh Phasing
208,0
207,8
207,6
207,4
207,2
207,0
206,8
206,6
50
51
52
53
54
55
56
57
58
Cam Angle

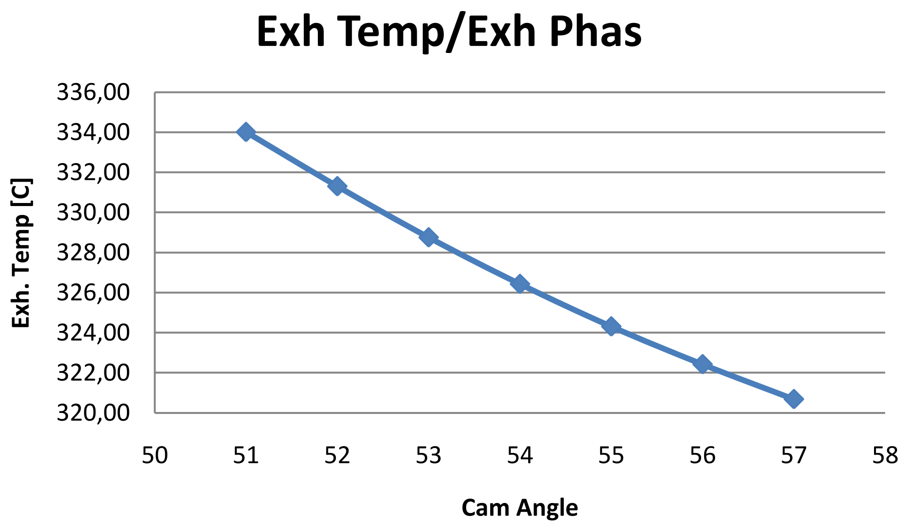
Exh Temp/Exh Phas
Exh. Temp [C]
336,00
334,00
332,00
330,00
328,00
326,00
324,00
322,00
320,00
50
51
52
53
54
55
56
57
58
Cam Angle

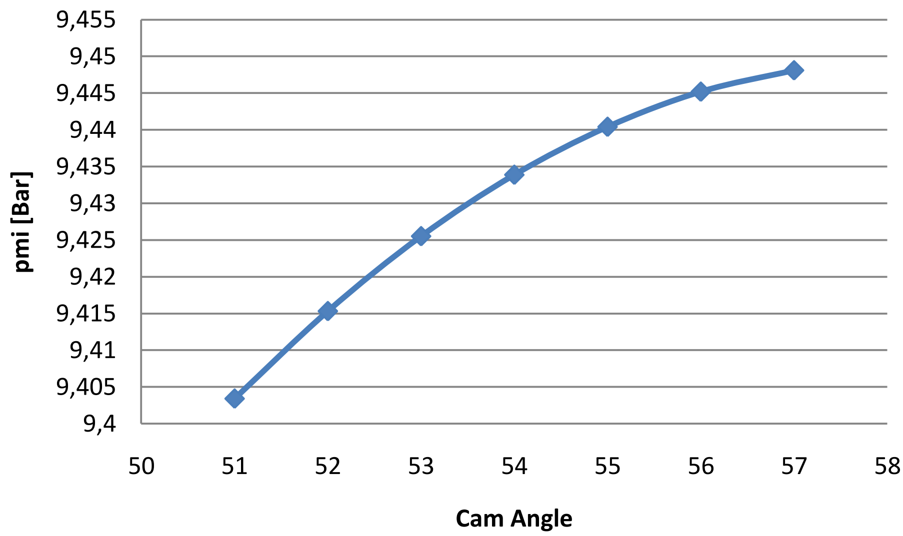
pmi [Bar]
9,455
9,45
9,445
9,44
9,435
9,43
9,425
9,42
9,415
9,41
9,405
9,4
50
51
52
53
54
55
56
57
58
Cam Angle

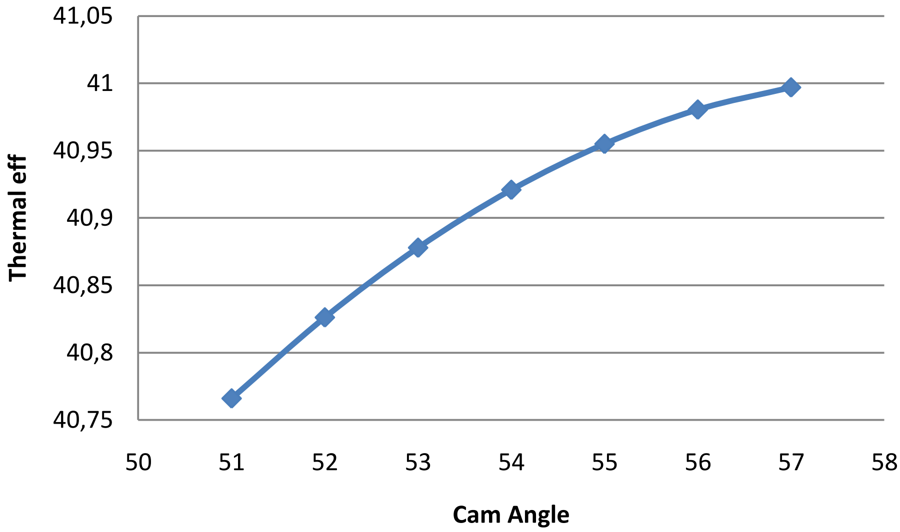
41,05
41
40,95
40,9
40,85
40,8
40,75
Thermal eff
50
51
52
53
54
55
56
57
58
Cam Angle

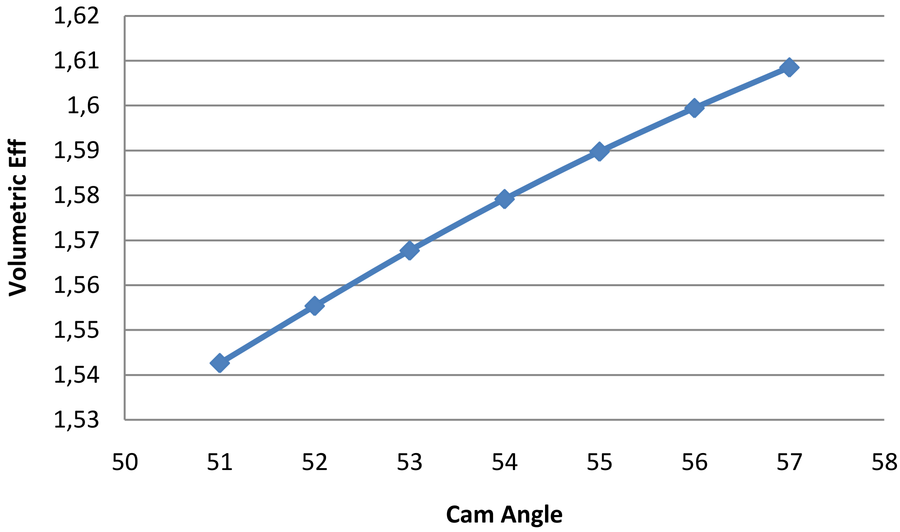
1,62
1,61
1,6
1,59
1,58
1,57
1,56
1,55
1,54
1,53
Volumetric Eff
50
51
52
53
54
55
56
57
58
Cam Angle

APPENDIX I: LATE EXHAUST PHASING AT 825 RPM AND 15464 NM

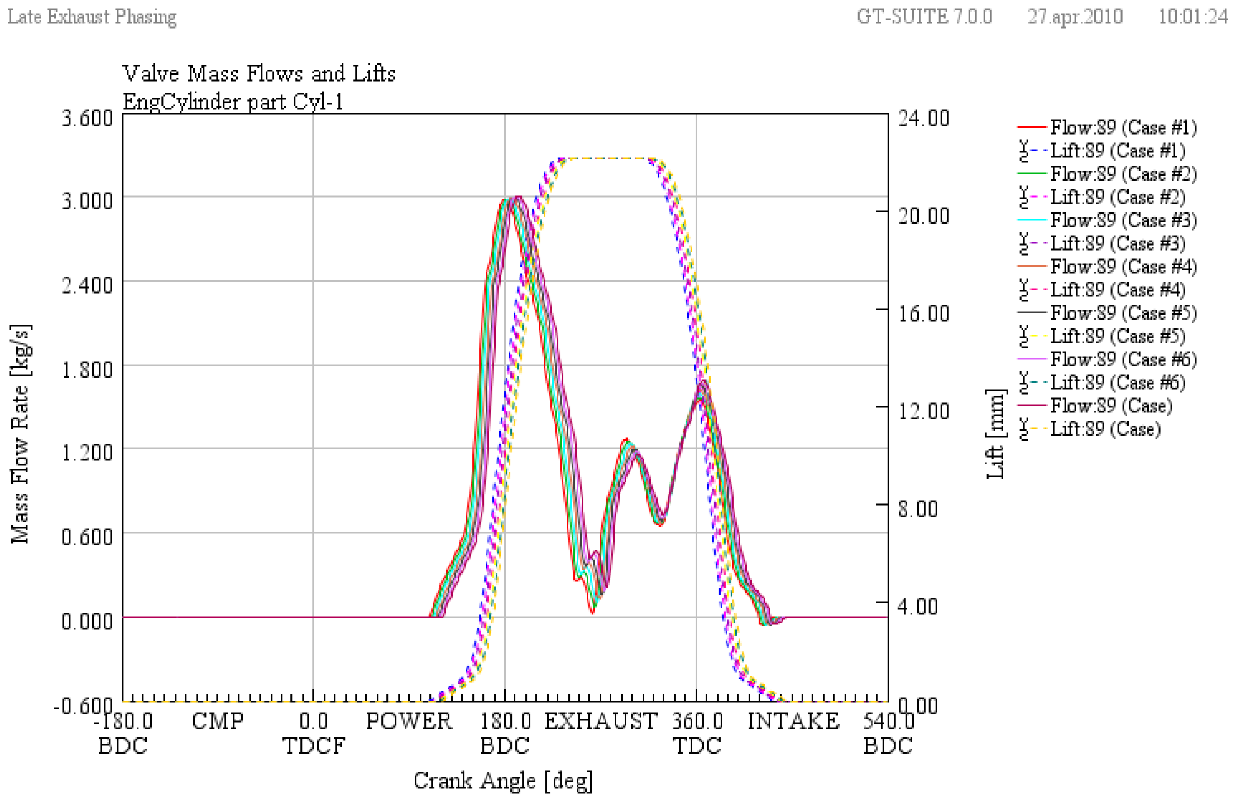

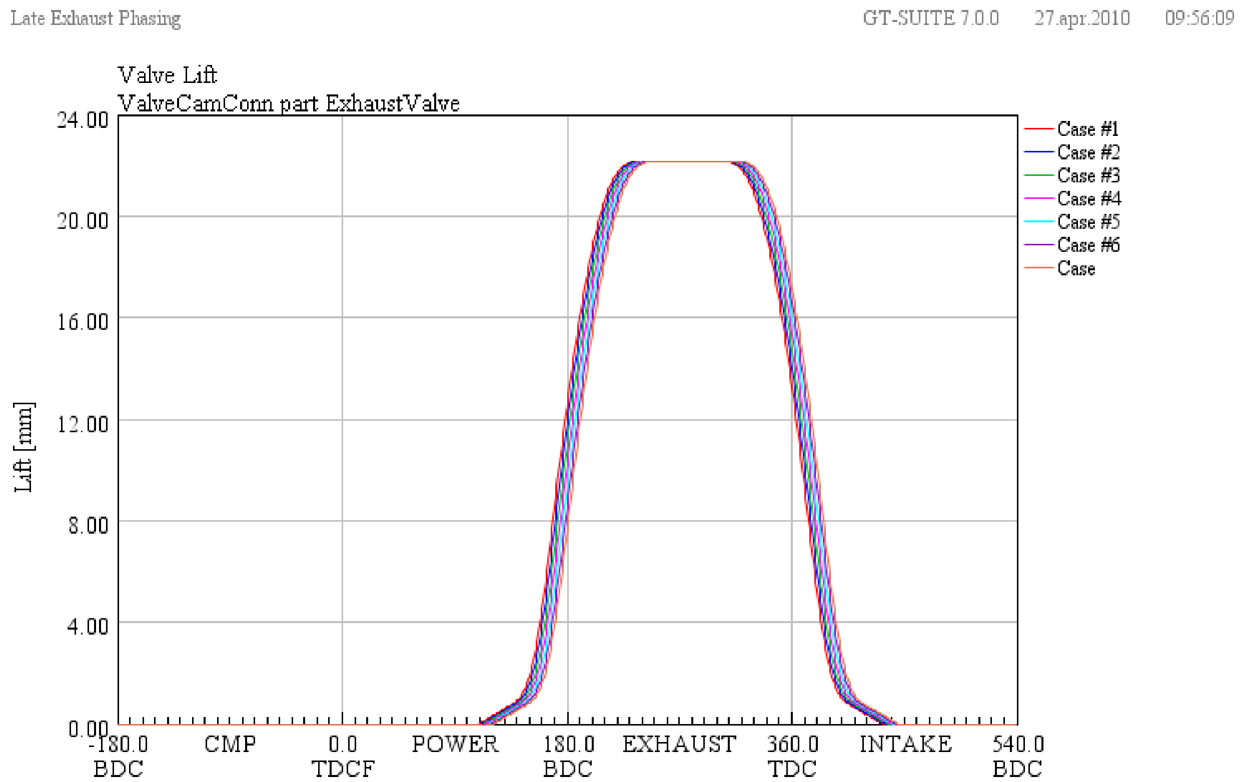

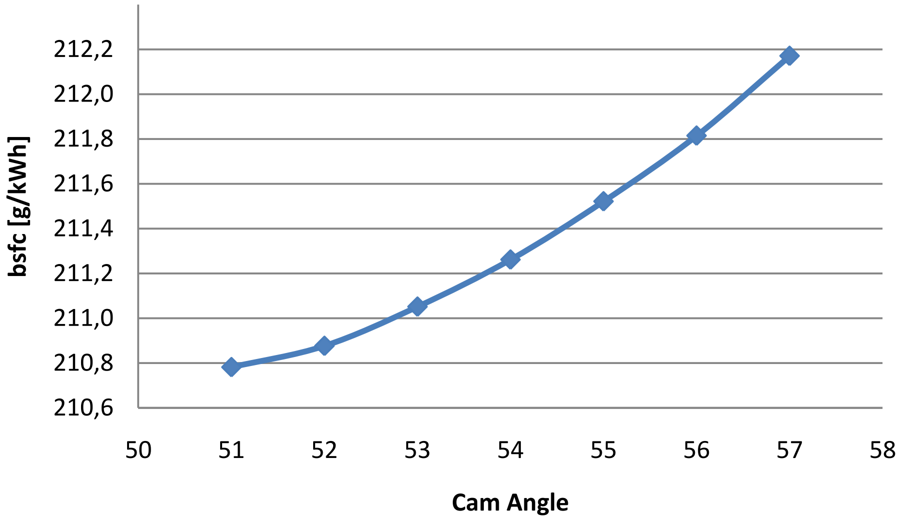
bsfc [g/kWh]
212,2
212,0
211,8
211,6
211,4
211,2
211,0
210,8
210,6
50
51
52
53
54
55
56
57
58
Cam Angle

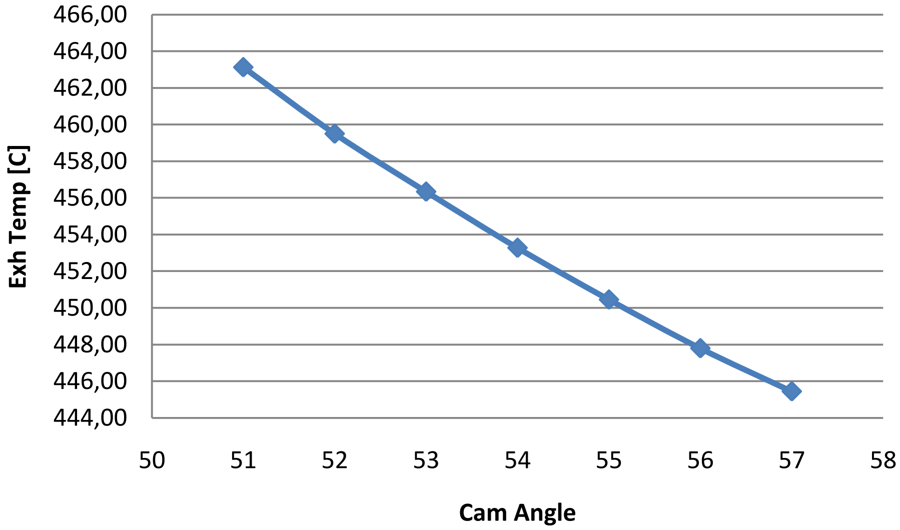
Exh Temp [C]
466,00
464,00
462,00
460,00
458,00
456,00
454,00
452,00
450,00
448,00
446,00
444,00
50
51
52
53
54
55
56
57
58
Cam Angle

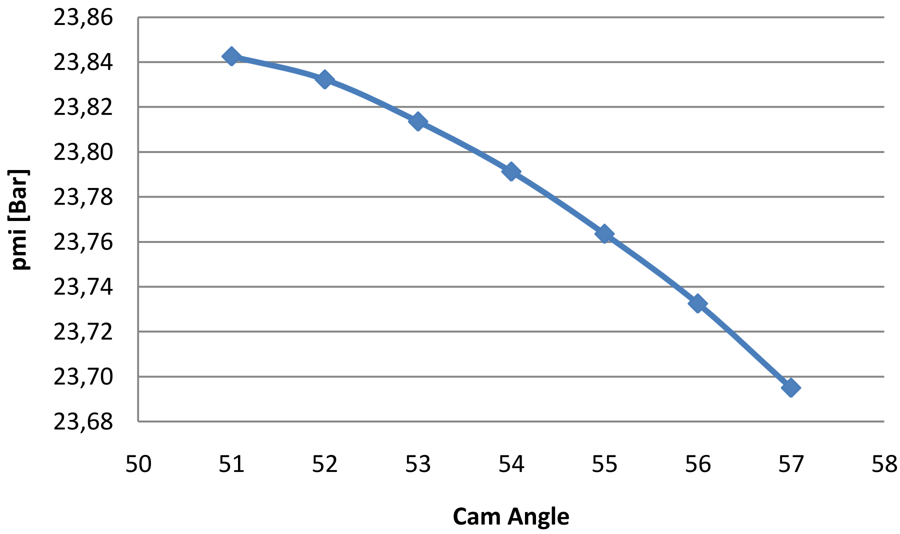
pmi [Bar]
23,86
23,84
23,82
23,80
23,78
23,76
23,74
23,72
23,70
23,68
50
51
52
53
54
55
56
57
58
Cam Angle

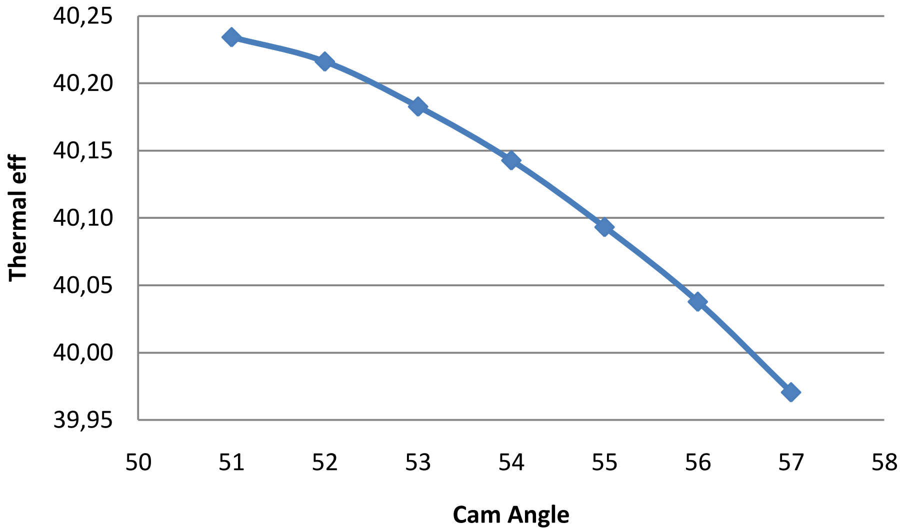
40,25
40,20
40,15
40,10
40,05
40,00
39,95
Thermal eff
50
51
52
53
54
55
56
57
58
Cam Angle

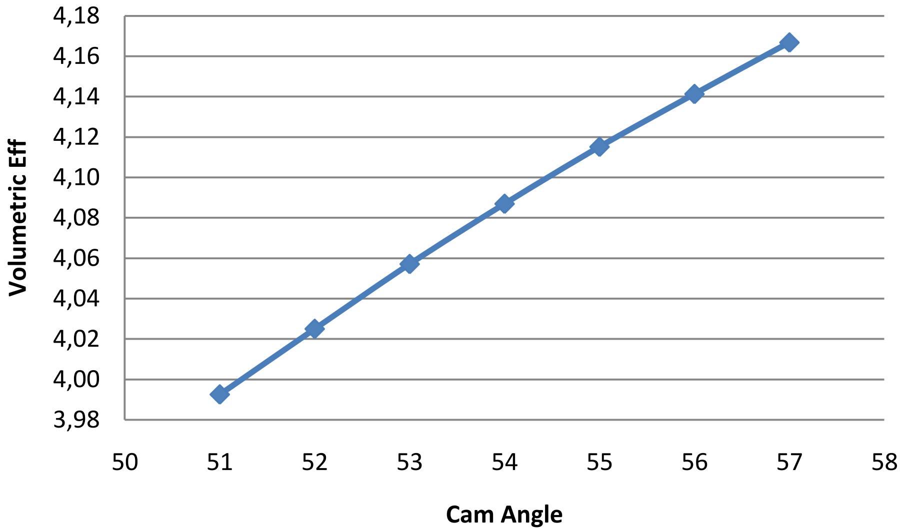
4,18
4,16
4,14
4,12
4,10
4,08
4,06
4,04
4,02
4,00
3,98
Volumetric Eff
50
51
52
53
54
55
56
57
58
Cam Angle

APPENDIX J: EARLY INLET PHASING AT 500 RPM AND 5735 NM

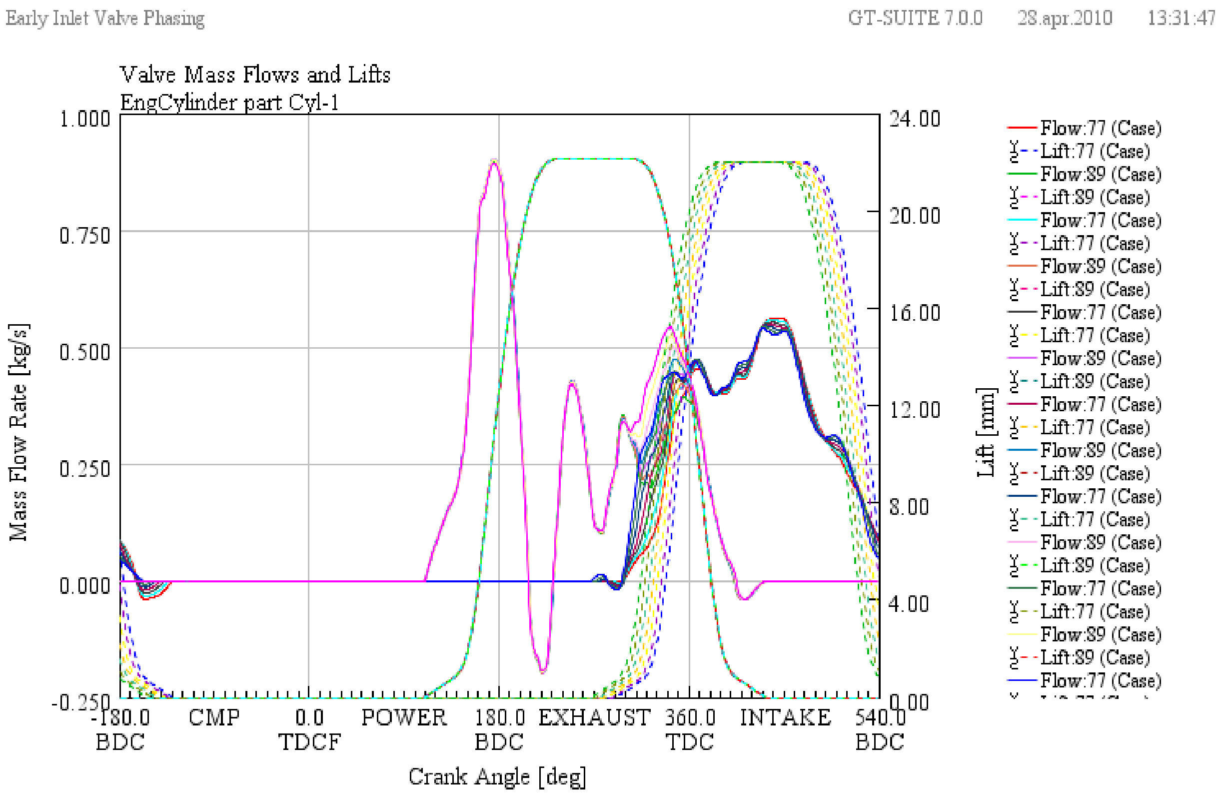

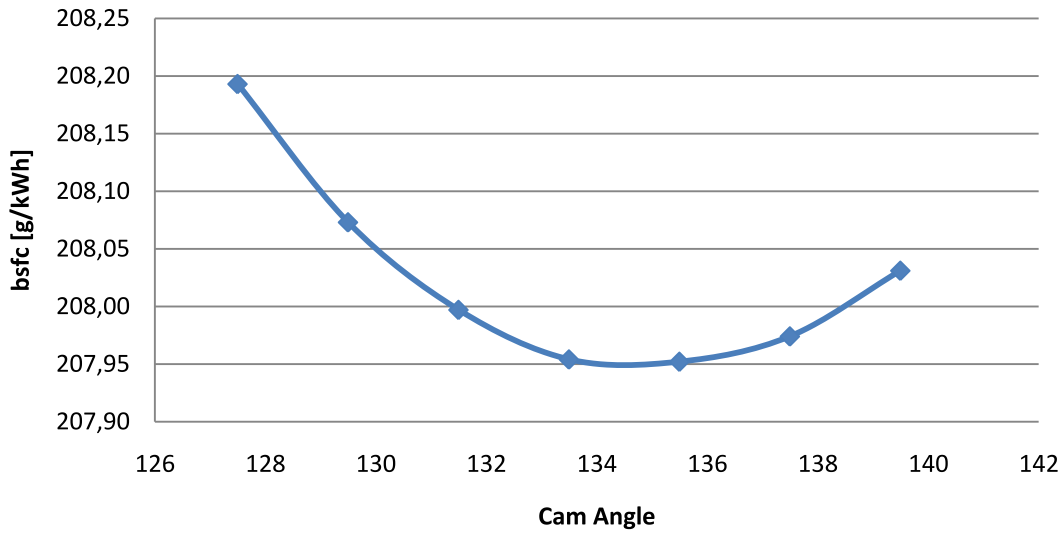

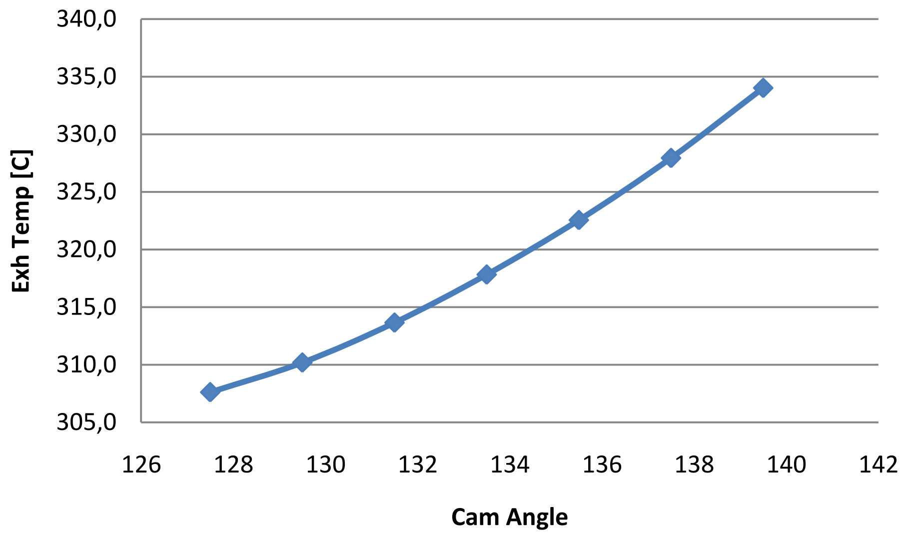
340,0
335,0
330,0
325,0
320,0
315,0
310,0
305,0
Exh Temp [C]
126
128
130
132
134
136
138
140
142
Cam Angle

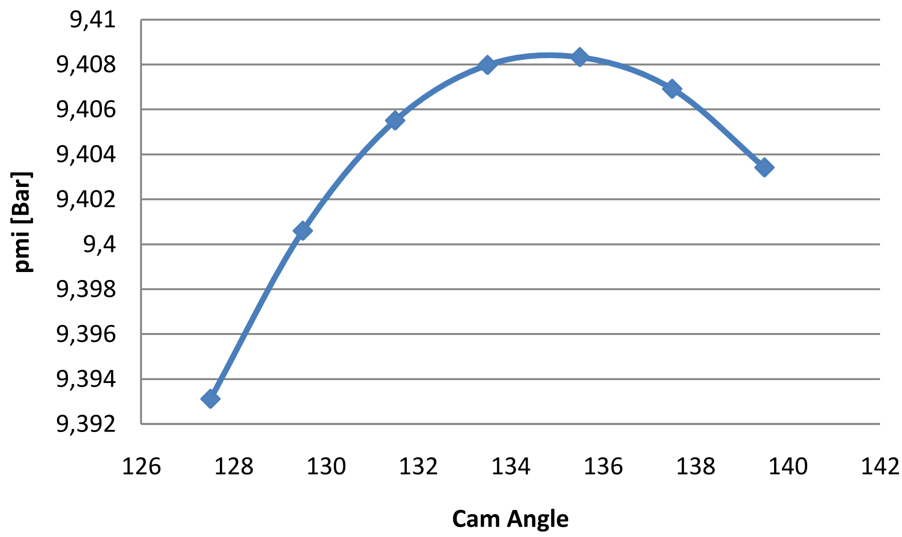
9,41
9,408
9,406
9,404
9,402
9,4
9,398
9,396
9,394
9,392
pmi [Bar]
126
128
130
132
134
136
138
140
142
Cam Angle

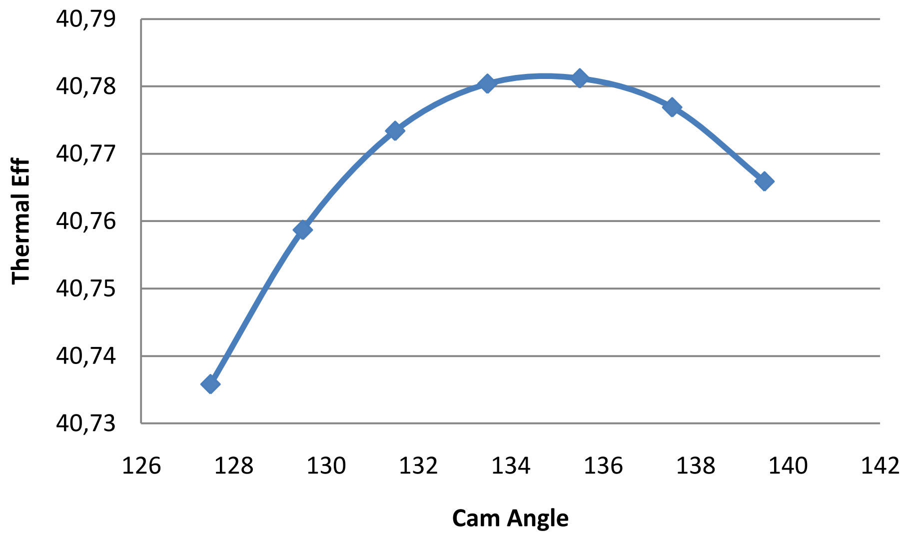
Thermal Eff
40,79
40,78
40,77
40,76
40,75
40,74
40,73
126
128
130
132
134
136
138
140
142
Cam Angle

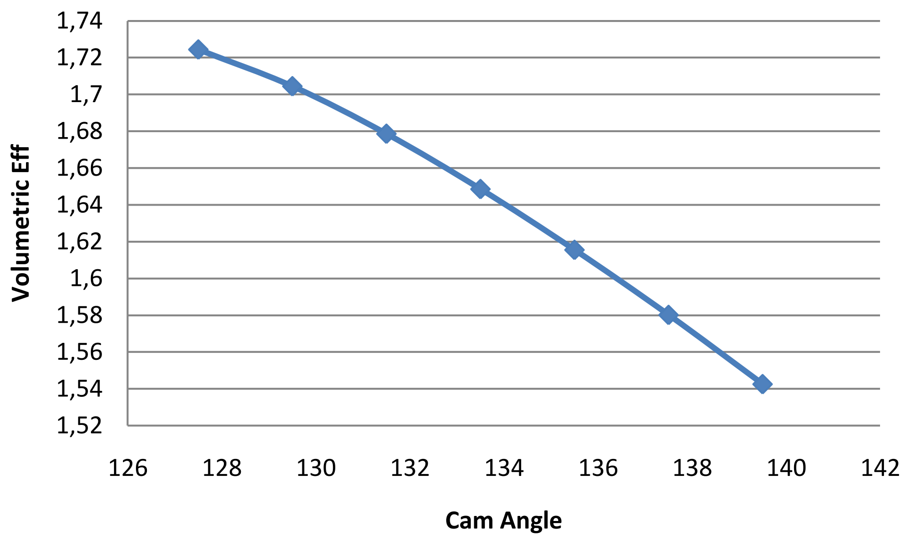
Volumetric Eff
1,74
1,72
1,7
1,68
1,66
1,64
1,62
1,6
1,58
1,56
1,54
1,52
126
128
130
132
134
136
138
140
142
Cam Angle

APPENDIX K: EARLY INLET PHASING AT 825 RPM AND 15464 NM

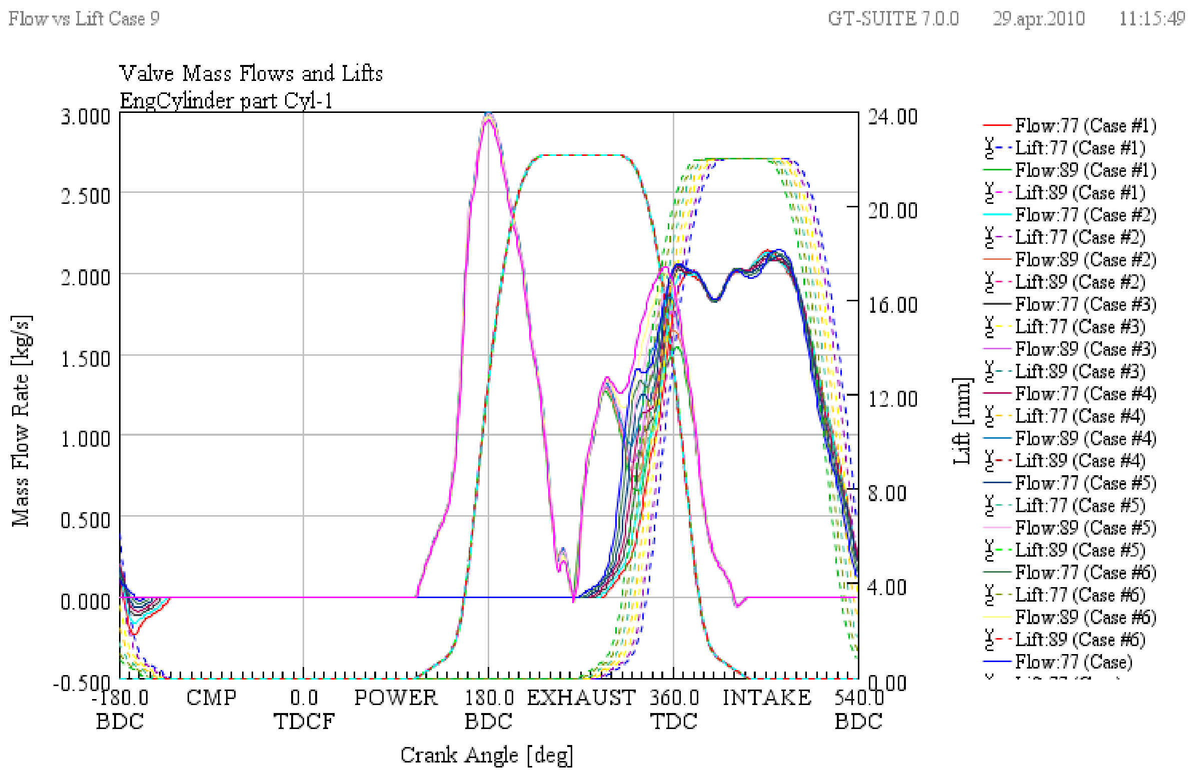

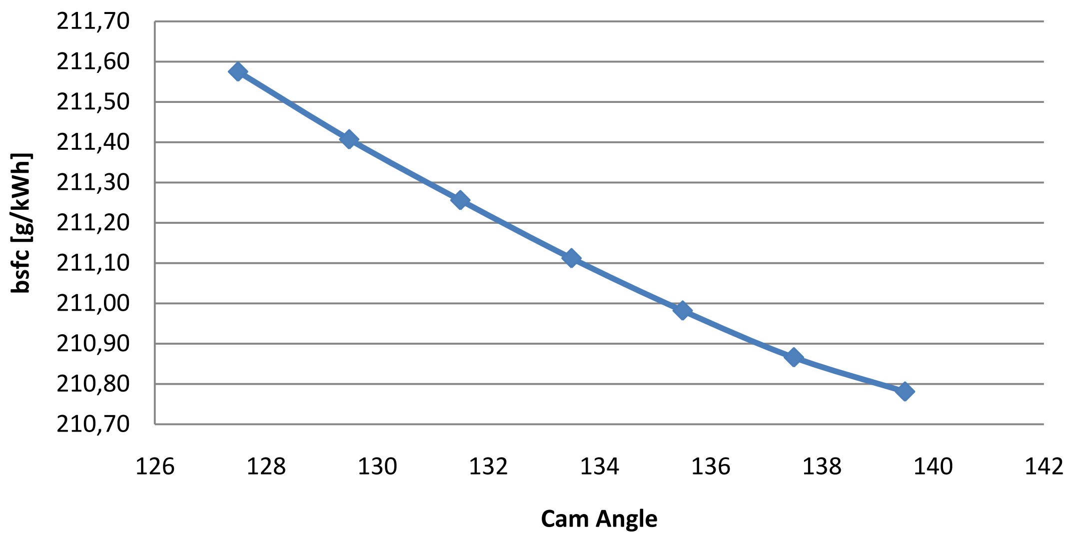

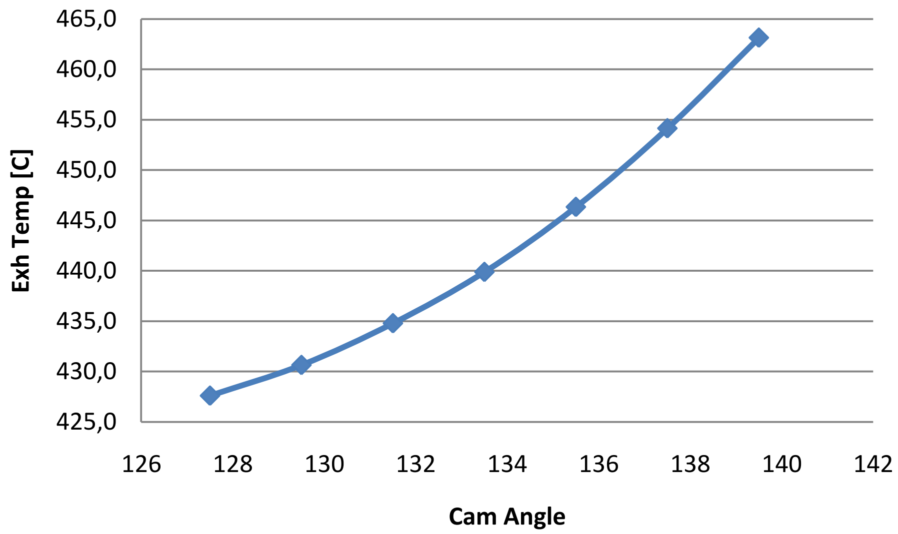
465,0
460,0
455,0
450,0
445,0
440,0
435,0
430,0
425,0
Exh Temp [C]
126
128
130
132
134
136
138
140
142
Cam Angle

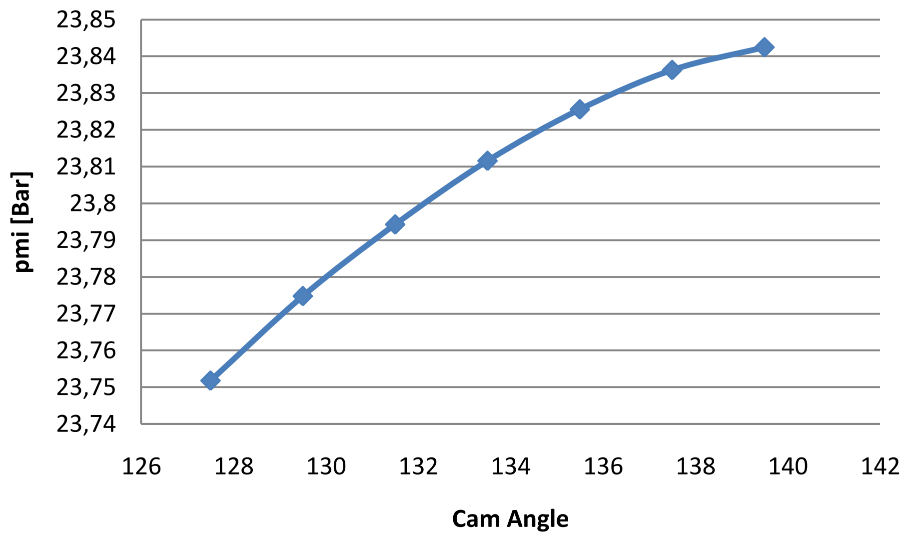
23,85
23,84
23,83
23,82
23,81
23,8
23,79
23,78
23,77
23,76
23,75
23,74
pmi [Bar]
126
128
130
132
134
136
138
140
142
Cam Angle

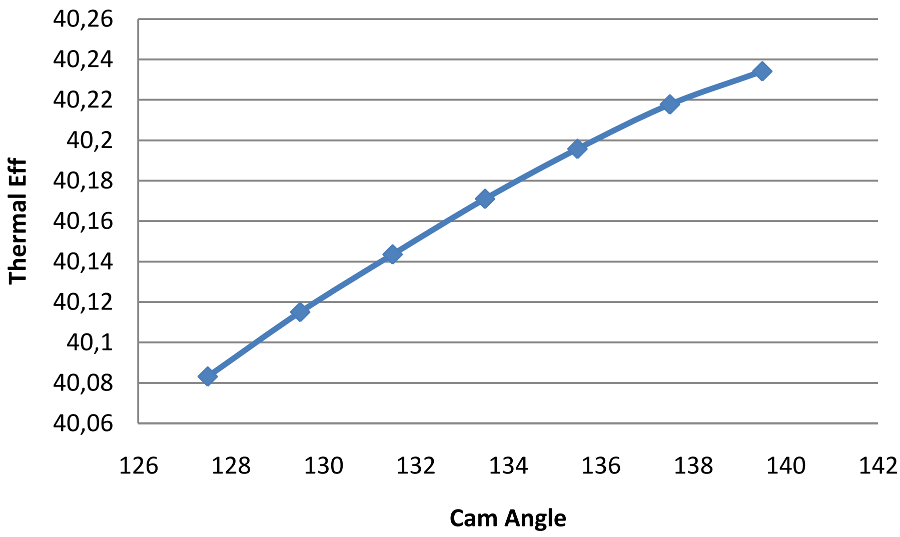
40,26
40,24
40,22
40,2
40,18
40,16
40,14
40,12
40,1
40,08
40,06
Thermal Eff
126
128
130
132
134
136
138
140
142
Cam Angle

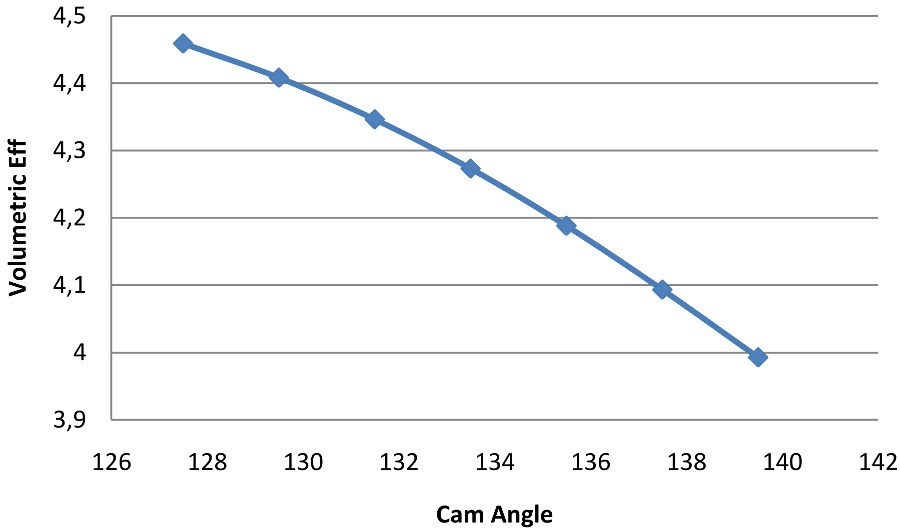
4,5
4,4
4,3
4,2
4,1
4
3,9
Volumetric Eff
126
128
130
132
134
136
138
140
142
Cam Angle

APPENDIX L: LATE INLET VALVE PHASING 500 RPM AND 5735 NM

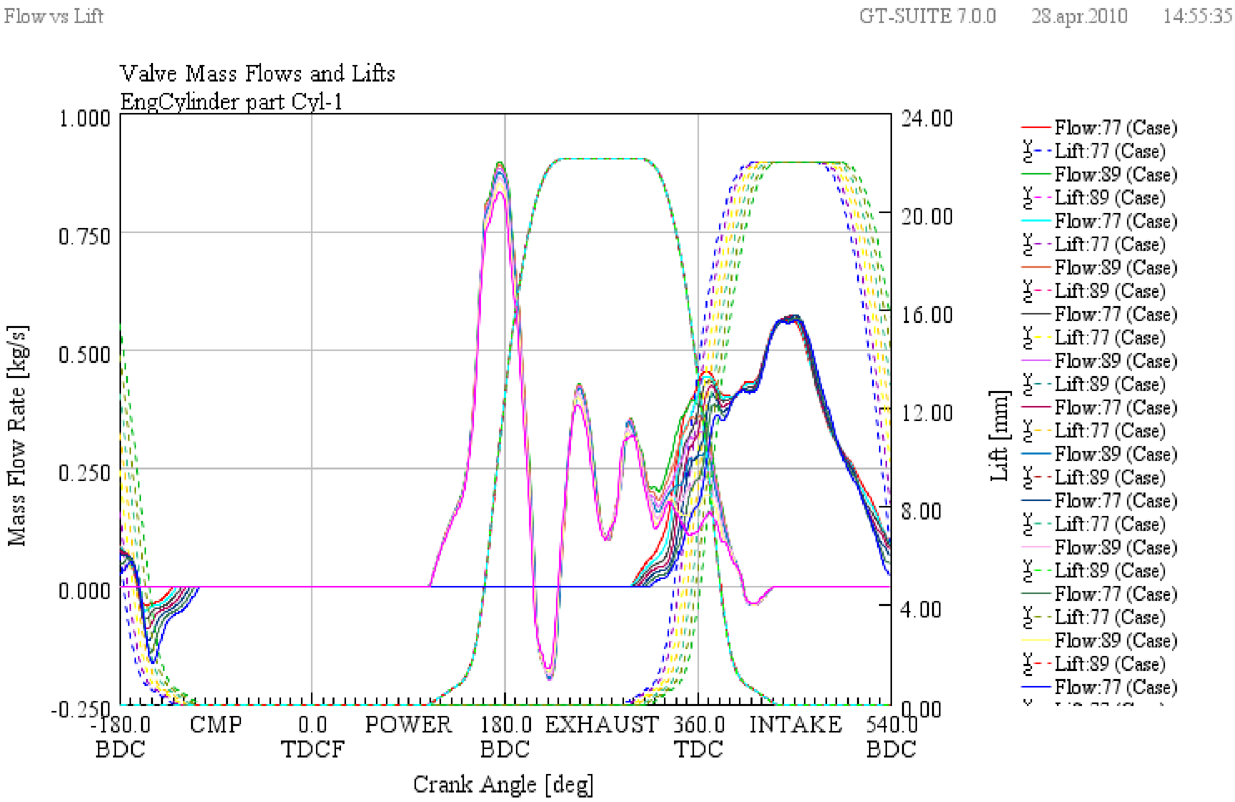

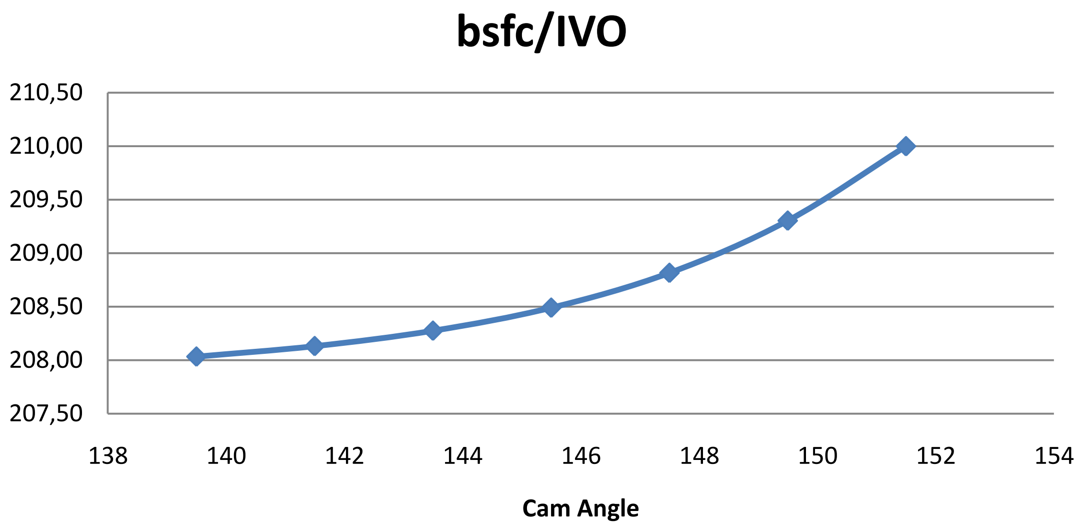

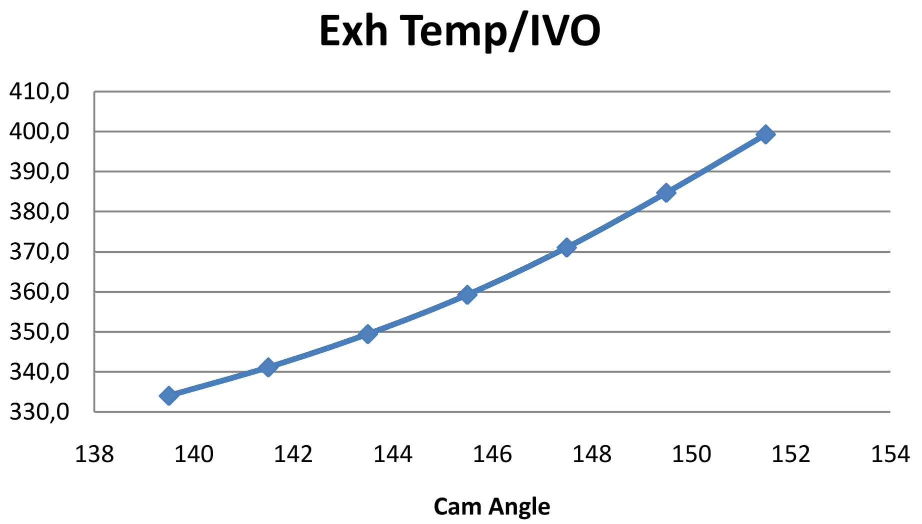
Exh Temp/IVO
410,0
400,0
390,0
380,0
370,0
360,0
350,0
340,0
330,0
138
140
142
144
146
148
150
152
154
Cam Angle

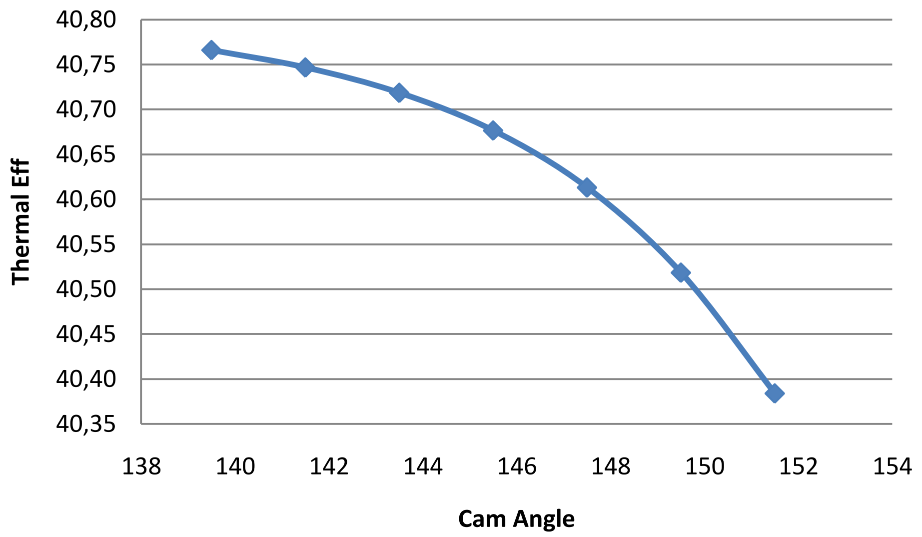
Thermal Eff
40,80
40,75
40,70
40,65
40,60
40,55
40,50
40,45
40,40
40,35
138
140
142
144
146
148
150
152
154
Cam Angle

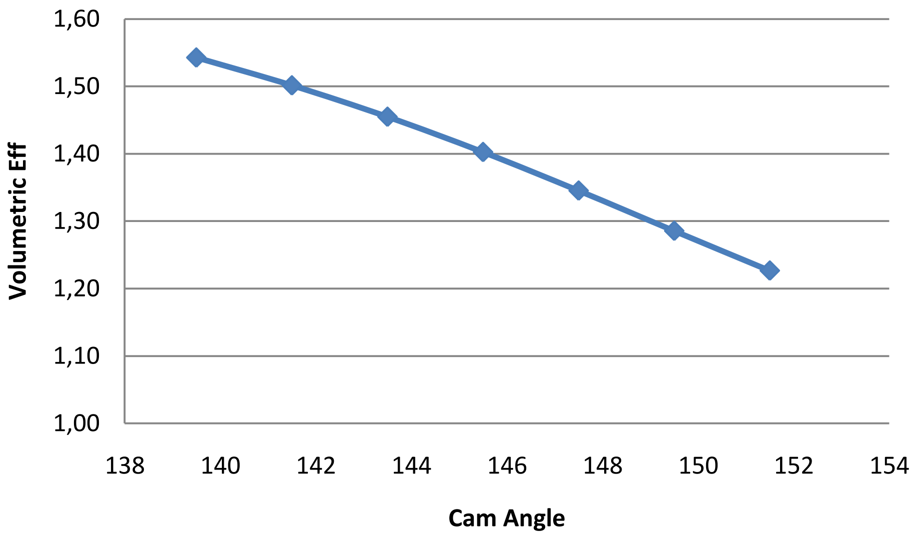
Volumetric Eff
1,60
1,50
1,40
1,30
1,20
1,10
1,00
138
140
142
144
146
148
150
152
154
Cam Angle

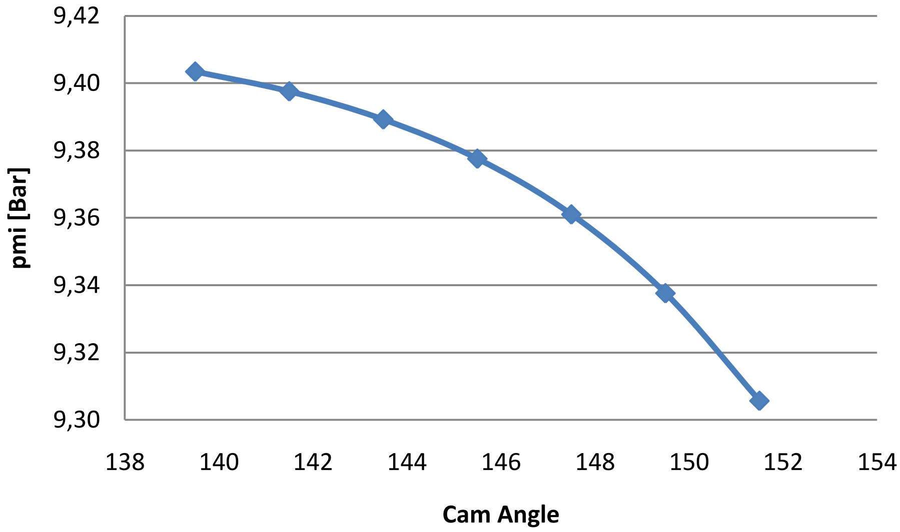
pmi [Bar]
9,42
9,40
9,38
9,36
9,34
9,32
9,30
138
140
142
144
146
148
150
152
154
Cam Angle

APPENDIX M: LATE INLET VALVE PHASING 825 RPM AND 15464 NM

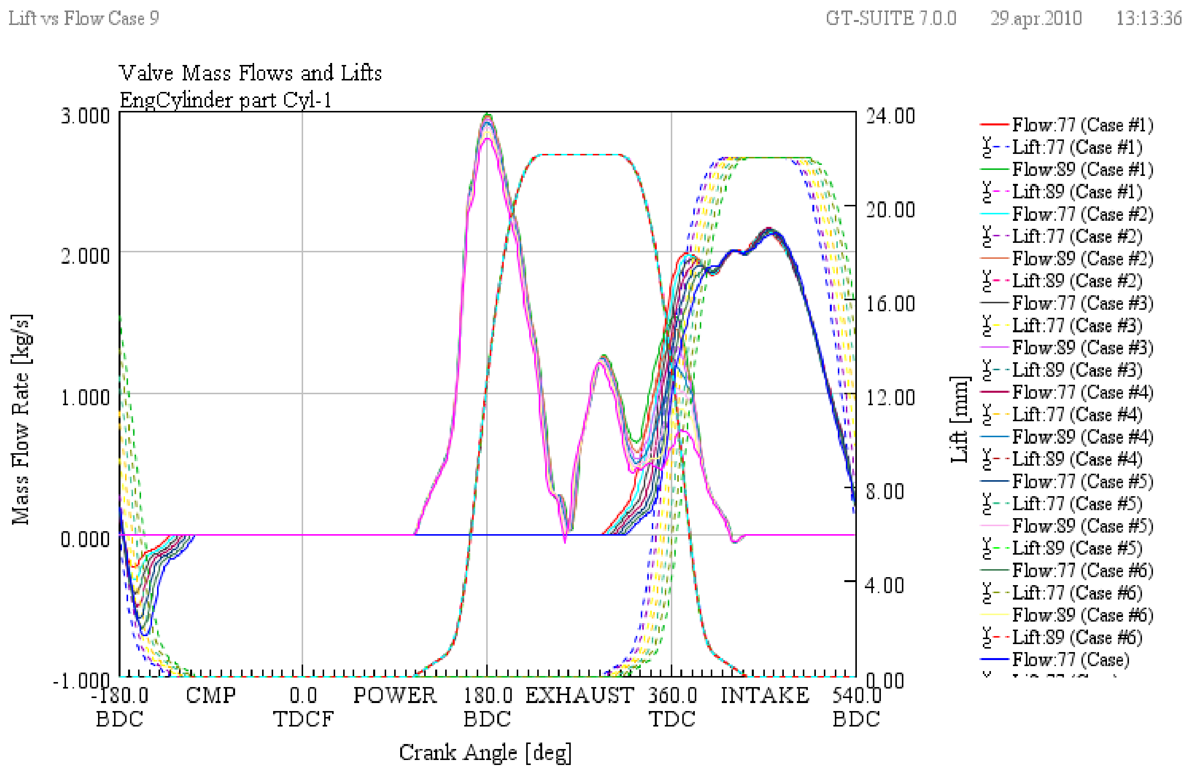

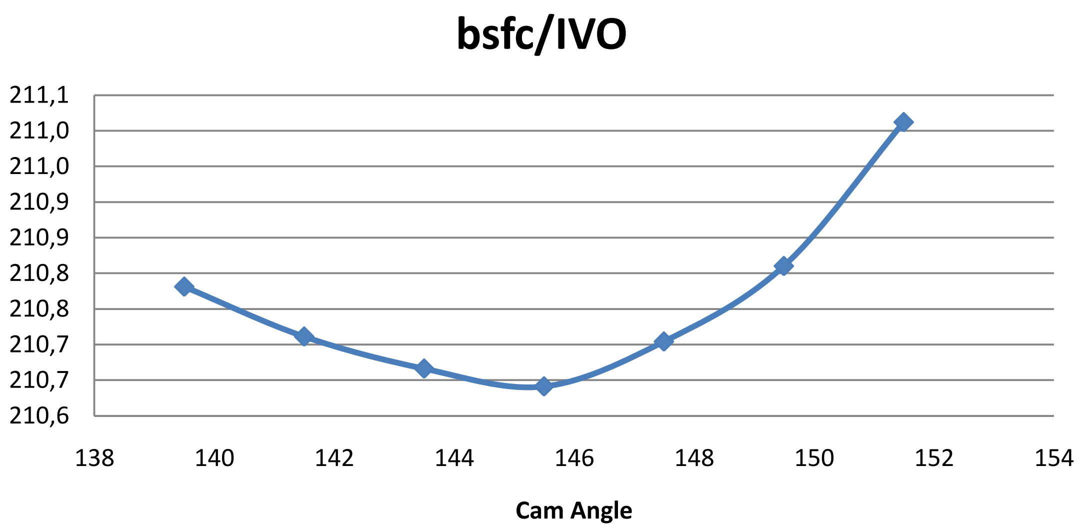

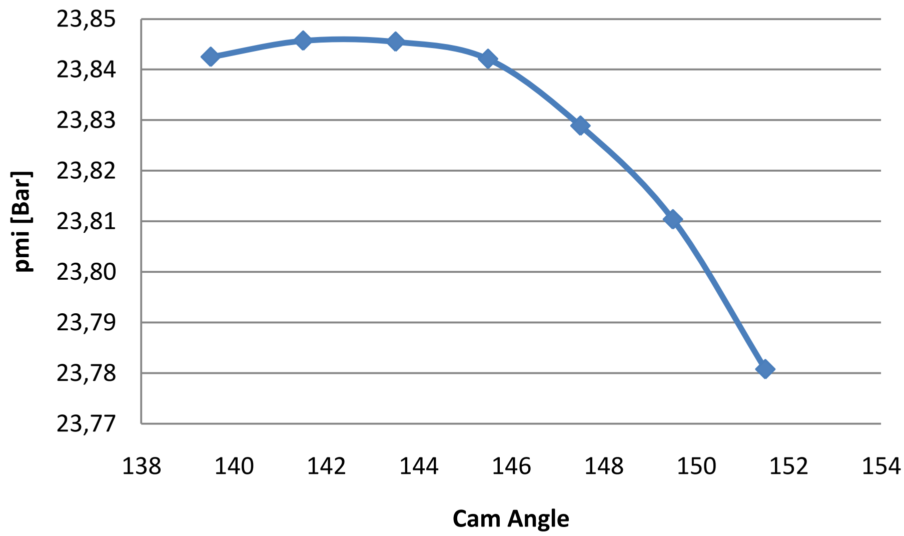
pmi [Bar]
23,85
23,84
23,83
23,82
23,81
23,80
23,79
23,78
23,77
138
140
142
144
146
148
150
152
154
Cam Angle

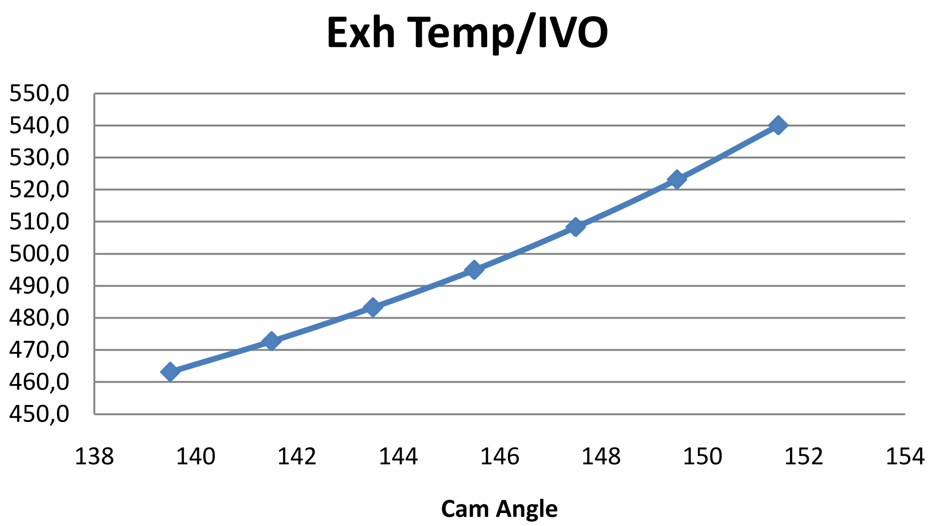
Exh Temp/IVO
550,0
540,0
530,0
520,0
510,0
500,0
490,0
480,0
470,0
460,0
450,0
138
140
142
144
146
148
150
152
154
Cam Angle

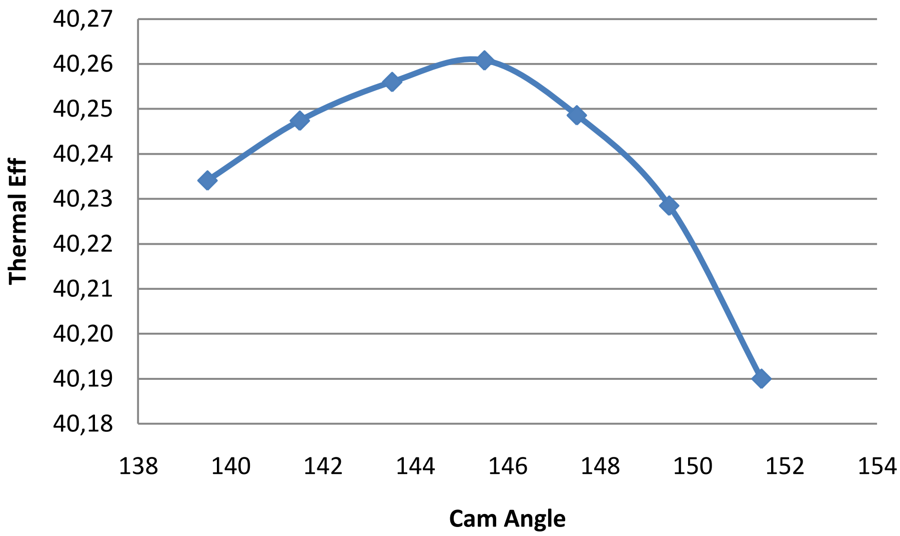
Thermal Eff
40,27
40,26
40,25
40,24
40,23
40,22
40,21
40,20
40,19
40,18
138
140
142
144
146
148
150
152
154
Cam Angle

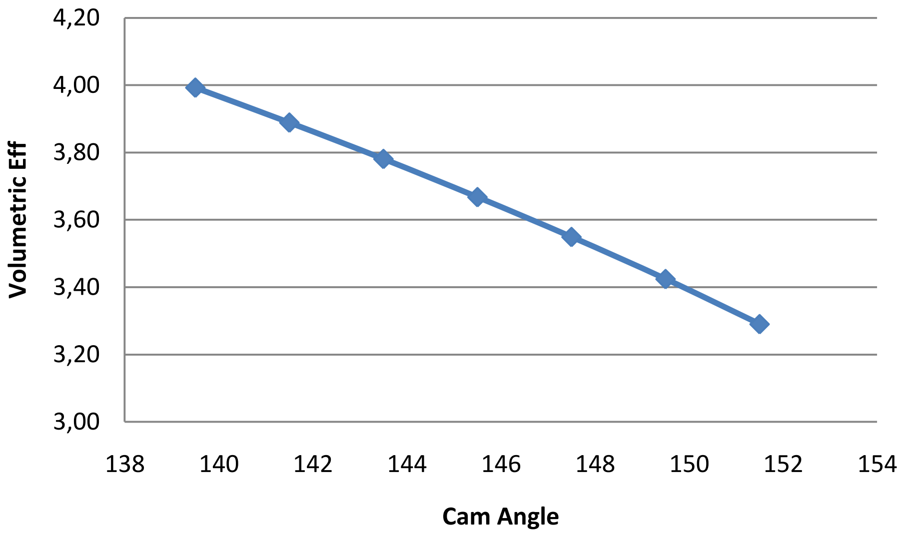
Volumetric Eff
4,20
4,00
3,80
3,60
3,40
3,20
3,00
138
140
142
144
146
148
150
152
154
Cam Angle

APPENDIX N: EARLY VALVE OPENING AT 500 RPM AND 5735 NM

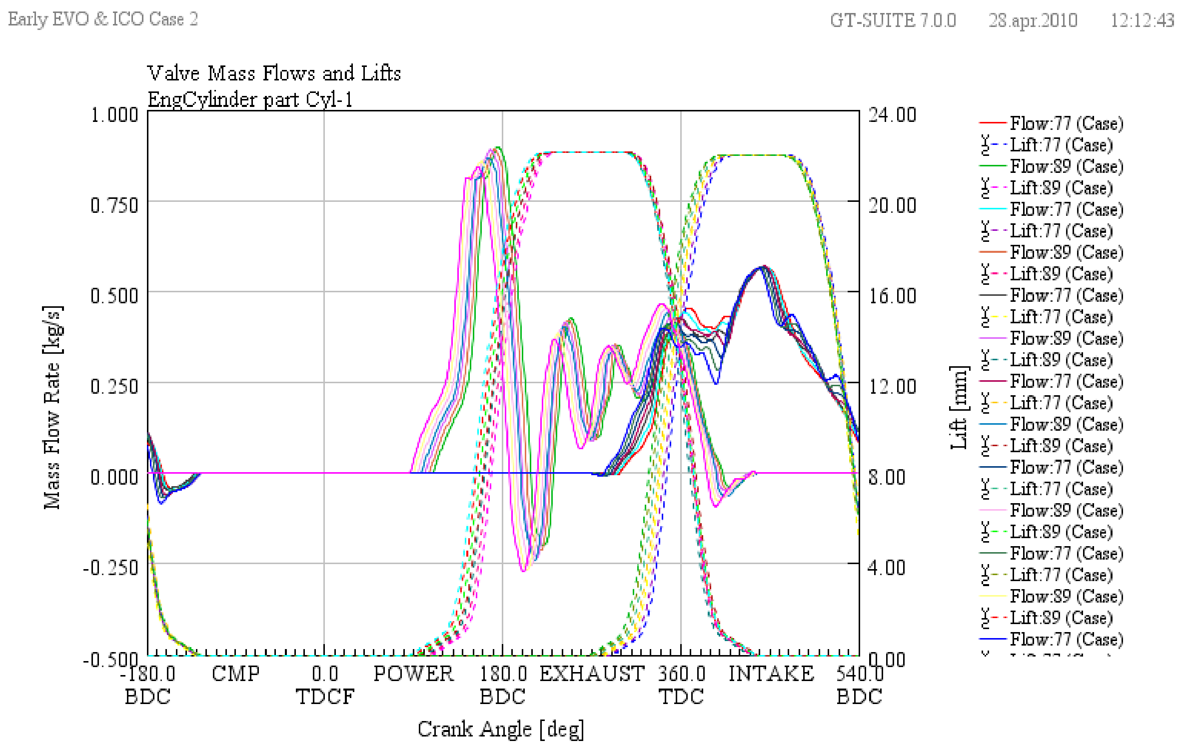

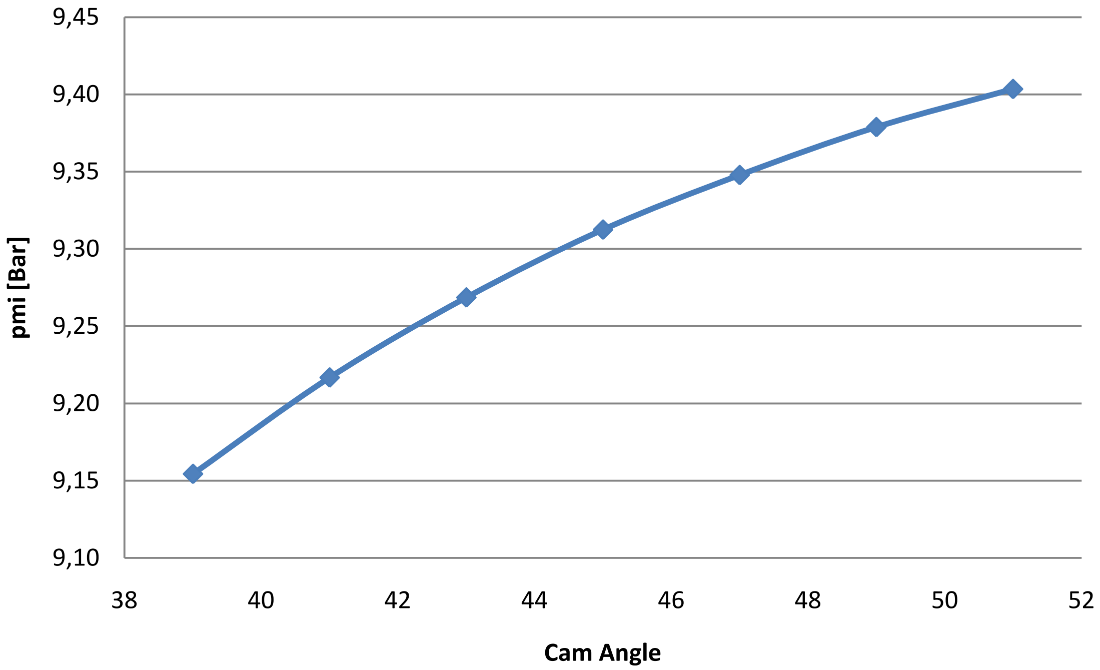

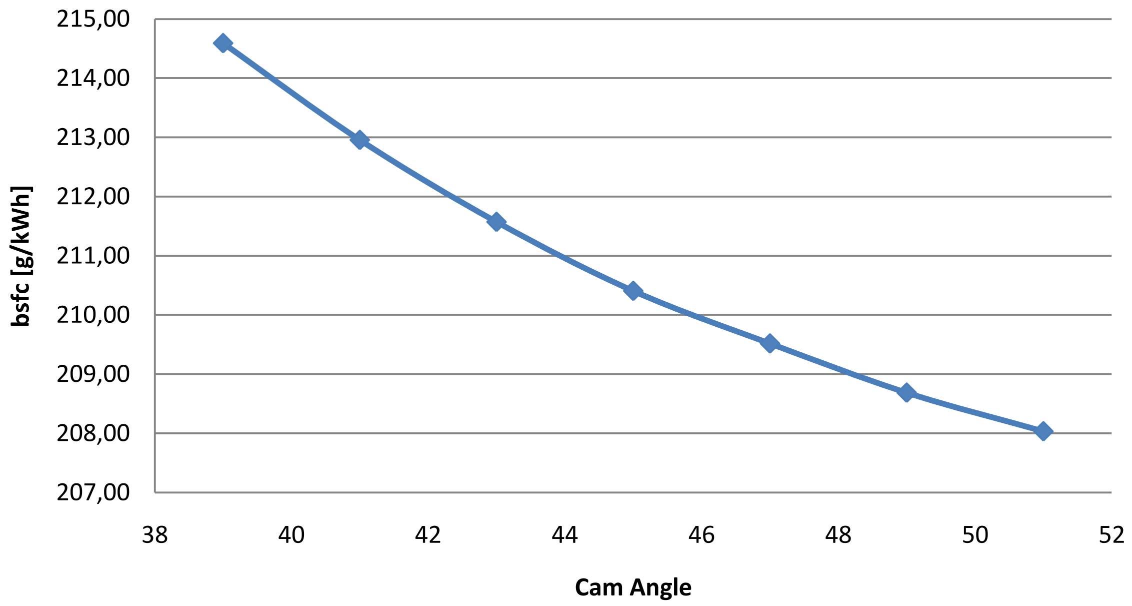
215,00
214,00
213,00
212,00
211,00
210,00
209,00
208,00
207,00
bsfc [g/kWh]
38
40
42
44
46
48
50
52
Cam Angle

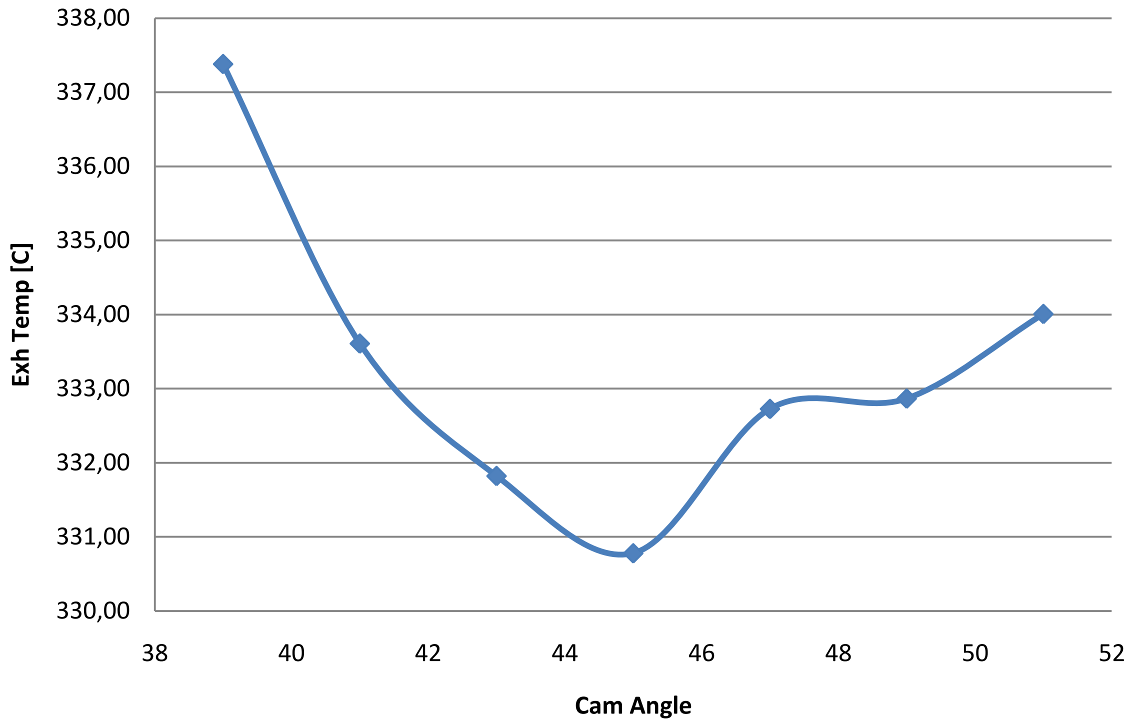
338,00
337,00
336,00
335,00
334,00
333,00
332,00
331,00
330,00
Exh Temp [C]
38
40
42
44
46
48
50
52
Cam Angle

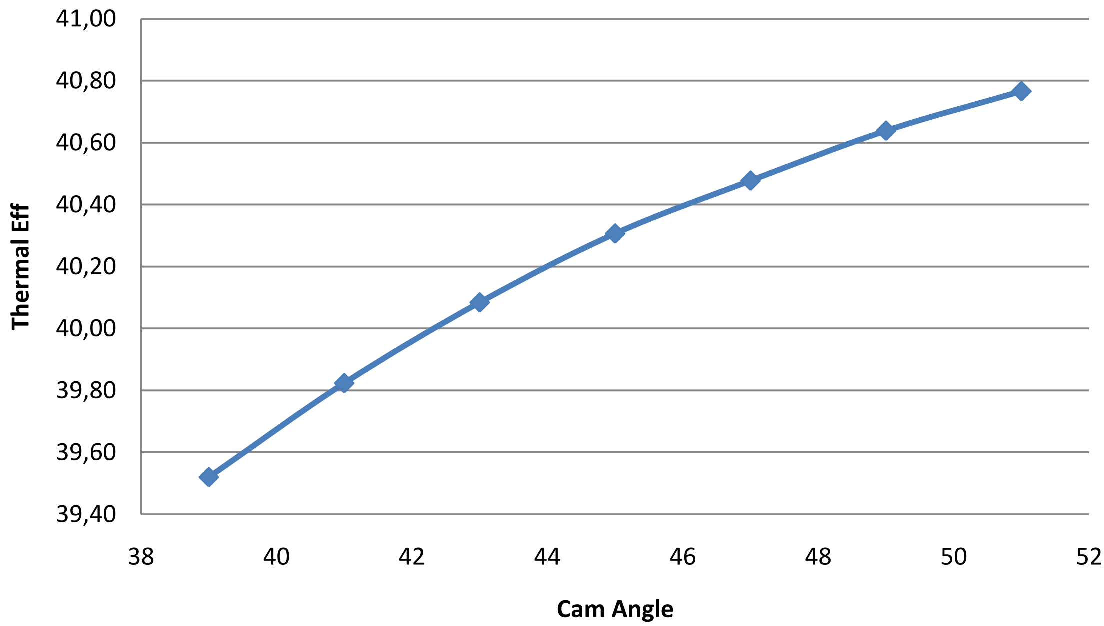
Thermal Eff
41,00
40,80
40,60
40,40
40,20
40,00
39,80
39,60
39,40
38
40
42
44
46
48
50
52
Cam Angle

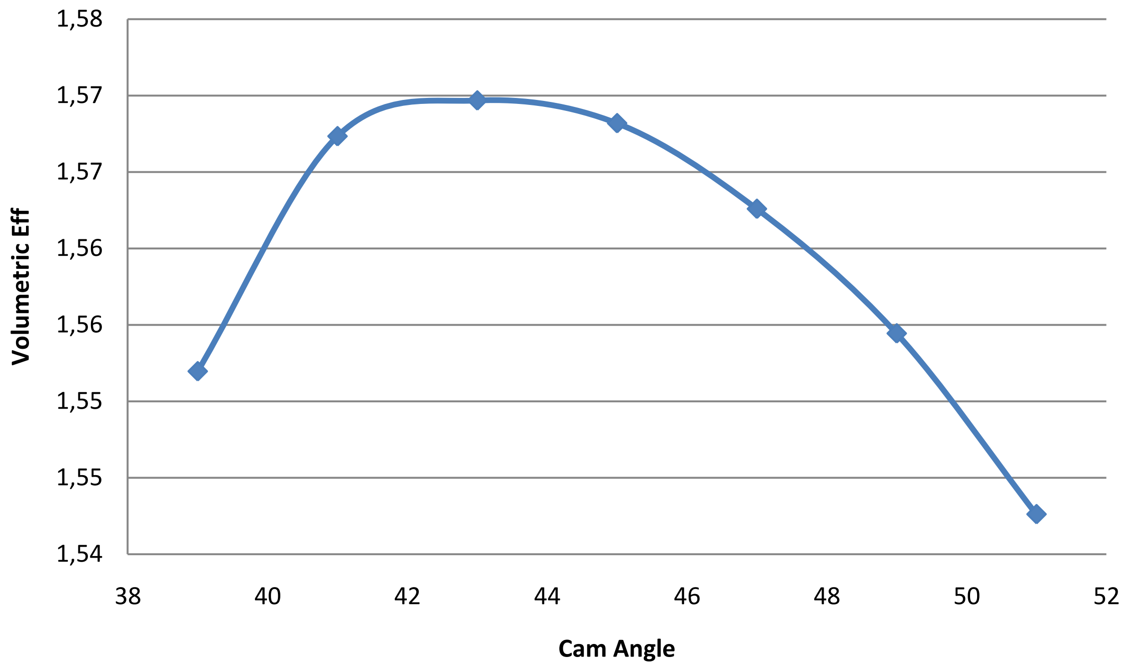
Volumetric Eff
1,58
1,57
1,57
1,56
1,56
1,55
1,55
1,54
38
40
42
44
46
48
50
52
Cam Angle

APPENDIX O: EARLY VALVE OPENING AT 825 RPM AND 15464 NM

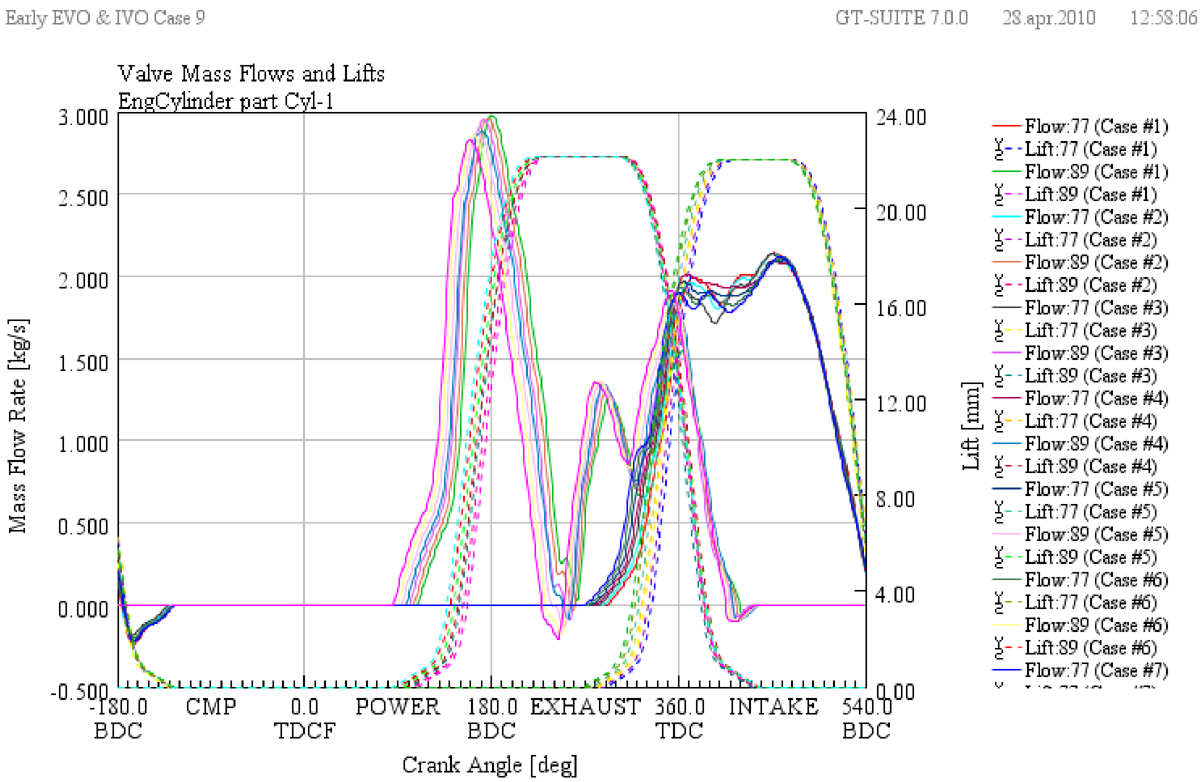

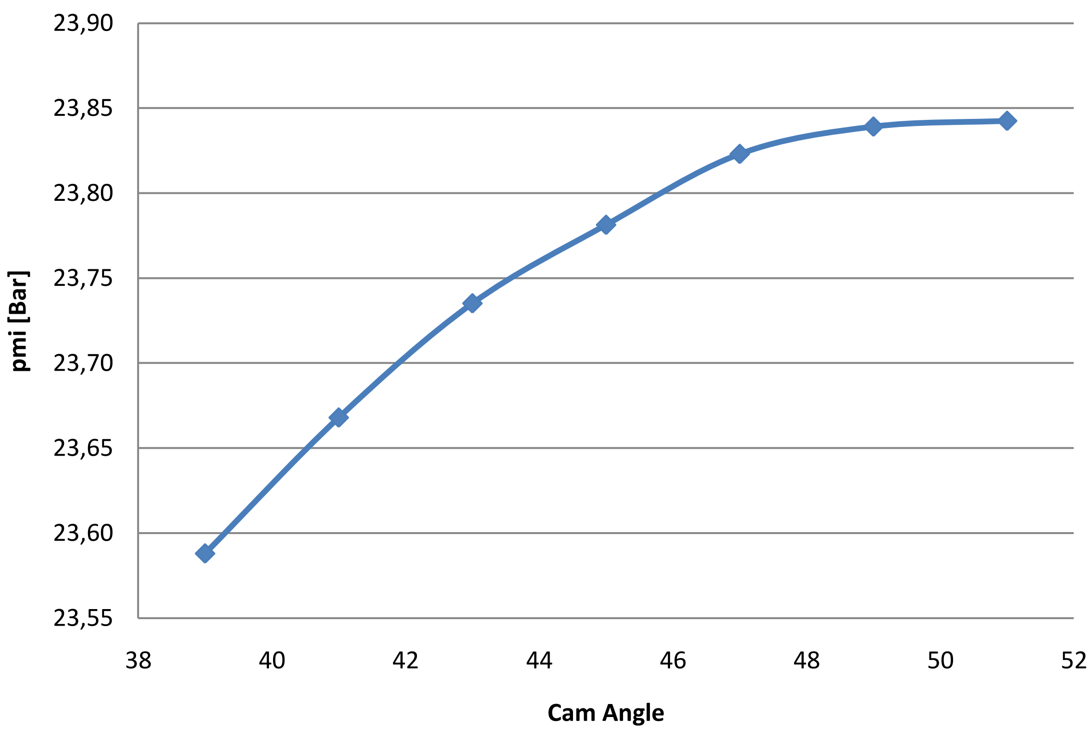

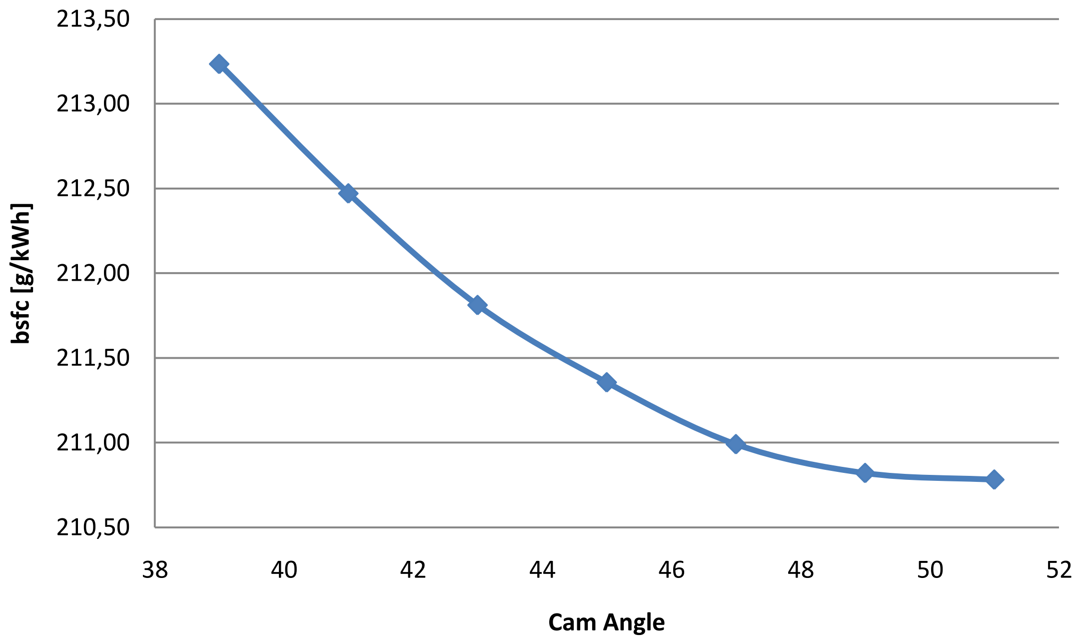
213,50
213,00
212,50
212,00
211,50
211,00
210,50
bsfc [g/kWh]
38
40
42
44
46
48
50
52
Cam Angle

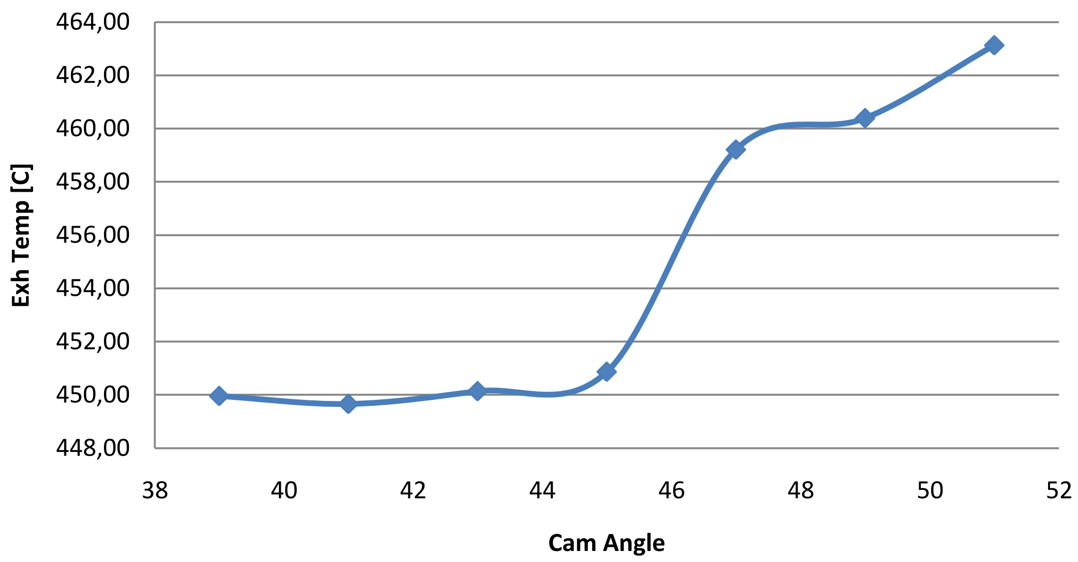
464,00
462,00
460,00
458,00
456,00
454,00
452,00
450,00
448,00
Exh Temp [C]
38
40
42
44
46
48
50
52
Cam Angle

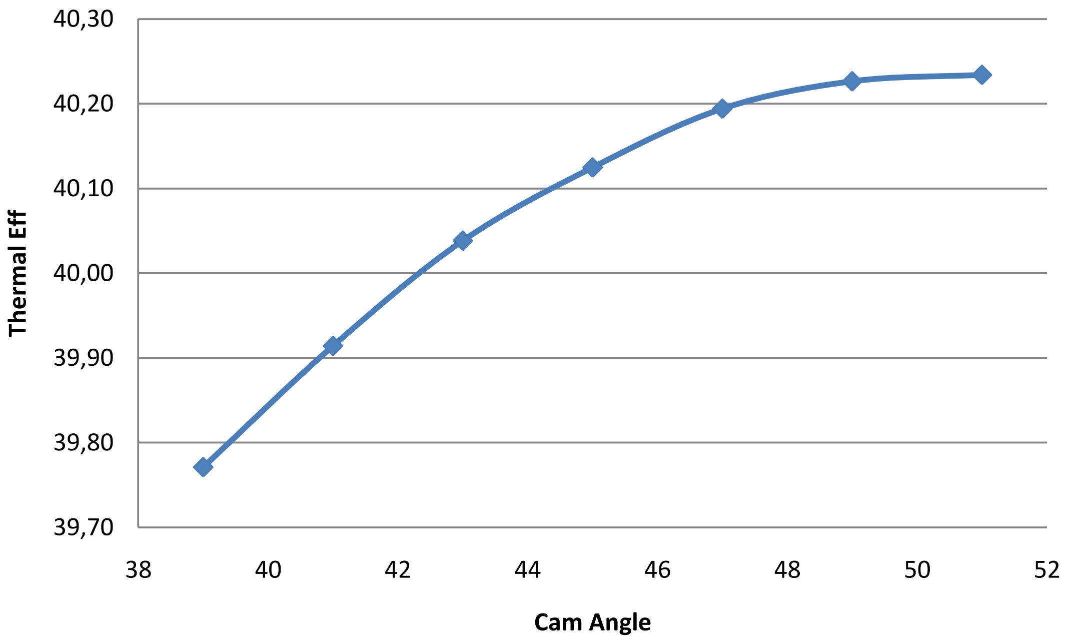
40,30
40,20
40,10
40,00
39,90
39,80
39,70
Thermal Eff
38
40
42
44
46
48
50
52
Cam Angle

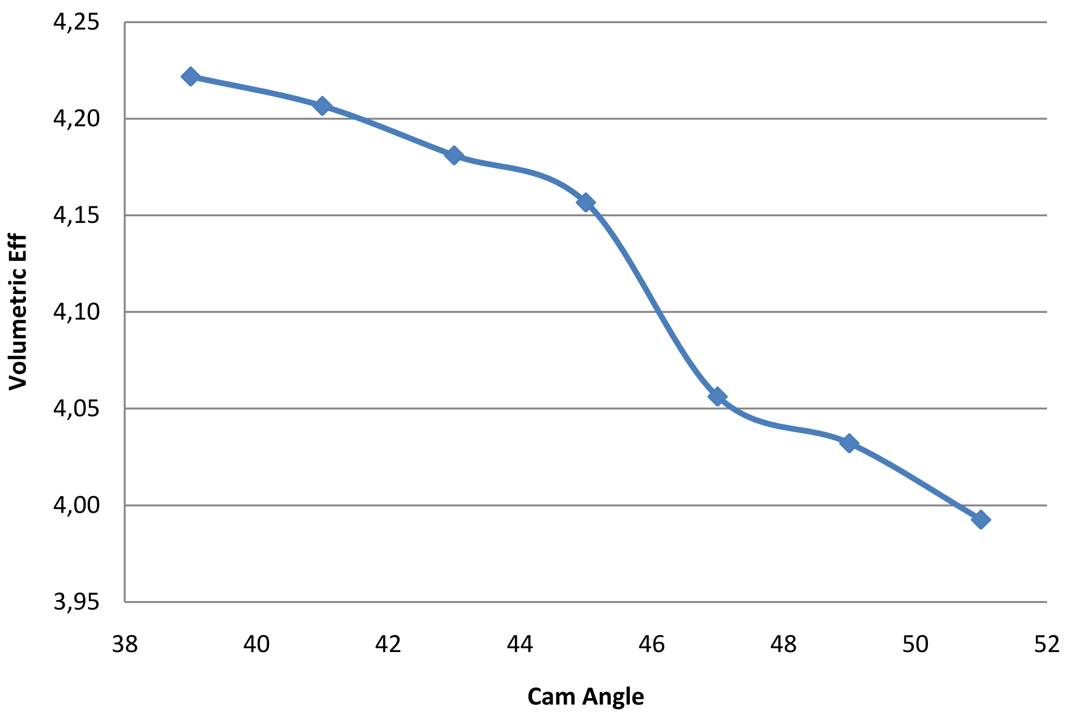
4,25
4,20
4,15
4,10
4,05
4,00
3,95
Volumetric Eff
38
40
42
44
46
48
50
52
Cam Angle

APPENDIX P: LATE VALVE OPENING AT 500 RPM AND 5735 NM

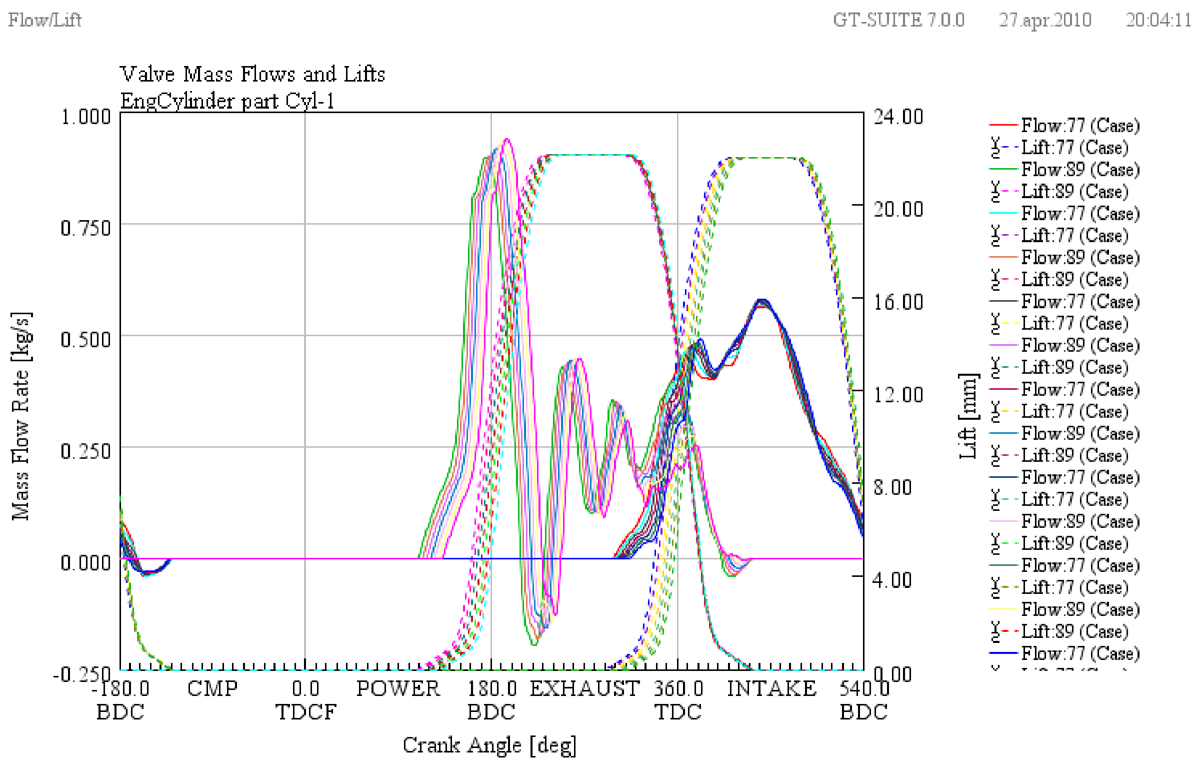

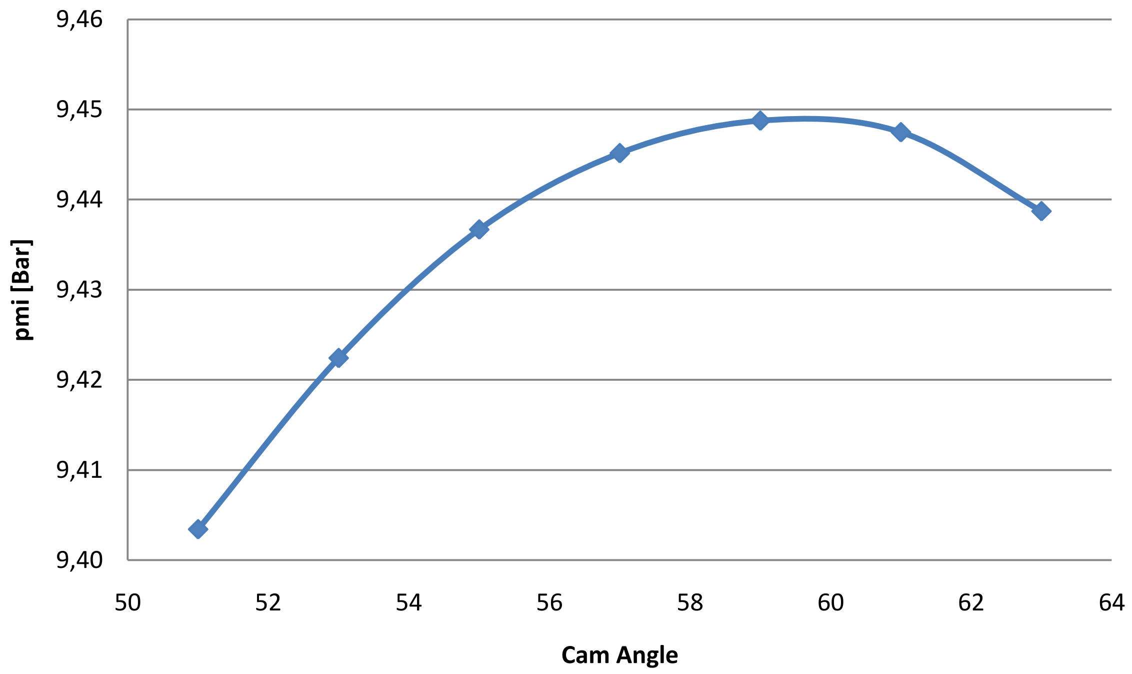

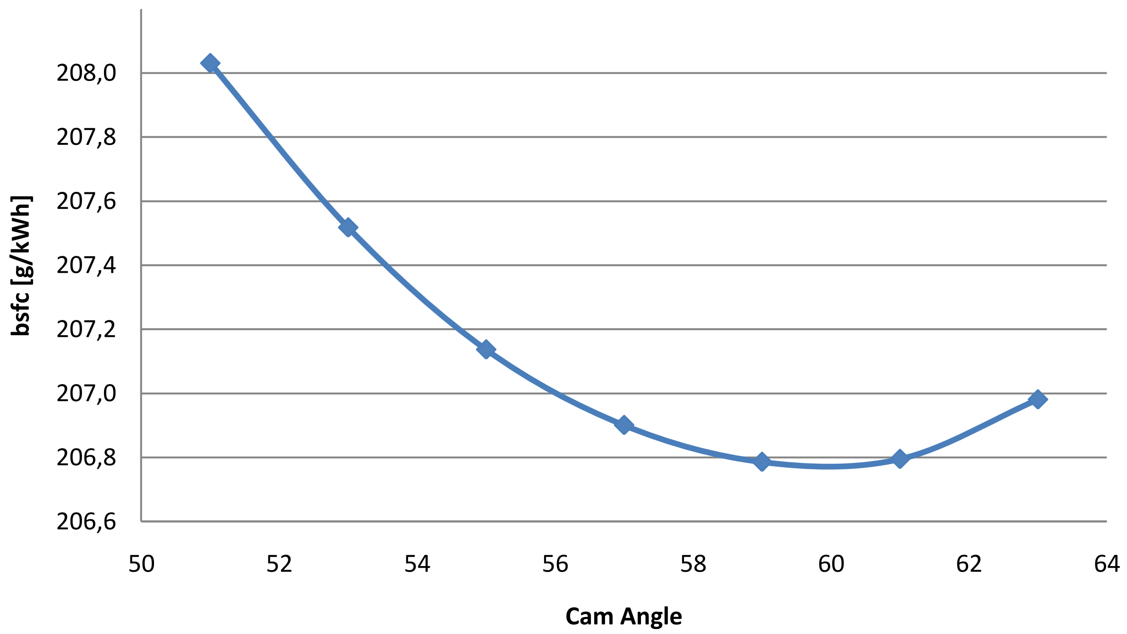
bsfc [g/kWh]
208,0
207,8
207,6
207,4
207,2
207,0
206,8
206,6
50
52
54
56
58
60
62
64
Cam Angle

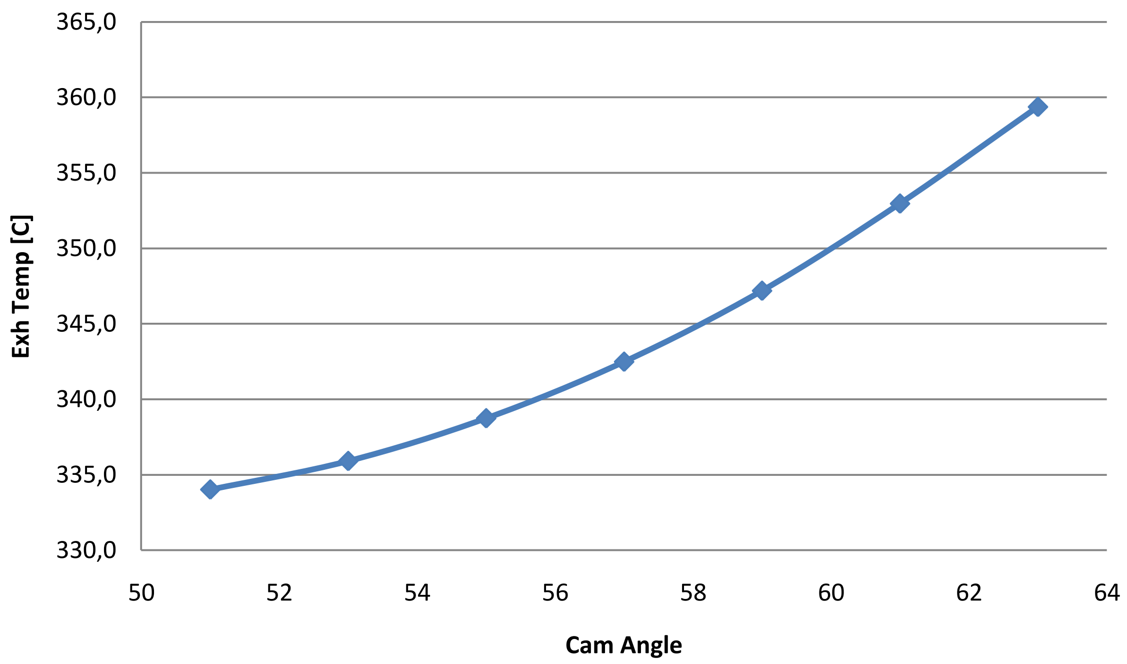
Exh Temp [C]
365,0
360,0
355,0
350,0
345,0
340,0
335,0
330,0
50
52
54
56
58
60
62
64
Cam Angle

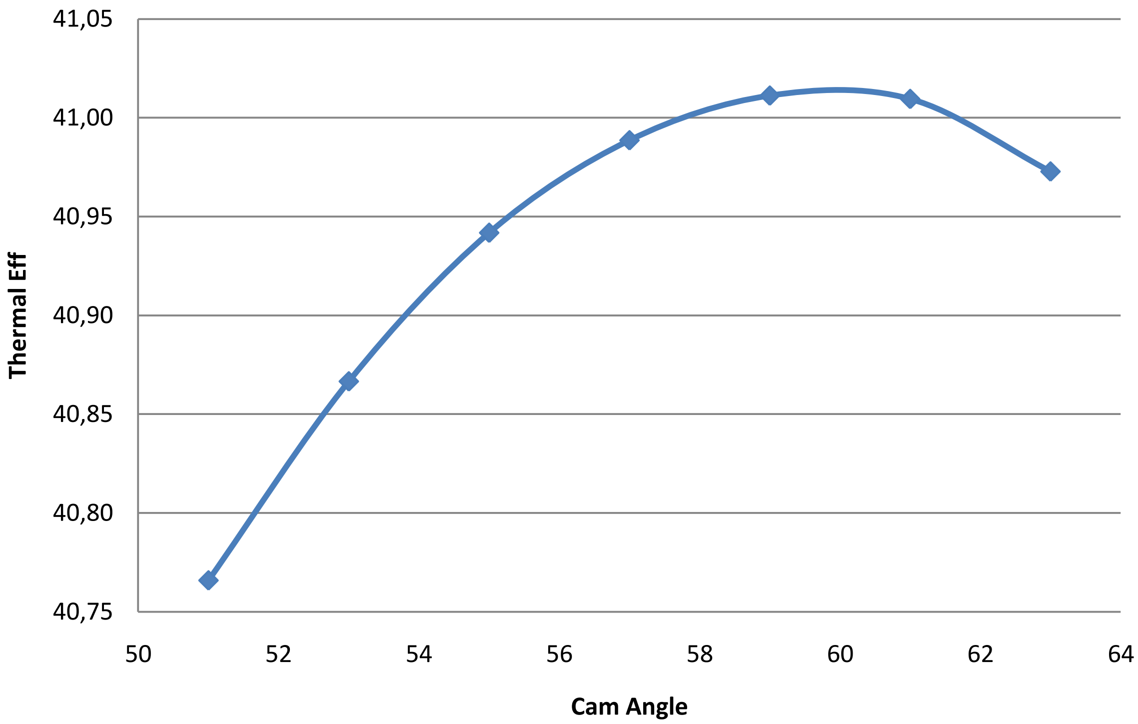
41,05
41,00
40,95
40,90
40,85
40,80
40,75
Thermal Eff
50
52
54
56
58
60
62
64
Cam Angle

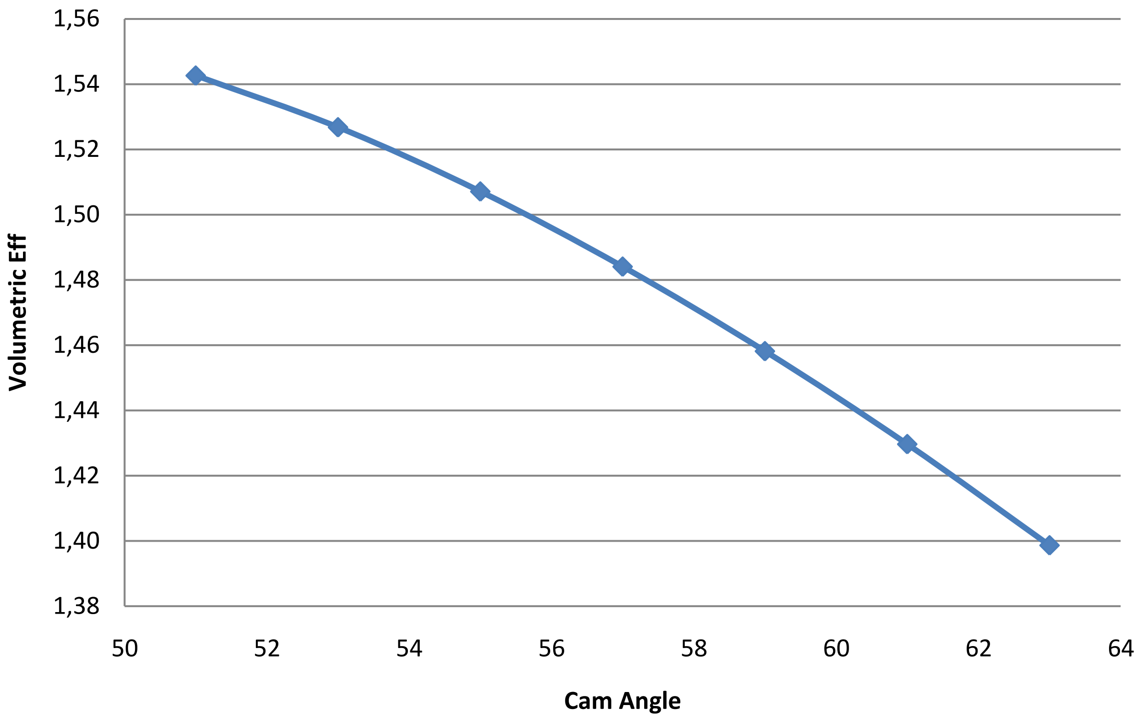
1,56
1,54
1,52
1,50
1,48
1,46
1,44
1,42
1,40
1,38
Volumetric Eff
50
52
54
56
58
60
62
64
Cam Angle

APPENDIX Q: LATE VALVE OPENING AT 825 RPM AND 15464 NM

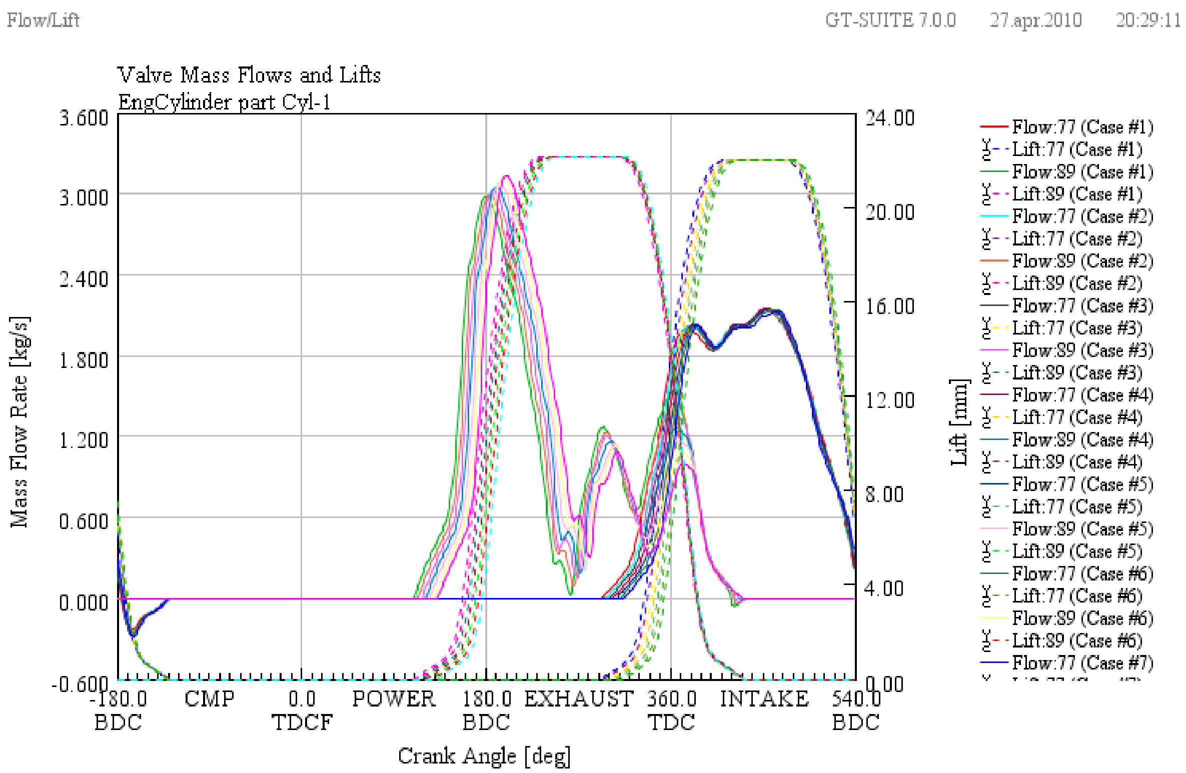

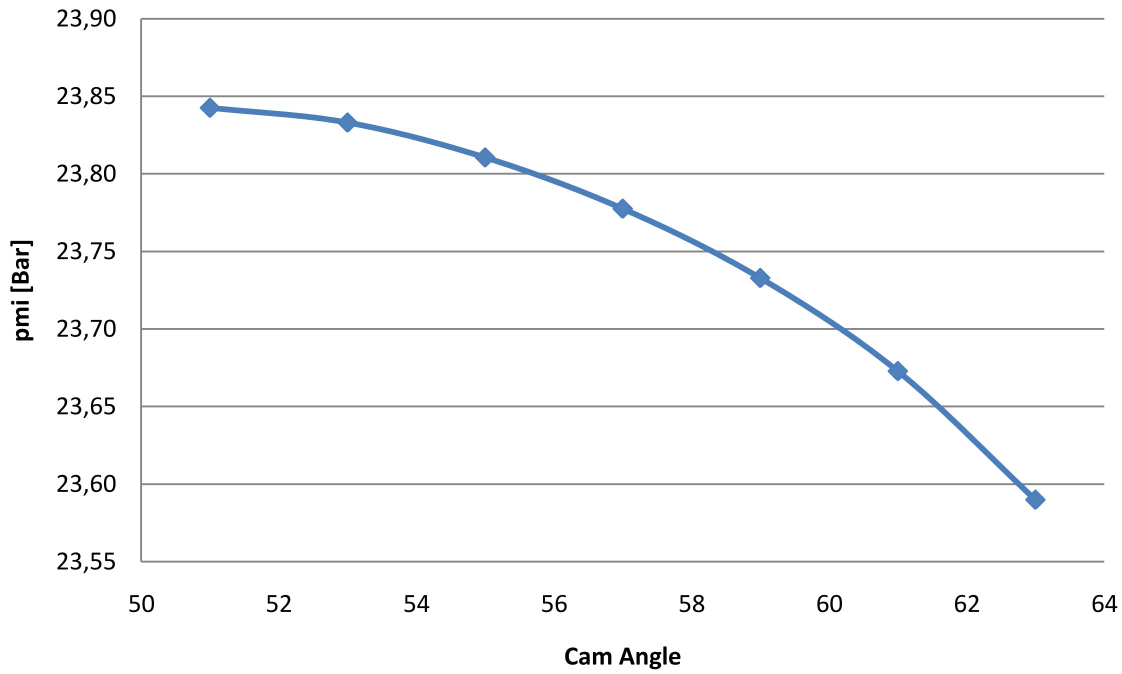

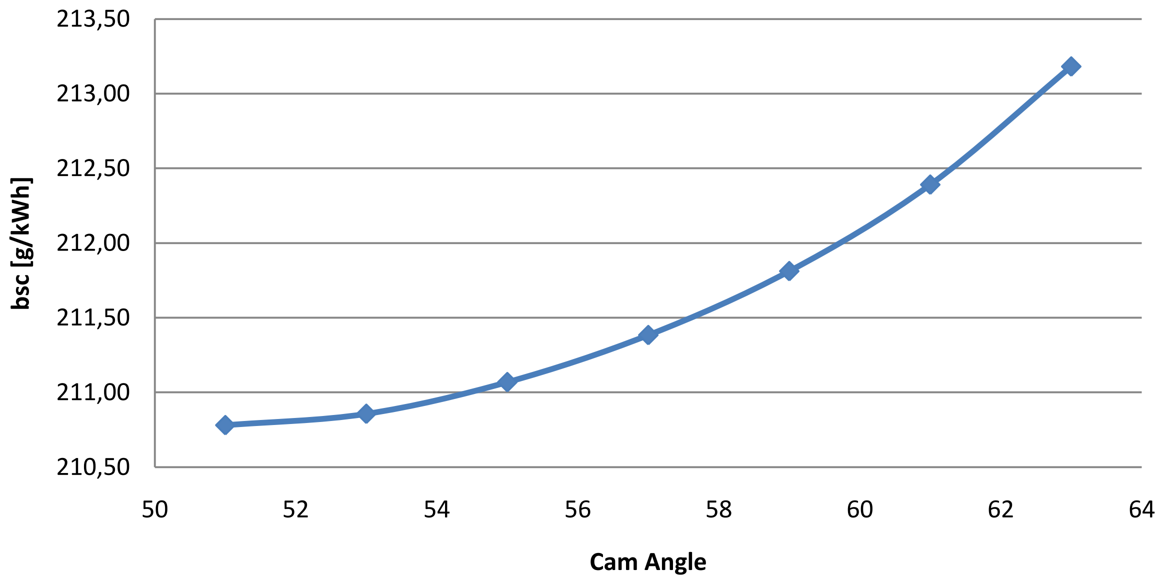
213,50
213,00
212,50
212,00
211,50
211,00
210,50
bsc [g/kWh]
50
52
54
56
58
60
62
64
Cam Angle

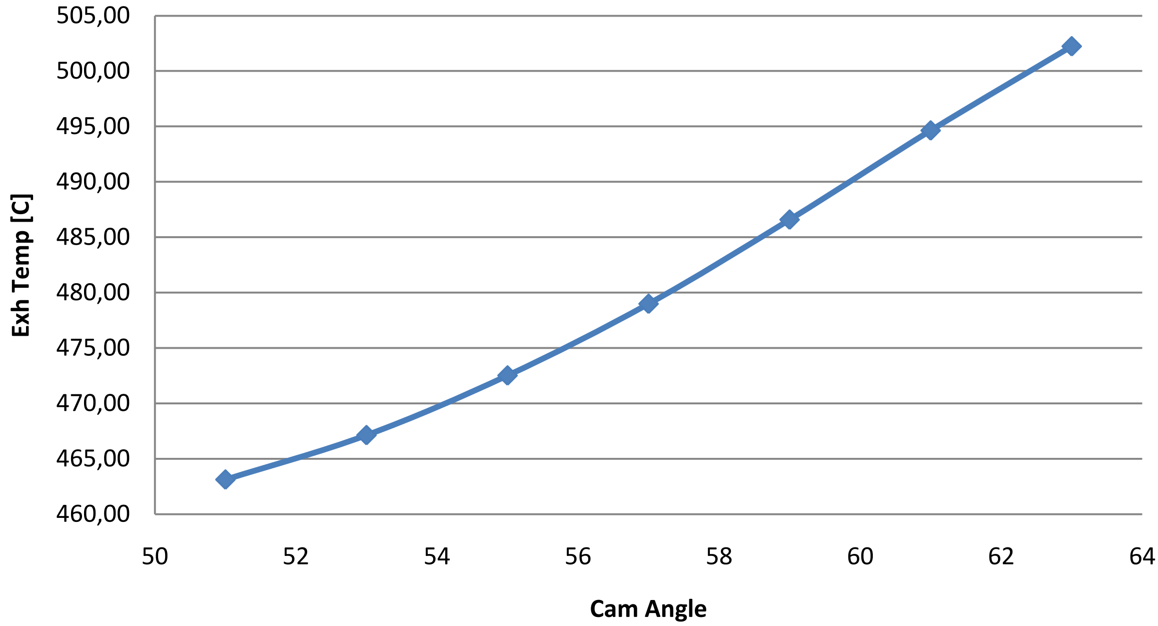
505,00
500,00
495,00
490,00
485,00
480,00
475,00
470,00
465,00
460,00
Exh Temp [C]
50
52
54
56
58
60
62
64
Cam Angle

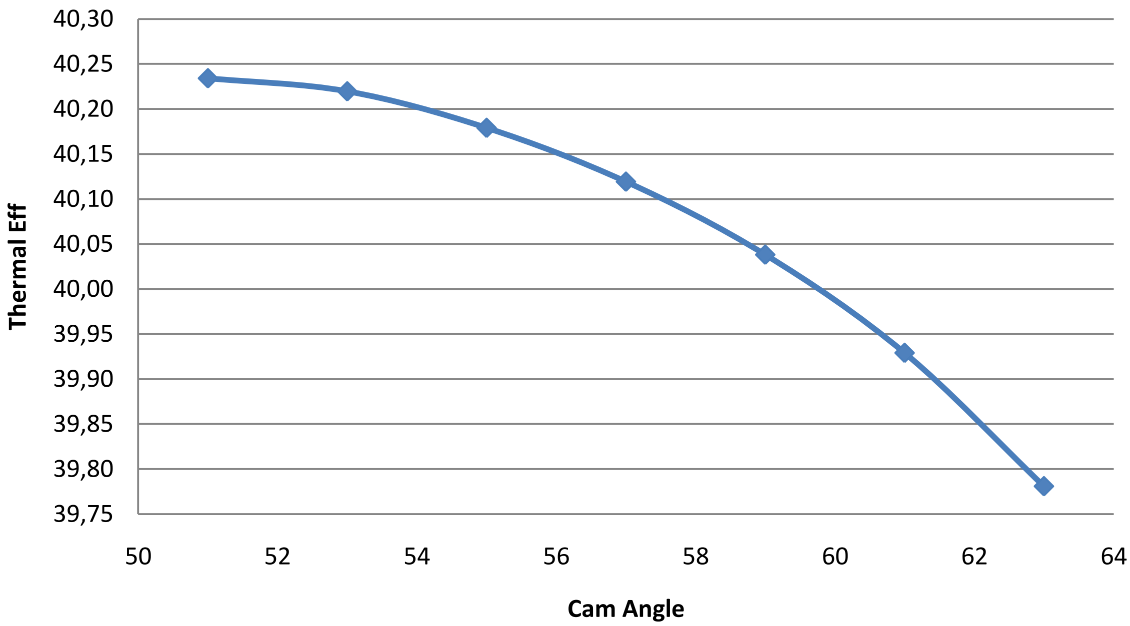
Thermal Eff
40,30
40,25
40,20
40,15
40,10
40,05
40,00
39,95
39,90
39,85
39,80
39,75
50
52
54
56
58
60
62
64
Cam Angle

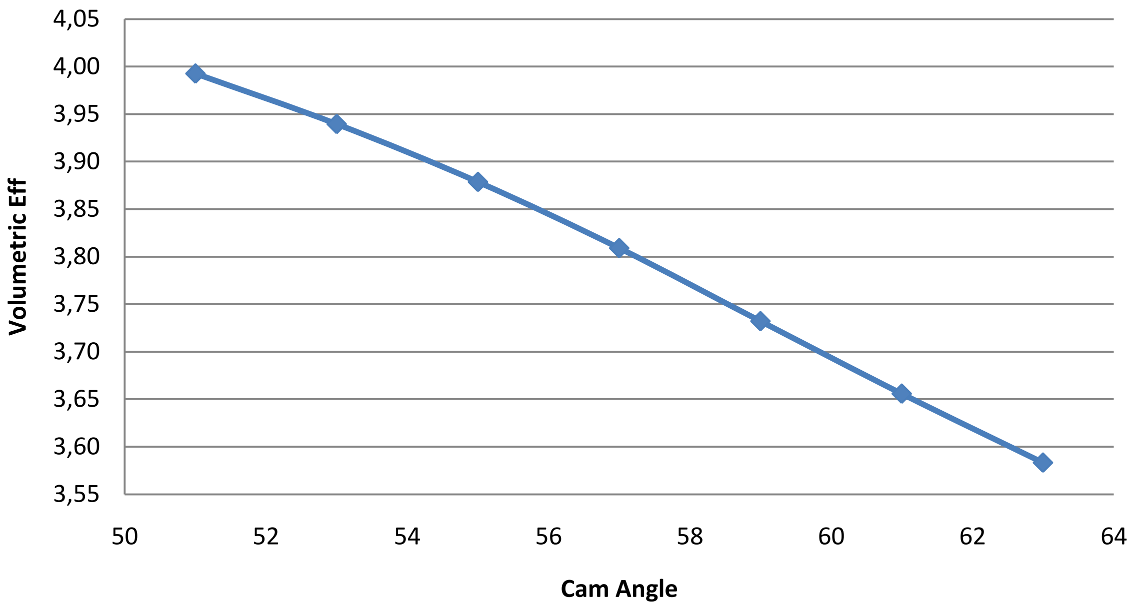
Volumetric Eff
4,05
4,00
3,95
3,90
3,85
3,80
3,75
3,70
3,65
3,60
3,55
50
52
54
56
58
60
62
64
Cam Angle

APPENDIX R: RETARDING CLOSING EVENTS AT 500 RPM AND 5735 NM

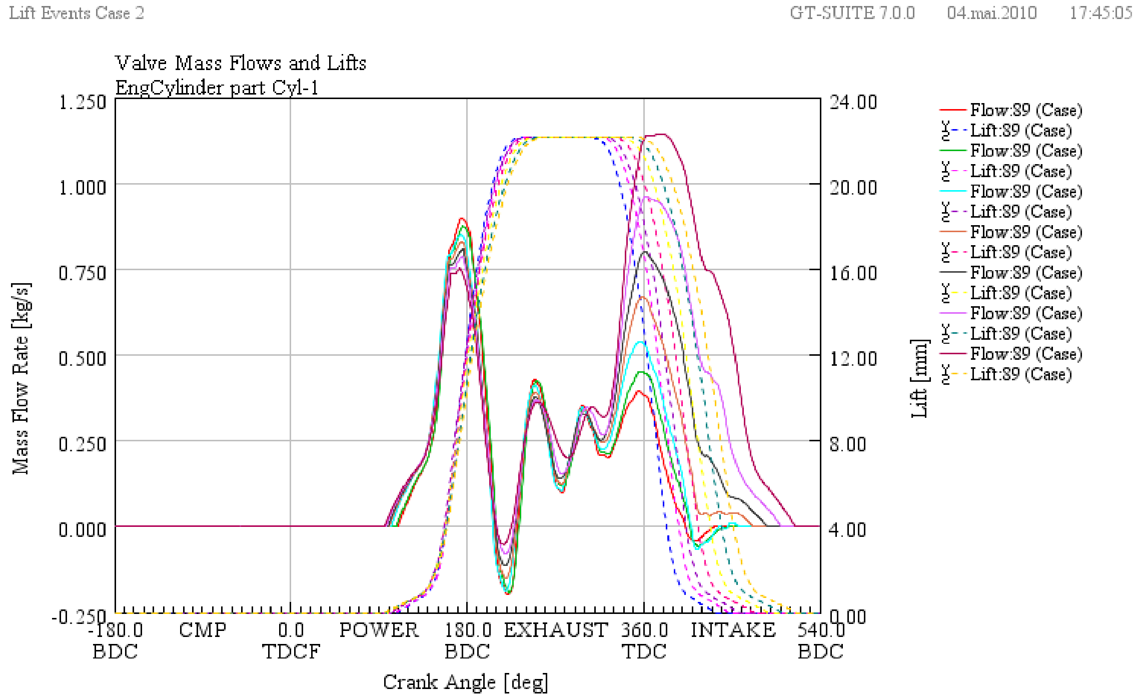

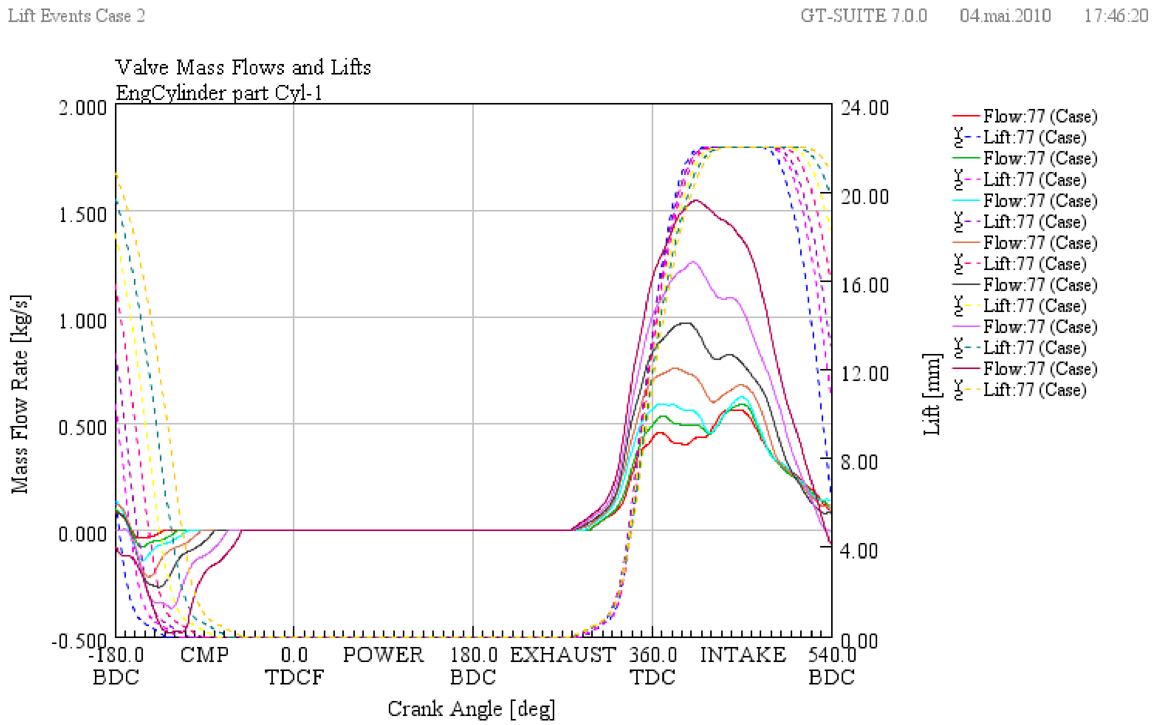

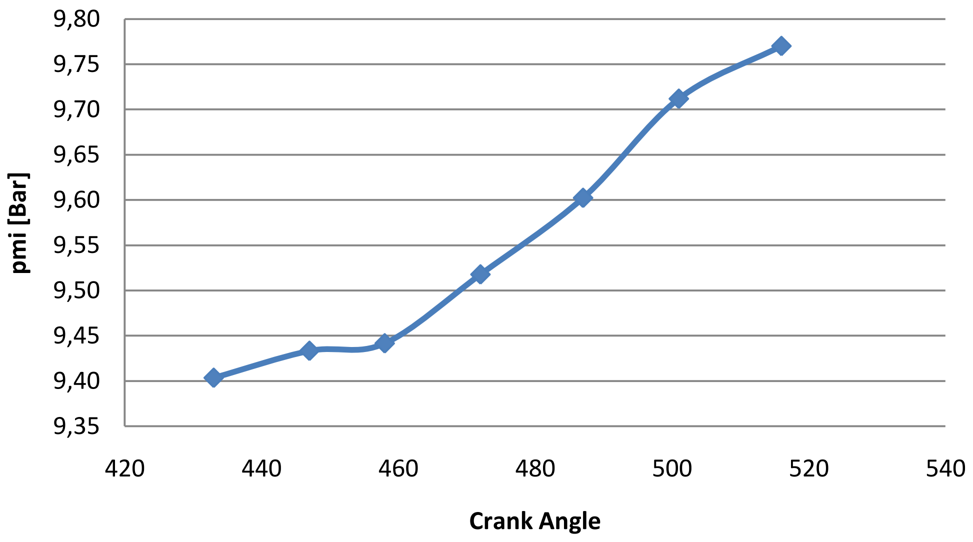
9,80
9,75
9,70
9,65
9,60
9,55
9,50
9,45
9,40
9,35
pmi [Bar]
420
440
460
480
500
520
540
Crank Angle

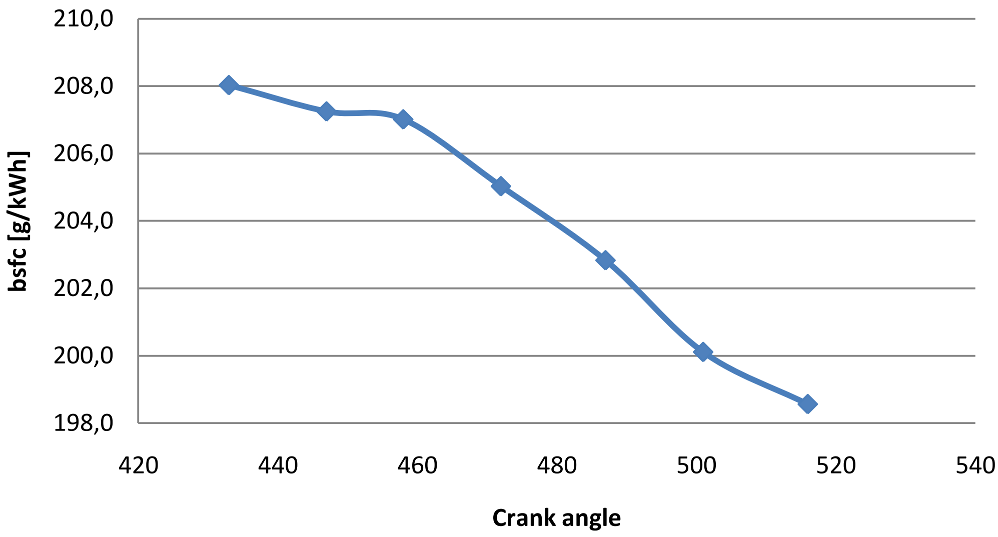
210,0
208,0
206,0
204,0
202,0
200,0
198,0
bsfc [g/kWh]
420
440
460
480
500
520
540
Crank angle

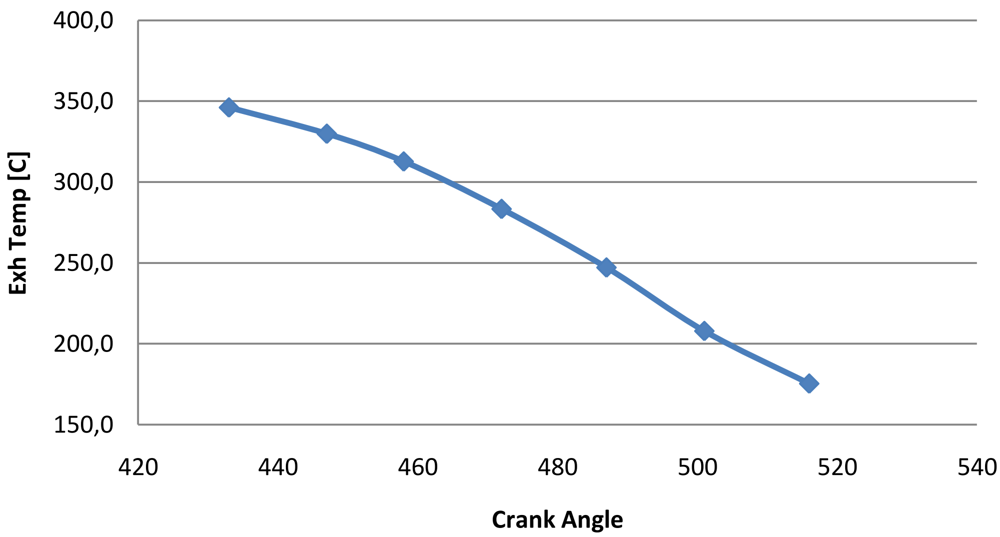
400,0
350,0
300,0
250,0
200,0
150,0
Exh Temp [C]
420
440
460
480
500
520
540
Crank Angle

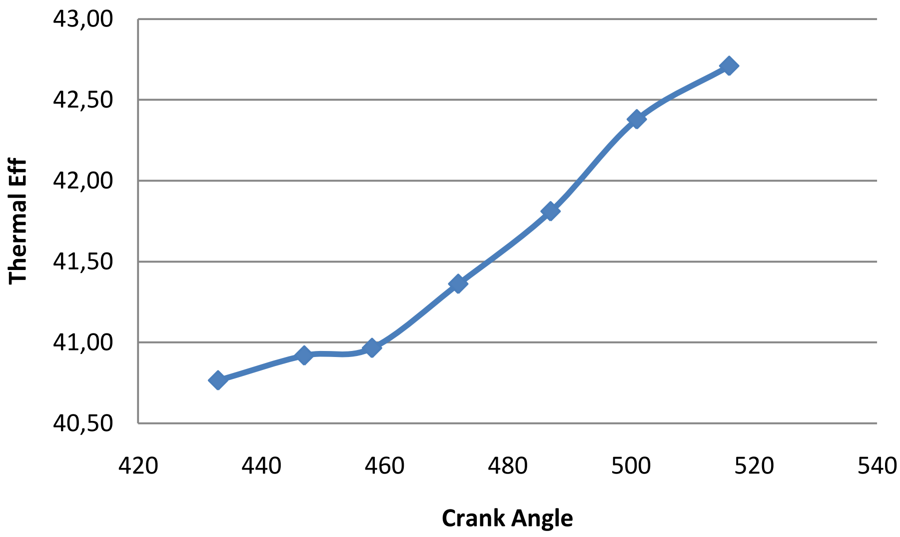
43,00
42,50
42,00
41,50
41,00
40,50
Thermal Eff
420
440
460
480
500
520
540
Crank Angle

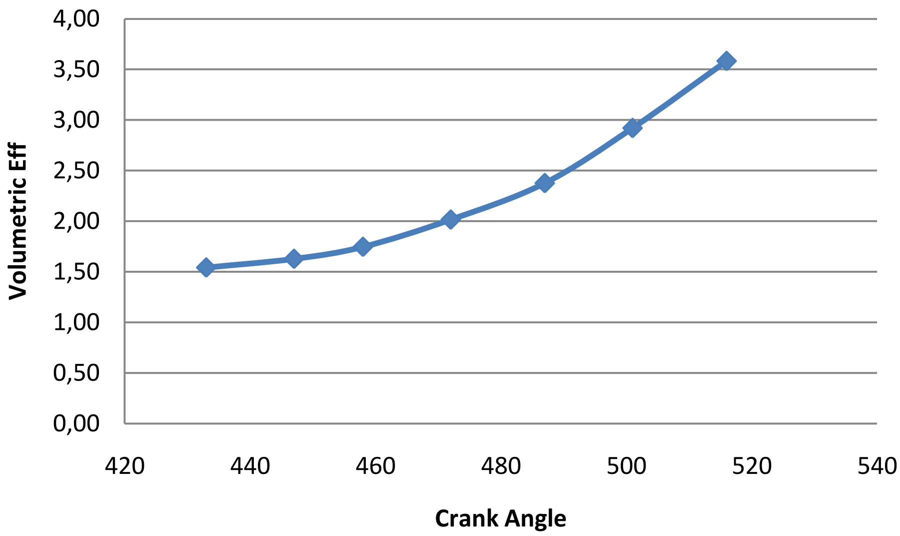
4,00
3,50
3,00
2,50
2,00
1,50
1,00
0,50
0,00
Volumetric Eff
420
440
460
480
500
520
540
Crank Angle

APPENDIX S: RETARDING CLOSING EVENTS AT 835 RPM AND 15464 NM

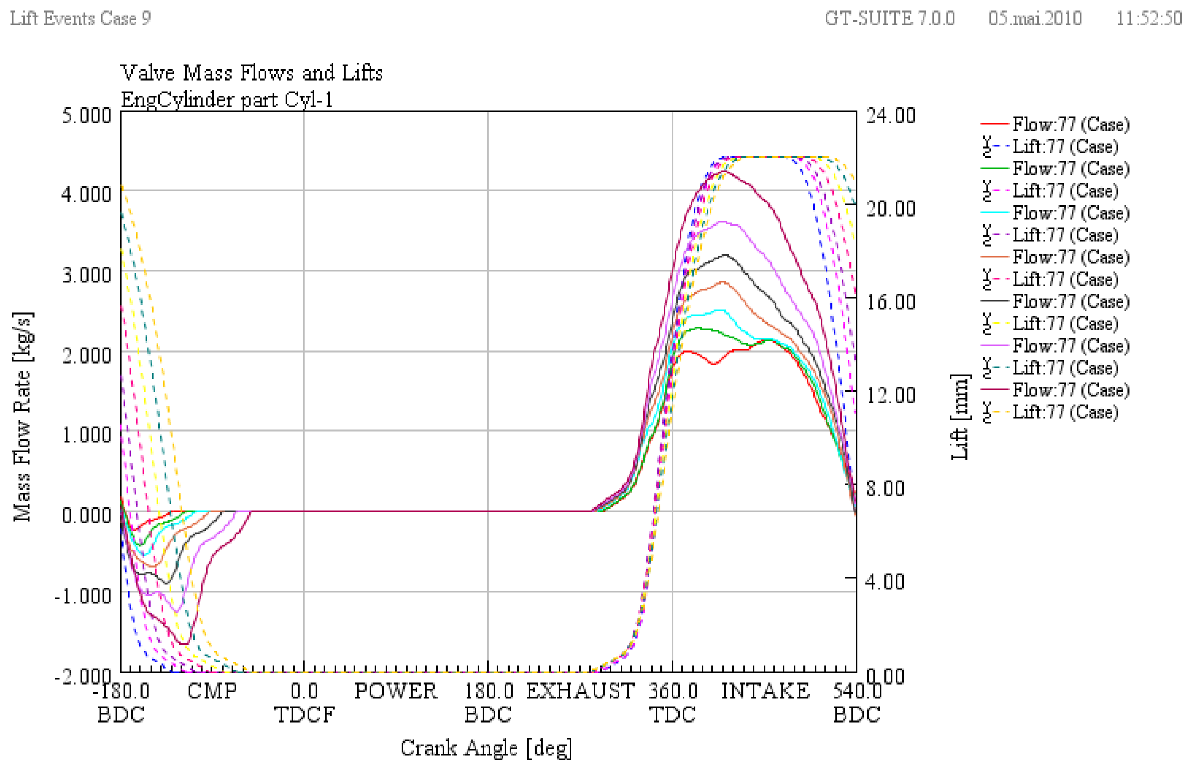

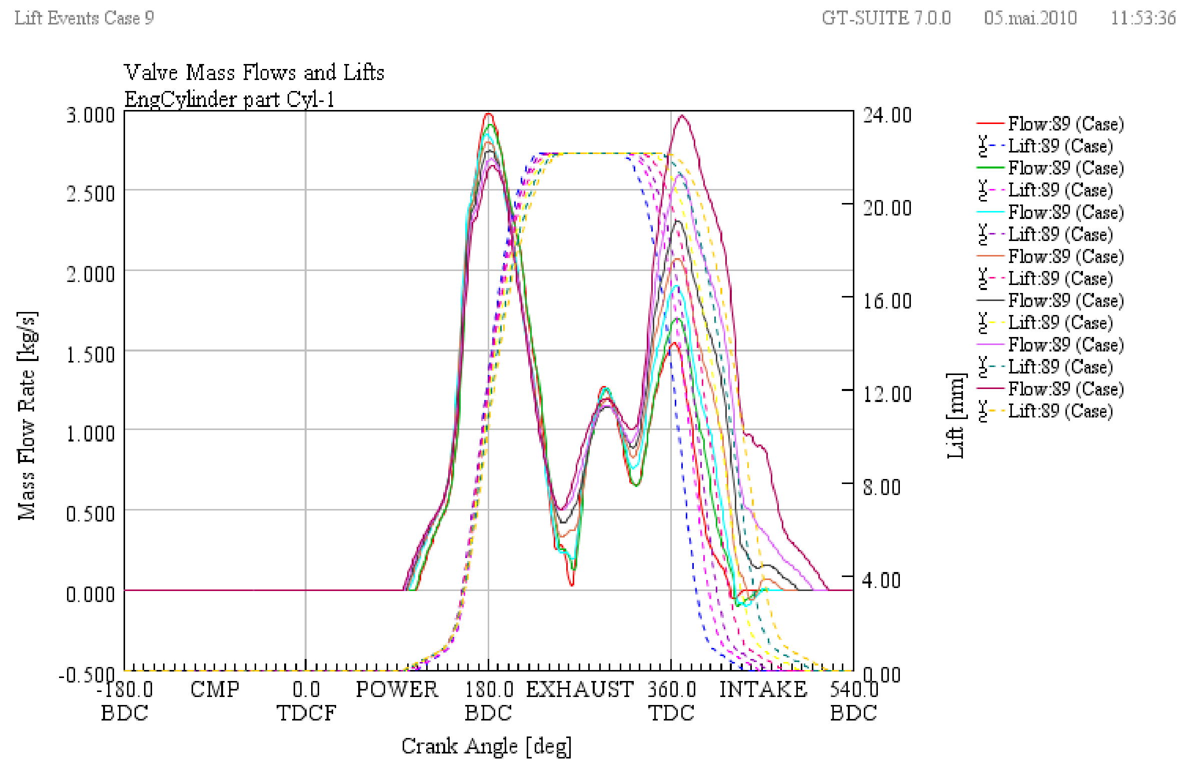

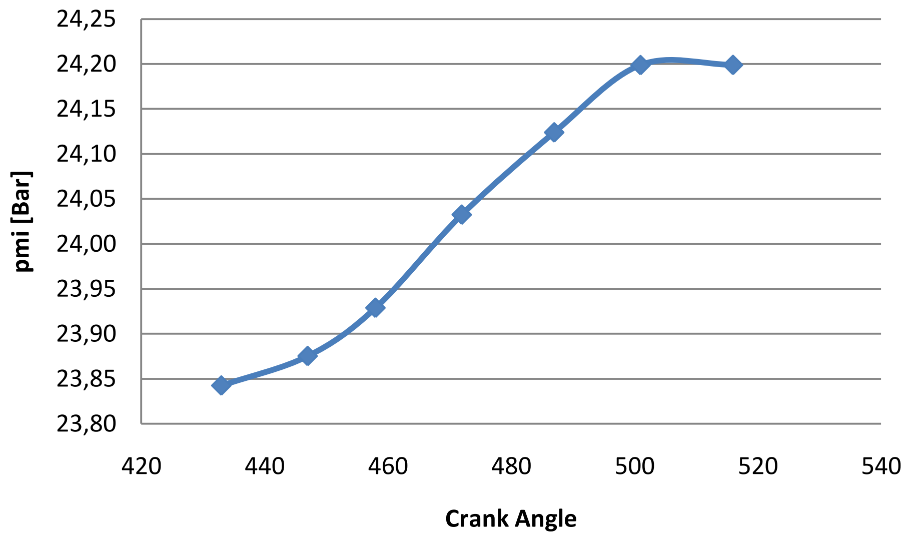
pmi [Bar]
24,25
24,20
24,15
24,10
24,05
24,00
23,95
23,90
23,85
23,80
420
440
460
480
500
520
540
Crank Angle

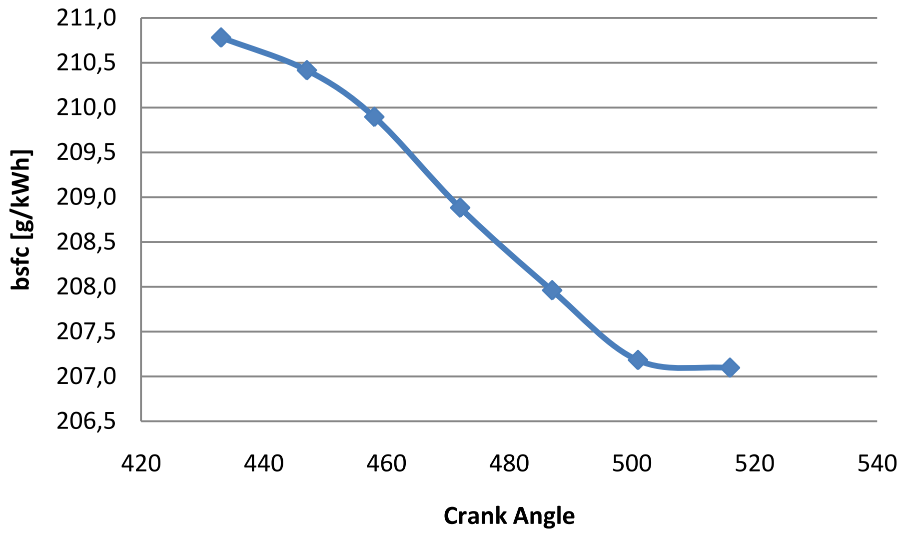
bsfc [g/kWh]
211,0
210,5
210,0
209,5
209,0
208,5
208,0
207,5
207,0
206,5
420
440
460
480
500
520
540
Crank Angle

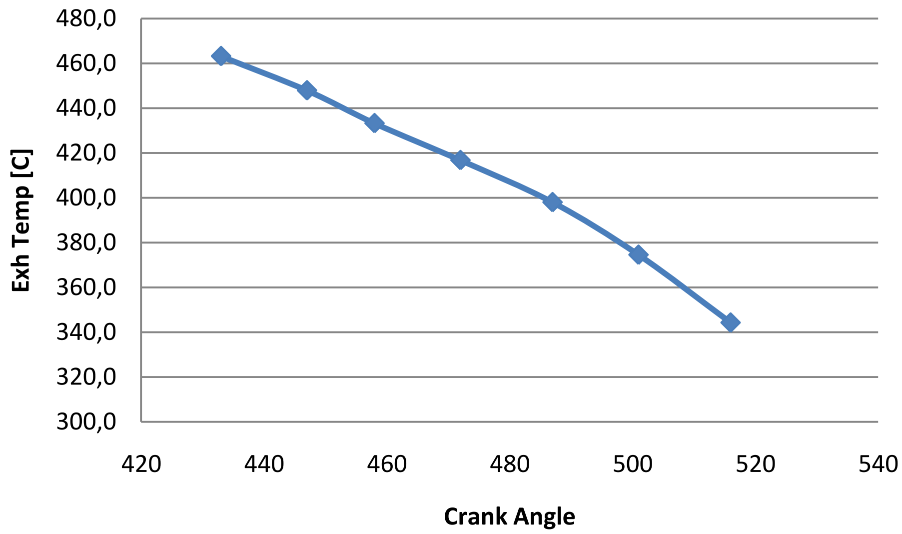
Exh Temp [C]
480,0
460,0
440,0
420,0
400,0
380,0
360,0
340,0
320,0
300,0
420
440
460
480
500
520
540
Crank Angle

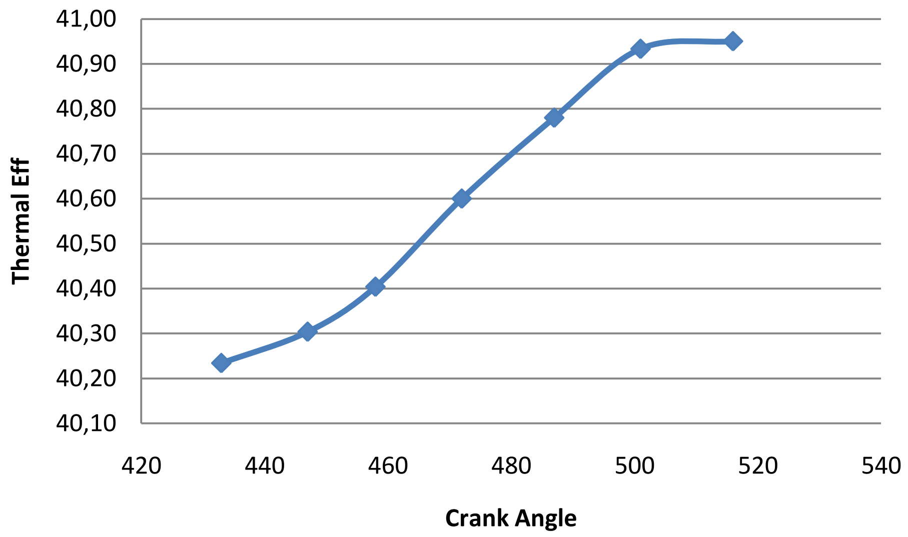
41,00
40,90
40,80
40,70
40,60
40,50
40,40
40,30
40,20
40,10
Thermal Eff
420
440
460
480
500
520
540
Crank Angle

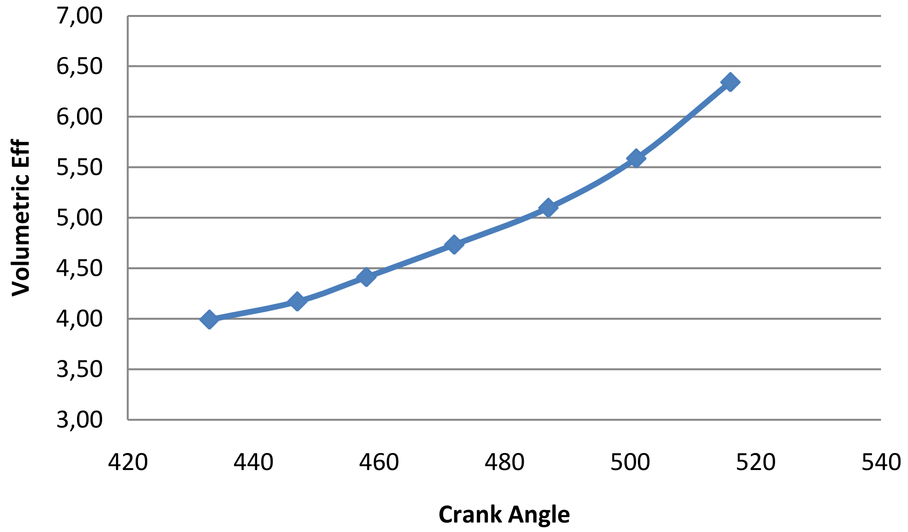
7,00
6,50
6,00
5,50
5,00
4,50
4,00
3,50
3,00
Volumetric Eff
420
440
460
480
500
520
540
Crank Angle

APPENDIX T: EMISSIONS

Early IVC at 500 rpm:

VVT Config	IVC [Cam Degrees]	CO (ppm)	CO2 (ppm)	Hydrocarbon (ppm)
Standard	277.3	1.35	53319.70	0.41
Early 1	271.4	1.37	53906.90	0.42
Early 2	265.5	1.36	53106.30	0.41
Early 3	259.6	1.30	50440.20	0.38
Early 4	253.7	1.24	47640.20	0.37
Early 5	247.8	1.16	44494.80	0.34
Early 6	243.0	1.10	42269.10	0.32
Early 7	237.1	1.02	39424.50	0.30
Early 8	231.2	0.93	35998.90	0.27
Early 9	225.3	0.84	32357.90	0.25

Early IVC at 825 rpm:

VVT Config	IVC [Cam Degrees]	CO (ppm)	CO2 (ppm)	Hydrocarbon (ppm)
Standard	277.3	0.87	57004.20	0.43
Early 1	271.4	0.87	57069.00	0.43
Early 2	265.5	0.86	56323.50	0.43
Early 3	259.6	0.85	55452.40	0.43
Early 4	253.7	0.81	53211.60	0.40
Early 5	247.8	0.79	51554.10	0.39
Early 6	242.0	0.75	48863.40	0.38
Early 7	236.1	0.71	46022.80	0.35
Early 8	230.2	0.66	42821.00	0.33
Early 9	224.3	0.61	39200.10	0.30

Late IVC at 500 rpm:

VVT Config	IVC [Cam Degrees]	CO (ppm)	CO2 (ppm)	Hydrocarbon (ppm)
Standard	277.3	1.35155	53319.7	0.40572
Late 1	283.2	1.3329	52354.7	0.398355
Late 2	287.1	1.30174	50817.8	0.382475
Late 3	293.0	1.22546	47668.5	0.360142
Late 4	298.9	1.15999	44735.9	0.341003
Late 5	304.7	1.29907	46948.4	0.356125
Late 6	310.6	1.51502	49734.9	0.381714

Late IVC at 825 rpm:

VVT Config	IVC [Cam Degrees]	CO (ppm)	CO2 (ppm)	Hydrocarbon (ppm)
Standard	296.0	0.87	57004.20	0.43
Late 1	303.0	0.86	56086.50	0.43
Late 2	311.0	0.86	56131.20	0.43
Late 3	318.5	0.84	54835.00	0.42
Late 4	326.5	0.83	53914.20	0.41
Late 5	334.5	0.81	52681.50	0.40
Late 6	342.0	0.79	50750.30	0.39
Late 7	350.0	0.79	49860.50	0.38

Late EVC and IVC at 825 rpm:

Case	EVC [Crank Angle]	IVC [Crank Angle]	CO (ppm)	CO2 (ppm)	Hydrocarbon (ppm)
1 (Standard)	433	591	0.87	57004.20	0.43
2	447	604	0.83	54925.10	0.42
3	458	614	0.77	52665.10	0.40
4	472	627	0.72	49965.30	0.38
5	487	641	0.67	47071.70	0.35
6	501	654	0.61	43121.90	0.32
7	516	668	0.53	37881.50	0.28

Late EVC and IVC at 825 rpm:

Case	EVC [Crank Angle]	IVC [Crank Angle]	CO (ppm)	CO2 (ppm)	Hydrocarbon(ppm)
1 (Standard)	433	591	1.35	53319.70	0.41
2	447	604	1.29	51347.30	0.40
3	458	614	1.18	48792.20	0.37
4	472	627	1.04	43574.50	0.33
5	487	641	0.88	37268.60	0.28
6	501	654	0.71	30419.70	0.23
7	516	668	0.58	24916.30	0.19

APPENDIX U: SYSTEM IMPLEMENTATION

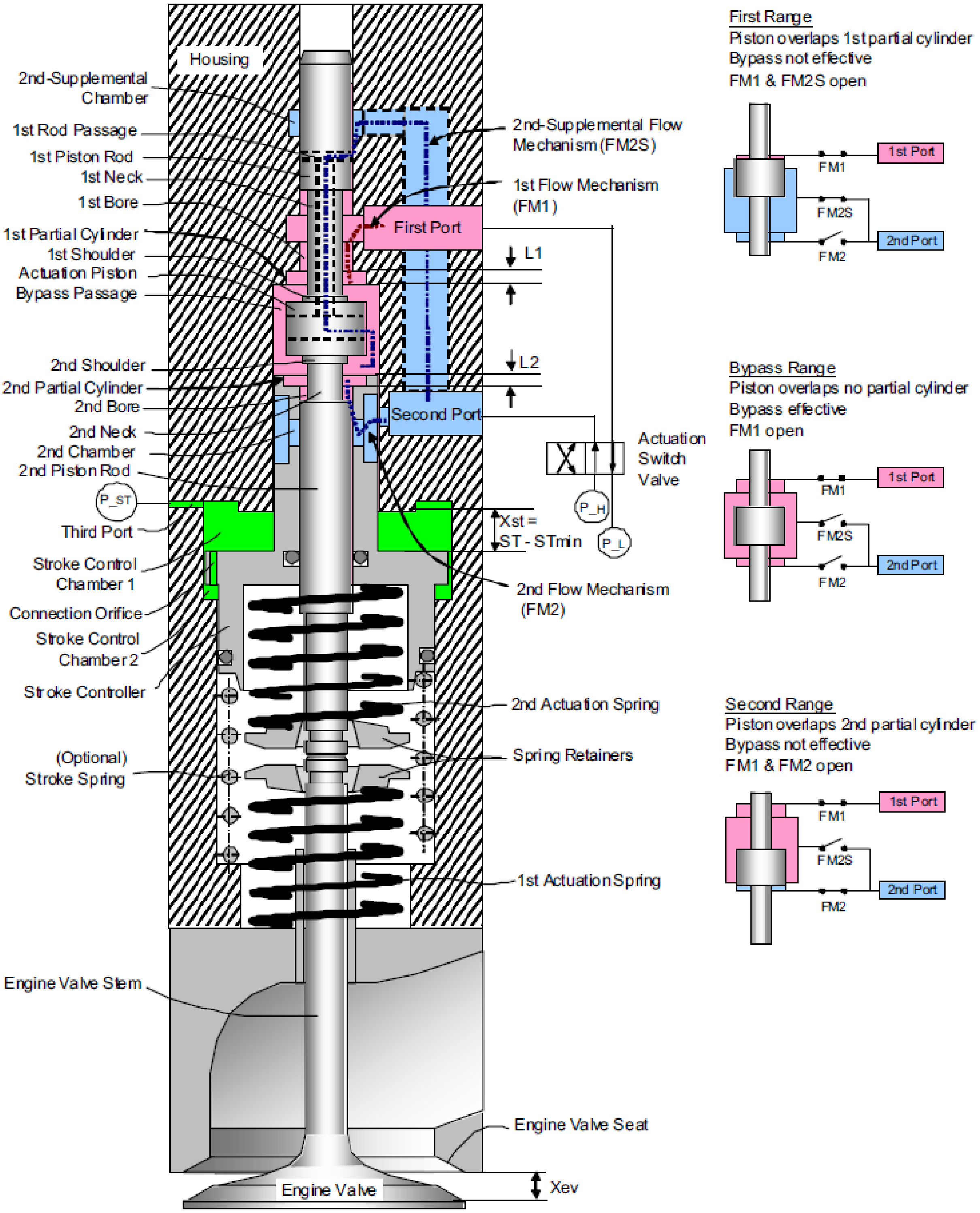

APPENDIX V: TECHNICAL DATA

PART 1

Rolls-Royce

TECHNICAL DATA.

TECHNICAL DATA

DRAWING NO.: LE908/62
MAIN ENGINE:KRM @ 720 rpm

APPLICATION: Marine Propulsion

MAIN ENGINE DATA				
NUMBER OF CYLINDERS	-	6	8	9
CYLINDER BORE	mm	250	250	250
PISTON STROKE	mm	300	300	300
RATED POWER(MCR), ENGINE	kW	1165	1555	1750
	bhp	1585	2115	2380
MEAN EFFECTIVE PRESSURE	bar	22.0	22.0	22.0
RATED SPEED	1/min	720	720	720
ENGINE SPEED, IDELING	1/min	450	450	450
MEAN PISTON SPEED	m/s	7.2	7.2	7.2
DISPLACEMENT	l	88	118	133
FUEL OIL DATA				
SPECIFIC FUEL CONSUMPTION	g/kWh	193	193	193
FUEL CONSUMPTION AT MCR	l/h	265	353	398
DAYTANK, 24HRS OPERATION	m³	6	8	10
START AIR DATA				
START AIR PRESSURE, MAX./MIN.	barg	30/15	30/15	30/15
AIR CONSUMPT. PER START(50°C)	m³n	0.50	0.50	0.50
NO OF STARTS, 125 l RECEIVER	-	4	4	4
NO OF STARTS, 250 l RECEIVER	-	8	8	8
LUBRICATION DATA				
LUBRICATING OIL	SAE 40			
MAIN PUMP CAPACITY	m³/h	18.8	24.0	24.0
LUB. OIL PRESSURE :				
- NORMAL	barg	4-5	4-5	4-5
- ALARM, PRESSURE LOW	barg	2.5	2.5	2.5
- START, STAND-BY PUMP	barg	2.2	2.2	2.2
- AUTOMATIC/MANUAL STOP	barg	1.7	1.7	1.7
TEMP. AT ENGINE INLET :				
- NORMAL	°C	60	60	60
- ALARM, TEMP. HIGH	°C	70	70	70
SPEC. LUB. OIL CONSUMPTION	g/kWh	0.80	0.80	0.80
LUB. OIL CONSUMPTION	l/h	1.0	1.4	1.5
LUB. OIL QUANTITY :				
- WET SUMP, MAXIMUM	l	500	740	810
- WET SUMP, MINIMUM	l	330	500	540
- DRY SUMP, SYSTEM TANK	l	1585	2115	2380
LUB. OIL COOLER :				
HEAT DISSIPATION	MJ/h	465	620	695
ROCKER ARM SYSTEM :				
LUB. OIL PUMP CAPACITY	l/h	270	270	270
LUB. OIL PRESSURE :				
- NORMAL	barg	0.5	0.5	0.5
- ALARM, PRESSURE LOW	barg	.2-.3	.2-.3	.2-.3
LUB. OIL, TANK VOLUME	l	40	40	40
COOLING WATER DATA				
TWO-STAGE CHARGE AIR COOLER :				
- LOW TEMP. STAGE :				
- MAX. INLET TEMP.	°C	37	37	37
- WATER FLOWRATE, MAX	m³/h	57.6	75.0	75.0
- HEAT DISSIPATION	MJ/h	550	615	715
- HIGH TEMP. STAGE :				
- WATER FLOWRATE, MAX	m³/h	28.8	52.0	58.5
- HEAT DISSIPATION	MJ/h	640	1180	1310

NOTE! 1 MJ/h = 239 kcal/h = 0.278 kW
MCR = Maximum Continuous Rating
m³n = Volume at 0°C and 1 atm

JACKET WATER SYSTEM:				
PUMP CAPACITY	m³/h	39	52	59
ALARM, PRESSURE LOW	barg	0.8	0.8	0.8
TEMP. AT ENGINE OUTLET :				
- NORMAL	°C	90	90	90
- ALARM, TEMP. HIGH	°C	95	95	95
- SHUT-DOWN, TEMP. HIGH	°C	98	98	98
TEMP RISE IN ENGINE, MAX	°C	7.2	7.2	7.2
- INCL. HIGH TEMP. CA-COOLER	°C	11.2	12.7	12.6
WATER QUANTITY, ENGINE BLOCK	l	240	300	330
EXPANSION TANK :				
- VOLUME, SINGLE-ENGINED	l	200	200	200
- VOLUME, MULTI-ENGINED	l	500	500	500
- HEIGHT ABOVE ENGINE	m	3-10	3-10	3-10
JACKET WATER COOLER :				
HEAT DISSIPATION, ENGINE	MJ/h	1180	1575	1770
- INCL. HIGH TEMP. CA-COOLER	MJ/h	1820	2750	3080
JACKET WATER WASTE HEAT RECOVERY				
WASTE HEAT, 100% LOAD, ±	MJ/h	1820	2750	3080
WASTE HEAT, 80% LOAD, ±	MJ/h	1345	1940	2200
WASTE HEAT, 50% LOAD, ±	MJ/h	800	3325	3790
AIR DATA				
TURBOCHARGER TYPE, BBC :	VTR-	214	254	254
CHARGE AIR COOLER TYPE :	UB-	17/33	29/36	29/36
AIR FLOW COMBUSTION	m³n/h	6700	8900	10000
CHARGE AIR PRESSURE, (±0.1)	barg	2.7	2.7	2.7
CHARGE AIR TEMP, NORMAL	°C	55-60	55-60	55-60
ALARM, TEMP HIGH	°C	65	65	65
AIR PRESS. IN ENGINE ROOM, MIN	mmWG	5	5	5
CHARGE AIR SUCTION DEPRESSION, AT COMPRESSOR INLET, MAX	mmWG	200	200	200
EXHAUST DATA				
MASS FLOW	kg/h	8900	11800	13300
VOLUME FLOW, AFTER TURBINE	m³/h	15800	21100	23700
TEMP., AFTER CYLINDER	°C	410	410	410
TEMP., AFTER TURBINE	°C	350	350	350
BACK PRESSURE, MAX	mmWG	300	300	300
PART LOAD DATA :				
MASS FLOW, 80% LOAD	kg/h	7400	9900	11100
TEMP., AFTER TURBINE	°C	325	325	325
MASS FLOW, 50% LOAD	kg/h	5500	7300	8300
TEMP., AFTER TURBINE	°C	290	290	290
RADIATION DATA				
- FROM ENGINE	MJ/h	180	240	275

Engine power definition is according to ISO 3046/1.
However the Engine ratings are valid for the following reference conditions :
Air inlet temperature . . . . max. + 45°C
Air inlet temperature . . . . min. + 0°C
Charge air low temp. fresh water inlet temp. . . . max. + 37°C
Relative humidity . . . . 60 %

Specific Fuel-Oil Consumption is measured on testbed according to ISO 3046-1, using diesel-oil with a net heating value of 42.7 MJ/kg and no engine-driven pumps.
With engine-driven pumps, add 1 g/kWh for each pump.

Specific Lubricating Oil Consumption is for guidance only.

Start Air Data based on remote and automatic starting.

Coolers to be dimensioned according to UBE recommendations:
- 20% overcapacity plus 10% fouling.

NOTE! Due to continuous development, some data may change.

13-AUG-01
ALO/SDF

Marine Propulsion Plant, K-engine

M/K/O 0801

Technical data.
Page 9

Rolls-Royce

PART 1

TECHNICAL DATA

DRAWING NO.: LE908/64
MAIN ENGINE:KRM @ 750 rpm

APPLICATION: Marine Propulsion

MAIN ENGINE DATA

NUMBER OF CYLINDERS	-	6	8	9
CYLINDER BORE	mm	250	250	250
PISTON STROKE	mm	300	300	300
RATED POWER(MCR), ENGINE	kW	1215	1620	1820
	bhp	1650	2205	2475
MEAN EFFECTIVE PRESSURE	bar	22.0	22.0	22.0
RATED SPEED	1/min	750	750	750
ENGINE SPEED, IDELING	1/min	450	450	450
MEAN PISTON SPEED	m/s	7.5	7.5	7.5
DISPLACEMENT	l	88	118	133
INERTIA OF ROTATING PARTS, ±	kgm^2	175	160	155

FUEL OIL DATA

SPECIFIC FUEL CONSUMPTION	g/kWh	193	193	193
FUEL CONSUMPTION AT MCR	l/h	275	368	413
DAYTANK, 24HRS OPERATION	m^3	7	9	10

START AIR DATA

START AIR PRESSURE, MAX./MIN.	barg	30/15	30/15	30/15
AIR CONSUMPT. PER START(50°C)	m^3n	0.50	0.50	0.50
NO OF STARTS, 125 l RECEIVER	-	4	4	4
NO OF STARTS, 250 l RECEIVER	-	8	8	8

LUBRICATION DATA

LUBRICATING OIL	SAE 40			
MAIN PUMP CAPACITY	m^3/h	19.6	25.0	25.0
LUB. OIL PRESSURE :				
- NORMAL	barg	4-5	4-5	4-5
- ALARM, PRESSURE LOW	barg	2.5	2.5	2.5
- START, STAND-BY PUMP	barg	2.2	2.2	2.2
- AUTOMATIC/MANUAL STOP	barg	1.7	1.7	1.7
TEMP. AT ENGINE INLET :				
- NORMAL	°C	60	60	60
- ALARM, TEMP. HIGH	°C	70	70	70
SPEC. LUB. OIL CONSUMPTION	g/kWh	0.80	0.80	0.80
LUB. OIL CONSUMPTION	l/h	1.1	1.4	1.6
LUB. OIL QUANTITY :				
- WET SUMP, MAXIMUM	l	500	740	810
- WET SUMP, MINIMUM	l	330	500	540
- DRY SUMP, SYSTEM TANK	l	1650	2205	2475
LUB. OIL COOLER :				
HEAT DISSIPATION	MJ/h	485	645	725
ROCKER ARM SYSTEM :				
LUB. OIL PUMP CAPACITY	l/h	270	270	270
LUB. OIL PRESSURE :				
- NORMAL	barg	0.5	0.5	0.5
- ALARM, PRESSURE LOW	barg	.2-.3	.2-.3	.2-.3
LUB. OIL, TANK VOLUME	l	40	40	40

COOLING WATER DATA

TWO-STAGE CHARGE AIR COOLER :				
- LOW TEMP. STAGE :				
- MAX. INLET TEMP.	°C	37	37	37
- WATER FLOWRATE, MAX	m^3/h	57.6	75.0	75.0
- HEAT DISSIPATION	MJ/h	575	670	765
- HIGH TEMP. STAGE :				
- WATER FLOWRATE, MAX	m^3/h	28.8	52.0	58.5
- HEAT DISSIPATION	MJ/h	665	1230	1365

NOTE! 1 MJ/h = 239 kcal/h = 0.278 kW
MCR = Maximum Continuous Rating
m^3n = Volume at 0°C and 1 atm

JACKET WATER SYSTEM:

PUMP CAPACITY	m^3/h	39	52	59
ALARM, PRESSURE LOW	barg	0.8	0.8	0.8
TEMP. AT ENGINE OUTLET :				
- NORMAL	°C	90	90	90
- ALARM, TEMP. HIGH	°C	95	95	95
- SHUT-DOWN, TEMP. HIGH	°C	98	98	98
TEMP RISE IN ENGINE, MAX	°C	7.5	7.5	7.5
- INCL. HIGH TEMP. CA-COOLER	°C	11.6	13.2	13.1
WATER QUANTITY, ENGINE BLOCK	l	240	300	330
EXPANSION TANK :				
- VOLUME, SINGLE-ENGINED	l	200	200	200
- VOLUME, MULTI-ENGINED	l	500	500	500
- HEIGHT ABOVE ENGINE	m	3-10	3-10	3-10
JACKET WATER COOLER :				
HEAT DISSIPATION, ENGINE	MJ/h	1230	1640	1840
- INCL. HIGH TEMP. CA-COOLER	MJ/h	1895	2870	3210
JACKET WATER WASTE HEAT RECOVERY				
WASTE HEAT, 100% LOAD, ±	MJ/h	1895	2870	3210
WASTE HEAT, 80% LOAD, ±	MJ/h	1400	2040	2295
WASTE HEAT, 50% LOAD, ±	MJ/h	830	3490	3930

AIR DATA

TURBOCHARGER TYPE, BBC :	VTR-	214	254	254
CHARGE AIR COOLER TYPE :	UB-	17/33	29/36	29/36
AIR FLOW COMBUSTION	m^3n/h	7100	9400	10600
CHARGE AIR PRESSURE, (±0.1)	barg	2.7	2.7	2.7
CHARGE AIR TEMP, NORMAL	°C	55-60	55-60	55-60
ALARM, TEMP HIGH	°C	65	65	65
AIR PRESS. IN ENGINE ROOM, MIN	mmWG	5	5	5
CHARGE AIR SUCTION DEPRESSION, AT COMPRESSOR INLET, MAX	mmWG	200	200	200

EXHAUST DATA

MASS FLOW	kg/h	9300	12500	14000
VOLUME FLOW, AFTER TURBINE	m^3/h	16600	22100	24600
TEMP., AFTER CYLINDER	°C	410	410	410
TEMP., AFTER TURBINE	°C	345	345	340
BACK PRESSURE, MAX	mmWG	300	300	300
PART LOAD DATA :				
MASS FLOW, 80% LOAD	kg/h	7800	10400	11700
TEMP., AFTER TURBINE	°C	320	320	320
MASS FLOW, 50% LOAD	kg/h	6000	8000	9000
TEMP., AFTER TURBINE	°C	285	285	285

RADIATION DATA

- FROM ENGINE	MJ/h	190	250	285

Engine power definition is according to ISO 3046/1.
However the Engine ratings are valid for the following reference conditions :
Air inlet temperature . . . . max. + 45°C
Air inlet temperature . . . . min. + 0°C
Charge air low temp. fresh water inlet temp. . . . max. + 37°C
Relative humidity . . . . 60 %

Specific Fuel-Oil Consumption is measured on testbed according to ISO 3046-1, using diesel-oil with a net heating value of 42.7 MJ/kg and no engine-driven pumps.
With engine-driven pumps, add 1 g/kWh for each pump.

Specific Lubricating Oil Consumption is for guidance only.

Start Air Data based on remote and automatic starting.

Coolers to be dimensioned according to UBE recommendations:
- 20% overcapacity plus 10% fouling.

NOTE! Due to continuous development, some data may change.

13-AUG-01
ALO/SDF

APPENDIX W: TEST BED DATA KRM-6

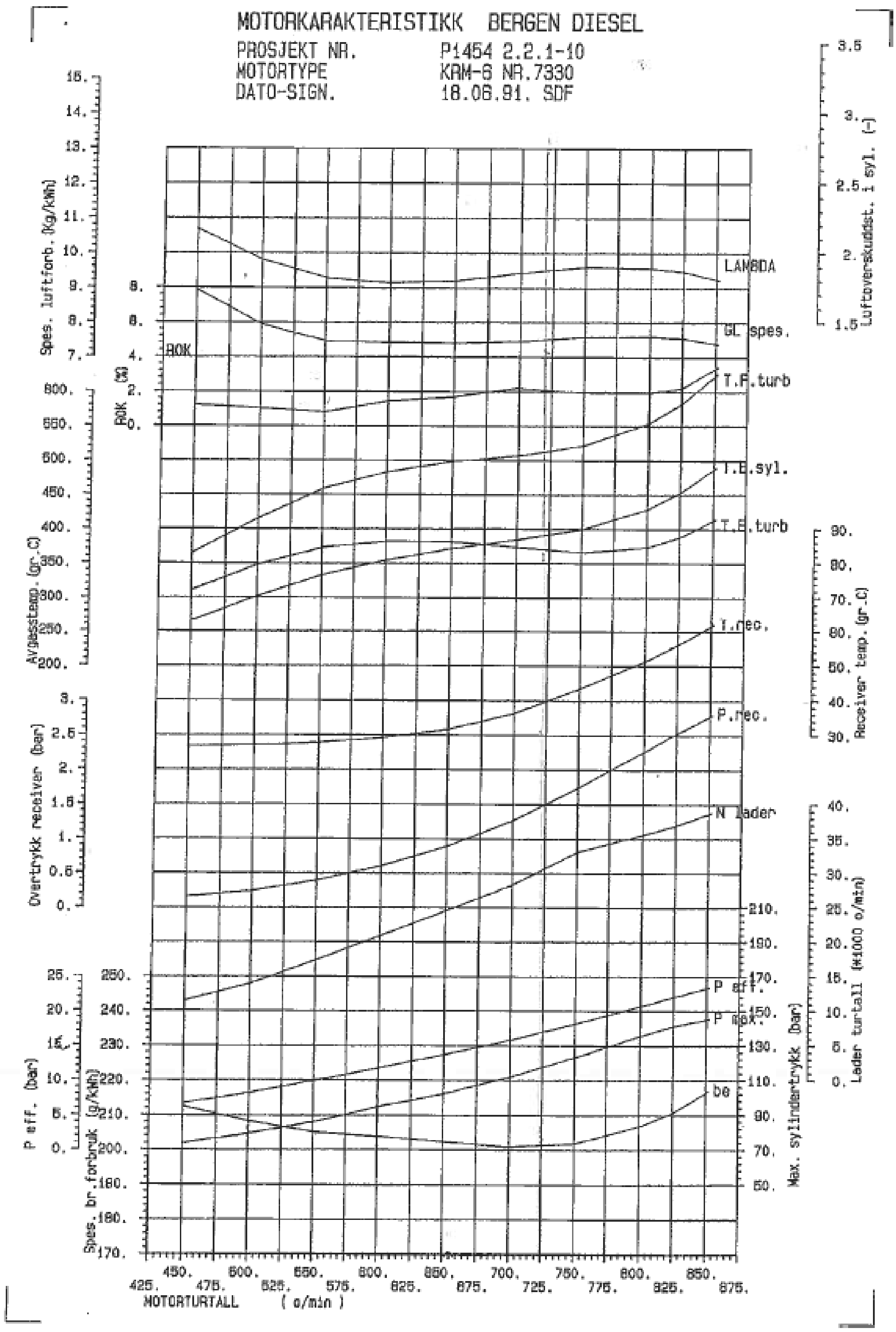

****

MOTORKARAKTERISTIKK BERGEN DIESEL

PROSJEKT :P1454 2.2.1-10

MOTORTYPE :KRM-6 NR.7330

****

FORS\K NR. 1 UTF\RT DATO: 18. 6.91. KLOKKESLETT: 14.42.35.

****

MOTOR-TURTALL	(o/min)	449.6	DREIEMOMENT	(Nm)	4693.
EFF.MIDDELTRYKK	(bar)	6.67	BREMSEKRAFT	(N)	5723.
YTELSE	(kW)	221.0	BRENNOLJEMENGDE	(kg)	5.569
MAKS.SYLINDERTRYKK	(bar)	73.7	BRENNOLJEMÅLING	(sek)	427.2
SPES.BRENNST.FORB.	(g/kWh)	212.4	PÅDRAG	(mm)	12.6
	(g/hkh)	156.2	BRENNOLJETEMP. F.MOTOR	(C)	34.2

****

LUFT-AVGASSDATA

	BAROMETER	(bar)	.996	TRYKKFALL LM.DYSE	(mbar)	1.50
density	TETTHET	(kg/m3)	1.179	TRYKKTAP LM.DYSE	(mbar)	.78
	TEMP.F.LM.DYSE	(C)	21.4	TRYKK F.LADER(abs)	(bar)	1.00
	TEMP.F.LADER	(C)	21.4	TRYKK REC. (abs)	(bar)	1.15
charger	TEMP.E.LADER	(C)	44.4	OVERTRYKK REC.	(bar)	.15
	TEMP.RECEIVER	(C)	26.7			
	KOEFF.LM.DYSE	(-)	.129	LADERTURTALL	(o/min)	11398.
air amount	LUFTMENGDE	(kg/s)	.55	LADERT.(298K)	(o/min)	11466.
	LUFTVOLUM	(m3/s)	.47	ADIAB.TEMP.STIGN.	(C)	12.2
	LUFTV.298K	(m3/s)	.47	TRYKKFORHOLD O.LADER	(-)	1.16
s. air consumpt	SP.LUFTF.	(kg/kWh)	8.94	ADIAB.VIRKNINGSGRAD	(-)	.53
	LAMBDA SYL.	(-)	2.17	LAMBDA AVGASS	(-)	2.96
	SPYLEFAKTOR	(-)	1.36			

TEMP.E.SYL.1	(C)	285.	TEMP. F.TURB. R1	(C)	372.
2	"	277.	" " R2	"	356.
3	"	235.	" " R3	"	0.
4	"	266.	MIDDEL F.TURB.	"	364.
5	"	270.	TEMP. E.TURBIN	"	310.
6	"	264.	AVGASSMENGDE	(kg/h)	2022.
7	"	0.	R\KMÅLING (1*BOSCH)	(%)	1.21
8	"	0.			
9	"	0.			
MIDDEL E.SYL.	"	266.			

****

KJ\LEVANN-SM\REOLJEDATA

KJ\LEVANN-TEMP. F.MOTOR	74.4	E.MOTOR	78.1	TRYKK E.MOTOR	1.7
SM\REOLJE-TRYKK F.FILTER	3.6	E.FILTER	3.8	DIFF.TRYKK	-.2
SM\REOLJE-TEMP. F.MOTOR	52.7	E.MOTOR	60.5		
DYSEOLJE -TEMP. F.DYSER	29.8	E.DYSER	31.9		

SJ\VANN-TEMP. (C)	F\R	ETTER	SJ\VANN-MENGDER (dm3/h)	
LADELUFTKJ\LER LT.	25.7	25.9	LADELUFTKJ\LER LT.	38862.
LADELUFTKJ\LER HT.	26.7	27.2	LADELUFTKJ\LER HT.	-11701.
SM\REOLJEKJ\LER	25.6	27.1	SM\REOLJEKJ\LER	31027.
FERSKVANNKJ\LER	25.6	28.1	FERSKVANNKJ\LER	39824.

****

```
************************************************************************
*                 MOTORKARAKTERISTIKK BERGEN DIESEL                    *
*                 PROSJEKT  :P1454 2.2.1-10                            *
*                 MOTORTYPE :KRM-6 NR.7330                             *
************************************************************************
FORS\K NR.   2    UTF\RT DATO: 18. 6.91.       KLOKKESLETT:  14.33.50.
************************************************************************

MOTOR-TURTALL        (o/min)   500.6  DREIEMOMENT            (Nm)   5732.
EFF.MIDDELTRYKK        (bar)    8.15  BREMSEKRAFT             (N)   6990.
YTELSE                  (kW)   300.4  BRENNOLJEMENGDE        (kg)      5.569
MAKS.SYLINDERTRYKK     (bar)    79.3  BRENNOLJEM]LING       (sek)    320.5
SPES.BRENNST.FORB.  (g/kWh)    208.2  P]DRAG                 (mm)     14.0
                    (g/hkh)    153.1  BRENNOLJETEMP. F.MOTOR (C)      34.2
************************************************************************

LUFT-AVGASSDATA

BAROMETER    (bar)     .996         TRYKKFALL LM.DYSE (mbar)      2.19
TETTHET     (kg/m3)   1.178         TRYKKTAP  LM.DYSE (mbar)      1.31
TEMP.F.LM.DYSE(C)     21.5          TRYKK F.LADER(abs)  (bar)      .99
TEMP.F.LADER   (C)    21.5          TRYKK REC.   (abs)  (bar)     1.24
TEMP.E.LADER   (C)    53.1          OVERTRYKK REC.      (bar)      .24
TEMP.RECEIVER  (C)    27.0

KOEFF.LM.DYSE (-)      .129         LADERTURTALL     (o/min) 13975.
LUFTMENGDE  (kg/s)     .66          LADERT.(298K)    (o/min) 14058.
LUFTVOLUM   (m3/s)     .56          ADIAB.TEMP.STIGN.      (C)     18.5
LUFTV.298K  (m3/s)     .57          TRYKKFORHOLD O.LADER (-)       1.24
SP.LUFTF.(kg/kWh)     7.94          ADIAB.VIRKNINGSGRAD  (-)        .58
LAMBDA SYL.    (-)    1.95          LAMBDA AVGASS        (-)       2.68
SPYLEFAKTOR    (-)    1.38


TEMP.E.SYL.1   (C) 325.             TEMP.  F.TURB. R1     (C)     421.
           2    "  317.              "        "    R2      "      409.
           3    "  269.              "        "    R3      "        0.
           4    "  299.             MIDDEL F.TURB.         "      415.
           5    "  303.             TEMP.  E.TURBIN        "      348.
           6    "  299.             AVGASSMENGDE       (kg/h)    2447.
           7    "    0.             R\KM]LING   (1*BOSCH) (%)       1.01
           8    "    0.
           9    "    0.
MIDDEL E.SYL.   "  302.
************************************************************************

KJ\LEVANN-SM\REOLJEDATA

KJ\LEVANN-TEMP.  F.MOTOR    74.3   E.MOTOR     78.2    TRYKK E.MOTOR  1.8
SM\REOLJE-TRYKK  F.FILTER    3.8   E.FILTER     4.0    DIFF.TRYKK     -.2
SM\REOLJE-TEMP.  F.MOTOR    52.3   E.MOTOR     60.3
DYSEOLJE -TEMP.  F.DYSER    30.3   E.DYSER     32.4

SJ\VANN-TEMP. (C)     F\R    ETTER  SJ\VANN-MENGDER   (dm3/h)

LADELUFTKJ\LER LT.  25.7    26.0   LADELUFTKJ\LER LT.        38641.
LADELUFTKJ\LER HT.  27.2    27.8   LADELUFTKJ\LER HT.       -11701.
SM\REOLJEKJ\LER     25.6    27.7   SM\REOLJEKJ\LER           30731.
FERSKVANNKJ\LER     25.6    28.6   FERSKVANNKJ\LER           39608.
************************************************************************
```

```
*********************************************************************
*                   MOTORKARAKTERISTIKK BERGEN DIESEL               *
*                   PROSJEKT  :P1454 2.2.1-10                       *
*                   MOTORTYPE :KRM-6 NR.7330                        *
*********************************************************************
FORS\K NR.    3     UTF\RT DATO: 18. 6.91.        KLOKKESLETT:  14.27. 4.
*********************************************************************

MOTOR-TURTALL        (o/min)   551.1  DREIEMOMENT             (Nm)   7009.
EFF.MIDDELTRYKK        (bar)     9.97 BREMSEKRAFT              (N)   8547.
YTELSE                  (kW)   404.4  BRENNOLJEMENGDE         (kg)      5.569
MAKS.SYLINDERTRYKK     (bar)    86.0  BRENNOLJEM]LING        (sek)    241.7
SPES.BRENNST.FORB.(g/kWh)      205.1  P]DRAG                  (mm)     15.7
                     (g/hkh)   150.8  BRENNOLJETEMP. F.MOTOR (C)      34.0
*********************************************************************

LUFT-AVGASSDATA

BAROMETER    (bar)     .996         TRYKKFALL LM.DYSE (mbar)        3.50
TETTHET    (kg/m3)    1.177         TRYKKTAP  LM.DYSE (mbar)        2.09
TEMP.F.LM.DYSE(C)    21.9           TRYKK F.LADER(abs)  (bar)        .99
TEMP.F.LADER   (C)   21.9           TRYKK REC.    (abs) (bar)       1.39
TEMP.E.LADER   (C)   67.5           OVERTRYKK REC.      (bar)        .40
TEMP.RECEIVER  (C)   27.8

KOEFF.LM.DYSE (-)      .129         LADERTURTALL      (o/min) 17384.
LUFTMENGDE  (kg/s)     .84          LADERT.(298K)     (o/min) 17477.
LUFTVOLUM   (m3/s)     .71          ADIAB.TEMP.STIGN.     (C)      29.2
LUFTV.298K  (m3/s)     .72          TRYKKFORHOLD O.LADER (-)        1.40
SP.LUFTF.(kg/kWh)     7.44          ADIAB.VIRKNINGSGRAD  (-)         .64
LAMBDA SYL.     (-)   1.82          LAMBDA AVGASS        (-)        2.55
SPYLEFAKTOR     (-)   1.41


TEMP.E.SYL.1   (C) 354.             TEMP.  F.TURB. R1     (C)    466.
           2    "  350.              "       "     R2      "     452.
           3    "  300.              "       "     R3      "       0.
           4    "  330.             MIDDEL F.TURB.         "     459.
           5    "  334.             TEMP.  E.TURBIN        "     373.
           6    "  332.             AVGASSMENGDE       (kg/h)   3092.
           7    "    0.             R\KM]LING  (1*BOSCH) (%)        .81
           8    "    0.
           9    "    0.
MIDDEL E.SYL.   "  333.
*********************************************************************

KJ\LEVANN-SM\REOLJEDATA

KJ\LEVANN-TEMP. F.MOTOR    74.1   E.MOTOR     78.4   TRYKK E.MOTOR   1.9
SM\REOLJE-TRYKK F.FILTER    4.0   E.FILTER     4.2   DIFF.TRYKK      -.2
SM\REOLJE-TEMP. F.MOTOR    51.0   E.MOTOR     61.4
DYSEOLJE -TEMP. F.DYSER    30.5   E.DYSER     32.7

SJ\VANN-TEMP. (C)    F\R    ETTER  SJ\VANN-MENGDER  (dm3/h)

LADELUFTKJ\LER LT.  25.7    26.4   LADELUFTKJ\LER LT.        38649.
LADELUFTKJ\LER HT.  27.7    28.3   LADELUFTKJ\LER HT.       -11701.
SM\REOLJEKJ\LER     25.6    28.5   SM\REOLJEKJ\LER           30848.
FERSKVANNKJ\LER     25.6    29.3   FERSKVANNKJ\LER           39628.
*********************************************************************
```

```
**********************************************************************
*                  MOTORKARAKTERISTIKK BERGEN DIESEL                 *
*                  PROSJEKT   :P1454 2.2.1-10                        *
*                  MOTORTYPE :KRM-6 NR.7330                          *
**********************************************************************
FORS\K NR.   4    UTF\RT DATO: 18. 6.91.       KLOKKESLETT:  14.21.48.
**********************************************************************

MOTOR-TURTALL       (o/min)   599.9  DREIEMOMENT             (Nm)   8218.
EFF.MIDDELTRYKK       (bar)   11.69  BREMSEKRAFT              (N)  10022.
YTELSE                (kW)    516.2  BRENNOLJEMENGDE         (kg)     5.569
MAKS.SYLINDERTRYKK   (bar)     94.5  BRENNOLJEM]LING        (sek)    190.6
SPES.BRENNST.FORB.(g/kWh)     203.8  P]DRAG                  (mm)     17.6
                  (g/hkh)     149.9  BRENNOLJETEMP. F.MOTOR  (C)      33.9
**********************************************************************

LUFT-AVGASSDATA

BAROMETER     (bar)     .996        TRYKKFALL LM.DYSE (mbar)       5.66
TETTHET     (kg/m3)    1.177        TRYKKTAP  LM.DYSE (mbar)       3.20
TEMP.F.LM.DYSE(C)     21.8          TRYKK F.LADER(abs)  (bar)       .99
TEMP.F.LADER   (C)    21.8          TRYKK REC.    (abs) (bar)      1.60
TEMP.E.LADER   (C)    85.3          OVERTRYKK REC.      (bar)       .60
TEMP.RECEIVER  (C)    29.2

KOEFF.LM.DYSE (-)      .129         LADERTURTALL      (o/min)  20908.
LUFTMENGDE  (kg/s)    1.06          LADERT.(298K)     (o/min)  21022.
LUFTVOLUM   (m3/s)     .90          ADIAB.TEMP.STIGN.     (C)     42.0
LUFTV.298K  (m3/s)     .91          TRYKKFORHOLD O.LADER  (-)     1.61
SP.LUFTF.(kg/kWh)     7.42          ADIAB.VIRKNINGSGRAD   (-)      .66
LAMBDA SYL.    (-)    1.78          LAMBDA AVGASS         (-)     2.56
SPYLEFAKTOR    (-)    1.44


TEMP.E.SYL.1   (C) 372.             TEMP.  F.TURB. R1     (C)    489.
           2   "   371.              "        "    R2     "      477.
           3   "   324.              "        "    R3     "        0.
           4   "   350.             MIDDEL F.TURB.        "      483.
           5   "   352.             TEMP.  E.TURBIN       "      381.
           6   "   356.             AVGASSMENGDE      (kg/h)    3935.
           7   "     0.             R\KM]LING  (1*BOSCH)  (%)      1.44
           8   "     0.
           9   "     0.
MIDDEL E.SYL.  "   354.
**********************************************************************

KJ\LEVANN-SM\REOLJEDATA

KJ\LEVANN-TEMP.  F.MOTOR    74.0   E.MOTOR    78.4   TRYKK E.MOTOR  2.0
SM\REOLJE-TRYKK F.FILTER    4.1    E.FILTER    4.3   DIFF.TRYKK     -.2
SM\REOLJE-TEMP.  F.MOTOR    52.5   E.MOTOR    62.8
DYSEOLJE -TEMP.  F.DYSER    30.5   E.DYSER    32.8

SJ\VANN-TEMP.  (C)    F\R    ETTER  SJ\VANN-MENGDER   (dm3/h)

LADELUFTKJ\LER LT.  25.6    27.0   LADELUFTKJ\LER LT.       38839.
LADELUFTKJ\LER HT.  27.7    28.2   LADELUFTKJ\LER HT.      -11701.
SM\REOLJEKJ\LER     25.5    28.6   SM\REOLJEKJ\LER          30491.
FERSKVANNKJ\LER     25.5    29.8   FERSKVANNKJ\LER          39681.
**********************************************************************
```

```
**********************************************************************
*                  MOTORKARAKTERISTIKK BERGEN DIESEL                 *
*                  PROSJEKT  :P1454 2.2.1-10                         *
*                  MOTORTYPE :KRM-6 NR.7330                          *
**********************************************************************
FORS\K NR.   5    UTF\RT DATO: 18. 6.91.       KLOKKESLETT:  14.17. 7.
**********************************************************************

MOTOR-TURTALL         (o/min)  649.0  DREIEMOMENT              (Nm)   9582.
EFF.MIDDELTRYKK         (bar)   13.63 BREMSEKRAFT               (N)  11685.
YTELSE                   (kW)  651.2  BRENNOLJEMENGDE          (kg)     5.569
MAKS.SYLINDERTRYKK      (bar)  102.2  BRENNOLJEM]LING         (sek)   152.1
SPES.BRENNST.FORB.(g/kWh)      202.4  P]DRAG                   (mm)    19.7
                      (g/hkh)  148.9  BRENNOLJETEMP. F.MOTOR  (C)      33.8
**********************************************************************

LUFT-AVGASSDATA

BAROMETER    (bar)     .996         TRYKKFALL LM.DYSE (mbar)       8.95
TETTHET    (kg/m3)    1.176         TRYKKTAP  LM.DYSE (mbar)       4.88
TEMP.F.LM.DYSE(C)    22.0           TRYKK F.LADER(abs)  (bar)       .99
TEMP.F.LADER    (C)  22.0           TRYKK REC.    (abs) (bar)      1.88
TEMP.E.LADER    (C) 106.0           OVERTRYKK REC.        (bar)     .88
TEMP.RECEIVER   (C)  31.7

KOEFF.LM.DYSE  (-)     .129         LADERTURTALL        (o/min) 24487.
LUFTMENGDE  (kg/s)    1.34          LADERT.(298K)       (o/min) 24612.
LUFTVOLUM   (m3/s)    1.14          ADIAB.TEMP.STIGN.       (C)     58.0
LUFTV.298K  (m3/s)    1.15          TRYKKFORHOLD O.LADER (-)       1.89
SP.LUFTF.(kg/kWh)     7.39          ADIAB.VIRKNINGSGRAD  (-)        .69
LAMBDA SYL.     (-)   1.80          LAMBDA AVGASS        (-)       2.57
SPYLEFAKTOR     (-)   1.43


TEMP.E.SYL.1    (C) 384.            TEMP.   F.TURB. R1      (C)     502.
            2    "  385.             "        "     R2       "      495.
            3    "  352.             "        "     R3       "        0.
            4    "  362.            MIDDEL F.TURB.           "      499.
            5    "  369.            TEMP.   E.TURBIN         "      381.
            6    "  375.            AVGASSMENGDE        (kg/h)     4944.
            7    "    0.            R\KM]LING   (1*BOSCH)  (%)        1.68
            8    "    0.
            9    "    0.
MIDDEL E.SYL.    "  371.
**********************************************************************

KJ\LEVANN-SM\REOLJEDATA

KJ\LEVANN-TEMP. F.MOTOR    73.8   E.MOTOR     78.4   TRYKK E.MOTOR   2.2
SM\REOLJE-TRYKK F.FILTER    4.2   E.FILTER     4.4   DIFF.TRYKK      -.2
SM\REOLJE-TEMP. F.MOTOR    53.8   E.MOTOR     63.9
DYSEOLJE -TEMP. F.DYSER    30.4   E.DYSER     32.7

SJ\VANN-TEMP. (C)     F\R    ETTER   SJ\VANN-MENGDER   (dm3/h)

LADELUFTKJ\LER LT.  25.7     27.9    LADELUFTKJ\LER LT.         38722.
LADELUFTKJ\LER HT.  28.4     28.8    LADELUFTKJ\LER HT.        -11701.
SM\REOLJEKJ\LER     25.6     28.8    SM\REOLJEKJ\LER            30683.
FERSKVANNKJ\LER     25.6     30.2    FERSKVANNKJ\LER            39594.
**********************************************************************
```

```
************************************************************************
*                  MOTORKARAKTERISTIKK BERGEN DIESEL              .   *
*                  PROSJEKT  :P1454 2.2.1-10                          *
*                  MOTORTYPE :KRM-6 NR.7330                           *
************************************************************************
FORS\K NR.   6    UTF\RT DATO: 18. 6.91.       KLOKKESLETT:  14. 9.35.
************************************************************************

MOTOR-TURTALL       (o/min)  698.9  DREIEMOMENT              (Nm) 11064.
EFF.MIDDELTRYKK       (bar)   15.74 BREMSEKRAFT               (N) 13493.
YTELSE                (kW)   809.7  BRENNOLJEMENGDE          (kg)    5.569
MAKS.SYLINDERTRYKK   (bar)   111.7  BRENNOLJEM]LING         (sek)   123.3
SPES.BRENNST.FORB.(g/kWh)    200.8  P]DRAG                   (mm)    22.1
                  (g/hkh)    147.7  BRENNOLJETEMP. F.MOTOR (C)      33.6
************************************************************************

LUFT-AVGASSDATA

BAROMETER    (bar)     .996       TRYKKFALL LM.DYSE (mbar)      14.10
TETTHET     (kg/m3)   1.177       TRYKKTAP  LM.DYSE (mbar)       7.73
TEMP.F.LM.DYSE(C)    21.8         TRYKK F.LADER(abs) (bar)        .99
TEMP.F.LADER   (C)   21.8         TRYKK REC.    (abs) (bar)       2.25
TEMP.E.LADER   (C)  131.4         OVERTRYKK REC.      (bar)       1.25
TEMP.RECEIVER  (C)   36.2

KOEFF.LM.DYSE (-)     .129        LADERTURTALL      (o/min)  28126.
LUFTMENGDE  (kg/s)    1.68        LADERT.(298K)     (o/min)  28278.
LUFTVOLUM   (m3/s)    1.43        ADIAB.TEMP.STIGN.     (C)     76.6
LUFTV.298K  (m3/s)    1.44        TRYKKFORHOLD O.LADER (-)       2.28
SP.LUFTF.(kg/kWh)     7.46        ADIAB.VIRKNINGSGRAD   (-)       .70
LAMBDA SYL.    (-)    1.85        LAMBDA AVGASS         (-)      2.62
SPYLEFAKTOR    (-)    1.41

TEMP.E.SYL.1   (C)  390.          TEMP.   F.TURB.  R1      (C)    508.
           2    "   398.           "         "     R2       "     505.
           3    "   373.           "         "     R3       "       0.
           4    "   369.          MIDDEL F.TURB.            "     507.
           5    "   382.          TEMP.   E.TURBIN          "     373.
           6    "   390.          AVGASSMENGDE          (kg/h)   6204.
           7    "     0.          R\KM]LING   (1*BOSCH)  (%)      2.20
           8    "     0.
           9    "     0.
MIDDEL E.SYL.   "   384.
************************************************************************

KJ\LEVANN-SM\REOLJEDATA

KJ\LEVANN-TEMP.  F.MOTOR    73.4   E.MOTOR     78.5   TRYKK E.MOTOR  2.3
SM\REOLJE-TRYKK F.FILTER     4.2   E.FILTER     4.4   DIFF.TRYKK     -.2
SM\REOLJE-TEMP.  F.MOTOR    55.8   E.MOTOR     66.0
DYSEOLJE  -TEMP.  F.DYSER   30.0   E.DYSER     32.3

SJ\VANN-TEMP.  (C)     F\R    ETTER  SJ\VANN-MENGDER   (dm3/h)

LADELUFTKJ\LER LT.  25.5    29.1   LADELUFTKJ\LER LT.        38481.
LADELUFTKJ\LER HT.  28.4    28.7   LADELUFTKJ\LER HT.       -11701.
SM\REOLJEKJ\LER     25.4    28.9   SM\REOLJEKJ\LER           30582.
FERSKVANNKJ\LER     25.4    30.7   FERSKVANNKJ\LER           39615.
************************************************************************
```

```
**********************************************************************
*                 MOTORKARAKTERISTIKK BERGEN DIESEL                  *
*                 PROSJEKT   :P1454 2.2.1-10                         *
*                 MOTORTYPE  :KRM-6 NR.7330                          *
**********************************************************************
FORS\K NR.   7    UTF\RT DATO: 18. 6.91.       KLOKKESLETT:  14. 4.23.
**********************************************************************

MOTOR-TURTALL       (o/min)   750.5  DREIEMOMENT            (Nm)  12780.
EFF.MIDDELTRYKK       (bar)   18.18  BREMSEKRAFT             (N)  15586.
YTELSE                (kW)   1004.4  BRENNOLJEMENGDE        (kg)    5.569
MAKS.SYLINDERTRYKK    (bar)   123.0  BRENNOLJEM]LING       (sek)    98.9
SPES.BRENNST.FORB.(g/kWh)     201.8  P]DRAG                 (mm)    26.1
                  (g/hkh)     148.4  BRENNOLJETEMP. F.MOTOR (C)     32.8
**********************************************************************

LUFT-AVGASSDATA

BAROMETER     (bar)     .996        TRYKKFALL LM.DYSE (mbar)     22.44
TETTHET     (kg/m3)    1.175        TRYKKTAP  LM.DYSE (mbar)     12.16
TEMP.F.LM.DYSE(C)      22.3         TRYKK F.LADER(abs) (bar)       .98
TEMP.F.LADER    (C)    22.3         TRYKK REC.   (abs) (bar)      2.74
TEMP.E.LADER    (C)   160.7         OVERTRYKK REC.     (bar)      1.74
TEMP.RECEIVER   (C)    43.4

KOEFF.LM.DYSE (-)       .129        LADERTURTALL      (o/min)  33066.
LUFTMENGDE  (kg/s)     2.12         LADERT.(298K)     (o/min)  33216.
LUFTVOLUM   (m3/s)     1.80         ADIAB.TEMP.STIGN.     (C)    98.2
LUFTV.298K  (m3/s)     1.83         TRYKKFORHOLD O.LADER  (-)     2.78
SP.LUFTF.(kg/kWh)      7.58         ADIAB.VIRKNINGSGRAD   (-)      .71
LAMBDA SYL.     (-)    1.90         LAMBDA AVGASS         (-)     2.65
SPYLEFAKTOR     (-)    1.39

TEMP.E.SYL.1    (C)  402.           TEMP.   F.TURB.  R1     (C)   523.
           2     "   414.            "        "      R2      "    519.
           3     "   392.            "        "      R3      "      0.
           4     "   384.           MIDDEL F.TURB.           "    521.
           5     "   397.           TEMP.   E.TURBIN         "    366.
           6     "   410.           AVGASSMENGDE        (kg/h)   7818.
           7     "     0.           R\KM]LING   (1*BOSCH)  (%)     1.93
           8     "     0.
           9     "     0.
MIDDEL E.SYL.    "   400.
**********************************************************************

KJ\LEVANN-SM\REOLJEDATA

KJ\LEVANN-TEMP.  F.MOTOR    73.2   E.MOTOR    78.8   TRYKK E.MOTOR   2.6
SM\REOLJE-TRYKK F.FILTER     4.4   E.FILTER    4.5   DIFF.TRYKK      -.1
SM\REOLJE-TEMP.  F.MOTOR    57.1   E.MOTOR    67.3
DYSEOLJE  -TEMP. F.DYSER    29.8   E.DYSER    32.1

SJ\VANN-TEMP.  (C)    F\R   ETTER  SJ\VANN-MENGDER   (dm3/h)

LADELUFTKJ\LER LT.  25.9    31.4   LADELUFTKJ\LER LT.       39350.
LADELUFTKJ\LER HT.  28.6    29.0   LADELUFTKJ\LER HT.      -11701.
SM\REOLJEKJ\LER     25.8    29.5   SM\REOLJEKJ\LER          30409.
FERSKVANNKJ\LER     25.8    31.8   FERSKVANNKJ\LER          40410.
**********************************************************************
```

```
*********************************************************************
*                  MOTORKARAKTERISTIKK BERGEN DIESEL                *
*                  PROSJEKT  :P1454 2.2.1-10                        *
*                  MOTORTYPE :KRM-6 NR.7330                         *
*********************************************************************
FORS\K NR.   8    UTF\RT DATO: 18. 6.91.       KLOKKESLETT:  14. 0.16.
*********************************************************************

MOTOR-TURTALL        (o/min)  800.5  DREIEMOMENT               (Nm)  14560.
EFF.MIDDELTRYKK        (bar)   20.71 BREMSEKRAFT                (N)  17756.
YTELSE                  (kW) 1220.6  BRENNOLJEMENGDE           (kg)     5.569
MAKS.SYLINDERTRYKK     (bar)  135.5  BRENNOLJEM]LING          (sek)    79.4
SPES.BRENNST.FORB.(g/kWh)     206.9  P]DRAG                    (mm)    28.4
                  (g/hkh)     152.2  BRENNOLJETEMP. F.MOTOR    (C)     32.0
*********************************************************************

LUFT-AVGASSDATA

BAROMETER    (bar)     .996       TRYKKFALL LM.DYSE (mbar)     33.19
TETTHET    (kg/m3)    1.177       TRYKKTAP  LM.DYSE (mbar)     17.90
TEMP.F.LM.DYSE(C)    21.8         TRYKK F.LADER(abs)  (bar)      .98
TEMP.F.LADER   (C)   21.8         TRYKK REC.    (abs) (bar)     3.25
TEMP.E.LADER   (C) 188.9          OVERTRYKK REC.      (bar)     2.26
TEMP.RECEIVER  (C)   51.3

KOEFF.LM.DYSE (-)      .129       LADERTURTALL       (o/min) 35581.
LUFTMENGDE  (kg/s)    2.58        LADERT.(298K)      (o/min) 35776.
LUFTVOLUM   (m3/s)    2.19        ADIAB.TEMP.STIGN.      (C)    118.3
LUFTV.298K  (m3/s)    2.24        TRYKKFORHOLD O.LADER   (-)      3.33
SP.LUFTF.(kg/kWh)     7.59        ADIAB.VIRKNINGSGRAD    (-)       .71
LAMBDA SYL.    (-)    1.89        LAMBDA AVGASS          (-)      2.59
SPYLEFAKTOR    (-)    1.37


TEMP.E.SYL.1    (C)  432.         TEMP.   F.TURB.  R1     (C)     556.
           2     "   445.          "        "      R2      "      552.
           3     "   420.          "        "      R3      "        0.
           4     "   407.         MIDDEL F.TURB.           "      554.
773        5     "   424.         TEMP.   E.TURBIN         "      374.
           6     "   444.         AVGASSMENGDE          (kg/h)   9523.
823        7     "     0.         R\KM}LING   (1*BOSCH)   (%)      1.93
           8     "     0.
           9     "     0.
MIDDEL E.SYL.    "   429.
*********************************************************************

KJ\LEVANN-SM\REOLJEDATA

KJ\LEVANN-TEMP.  F.MOTOR    72.8   E.MOTOR    79.1   TRYKK E.MOTOR  2.7
SM\REOLJE-TRYKK  F.FILTER    4.4   E.FILTER    4.6   DIFF.TRYKK     -.1
SM\REOLJE-TEMP.  F.MOTOR    57.5   E.MOTOR    67.9
DYSEOLJE  -TEMP. F.DYSER    29.6   E.DYSER    31.7

SJ\VANN-TEMP.  (C)      F\R    ETTER   SJ\VANN-MENGDER   (dm3/h)

LADELUFTKJ\LER LT.  25.0    32.7   LADELUFTKJ\LER LT.        39118.
LADELUFTKJ\LER HT.  28.8    29.1   LADELUFTKJ\LER HT.       -11700.
SM\REOLJEKJ\LER     24.9    28.8   SM\REOLJEKJ\LER           31542.
FERSKVANNKJ\LER     24.9    32.3   FERSKVANNKJ\LER           40373.
*********************************************************************
```

```
*********************************************************************
*                   MOTORKARAKTERISTIKK BERGEN DIESEL               *
*                   PROSJEKT   :P1454 2.2.1-10                      *
*                   MOTORTYPE :KRM-6 NR.7330                        *
*********************************************************************
FORS\K NR.   9   UTF\RT DATO: 18. 6.91.      KLOKKESLETT:  13.53.25.
*********************************************************************

MOTOR-TURTALL       (o/min)  824.9  DREIEMOMENT            (Nm) 15485.
EFF.MIDDELTRYKK      (bar)   22.02  BREMSEKRAFT             (N) 18884.
YTELSE               (kW)  1337.6  BRENNOLJEMENGDE         (kg)     5.569
MAKS.SYLINDERTRYKK  (bar)   141.2  BRENNOLJEMJLING        (sek)    71.2
SPES.BRENNST.FORB.(g/kWh)   210.5  PJDRAG                  (mm)    30.3
                  (g/hkh)   154.8  BRENNOLJETEMP. F.MOTOR  (C)     31.3
*********************************************************************

LUFT-AVGASSDATA

BAROMETER    (bar)     .996      TRYKKFALL LM.DYSE (mbar)     39.25
TETTHET     (kg/m3)   1.178      TRYKKTAP  LM.DYSE (mbar)     21.32
TEMP.F.LM.DYSE(C)    21.7       TRYKK F.LADER(abs) (bar)       .98
TEMP.F.LADER   (C)   21.7       TRYKK REC.    (abs) (bar)     3.52
TEMP.E.LADER   (C)  203.9       OVERTRYKK REC.      (bar)     2.52
TEMP.RECEIVER  (C)   56.1

KOEFF.LM.DYSE (-)     .129      LADERTURTALL       (o/min) 36903.
LUFTMENGDE  (kg/s)   2.80       LADERT.(298K)      (o/min) 37111.
LUFTVOLUM   (m3/s)   2.38       ADIAB.TEMP.STIGN.     (C)    127.9
LUFTV.298K  (m3/s)   2.44       TRYKKFORHOLD O.LADER  (-)      3.61
SP.LUFTF.(kg/kWh)    7.54       ADIAB.VIRKNINGSGRAD   (-)       .70
LAMBDA SYL.    (-)   1.87       LAMBDA AVGASS         (-)      2.52
SPYLEFAKTOR    (-)   1.35


TEMP.E.SYL.1   (C)  463.        TEMP.   F.TURB. R1     (C)     583.
           2    "   470.          "       "     R2      "      581.
           3    "   442.          "       "     R3      "        0.
           4    "   427.        MIDDEL F.TURB.          "      582.
           5    "   445.        TEMP.   E.TURBIN        "      388.
           6    "   468.        AVGASSMENGDE        (kg/h) 10365.
           7    "     0.        R\KMJLING   (1*BOSCH)  (%)      2.20
           8    "     0.
           9    "     0.
MIDDEL E.SYL.   "   453.
*********************************************************************

KJ\LEVANN-SM\REOLJEDATA

KJ\LEVANN-TEMP.  F.MOTOR    72.3   E.MOTOR    79.3   TRYKK E.MOTOR   2.7
SM\REOLJE-TRYKK F.FILTER    4.5   E.FILTER    4.6   DIFF.TRYKK      -.1
SM\REOLJE-TEMP.  F.MOTOR    57.6   E.MOTOR    68.1
DYSEOLJE -TEMP.  F.DYSER    29.4   E.DYSER    31.3

SJ\VANN-TEMP.  (C)    F\R    ETTER  SJ\VANN-MENGDER  (dm3/h)

LADELUFTKJ\LER LT.  23.8   33.0   LADELUFTKJ\LER LT.       38518.
LADELUFTKJ\LER HT.  28.6   28.7   LADELUFTKJ\LER HT.      -11700.
SM\REOLJEKJ\LER     23.7   27.7   SM\REOLJEKJ\LER          31170.
FERSKVANNKJ\LER     23.7   32.1   FERSKVANNKJ\LER          39641.
*********************************************************************
```

APPENDIX X: "WIEBECOMB"

Submitted electronically due to formatting challenges. See attached CD-rom for "WiebeComb.xls".